

(NASA-CR-121213) ADVANCED HYDROGEN/OXYGEN
THRUST CHAMBER DESIGN ANALYSIS Final
Report, Jul. 1972 - May 1973 (Rockwell
International Corp., Canoga Park) 252 p
HC \$14.75

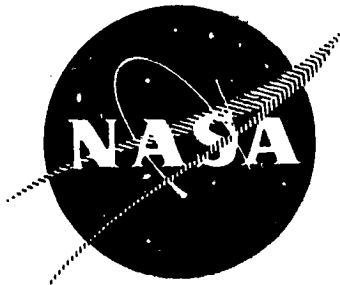
N74-12446

Unclas
23017

CSCI 21H G3/28

NASA CR-121213

R-9258



ADVANCED HYDROGEN/OXYGEN
THRUST CHAMBER DESIGN ANALYSIS

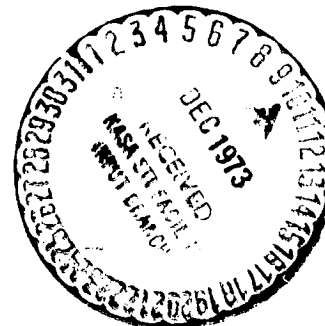
by J. M. Shoji

ROCKETDYNE DIVISION
ROCKWELL INTERNATIONAL

prepared for

NATIONAL AERONAUTICS AND SPACE ADMINISTRATION

NASA Lewis Research Center
Contract NAS 3-16774



FOREWORD

This technical report presents the results of the Advanced Hydrogen/Oxygen Thrust Chamber Design Analysis Program. The studies were conducted by Rocketdyne Division, Rockwell International, during the period 13 July 1972 to 11 May 1973 as part of National Aeronautics and Space Administration, Lewis Research Center, Contract NAS3-16774.

The NASA-LeRC Project Manager was Mr. H. G. Price. Mr. H. G. Diem was the Rocketdyne Program Manager.

The computer programs and manuals have been submitted separately.

ACKNOWLEDGMENTS

The work presented in this volume represents the concerted effort and expertise of many members of the Rocketdyne organization. Contributions of major significance were made by the following personnel:

D. S. Jenkins	- Program Management
W. R. Wagner	- Technical Review
N. E. Bergstresser	- Stress and Cycle Life Analysis
G. J. Leake	- Stress and Cycle Life Analysis
H. E. Marker	- Thrust Chamber Design
G. Janson	- Thrust Chamber Design
R. D. Huxsol	- Thrust Chamber Design
J. G. Gerstley	- Computer Manual and Programming
G. S. Osugi	- Computer Manual
B. L. McFarland	- Computer Manual and Programming
R. D. Tobin	- Computer Manual
J. F. Newell	- Computer Program

PRECEDING PAGE BLANK NOT FILMED

TABLE OF CONTENTS

Summary	1
Introduction	3
Conclusions	5
Task I: Base Designs and Analysis	7
Thrust Chamber Design Criteria	7
Tubular Wall Configurations (1-1/2 Pass Cooling Circuit)	17
Channel Wall Combustor/Tubular Nozzle Configuration (1-1/2 Pass Cooling Circuit)	47
Channel Wall Combustor/Tubular Nozzle (Split-Flow Cooling Circuit)	76
Configuration Selection	101
Transient Analysis	123
Task II: Off-Design Life Evaluation	137
Off-Design Thrust Chamber Parameters	137
Analysis and Results	137
Task III: Perturbation of Reference-Point Operating Conditions	147
Cycle Life Perturbation ($P_c = 1900$ psia or 1.31×10^7 N/m ²)	147
Chamber Pressure Perturbation (300-Cycle Life)	159
Task IV: Computer Programming	195
<u>Appendix A</u>	197
Stress and Life Cycle Evaluation	197
Fatigue Properties	197
Stress Rupture Properties	202
Material Damage Fractions	202
Life Equation	203
Stress and Strain Analysis	211
<u>Appendix B</u>	211
Duty Cycle Life Evaluation Method	211
Fatigue Damage	211
Creep Damage	212
Total Damage	213
References	213

PRECEDING PAGE BLANK NOT FILMED

ILLUSTRATIONS

1.	Zr-Cu Channel Wall Combustor/A-286 Tubular Nozzle Configuration With Split-Flow Cooling Circuit	4
2.	Task I Configurations	8
3.	Combustion Chamber Configuration	11
4.	20K Pounds (8.896×10^4 N) Thrust Chamber Combustion Chamber Contour	12
5.	20K Pounds (8.896×10^4 N) Thrust Chamber Nozzle Contour	13
6.	20K Pounds (8.896×10^4 N) Thrust Chamber-Combustor Gas-Side Heat Transfer Coefficient Distribution	14
7.	20K Pounds (8.896×10^4 N) Thrust Chamber--Nozzle Heat Transfer Coefficient Distribution ($\epsilon = 1$ to $\epsilon = 100$)	15
8.	20K Pounds (8.896×10^4 N) Thrust Chamber--Nozzle Heat Transfer Coefficient Distribution ($\epsilon = 100$ to $\epsilon = 400$)	16
9.	Zr-Cu Tubular Configuration--Variation of Coolant Pressure Drop and Wall Temperature With Number of Tubes	18
10.	NARloy Tubular Configuration--Variation of Coolant Pressure Drop and Wall Temperature With Number of Tubes	19
11.	Coolant Tube Weight Variation With Number of Tubes-- Zr-Cu Tubular Configuration	20
12.	Coolant Tube Weight Variation With Number of Tubes-- NARloy-Z Tubular Configuration	21
13.	Tube R/t Versus Allowable Coolant Pressure for Zirconium-Copper (Basic Structural Criteria)	23
14.	Tube R/t Versus Allowable Coolant Pressure for NARloy-Z (Basic Structural Criteria)	24
15.	Variation of Coolant Pressure and Wall Temperature Just Upstream of Coolant Inlet With Coolant Inlet Area Ratio-- Zr-Cu Tubular Configuration	25
16.	Coolant Tube Weight Variation With Coolant Inlet Area Ratio-- Zr-Cu Tubular Configuration	26
17.	Variation of Coolant Pressure and Wall Temperature Just Upstream of Tube Splice With Tube Splice Area Ratio-- Zr-Cu Tubular Configuration	27
18.	Coolant Tube Weight Variation With Tube Splice Area Ratio-- Zr-Cu Tubular Configuration	28
19.	Wall Temperature Variation With Tube Wall Thickness (Constant Outside Diameter)--Zr-Cu Tubular Configuration	29
20.	Selected Zr-Cu Tubular Configuration	30
21.	Coolant Static Pressure Distribution for the Selected Zr-Cu Tubular Configuration	32
22.	Temperature Distributions for the Selected Zr-Cu Tubular Configuration	33
23.	Tube Wall Temperature Distribution ($X = -0.8$ Inch or -2.03 CM)	34
24.	Variation of Damage Fraction and Yield Strength Safety Factor With Number of Tubes for NARloy-Z	35
25.	Coolant Mass Velocity Ratio Variation With Number of Tubes--NARloy-Z	36
26.	Creep Damage Fraction for the NARloy-Z Tubular Configuration	37
27.	Selected NARloy-Z Tubular Configuration	27

28.	Coolant Static Pressure Distribution for the Selected NARloy Tubular Configuration	39
29.	Temperature Distribution for the Selected NARloy-Z Tubular Configuration	40
30.	Zr-Cu Tubular Wall Configuration (1-1/2 Pass Cooling Circuit)	43
31.	NARloy-Z Tubular Wall Configuration (1-1/2 Pass Cooling Circuit)	45
32.	Chamber Jacket Thickness Distribution for the Tubular Wall Configuration (1-1/2 Pass Cooling Circuit)	48
33.	A-286 Nozzle (Round Tube Configuration) Coolant Pressure Drop Variation With Number of Tubes and Combustor-Nozzle Joint Area Ratio	49
34.	A-286 Nozzle (Booked Tube Configurations) Gas-Side Wall Temperature Distributions	51
35.	Selected A-286 Nozzle Configuration (1-1/2 Pass Cooling Circuit)	52
36.	Coolant Static Pressure Distribution for the Selected A-286 Nozzle (1-1/2 Pass Cooling Circuit)	53
37.	Temperature Distributions for the Selected A-286 Nozzle (1-1/2 Pass Cooling Circuit)	54
38.	Basic Structural Criteria for Zirconium-Copper	55
39.	Basic Structural Criteria for NARloy-Z	56
40.	Fatigue Damage Fraction Variation With Wall Temperature for Zr-Cu Channel Configuration (1-1/2 Pass Cooling Circuit)	58
41.	Zr-Cu Combustor (1-1/2 Pass Cooling Circuit) Channel Width Influence on Coolant Pressure Drop	59
42.	Chamber Coolant Pressure Drop and Weight Variation With Combustor-Nozzle Joint Area Ratio for Zr-Cu Combustor/A-286 Nozzle (1-1/2 Pass Cooling Circuit)	60
43.	Channel Dimensions of the Selected Zr-Cu Channel Wall Combustor Configuration (1-1/2 Pass Cooling Circuit)	61
44.	Temperature Distributions for the Selected Zr-Cu Channel Wall Combustor Configuration (1-1/2 Pass Cooling Circuit)	62
45.	Maximum Allowable Wall Temperature to Meet Life Cycle Requirements (NARloy-Z)	63
46.	NARloy-Z Combustor (1-1/2 Pass Cooling Circuit) Channel Width-to-Wall Thickness Ratio Influence	65
47.	Channel Dimensions of the Selected NARloy-Z Channel Wall Combustor Configuration (1-1/2 Pass Cooling Circuit)	66
48.	Temperature Distributions for the Selected NARloy-Z Channel Wall Combustor Configuration (1-1/2 Pass Cooling Circuit)	57
49.	Zr-Cu Channel Wall Combustor/A-286 Tubular Nozzle Configuration (1-1/2 Pass Cooling Circuit)	71
50.	NARloy-Z Channel Wall Combustor/A-286 Tubular Nozzle Configuration (1-1/2 Pass Cooling Circuit)	73
51.	Chamber Jacket Thickness Distribution for the Channel Wall Combustor/Tubular Nozzle Configuration (1-1/2 Pass Cooling Circuit)	75
52.	Candidate A-286 Nozzle Split-Flow Cooling Circuits	77

53.	A-286 Nozzle Split-Flow Circuit (Round Tube Configuration) Coolant Pressure Drop and Wall Temperature Variation With Number of Tubes	78
54.	A-286 Nozzle (Round Tube Configuration) Tube Weight Variation With Number of Tubes (Uppass Coolant Circuit)	79
55.	A-286 Nozzle Split-Flow Circuit (Round Tubes) Tube Diameter Variation With Number of Tubes	80
56.	Uppass Booked A-286 Nozzle Configurations (Split-Flow Cooling Circuit)	81
57.	Nozzle Coolant Pressure Drop Influence on Maximum Wall Temperature for Uppass A-286 Nozzle (Split-Flow Cooling Circuit)	82
58.	Selected A-286 Nozzle Configuration (Split-Flow Cooling Circuit)	83
59.	Coolant Static Pressure Distribution for the Selected A-286 Nozzle (Split-Flow Cooling Circuit)	84
60.	Temperature Distributions for the Selected A-286 Nozzle (Split-Flow Cooling Circuit)	85
61.	NARloy-Z Combustor (Split-Flow Cooling Circuit) Channel Width- to-Wall Thickness Ratio Influence	87
62.	Combustor and Nozzle Coolant Pressure Variation With Joint Area Ratio (Split-Flow Cooling Circuit)	88
63.	Combustor Liner and/or Nozzle Tube Weight Variation With Joint Area Ratio (Split-Flow Cooling Circuit)	89
64.	Channel Dimensions of the Selected NARloy-Z Channel Wall Combustor Configuration (Split-Flow Cooling Circuit)	90
65.	Temperature Distributions for the Selected NARloy-Z Channel Wall Combustor Configuration (Split-Flow Cooling Circuit)	91
66.	Influence of Channel Width on Combustor Coolant Pressure Drop on the Zr-Cu Combustor (Split-Flow Cooling Circuit)	92
67.	Channel Dimensions of the Selected Zr-Cu Channel Wall Combustor Configuration (Split-Flow Cooling Circuit)	93
68.	Temperature Distributions for the Selected Zr-Cu Channel Wall Combustor Configuration (Split-Flow Cooling Circuit)	94
69.	Zr-Cu Channel Wall Combustor/A-286 Tubular Nozzle Configuration (Split-Flow Cooling Circuit)	97
70.	NARloy-Z Channel Wall Combustor/A-286 Tubular Configuration (Split-Flow Cooling Circuit)	99
71.	Selected Task I Configurations	102
72.	Finite Element Model (NARloy-Z Tubular Configuration at $X = -0.8$ Inch or -2.03 cm)	106
73.	NARloy-Z Channel Wall Finite Element Stress Analysis Model	107
74.	Variations of Combustor Coolant Pressure Drop and Channel Depth With Maximum Wall Temperature for Split-Flow Cooling Circuit NARloy-Z Combustor	109
75.	Variation of Combustor Coolant Pressure Drop and Minimum Channel Depth With Maximum Gas-Side Wall Temperature for Split-Flow Cooling Circuit Zr-Cu Combustor	111
76.	Variation of Combustor Coolant Pressure Drop and Minimum Channel Depth With Maximum Gas-Side Wall Temperature for 1-1/2-Pass Cooling Circuit Zr-Cu Combustor	112

77.	Channel Dimensions of the Final Zr-Cu Channel Wall Combustor Configuration (Split-Flow Cooling Circuit)	113
78.	Coolant Static Pressure Distribution for the Final Zr-Cu Combustor Configuration (Split-Flow Cooling Circuit)	114
79.	Temperature Distribution for the Final Zr-Cu Channel Wall Combustor Configuration (Split-Flow Cooling Circuit)	115
80.	Two-Dimensional Wall Temperature Distribution in Throat Region for Final Zr-Cu Combustor (Split-Flow Cooling Circuit)	116
81.	Channel Dimensions of the Final Zr-Cu Channel Wall Combustor Configuration (1-1/2 Pass Cooling Circuit)	117
82.	Coolant Static Pressure Distribution for the Final Zr-Cu Combustor Configuration (1-1/2 Pass Cooling Circuit)	118
83.	Temperature Distribution for the Final Zr-Cu Channel Wall Combustor Configuration (1-1/2 Pass Cooling Circuit)	119
84.	Two-Dimensional Wall Temperature Distribution in Throat Region for Final Zr-Cu Combustor (1-1/2 Pass Cooling Circuit)	120
85.	Zr-Cu Channel Wall Finite Element Stress Analysis Model	122
86.	Final Zr-Cu Channel Wall Combustor/A-286 Tubular Nozzle Configuration-- $P_c = 1900$ psia or 1.31×10^7 N/m ² (Split-Flow Cooling Circuit)	125
87.	Final Zr-Cu Channel Wall Combustor/A-286 Tubular Nozzle Configuration-- $P_c = 1900$ psia or 1.31×10^7 N/m ² (1-1/2 Pass Cooling Circuit)	127
88.	Engine Start Transients	129
89.	Engine Shutdown Transients	130
90.	Zr-Cu Combustor Channel Wall Temperature Engine Start Transient at X = -0.5 Inch (-1.27 cm) (Split-Flow Cooling Circuit)	132
91.	Zr-Cu Combustor Channel Wall Temperature Engine Start Transients at X = -0.5 Inch (-1.27 cm) (1-1/2 Pass Cooling Circuit)	133
92.	Zr-Cu Combustor Channel Wall Temperature Engine Shutdown Transients at X = -0.5 Inch (-1.27 cm) (Split-Flow Cooling Circuit)	134
93.	Zr-Cu Combustor Channel Wall Temperature Engine Shutdown Transients at X = -0.5 Inch (-1.27 cm) (1-1/2 Pass Cooling Circuit)	135
94.	Task II - Off-Design Life Evaluation	138
95.	Duty Cycle Temperature Variation at Critical Location (X = -0.5 Inch or -1.27 cm) - Case No. 1	140
96.	Duty Cycle Coolant Static Pressure Variation at Critical Location (X = -0.5 Inch or -1.27 cm) - Case No. 1	141
97.	Task III - Combustion Chamber Contours	150
98.	Approximate Variation of Combustor Coolant Pressure Drop With Maximum Wall Temperature	151
99.	Approximate Variation of Maximum Wall Temperature With Number of Thermal Cycles	152
100.	70 Cycle Life Zr-Cu Combustor Channel Dimensions ($P_c = 1900$ psia or 1.31×10^7 N/m ² , $MR_{T/C} = 6.5$)	154
101.	70 Cycle Life Zr-Cu Combustor Wall Temperature Distribution ($P_c = 1900$ psia or 1.31×10^7 N/m ² , $MR_{T/C} = 6.5$)	155

102.	70 Cycle Life Zr-Cu Channel Wall Combustor/A-286 Tubular Nozzle Configuration ($P_c = 1900$ psia or 1.31×10^7 N/m ² , $MR_{T/C} = 6.5$)	157
103.	700 Cycle Life Zr-Cu Combustor Channel Dimensions ($P_c = 1900$ psia or 1.31×10^7 N/m ² , $MR_{T/C} = 6.5$)	161
104.	700 Cycle Life Zr-Cu Combustor Wall Temperature Distribution ($P_c = 1900$ psia or 1.31×10^7 N/m ² , $MR_{T/C} = 6.5$)	162
105.	700 Cycle Life Zr-Cu Channel Wall Combustor/A-286 Tubular Nozzle Configuration ($P_c = 1900$ psia or 1.31×10^7 N/m ² , $MR_{T/C} = 6.5$)	163
106.	A-286 Nozzle Split-Flow Circuit (Round Tubes) Coolant Pressure Drop and Wall Temperature Variation With Number of Tubes ($P_c = 1600$ or 1.103×10^7 N/m ²), $MR_{T/C} = 6.5$	166
107.	A-286 Nozzle Split-Flow Circuit (Round Tubes) Tube Diameter and Weight Variation With Number of Tubes ($P_c = 1600$ psia or 1.103×10^7 N/m ²), $MR_{T/C} = 6.5$	167
108.	Booked A-286 Nozzle Configurations (Split-Flow Cooling Circuit)-- $P_c = 1600$ psia (1.103×10^7 N/m ²), $MR_{T/C} = 6.5$	168
109.	Nozzle Coolant Pressure Drop Influence on Maximum Wall Temperature ($P_c = 1600$ psia or 1.103×10^7 N/m ² , $MR_{T/C} = 6.5$)	169
110.	A-286 Tubular Nozzle Tube Dimensions ($P_c = 1600$ psia or 1.103×10^7 N/m ² , $MR_{T/C} = 6.5$)	170
111.	Nozzle Coolant Static Pressure Distribution ($P_c = 1600$ psia or 1.103×10^7 N/m ² , $MR_{T/C} = 6.5$)	171
112.	Nozzle Temperature Distributions ($P_c = 1600$ psia or 1.103×10^7 N/m ² , $MR_{T/C} = 6.5$)	172
113.	Combustor Coolant Pressure Drop and Liner Weight Variation With Combustor-Nozzle Joint Area Ratio ($P_c = 1600$ psia or 1.103×10^7 N/m ² , $MR_{T/C} = 6.5$, 300 Cycle Life)	174
114.	Minimum Land Width (Number of Channels) Influence on Combustor Coolant Pressure Drop ($P_c = 1600$ psia or 1.103×10^7 N/m ² , $MR_{T/C} = 6.5$, 300 Cycle Life)	175
115.	Zr-Cu Combustor Channel Dimensions ($P_c = 1600$ psia or 1.103×10^7 N/m ² , $MR_{T/C} = 6.5$, 300 Cycle Life)	177
116.	Zr-Cu Combustor Coolant Static Pressure Distribution ($P_c = 1600$ psia or 1.103×10^7 N/m ² , $MR_{T/C} = 6.5$, 300 Cycle Life)	178
117.	Zr-Cu Combustor Wall Temperature Distribution ($P_c = 1600$ psia or 1.103×10^7 N/m ² , $MR_{T/C} = 6.5$, 300 Cycle Life)	179
118.	1600 psia (1.103×10^7 N/m ²) Chamber Pressure Zr-Cu Channel Wall Combustor/A-286 Tubular Nozzle Configuration (Split-Flow Cooling Circuit)	181
119.	A-286 Nozzle Tube Dimensions ($P_c = 2100$ psia or 1.448×10^7 N/m ² , $MR_{T/C} = 6.5$)	183
120.	Nozzle Coolant Static Pressure Distribution ($P_c = 2100$ psia or 1.448×10^7 N/m ² , $MR_{T/C} = 6.5$)	184
121.	A-286 Nozzle Temperature Distributions ($P_c = 2100$ psia or 1.448×10^7 N/m ² , $MR_{T/C} = 6.5$)	185
122.	Combustor Coolant Pressure Drop and Liner Weight Variation With Combustor-Nozzle Joint Area Ratio ($P_c = 2100$ psia or 1.448×10^7 N/m ² , $MR_{T/C} = 6.5$, 300 Cycle Life)	186

123.	Zr-Cu Combustor Channel Dimensions ($P_C = 2100$ psia or 1.448×10^7 N/m ² , $MR_{T/C} = 6.5$, 300 Cycle Life)	188
124.	Zr-Cu Combustor Coolant Static Pressure Distribution ($P_C = 2100$ psia or 1.448×10^7 N/m ² , $MR_{T/C} = 6.5$, 300 Cycle Life)	189
125.	Zr-Cu Combustor Wall Temperature Distribution ($P_C = 2100$ psia or 1.448×10^7 N/m ² , $MR_{T/C} = 6.5$, 300 Cycle Life)	190
126.	2100 psia (1.448×10^7 N/m ²) Chamber Pressure Zr-Cu Channel Wall Combustor/A-286 Tubular Nozzle Configuration (Split-Flow Cooling Circuit)	191
127.	NARloy-Z Thermal Fatigue Life	198
128.	Zirconium-Copper Thermal Fatigue Life	199
129.	NARloy-Z Stress Rupture	200
130.	Zirconium-Copper Stress Rupture	201
131.	NARloy-Z Yield and Ultimate Strengths	204
132.	Zirconium-Copper Yield and Ultimate Strength	205
133.	Thick Wall Tube Hoop Stress Factors	207

TABLES

I.	20K Pounds (8.896×10^4 N) Thrust Engine Parameters	9
II.	Combustion Gas Properties	17
III.	Selected Tubular Configurations	41
IV.	A-286 Nozzle (1-1/2 Pass Cooling Circuit) Comparison	50
V.	Comparison of Selected 1-1/2 Pass Cooling Circuit Channel Wall Combustors	68
VI.	Selected A-286 Tubular Nozzle/Channel Wall Combustor Configuration (1-1/2 Pass Cooling Circuit)	69
VII.	Comparison of Selected Split-Flow Cooling Circuit Channel Wall Combustors	95
VIII.	Selected A-286 Tubular Nozzle/Channel Wall Combustor Configurations (Split-Flow Cooling Circuit)	96
IX.	Coolant Circuit Overall Comparisons (NARloy-Z Configurations)	103
X.	Coolant Circuit Overall Comparisons (Zr-Cu Configurations)	104
XI.	NARloy-Z Channel Wall and Tubular Wall Finite Element Stress Analysis Results	108
XII.	Zr-Cu Channel Wall Finite Element Stress Analysis Results	121
XIII.	Coolant Circuit Comparison (Zr-Cu Channel Wall Combustor/A-286 Tubular Nozzle)	124
XIV.	Pertinent Off-Design Thrust Chamber Parameters	139
XV.	Off-Design Life Evaluation - Heat Transfer Summary	142
XVI.	Off-Design Life Analysis Summary (Station X = -0.5 Inch or -1.27 cm)	143
XVII.	Off-Design Life Analysis Results (Station X = -0.5 Inch or -1.27 cm)	144
XVIII.	Task III: Design Perturbations	148
XIX.	Design Perturbation Thrust Chamber Parameters	149
XX.	Low Cycle Life Thrust Chamber Stress/Cycle Life Results	153
XXI.	High Cycle Life Thrust Chamber Stress/Cycle Life Results	160
XXII.	Cycle Life Perturbation Summary	165
XXIII.	1600 psia (1.103×10^7 N/m ²) Chamber Pressure Thrust Chamber Stress/Cycle Life Results	176
XXIV.	2100 psia (1.448×10^7 N/m ²) Chamber Pressure Thrust Chamber Stress/Cycle Life Results	187
XXV.	Chamber Pressure Perturbation Summary	194

SUMMARY

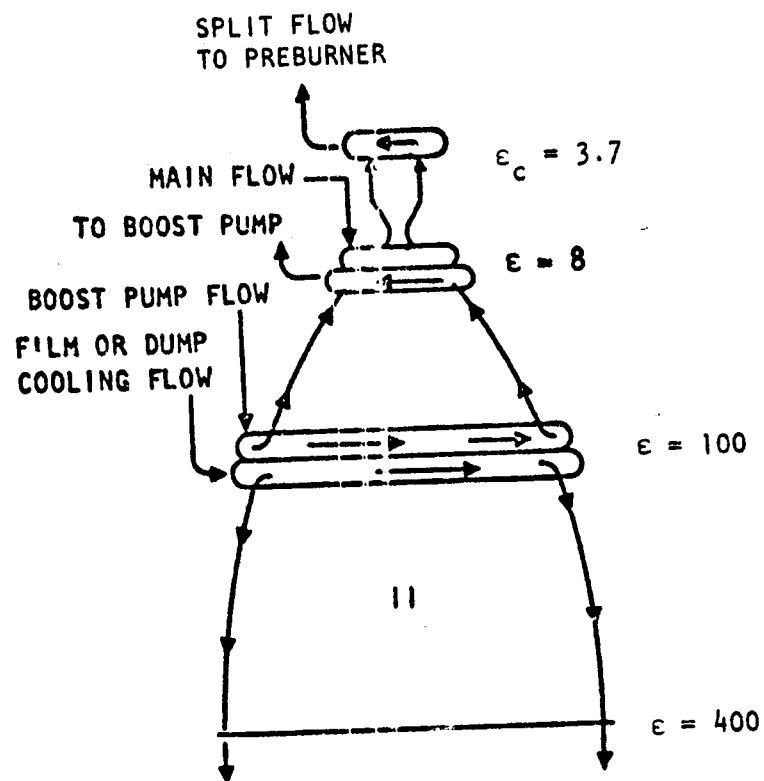
The nominal 1900-psia (1.31×10^7 N/m²) chamber pressure, 300-cycle life thrust chamber was a Zr-Cu channel wall combustor with an A-286 tubular wall nozzle attached at an area ratio of 8-to-1. The thrust chamber was cooled using a split-flow circuit (Fig. 1) in which the available coolant flow was divided between the combustor and nozzle, and the cooling was performed in a parallel uppass circuit. This configuration was selected after a detailed evaluation of an all tubular (Zr-Cu or NARloy-Z) wall thrust chamber and a channel wall combustor/A-286 tubular nozzle configuration with a 1-1/2 pass cooling circuit. The split-flow configuration was selected since it represented the more critical design from the standpoint of minimum channel dimensions. The cycle life capability of the selected thrust chamber configuration was evaluated for three different duty cycle operations (Task II) that included tank head idle, full and intermediate thrust levels, and off-design mixture ratios. The duty cycles analyzed only resulted in minor changes in cycle life. Also, the influence of the design cycle life and the design chamber pressure on the thrust chamber design was analyzed in Task III. Increased cycle life resulted in a substantial increase in coolant pressure drop because of the required lower gas-side wall temperatures. For Zr-Cu both the low and high cycle life thrust chambers were limited because of the basic structural requirements. For the 1600-psia (1.103×10^7 N/m²) to 2100 psia (1.448×10^7 N/m²) chamber pressures investigated, coolant pressure drop was approximately proportional to chamber pressure and the combined combustor liner and nozzle tube weight decreased with increase in chamber pressure. A number of improvements and modifications were made to the regenerative cooling design/analysis computer program during this contract.

INTRODUCTION

The thermal and cycle life characteristics of a 20,000-pound (8.896×10^4 newtons) staged combustion cycle bell thrust chamber were evaluated during a 9-month study. Only the portion of the 400-to-1 area ratio thrust chamber from the injector plane to a nozzle area ratio of 100-to-1 was evaluated for this regenerative cooled design. The remaining portion of the nozzle was assumed to be film and/or dump-cooled with a small amount of fuel flow.

The study was divided into four areas of investigation as follows:

1. Base design was selected from an evaluation of different coolant passage configurations and coolant circuits. These designs were determined for steady-state conditions. The final selection was made from two configurations that were selected for, and subjected to, a transient analysis investigation.
2. The influence on the cycle life of the selected configuration was investigated for three different duty cycles.
3. The influences of design cycle life and design chamber pressure on thrust chamber design were determined.
4. Modifications and improvements were made to the regenerative cooling design/analysis computer program.



UPPASS COMBUSTOR,
 UPPASS UPPER NOZZLE, AND DUMP,
 RADIATION, OR RADIATOR/FILM-
 COOLED LOWER NOZZLE

Figure 1. Zr-Cu Channel Wall Combustor/A-286 Tubular
 Nozzle Configuration With Split-Flow
 Cooling Circuit

CONCLUSIONS

The overall conclusions of the analysis tasks performed in this contract included:

1. The nominal 300-cycle life with the 20,000-pound (8.896×10^4 N), 1900 psia (1.31×10^7 N/m²) chamber pressure thrust chamber was easily accomplished with a coolant pressure drop equal to approximately 32 percent of chamber pressure.
2. The two candidate combustor materials, Zr-Cu and NARloy-Z, evaluated for the three configurations, required distinctly different thrust chamber designs because of differences in strength and life characteristics.
3. The NARloy-Z designs provided substantially lower coolant pressure drops and lower or equal chamber basic weights.
4. The all tubular configurations (1-1/2 pass cooling circuit) resulted in relatively high coolant pressure drops and tube weights because of the higher than one-dimensional (flat plate) gas-side wall temperature and the low strength of the copper alloys.
5. For the all tubular configurations, the Zr-Cu design was limited because of the yield safety factor and the NARloy-Z design was limited because of the creep damage fraction.
6. For the channel combustors, both the Zr-Cu and NARloy-Z designs were limited because of the fatigue damage fraction. The Zr-Cu design was limited to a maximum gas-side wall temperature, but the maximum allowable wall temperature for the NARloy-Z design could be increased through a decrease in channel width-to-wall thickness ratio (a/t).
7. For the tubular nozzle/channel wall combustor configurations, a booked tube up-pass circuit provided satisfactory cooling with low coolant pressure drops and tube weights.
8. The optimum channel width of the Zr-Cu and NARloy-Z channel wall combustors led to the small channel widths (less than 0.040-inch or 0.1016 cm).
9. The engine start and shutdown investigated did not govern the cycle life of the nominal thrust chamber design.
10. Duty cycle operations involving different thrust levels and off-design mixture ratios did not significantly alter the nominal cycle life.
11. Because of the relatively high heat fluxes involved, increasing the design cycle life requirements substantially increased the coolant pressure drop. If the design cycle life of this thrust chamber is to be significantly increased above the nominal 300 cycles, a different combustor liner material and/or a different thrust chamber design technique must be employed.

12. As the design chamber pressure of the 20,000-pound (8.896×10^4 N) thrust chamber was increased from 1600 psia (1.103×10^7 N/m²) to 2100 psia (1.448×10^7 N/m²), the coolant pressure drop percentage of chamber pressure increased from 21 to 38 percent; however, the combined combustor liner and nozzle tube weight decreased.

TASK I: BASE DESIGNS AND ANALYSIS

THRUST CHAMBER DESIGN CRITERIA

In Task I (Base Designs and Analysis), three thrust chamber configurations were designed and evaluated to meet the required nominal 300 major thermal cycles. These configurations are schematically shown in Fig. 2 and were:

1. Tubular wall configuration with a 1-1/2 pass cooling circuit.
2. Channel wall combustor/tubular nozzle configuration with a 1-1/2 pass cooling circuit.
3. Channel wall combustor/tubular nozzle configuration with a split-flow cooling circuit.

In all configurations the nozzle from an area ratio of 100 to 400 was assumed to be dump-cooled and/or film cooled and was not evaluated in this contract.

The all tubular configuration consisted of zirconium-copper (Zr-Cu) or NARloy-Z tubes to an area ratio of 100. The 1-1/2 pass cooling circuit was formed with one tube down and two tubes up to minimize coolant pressure drop. Also, to minimize coolant pressure drop, the coolant inlet and tube-splice locations were to be determined. The channel wall combustor/tubular nozzle with the 1-1/2 pass cooling circuit was basically the same as the all tubular configuration except that the nozzle tubes were A-286 and the Zr-Cu or NARloy-Z combustor was cooled with channels instead of tubes. In split-flow cooling circuit configuration, the available coolant flow was divided and the A-286 tubular nozzle and the Zr-Cu or NARloy-Z channel wall combustor were cooled in parallel. In all three configurations, the coolant inlet, tube splice, and combustor-nozzle joint locations were selected based on a compromise to achieve minimum coolant pressure drop and low thrust chamber weight.

The tubular nozzle of the channel wall combustor/tubular nozzle configurations was specified to be A-286.

The thrust chambers were designed to meet the following structural requirements:

$$\sigma \leq \frac{F_{\text{yield}}}{1.2} \quad \text{and} \quad \leq \frac{F_{\text{ultimate}}}{1.5}$$

A life cycle safety of 4.0 and typical material properties were used for the nominal 300-cycle life requirement. The simplified method of stress and life cycle evaluation used is presented in Appendix A. Finite element stress analyses were also performed for the final selected designs.

From engine system analyses performed as part of the Advanced O₂/H₂ Engine Preliminary Design Program (Contract NAS3-16751), the pertinent thrust chamber parameters shown in Table I were determined for the 1900-psia ($1.310 \times 10^7 \text{ N/m}^2$)

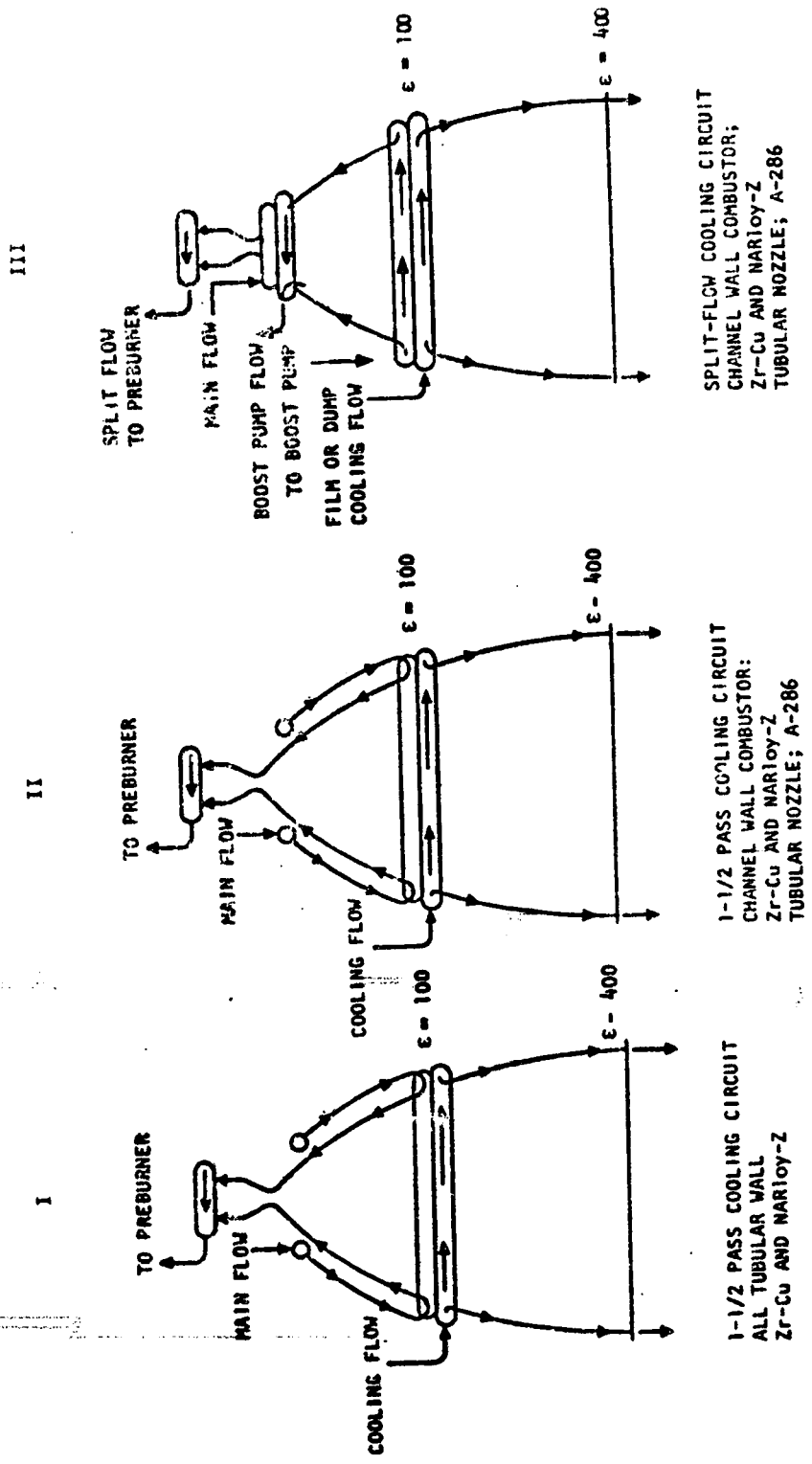


Figure 2. Task I Configurations

TABLE I. 20K POUNDS (8.896×10^4 N) THRUST ENGINE PARAMETERS

Propellant	Oxygen/Hydrogen
Vacuum thrust	20,000 pounds (8.896×10^4 newtons)
Chamber pressure	1900 psia (1.31×10^7 N/m ²)
Mixture ratio (Thrust chamber)	6.5
Nozzle area ratio	400-to-1
Nozzle percent length	80 percent
Combustion chamber contraction ratio	3.7
Combustion chamber length	10 inches (25.4 cm)
Total fuel flowrate (coolant)	6.0 lb/sec (2.72 Kg/sec)
Dump-cooled nozzle coolant flowrate ($\epsilon = 100$ to 400)	0.5 lb/sec (0.1816 Kg/sec)
Collant inlet temperature	90 R (50 K)
<u>Cooling Circuit:</u>	<u>Split-Flow</u>
Available regenerative coolant flowrates	1-1/2 Pass 5.6 lb/sec (2.54 Kg/sec)
Coolant jacket outlet pressures	3800 psia 7×10^7 N/m ² -- Combustor (2.62×10^7 N/m ²) (2.48×10^7 N/m ²) 3.808 lb/sec -- Combustor (1.728 Kg/sec) 1.792 lb/sec -- Nozzle (0.814 Kg/sec) 3600 psia 7×10^7 N/m ² -- Combustor (2.48×10^7 N/m ²) 4200 psia -- Nozzle (2.895×10^7 N/m ²)

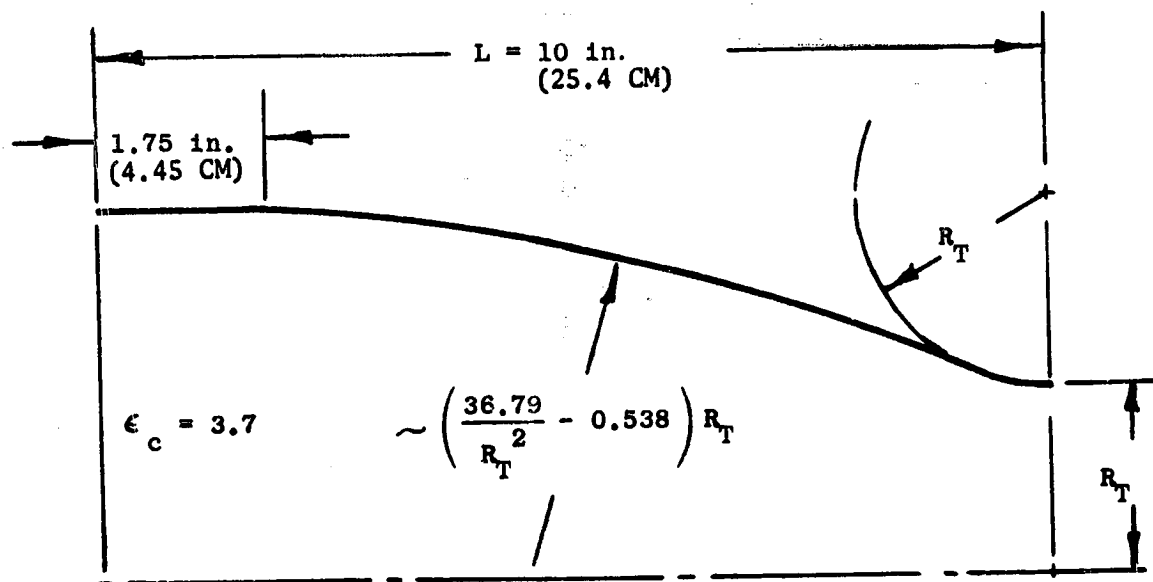
design chamber pressure. The dump cooled and/or film coolant flowrate was assumed to be 0.4 lb/sec (0.1816 kg/sec). A combustion chamber contour of the type suggested by NASA-LeRC (Fig. 3) was evaluated. Using the computed throat radius of 1.29-inches (3.275 cm), the resulting thrust chamber contour is shown in Fig. 4 and 5. The 3.7-to-1 contraction ratio would provide a reasonable heat input and reduce the tendency for boundary layer separation that can induce high peak heat fluxes. An initial mixing and combustion zone is provided by the 1.75-inch (4.44 cm) cylindrical section. The large radius contour allows early boundary layer attachment (tendency toward low peak heat flux), minimum tendency for boundary layer separation, and a low heat input. The small upstream radius of curvature (equal to the throat radius) minimizes the area exposed to high heat fluxes.

The RAO optimum bell nozzle contour for the 400 to 1 area ratio and 80-percent length is shown in Fig. 5. The contour was developed using the method of characteristics with a conventional $0.392 R_T$ throat radius of curvature. Chemical equilibrium oxygen/hydrogen combustion gas properties were used in determining the nozzle contour.

Combustion gas properties for the 1900 psia ($1.31 \times 10^7 \text{ N/m}^2$) chamber pressure and a thrust chamber mixture ratio of 6.5 are presented in Table II. These properties are for ambient (537 R or 298 K) hydrogen. For the design condition, the gas-side heat transfer coefficient distributions shown in Fig. 6 through 8 were determined. The combustion chamber distributions were developed analytically and through extrapolation of test data measured from a water-cooled combustion chamber of approximately the same size. As shown in Fig. 6, the peak experimental film coefficient was 35-percent and 21-percent higher than the predicted values for the boundary layer starting at 8.25-inches (20.95 cm) and 4-inches (10.17 cm) upstream of the throat, respectively. To provide a conservative thrust chamber design, the extrapolated test data distribution was used in the coolant passage designs performed. The gas-side heat transfer coefficient distribution for the 400 to 1 nozzle is shown in Fig. 7 and 8.

In the design and analysis of the Task I configurations, several assumptions were made that included:

1. Maximum coolant curvature enhancement factor = 1.4
2. Internal tube or channel roughness = 60 microinches
3. Ripple factor ($\frac{\text{Heat Input Surface Area}}{\text{Project Area}}$)
 - a. Tube ripple factor = 1.15
 - b. Channel ripple factor = 1.00
4. Coolant pressure drop included:
 - a. Two velocity head return manifold loss
 - b. One velocity head exit loss
5. Channel design limitations:
 - a. Maximum ratio of channel depth-to-channel width = 3.0
 - b. Bi-width channel
 - c. Minimum channel and land width = 0.040-inch (0.1017 cm)
 - d. Minimum hot-gas wall thickness = 0.027-inch (0.0686 cm)



NOTE: LARGE RADIUS CONTOUR IS TO
 BE TANGENT TO CYLINDRICAL
 SECTION AND UPSTREAM THROAT
 RADIUS OF CURVATURE.
 EQUATION PRESENTED FOR THE
 LARGE RADIUS RESULTS IN THE
 RADIUS IN INCHES.

Figure 3. Combustion Chamber Configuration

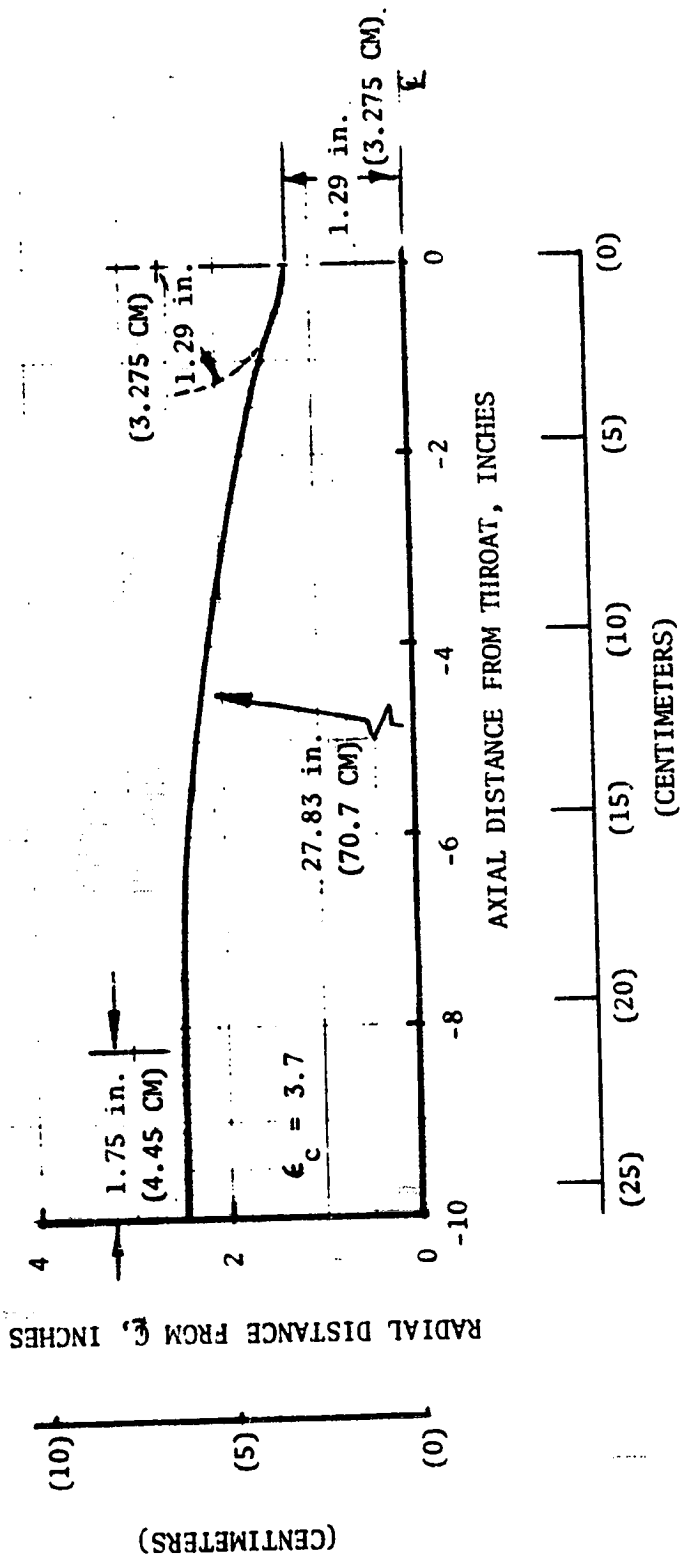


Figure 4. 20K Pounds (8.896×10^4 N) Thrust Chamber Combustion Chamber Contour

Area Ratio: 400 to 1
 Percent Length: 80
 Throat Radius of Curvature: 0.506 inch (1.284 CM)

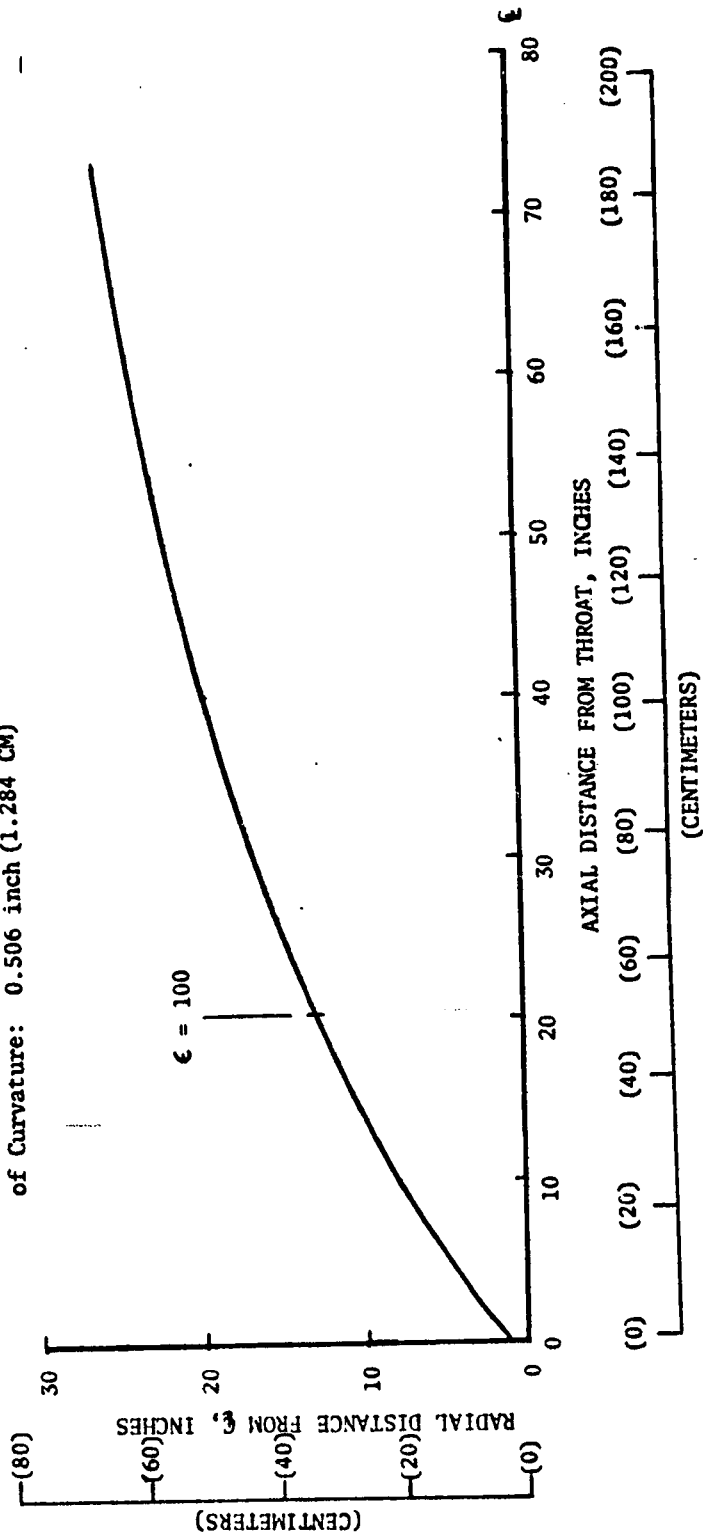


Figure 5. 20K Pounds (8.896×10^4 N) Thrust Chamber Nozzle Contour

Propellant: O_2/H_2
 P_c : 1900 psia (1.31×10^7 N/M²)
 $MR_{T/C}$: 6.5

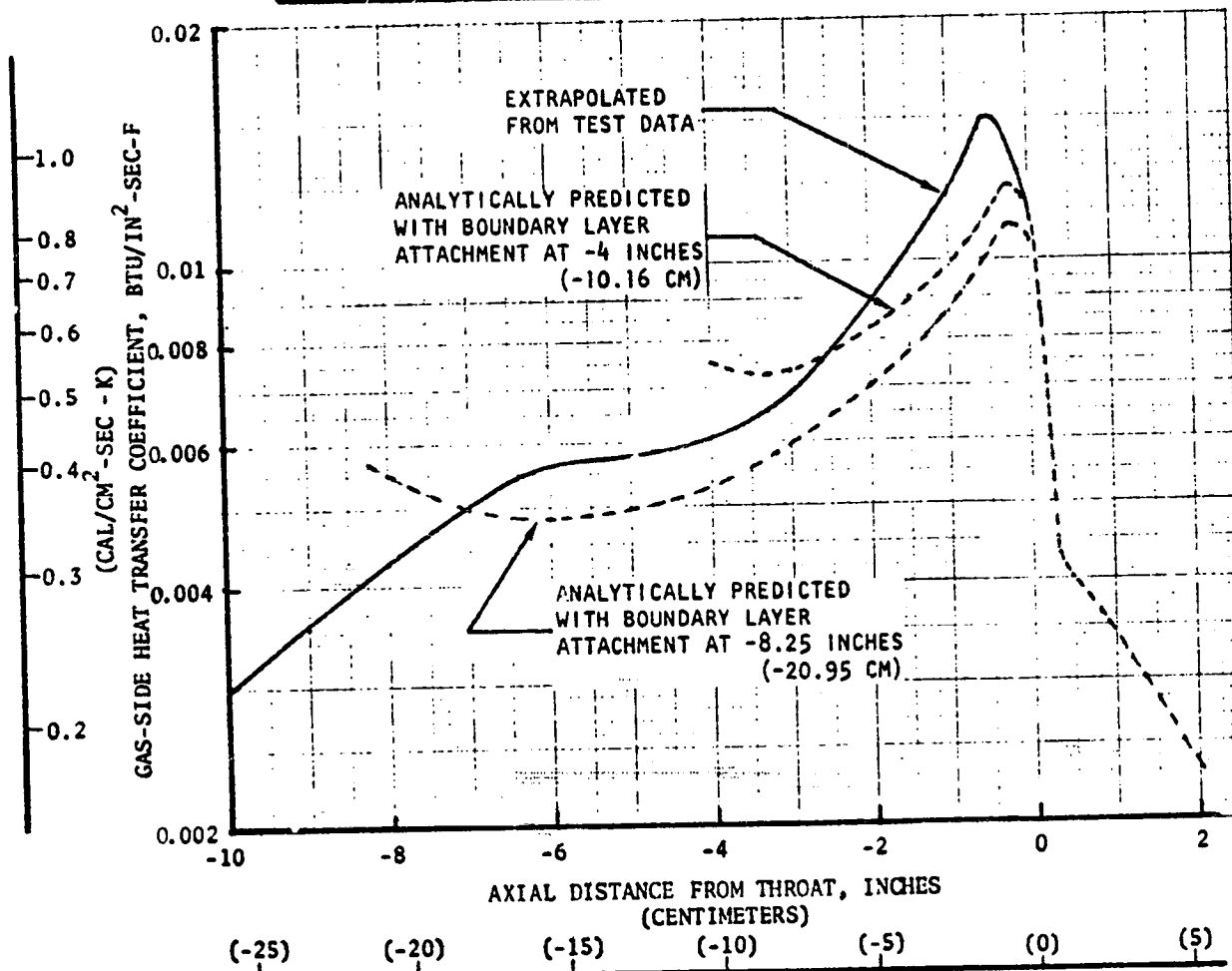


Figure 6. 20K Pounds (8.896×10^4 N) Thrust Chamber-Combustor Gas-Side Heat Transfer Coefficient Distribution

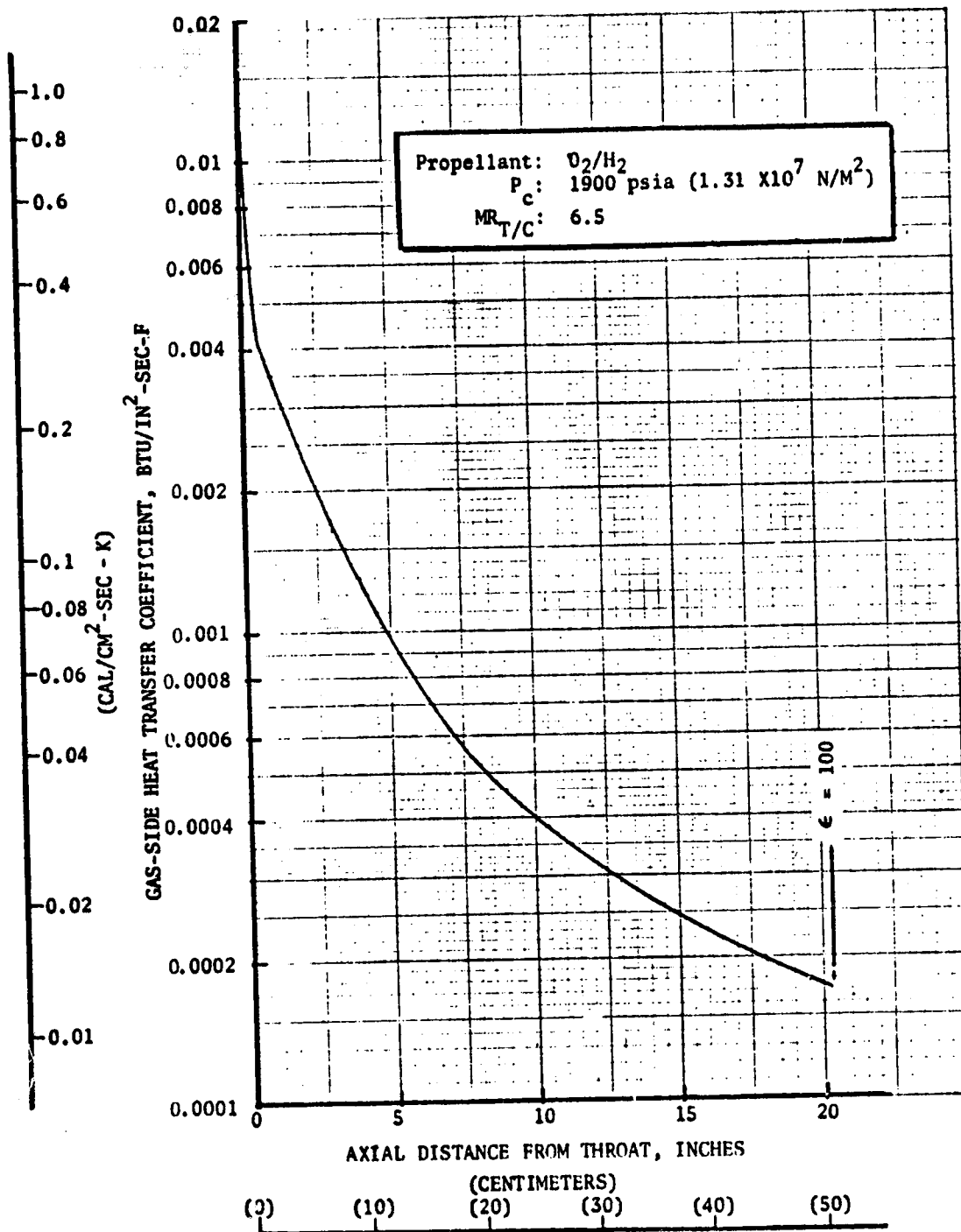


Figure 7. 20K Pounds (8.896×10^4 N) Thrust Chamber -- Nozzle Heat Transfer Coefficient Distribution ($\epsilon = 1$ to $\epsilon = 100$)

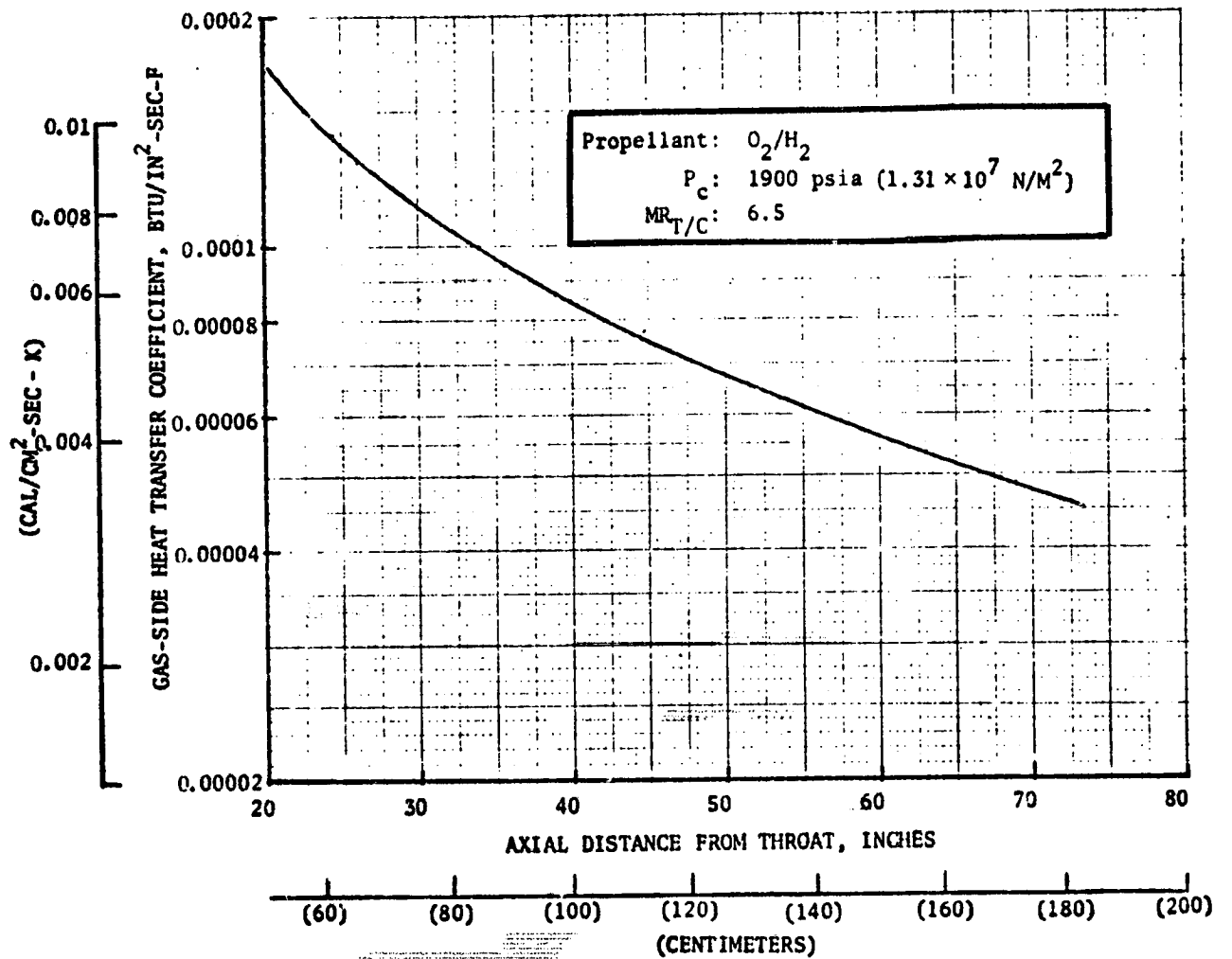


Figure 8. 20K Pounds (8.896×10^4 N) Thrust Chamber -- Nozzle
 Heat Transfer Coefficient Distribution
 ($\epsilon = 100$ to $\epsilon = 400$)

TABLE II. COMBUSTION GAS PROPERTIES

Propellant	O ₂ /H ₂ (537 R or 298 K)
Chamber Pressure	1900 psia (1.31 x 10 ⁷ N/m ²)
Mixture Ratio	6.5
Combustion Temperature	6658 R (3700 K)
Molecular Weight	14.156
Specific Heat Ratio	1.139
Specific Heat (Frozen)	0.855 Btu/lb-R (0.855 cal/gm K)
Viscosity	6.54 x 10 ⁻⁶ lb/in-sec (1.168 x 10 ⁻⁶ kg/gm sec)
Prandtl	0.8285

Ideally, from a heat transfer standpoint, a variable channel width would be desirable; however, to reduce fabrication cost, a step-width or bi-width channel was considered. The chamber "throat region" (approximately 2-inches (5.08 cm) upstream to 1-inch (2.54 cm) downstream of the throat) was assumed to have one value of channel width and the rest of the channel wall combustor had a larger value. This approach eliminates the extremely wide land width that normally results from a constant channel width design. For a specified wall temperature distribution, this type of design will reduce the coolant pressure drop considerably, compared to a constant channel width design. Because of channel machining difficulties, the maximum channel depth-to-channel width ratio was limited to 3.0; the minimum channel and land width to 0.040-inch (0.1017 cm), and the minimum hot-gas wall thickness to 0.027-inch (0.0686 cm). Minimum hot-gas wall thicknesses of 0.025-inch (0.0635 cm) and 0.023-inch (0.0584 cm) were evaluated for NARloy-Z channel wall configurations in the Task I steady-state design and analysis. After the Task I design review, the allowable minimum wall thickness was limited to 0.027-inch (0.0686 cm) to reflect current state-of-the-art fabrication techniques for channel wall bell-type thrust chambers.

TUBULAR WALL CONFIGURATIONS (1-1/2 PASS COOLING CIRCUIT)

Since the most critical stress-life thrust chamber section is normally located at the position yielding the maximum gas-side wall temperature, the coolant inlet and tube splice locations for the all tubular configuration were arbitrarily selected and fixed, and parametric heat transfer data were generated for the critical location (approximately X = -0.8-inch or -2.03 cm) by varying the number of tubes (Fig. 9 through 12). For Zr-Cu, a tube wall thickness of 0.020-inch (0.0508 cm) was used. Because its yield strength is higher, the tube wall thickness for NARloy-Z was reduced to 0.015-inch (0.0381 cm). To minimize the coolant tube weight, designs were determined using round tubes. As the number of tubes was increased (the coolant mass velocity increases), the gas-side wall temperature decreased as shown in Fig. 9 and 10. The wall temperatures presented were obtained from two-dimensional thermal analyses. For

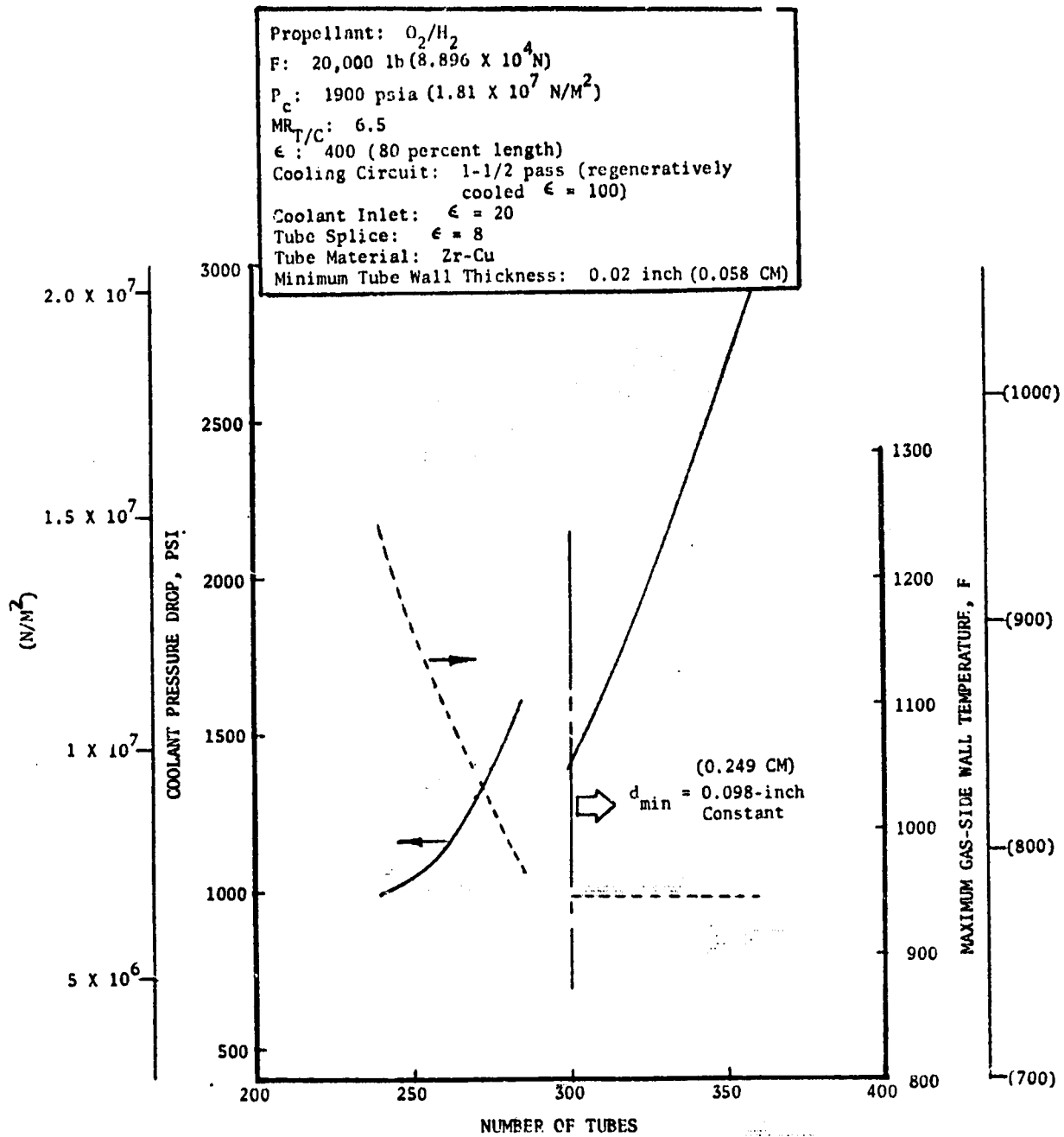


Figure 9. Zr-Cu Tubular Configuration -- Variation of Coolant Pressure Drop and Wall Temperature with Number of Tubes

Cooling Circuit: 1-1/2 pass
 (Regeneratively
 Cooled to $\epsilon = 100$)
 Coolant Inlet: $\epsilon = 20$
 Tube Splice: $\epsilon = 8$
 Tube Material: NARloy-Z
 Minimum Tube Wall Thickness: 0.015-inch (0.0381 cm)

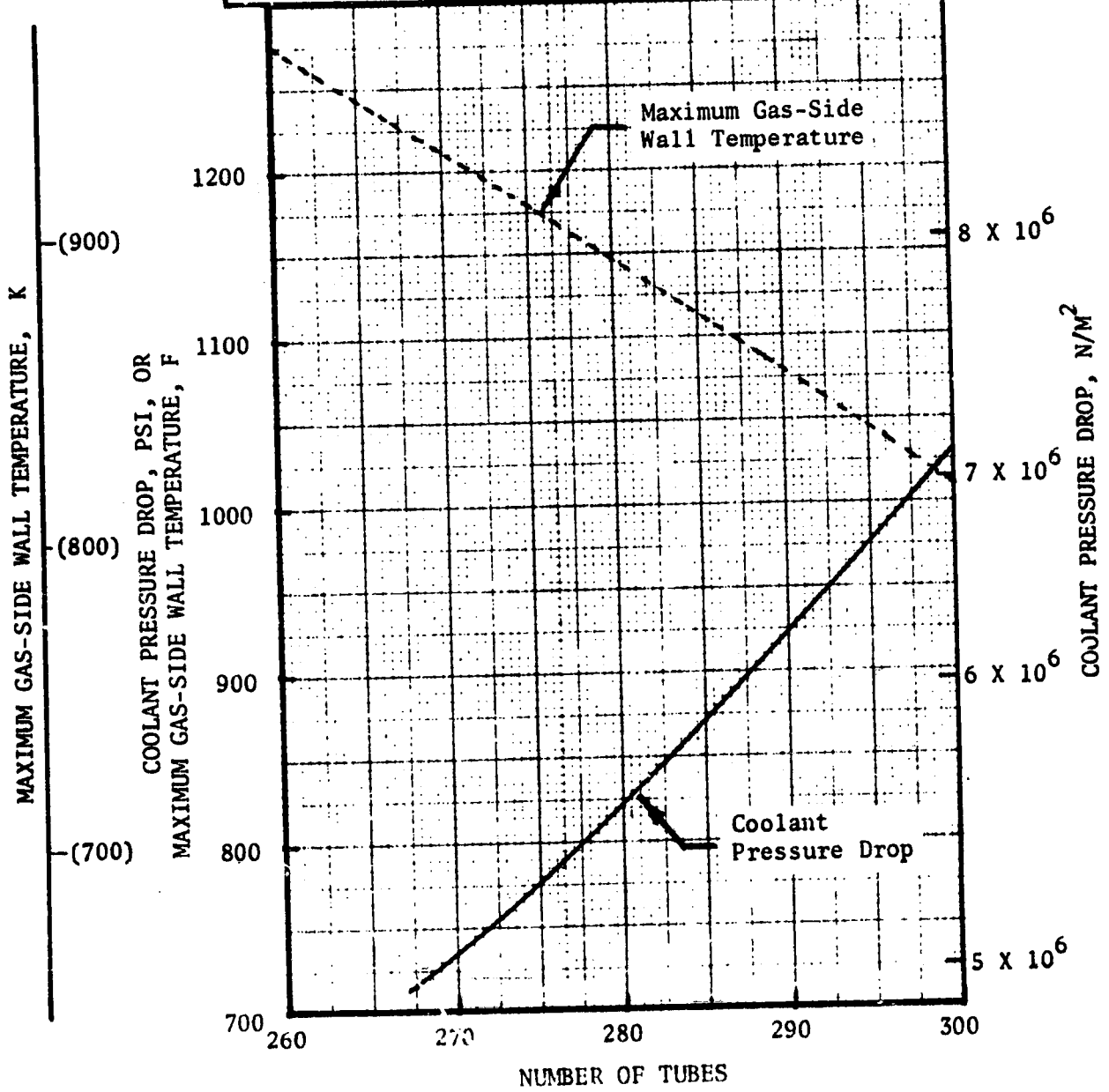


Figure 10. NARloy Tubular Configuration -- Variation of Coolant Pressure Drop and Wall Temperature With Number of Tubes

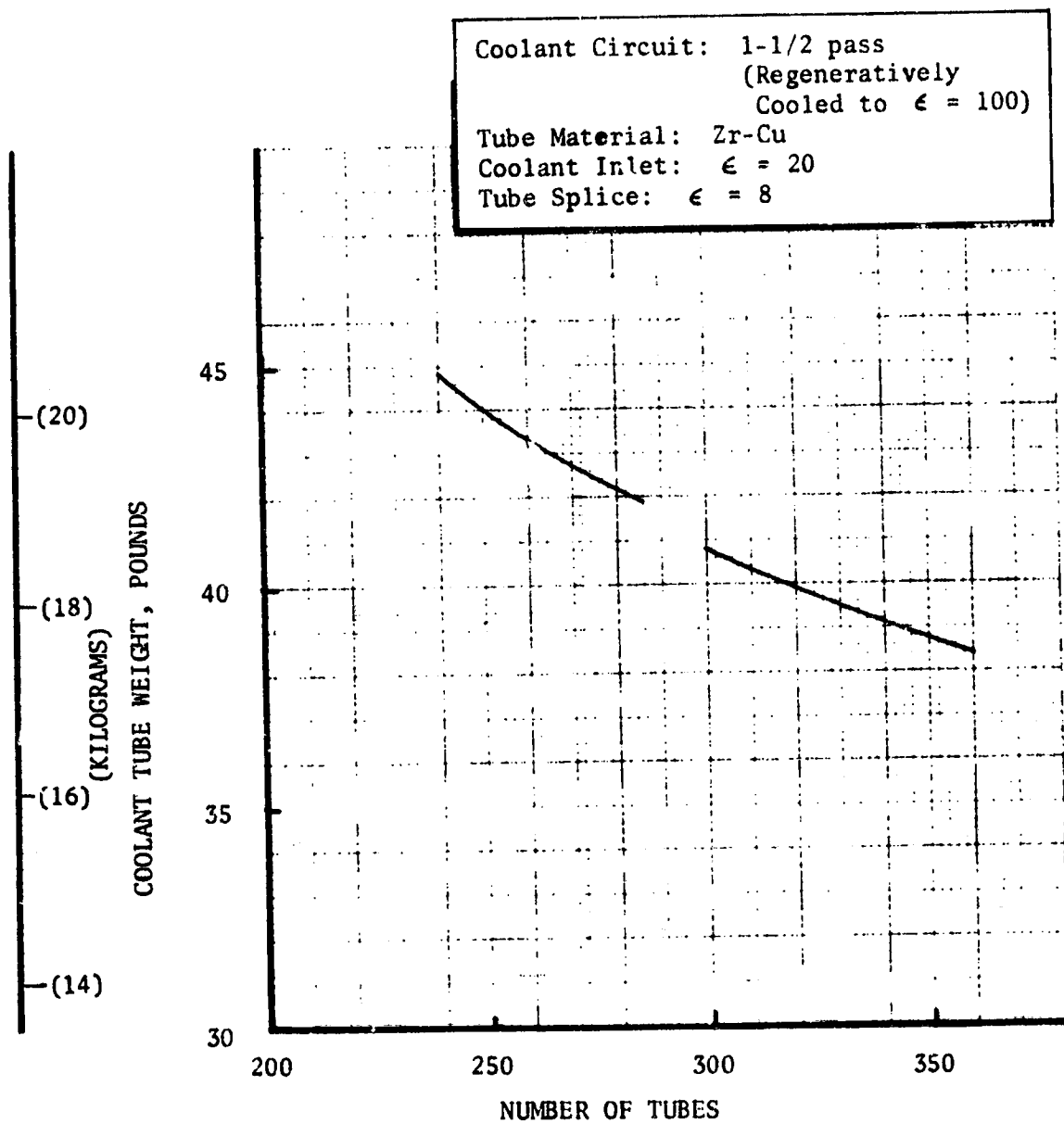


Figure 11. Coolant Tube Weight Variation With Number of Tubes -- Zr-Cu Tubular Configuration

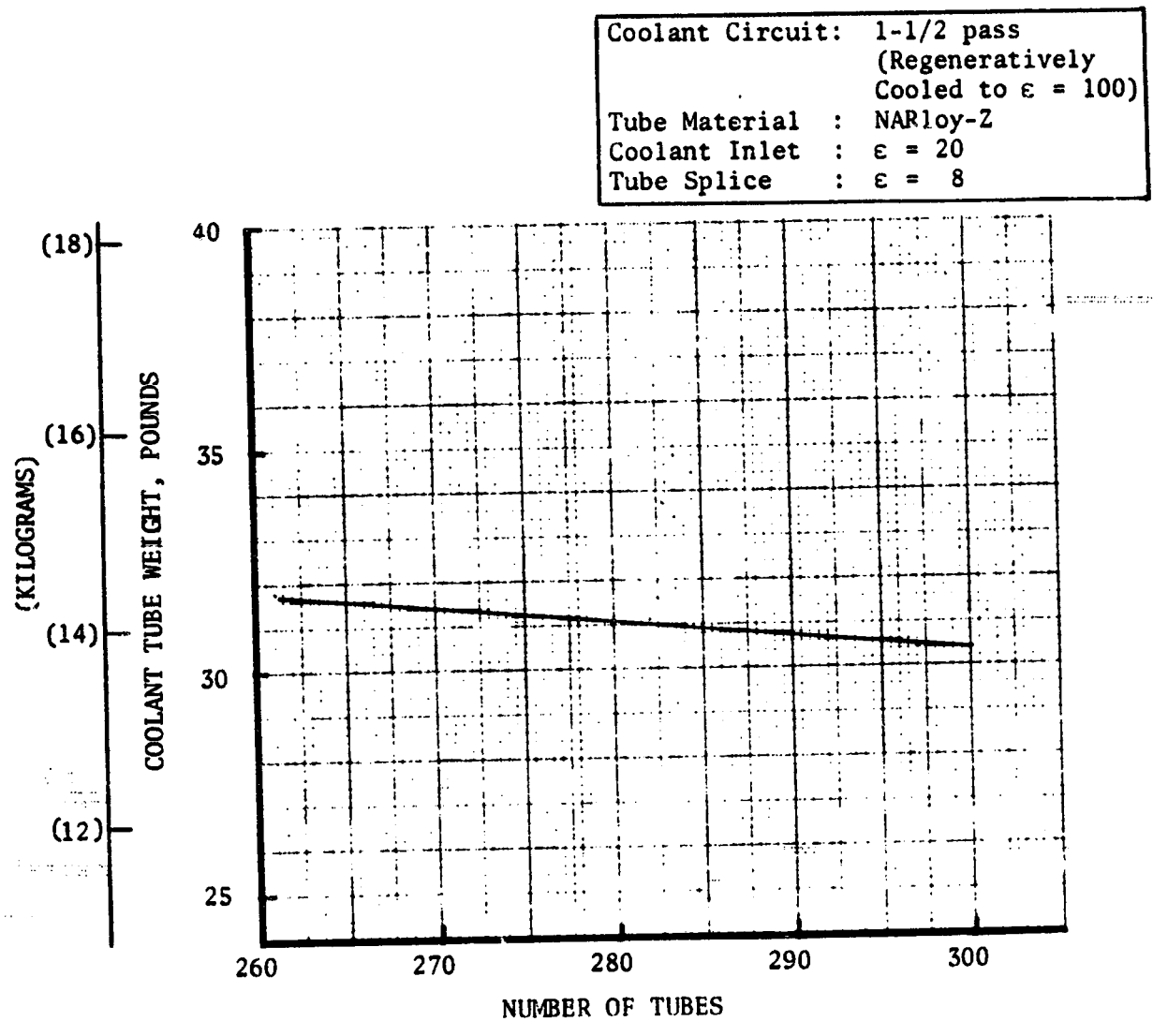


Figure 12. Coolant Tube Weight Variation with Number of Tubes -- NARloy-Z Tubular Configuration

the Zr-Cu designs with greater than 300 tubes, a slightly "booked" tube (not round) was used in the throat region to minimize the pressure drop. As the number of tubes was increased, the tube wall thickness at the higher area ratios was reduced, since the structural safety factors could be achieved with the smaller tube diameters. The result, as illustrated in Fig. 11 and 12, was a decrease in tube weight.

Using the stress and life evaluation criteria set forth in Appendix A, parametric curves of allowable pressure versus tube inside radius-to-wall thickness ratio were determined for Zr-Cu and NARloy-Z as shown in Fig. 13 and 14, respectively. From these thermal and structural data, two tubular designs were selected:

Zr-Cu	252 tubes
	Minimum tube wall thickness = 0.02-inch (0.0508 cm)
NARloy-Z:	288 tubes
	Minimum tube wall thickness = 0.015-inch (0.0381 cm)

With the 252 Zr-Cu tubes and the tube splice fixed at an area ratio of 8-to-1, the coolant inlet area ratio was varied from 20 to 100 to investigate the influences on coolant pressure drop, wall temperature, and tube weight. As shown in Fig. 15, an increase of the coolant inlet area ratio reduced the pressure drop significantly with a small change in the wall temperature just upstream of the inlet. The reduced pressure drop reflects the decreased distance traveled by the coolant as well as the decreased coolant velocity near the inlet. However, increasing the inlet area ratio resulted in an increase in coolant tube weight (Fig. 16), which was due to the increased tube wall thickness required as the tube diameter increased. Therefore, a tradeoff of coolant pressure drop and chamber weight was necessary. As shown in Fig. 15 and 16, a coolant inlet area ratio of 100-to-1 reduced the coolant pressure drop approximately 70 psi ($4.83 \times 10^5 \text{ N/m}^2$) compared to the 20-to-1 inlet area ratio at the expense of 13.5 pounds (0.611 kg) of additional tube weight. A coolant inlet area ratio of 40-to-1 reduced pressure drop by 50 psi or $3.445 \times 10^5 \text{ N/m}^2$ (71.5 percent of the total savings) and only increased tube weight by 1.5 pounds (0.68 kg); therefore, a coolant inlet area ratio of 40-to-1 was selected. In a similar manner, the tube splice area ratio of 8-to-1 was selected from the data presented in Fig. 17 and 18.

Because the thermal conductivity of Zr-Cu is high, an increase in tube wall thickness (increased coolant mass velocity) resulted in a decrease in wall temperature as shown in Fig. 19. To achieve a wall temperature less than 1000 F (812 K) in the combustion chamber, a tube wall thickness of 0.05-inch (0.127 cm) was selected. The final Zr-Cu tubular configuration is illustrated in Fig. 20. The 1-1/2 pass cooling circuit is arranged so that the coolant (hydrogen) enters at an area ratio of 40-to-1 into 84 tubes, traverses to 100-to-1 area ratio, turns around, and returns up 168 tubes. At an area ratio of 8-to-1, a 2-to-1 tube splice exists resulting in 84 tubes in the combustion chamber. The selected Zr-Cu tubular design resulted in a coolant pressure drop of 996 psi ($6.86 \times 10^6 \text{ N/m}^2$) and a coolant tube weight of 46.2 pounds (20.95 kg). The coolant static pressure and wall temperature distributions for the selected

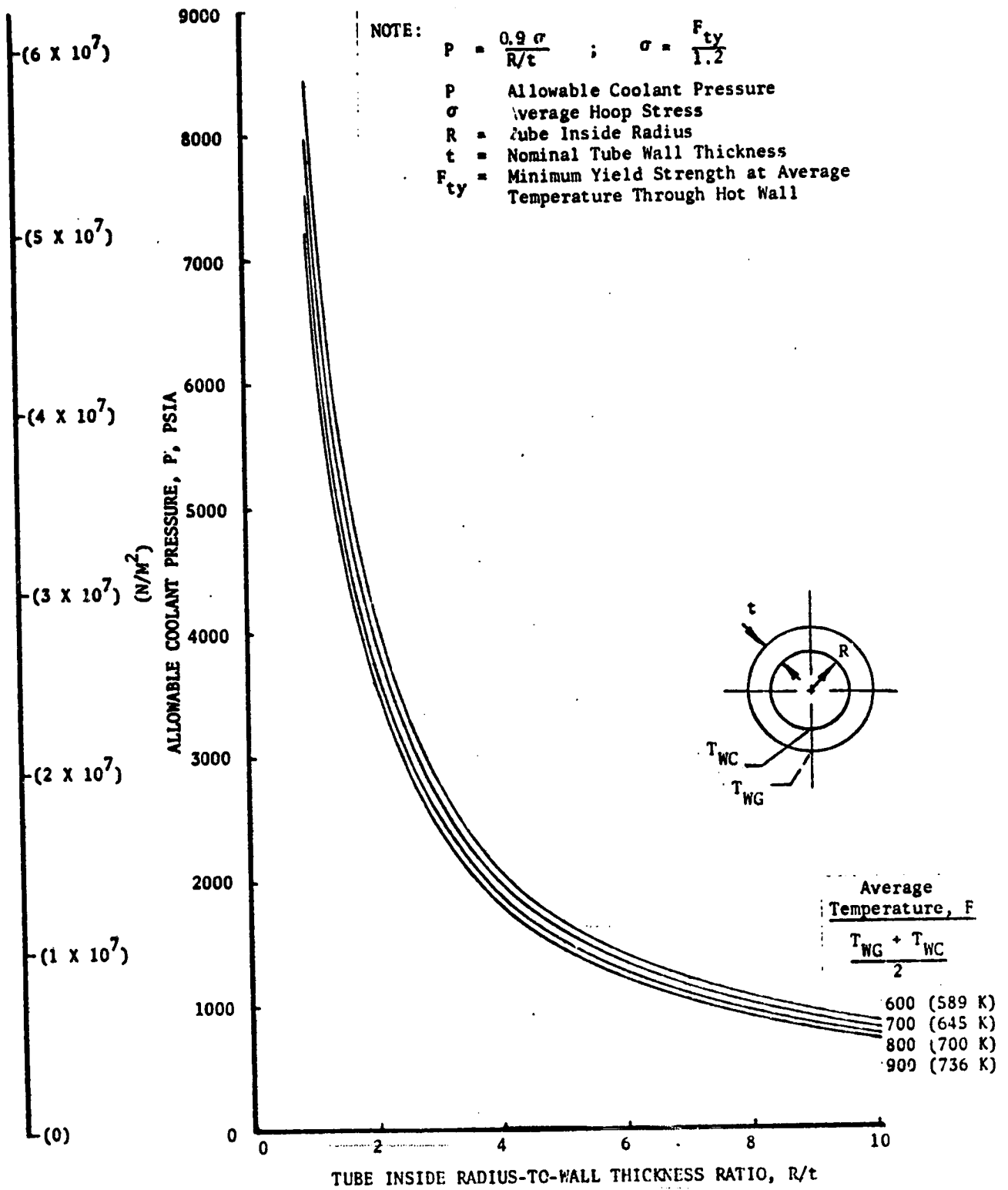


Figure 13. Tube R/t Versus Allowable Coolant Pressure for Zirconium-Copper (Basic Structural Criteria)

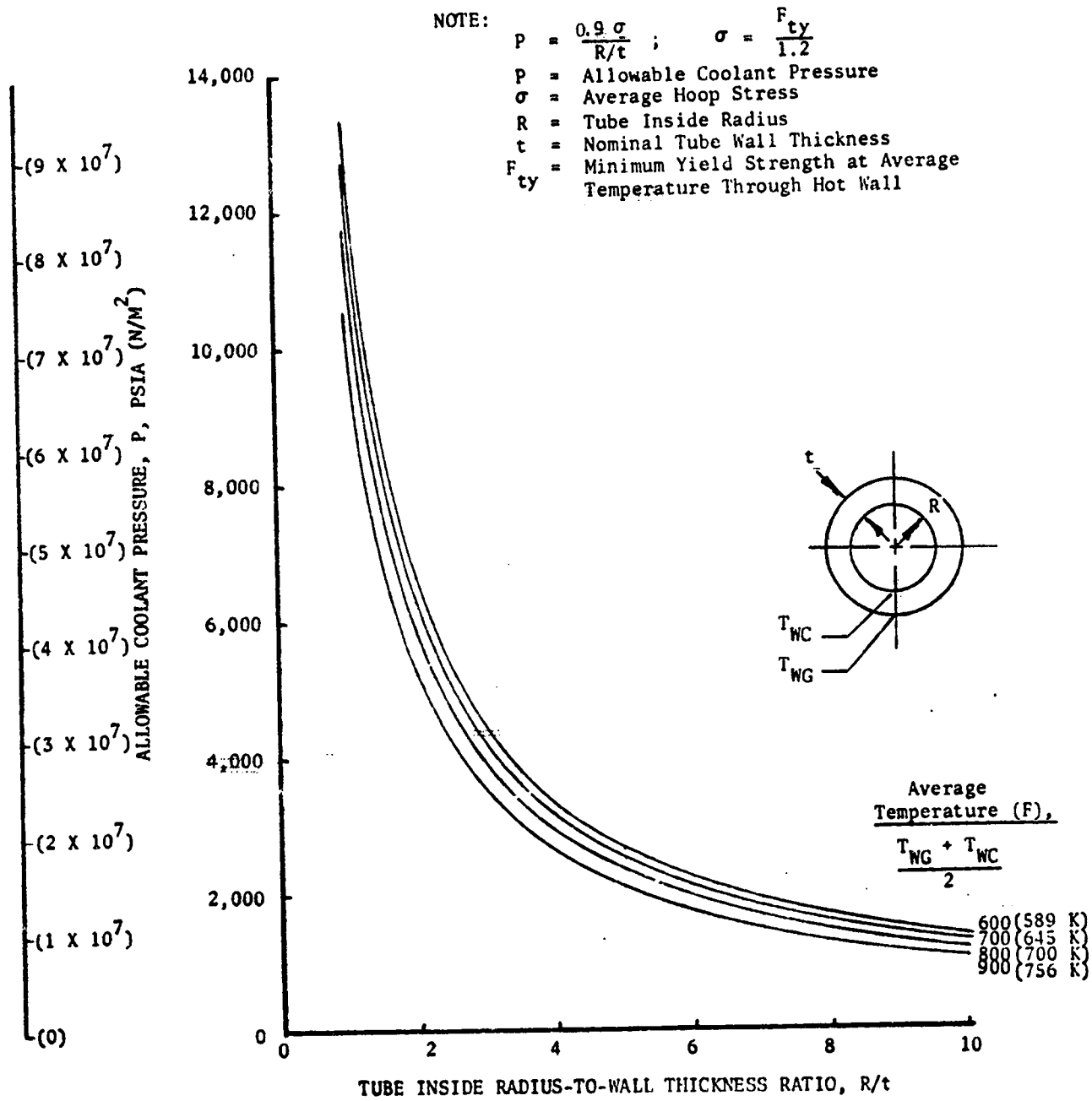


Figure 14. Tube R/t Versus Allowable Coolant Pressure for NARloy-Z (Basic Structural Criteria)

Coolant Circuit: 1-1/2 Pass (Regeneratively
 Cooled to $\epsilon = 100$)
 Tube Material: Zr-Cu
 Maximum Number of Tubes: 252
 Tube Splice: $\epsilon = 8$

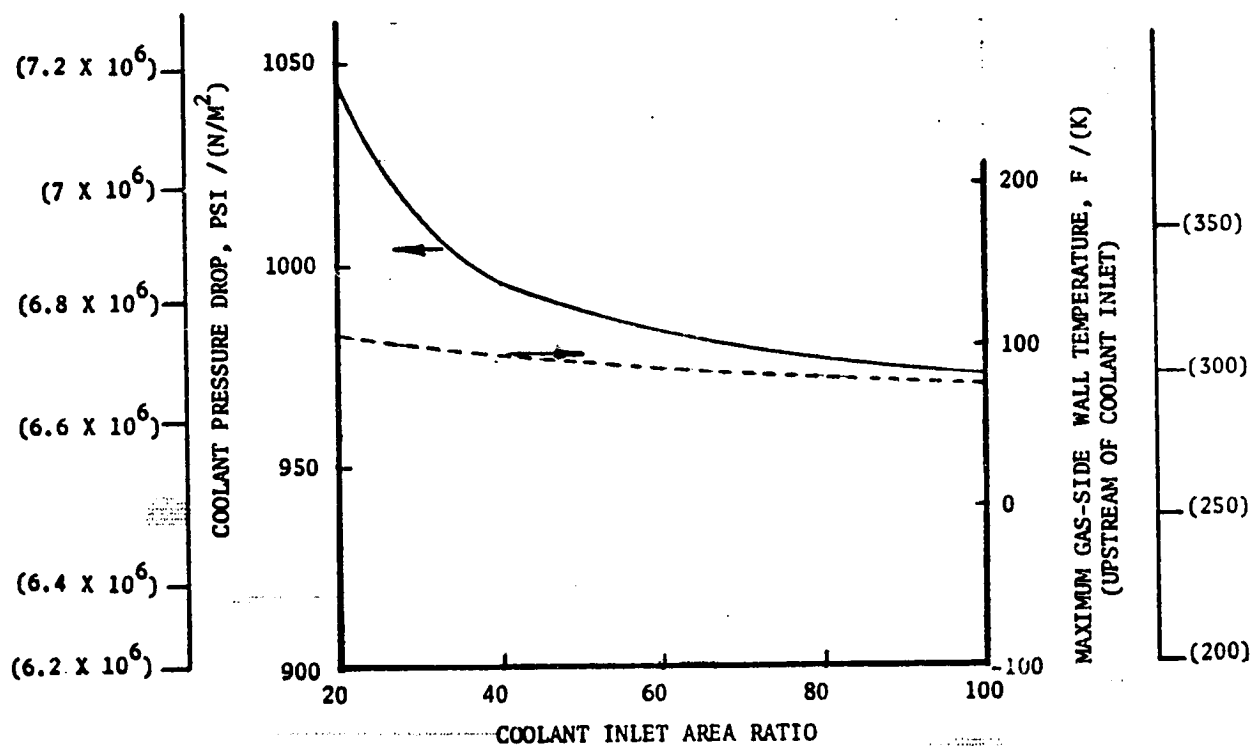


Figure 15. Variation of Coolant Pressure and Wall Temperature Just Upstream of Coolant Inlet With Coolant Inlet Area Ratio -- Zr-Cu Tubular Configuration

Coolant Circuit: 1-1/2 Pass (Regeneratively
Cooled to $\epsilon = 100$)
 Tube Material: Zr-Cu
 Maximum Number of Tubes: 252
 Tube Splice: $\epsilon = 8$

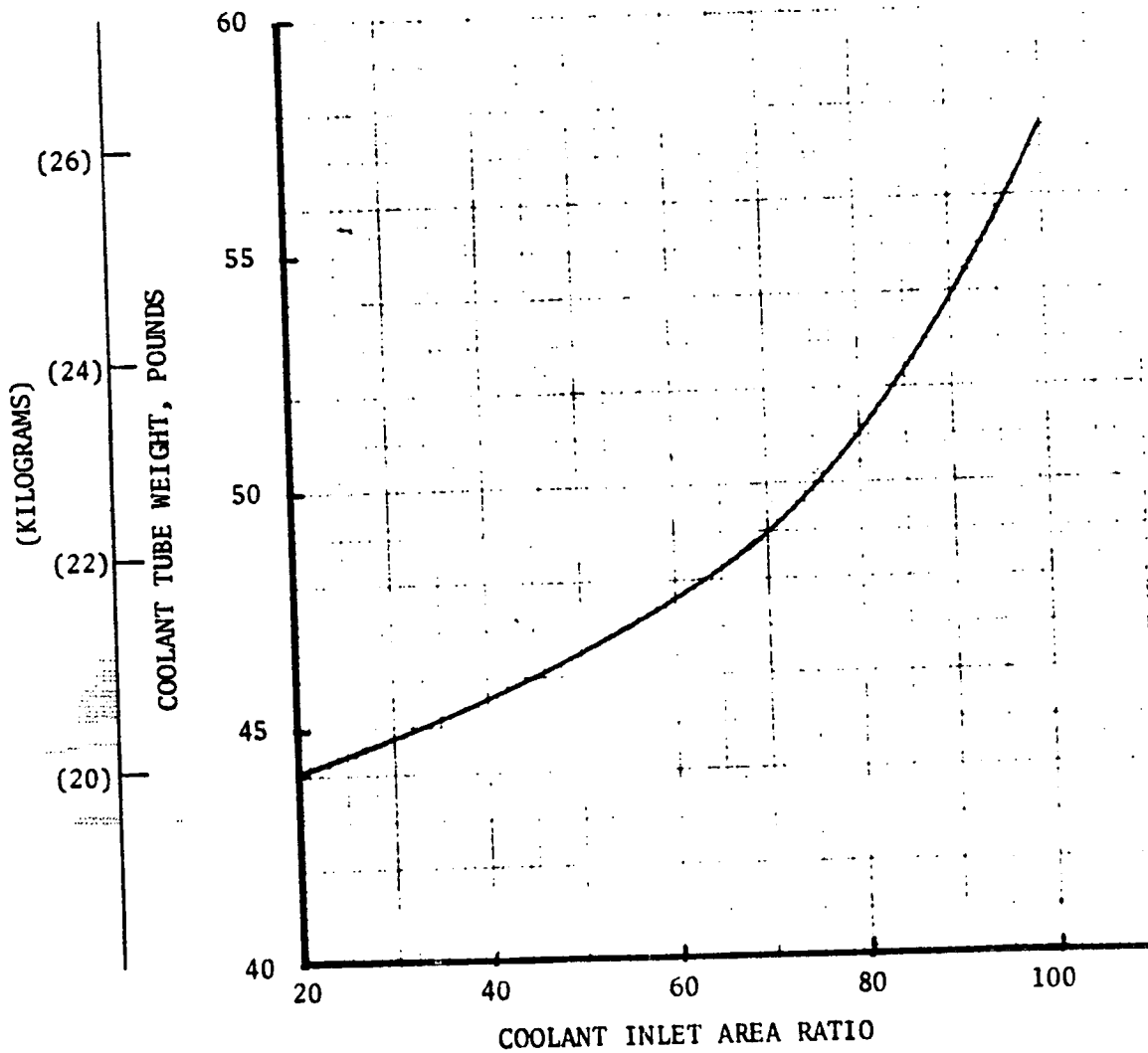


Figure 16. Coolant Tube Weight Variation With Coolant Inlet Area Ratio -- Zr-Cu Tubular Configuration

Coolant Circuit: 1-1/2 Pass (Regeneratively Cooled to $\epsilon = 100$)
 Tube Material: Zr-Cu
 Maximum Number of Tubes: 252
 Coolant Inlet Area Ratio: 40

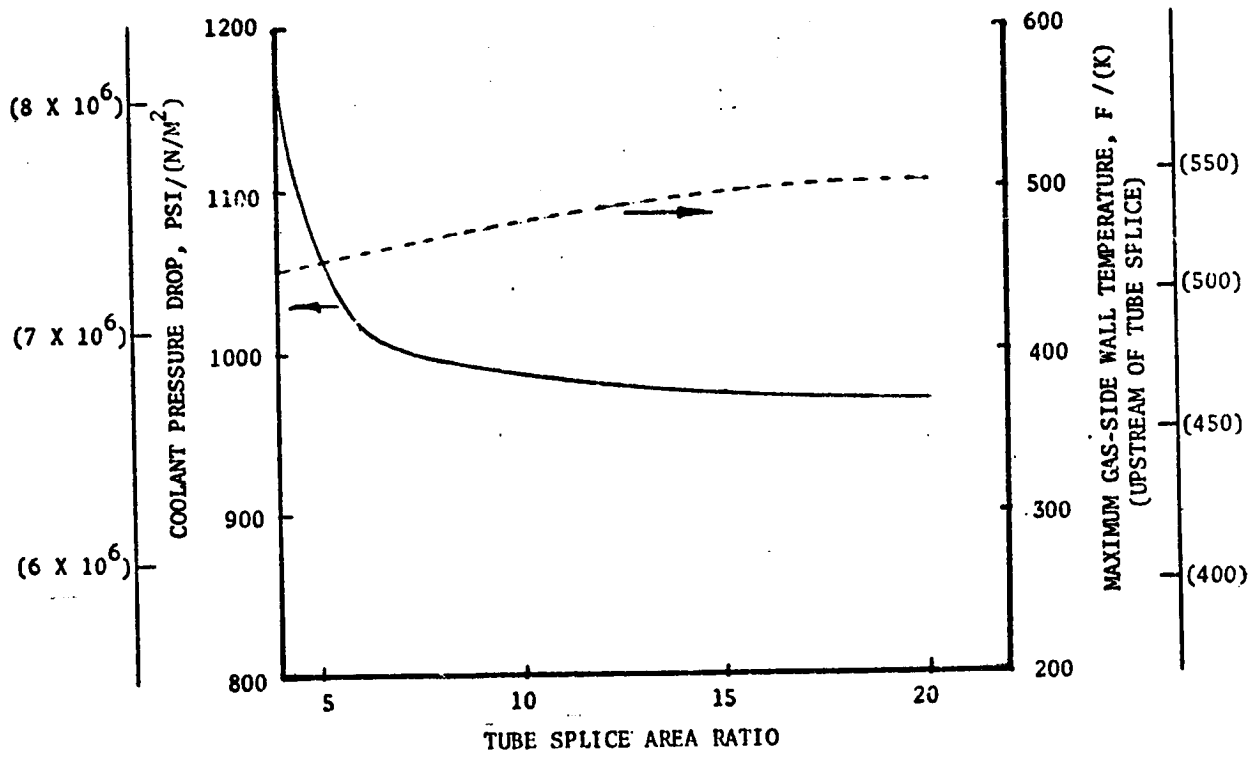


Figure 17. Variation of Coolant Pressure and Wall Temperature Just Upstream of Tube Splice With Tube Splice Area Ratio -- Zr-Cu Tubular Configuration

Coolant Circuit: 1-1/2 Pass Regeneratively
Cooled to $\epsilon = 100$)

Tube Material: Zr-Cu
Maximum Number of Tubes: 252
Coolant Inlet: $\epsilon = 40$

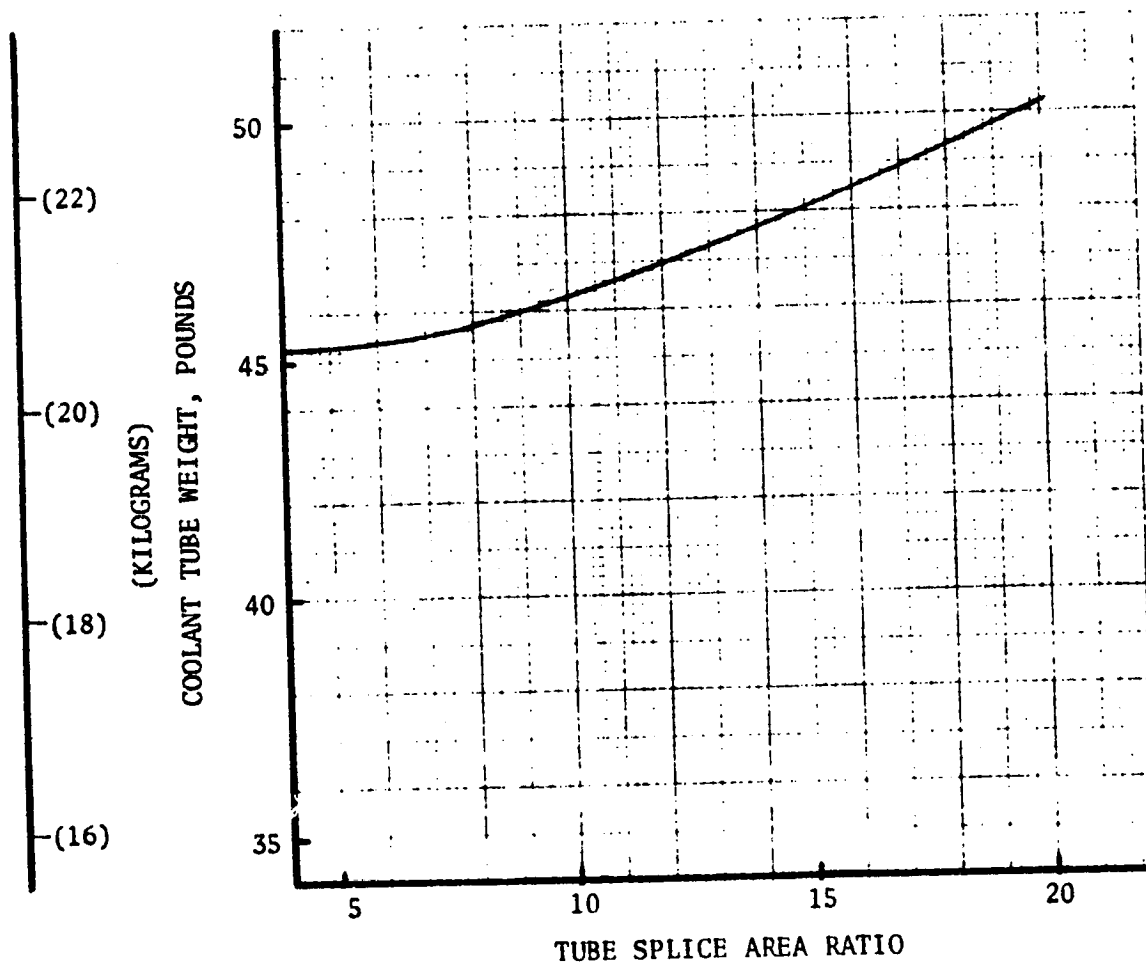


Figure 18. Coolant Tube Weight Variation With Tube Splice Area Ratio -- Zr-Cu Tubular Configuration

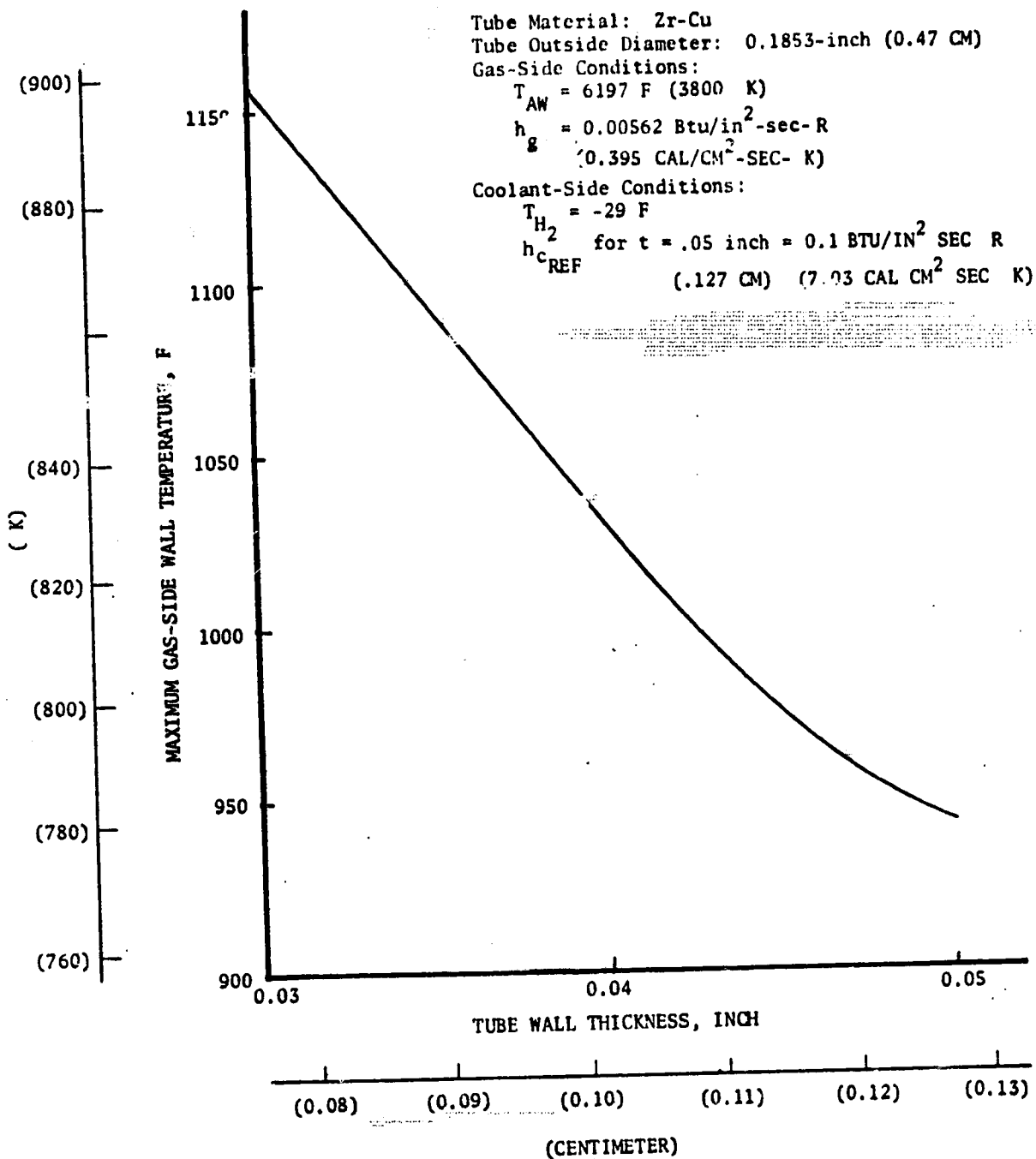


Figure 19. Wall Temperature Variation With Tube Wall Thickness (Constant Outside Diameter) -- Zr-Cu Tubular Configuration

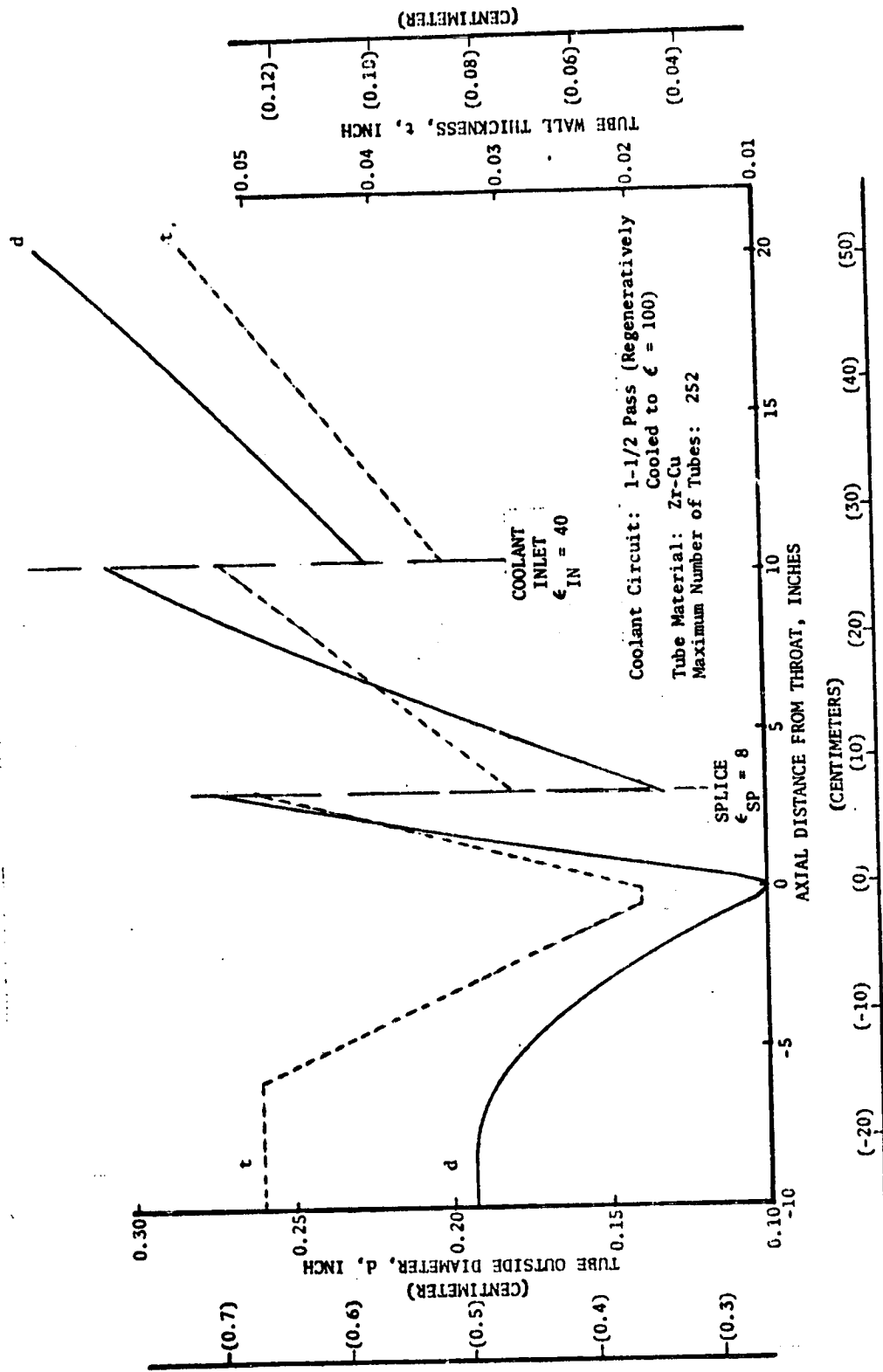


Figure 20. Selected Zr-Cu Tubular Configuration

design are presented in Fig. 21 and 22. The wall temperature distribution shown in Fig. 23 was determined using a two-dimensional tube thermal model for $X = -10.0$ inches (-25.4 cm) to $+9.566$ inches ($+24.25$ cm). For locations downstream of 10 inches (25.4 cm) from the throat, the one-dimensional values were used. The two-dimensional tube wall temperature distribution of the critical stress-life location ($X = -0.8$ -inch or 2.03 cm) is presented in Fig. 23.

From the parametric heat transfer data for the NARloy-Z tubular configuration at the critical location, structural and life analyses resulted in the data presented in Fig. 24. In all the NARloy-Z configurations evaluated, the creep damage fraction was the governing portion of the total damage fraction. The design consisting of a maximum of 288 tubes met the basic structural and life requirements; however, the yield safety factor (1.44) and the damage fraction (0.724) could be reduced and increased, respectively. This was attempted for 291 tubes through a decrease in tube wall thickness (increased r/t). As shown in Fig. 24, the yield safety factor was closer to the limit of 1.2, but the damage fraction exceeded 1.0. With this decrease in wall thickness, and increased number of tubes (approximately 297) would result in a design closer to the structural and life cycle limits. As shown in Fig. 25, the coolant mass velocity at the critical location would be approximately the same as the 288 tube design with a slight increase in r/t. However, this increase in r/t would require a lower maximum gas-side wall temperature to achieve the same creep damage fraction (Fig. 26) that, in turn, would require an increase in coolant pressure drop. Therefore, the 288-tube design was selected as the final NARloy-Z tubular configuration.

As for the Zr-Cu design, the coolant inlet and tube splice was varied independently, and the same inlet and splice area ratios were selected for the NARloy-Z tube design. The tube dimensions for the NARloy-Z tubular configuration are shown in Fig. 27. The 288 tubes become 96 tubes in the combustion chamber with a 0.015-inch (0.0381 cm) minimum tube wall thickness. The resultant coolant static pressure and wall temperature distributions are presented in Fig. 28 and 29. This selected NARloy-Z design had a coolant pressure drop of 854 psi (5.88×10^6 N/m²), a coolant tube weight of 32.2 pounds (14.6 kg), and a maximum gas-side wall temperature of 1090 F (862 K).

A summary of the Zr-Cu and the NARloy-Z tubular wall designs is presented in Table III. The NARloy-Z design resulted in a 142 psi (9.78×10^5 N/m²) lower coolant pressure drop and a 14 pounds (6.35 kg) lower tube weight. As shown in Table III, the Zr-Cu design was limited by the yield safety factor of 1.22 and not by the damage fraction of 0.40. The creep portion of the total damage fraction limited the NARloy-Z design.

The structural nozzle hatband spacing was determined using a minimum hatband cross-sectional area of 0.00192 in² (0.01238 cm²). For the design criteria of 1.2 safety factor on yield strength and 1.5 on ultimate strength, five hatbands were required. As shown in the design drawings (Fig. 30 and 31), the inlet and return manifolds serve as two of the bands. The other hatbands are flat INCO 718 bands. To achieve a band that would be reasonable from a fabrication standpoint, the cross-sectional area was increased to 0.015 in² (0.0967 cm²). The INCO 718 combustor jacket for the tubular configurations started at an area

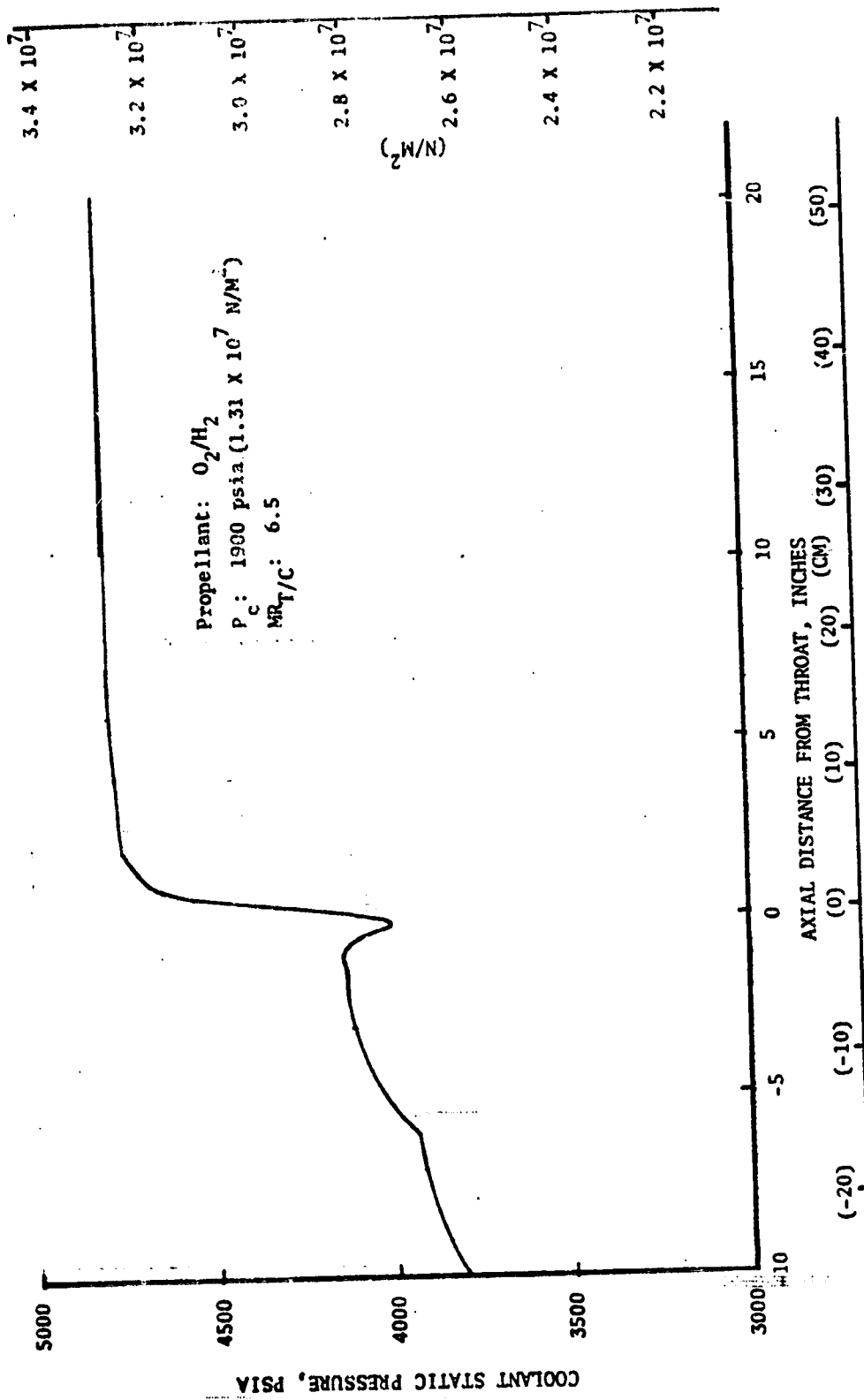


Figure 21. Coolant Static Pressure Distribution for the Selected Zr-Cu Tubular Configuration

Coolant Circuit: 1-1/2 Pass (Regeneratively Cooled to $\epsilon = 100$)
 Tube Material: Zr-Cu
 Maximum Number of Tubes: 252

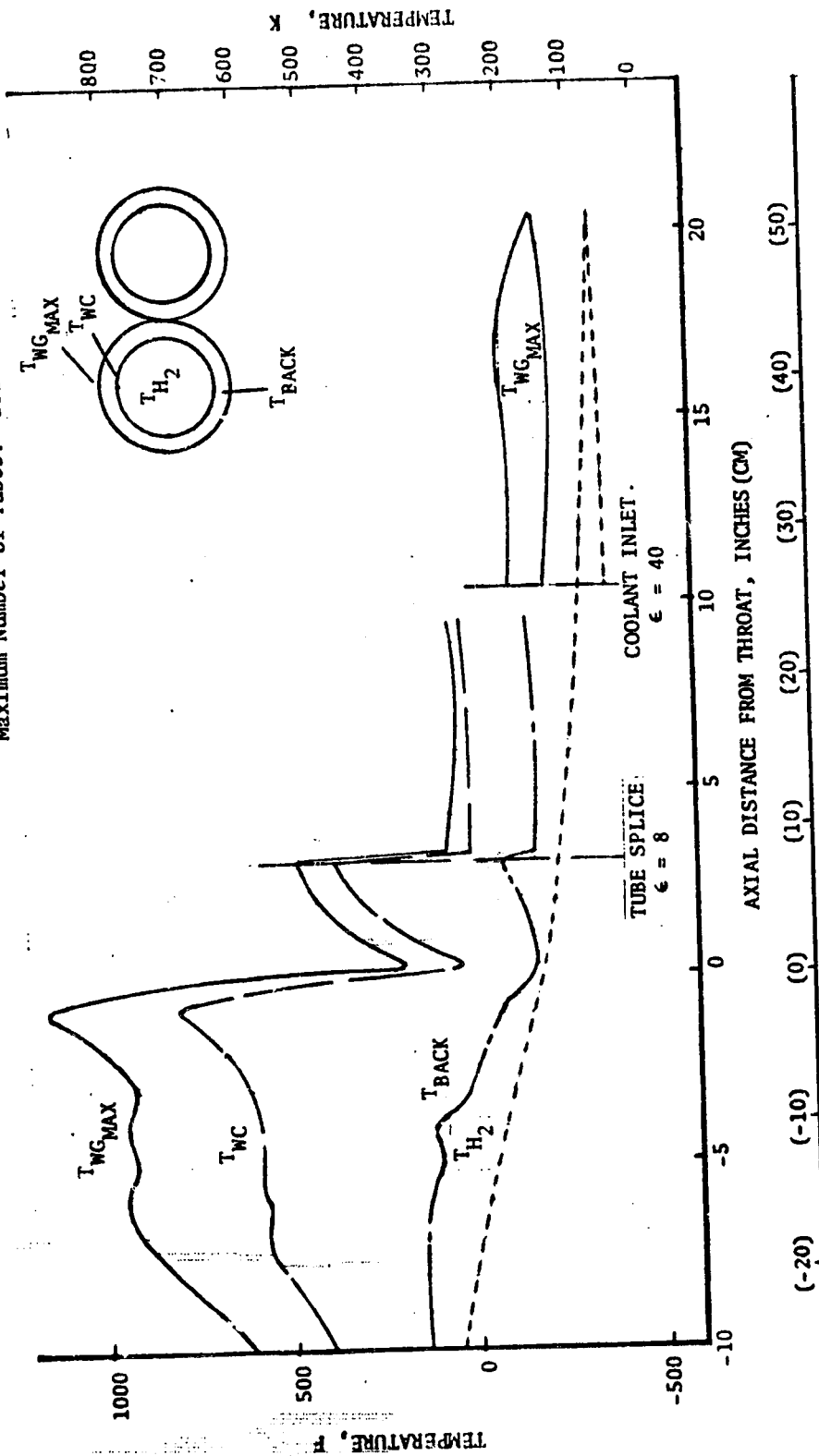
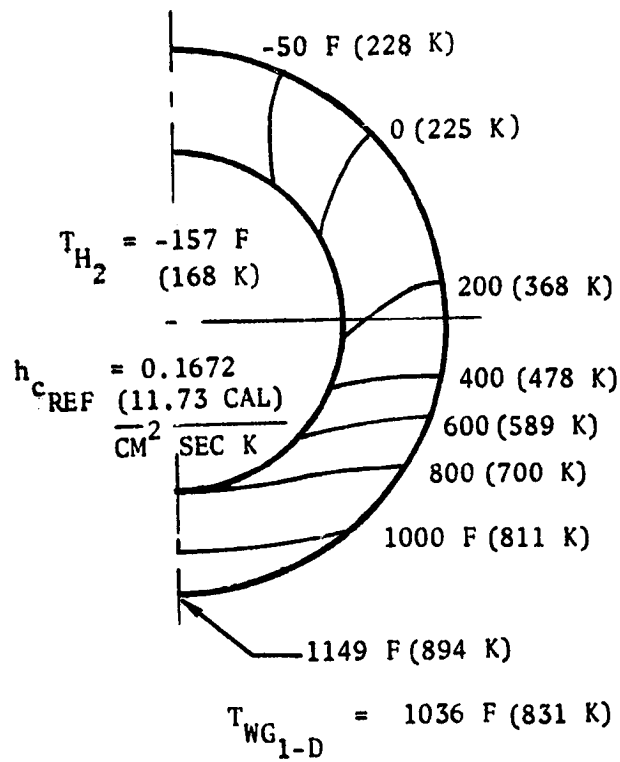


Figure 22. Temperature Distributions for the Selected Zr-Cu Tubular Configuration

Tube Material: Zr-Cu
 Tube Outside Diameter: 0.1134-inch (0.288-CM)
 Tube Wall Thickness: 0.0217-inch (0.0552-CM)



$T_{AW} = 6190 \text{ F (3695 K)}$
 $h_g = 0.0133 \text{ Etu/in}^2\text{-sec-F}$
 $(0.934 \text{ CAL/CM}^2\text{-SEC-K})$

Figure 23. Tube Wall Temperature Distribution
 (X = -0.8 Inch or -2.03 CM)

Coolant Circuit: 1-1/2 Pass (Regeneratively Cooled to $\epsilon = 100$)
 Tube Material: NARloy-Z
 Coolant Inlet: $\epsilon = 20$
 Tube Splice: $\epsilon = 8$

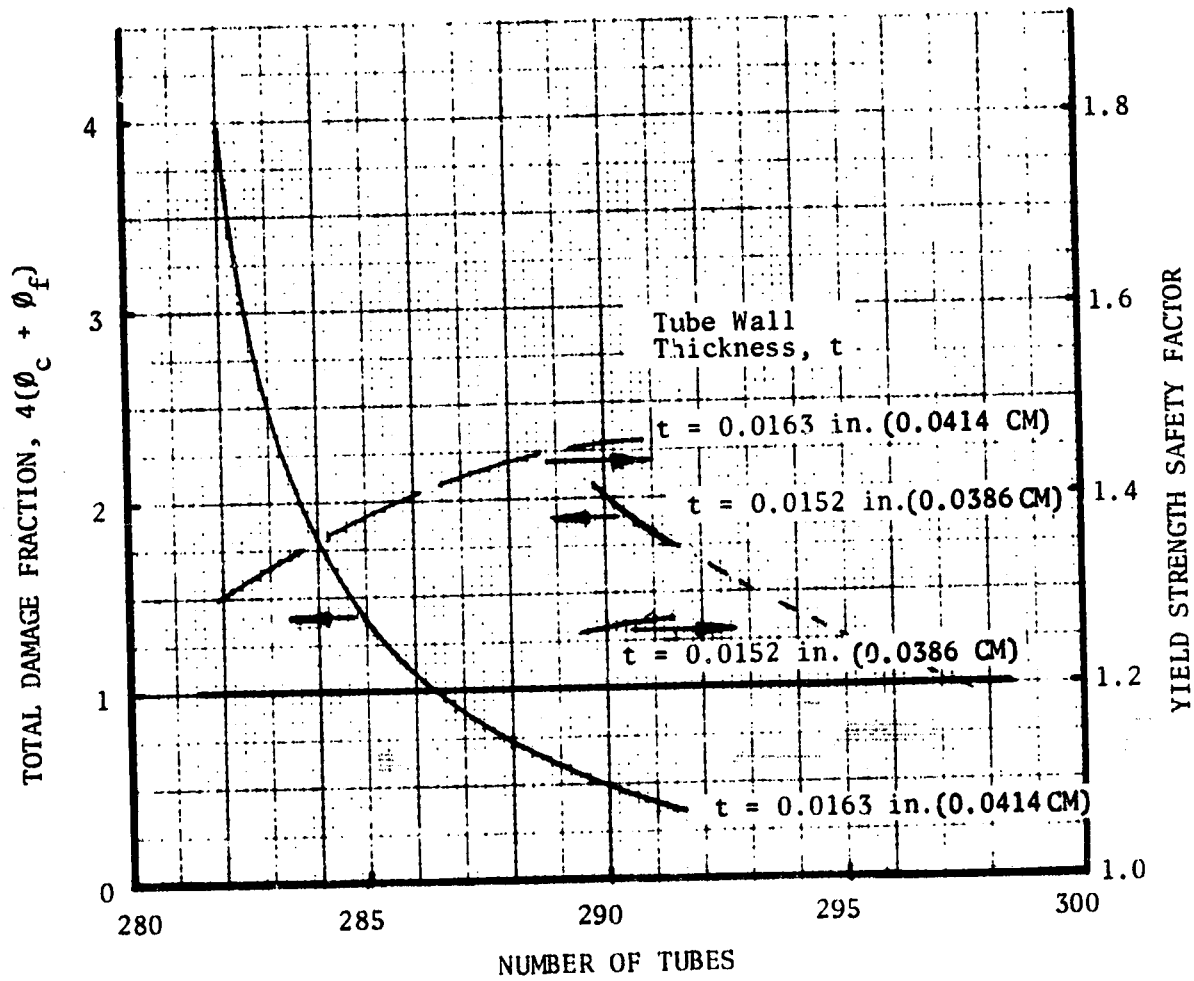


Figure 24. Variation of Damage Fraction and Yield Strength Safety Factor With Number of Tubes for NARloy-Z

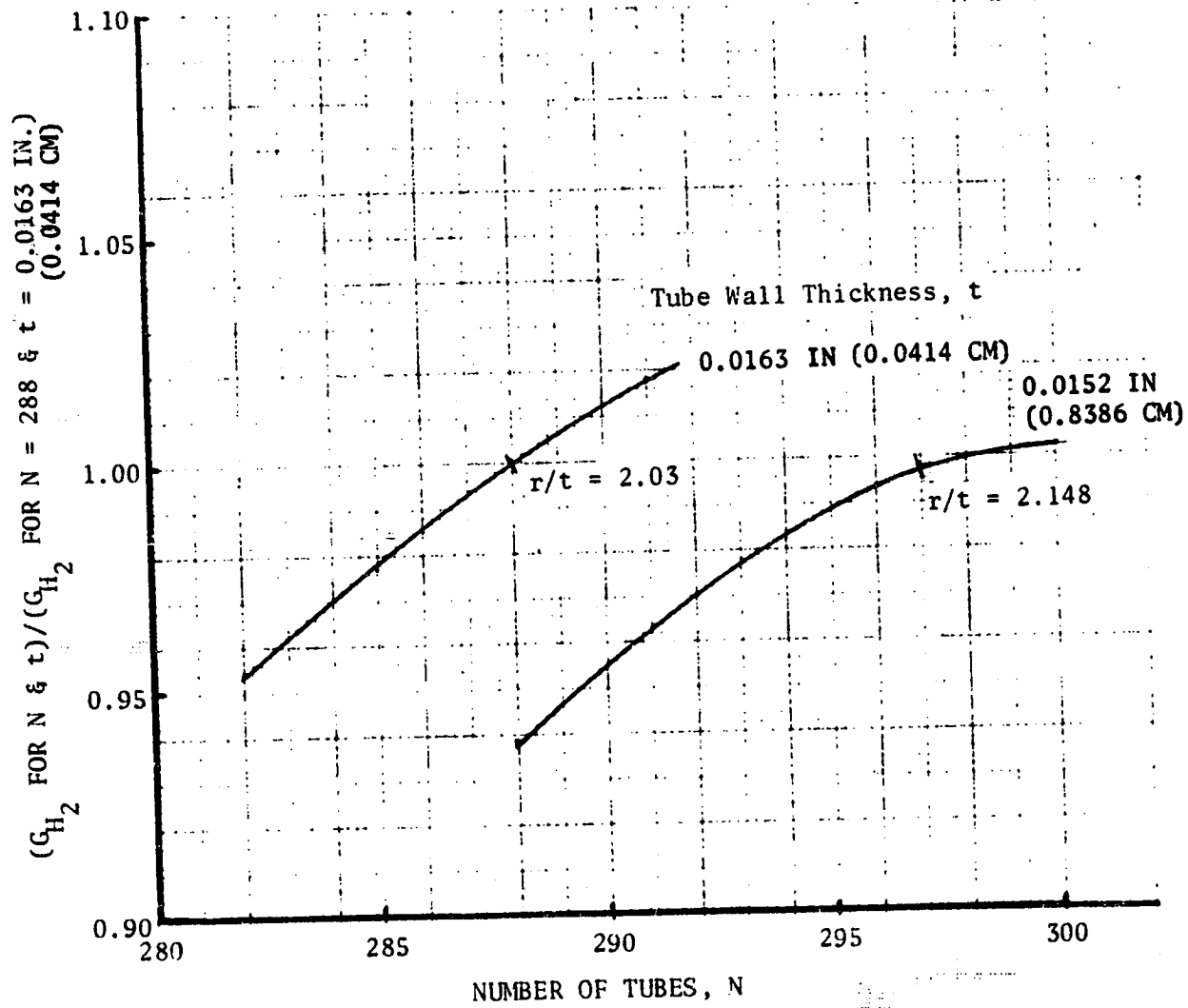


Figure 25. Coolant Mass Velocity Ratio Variation With Number of Tubes -- NARloy-Z

Note:

⊙ Calculated Values

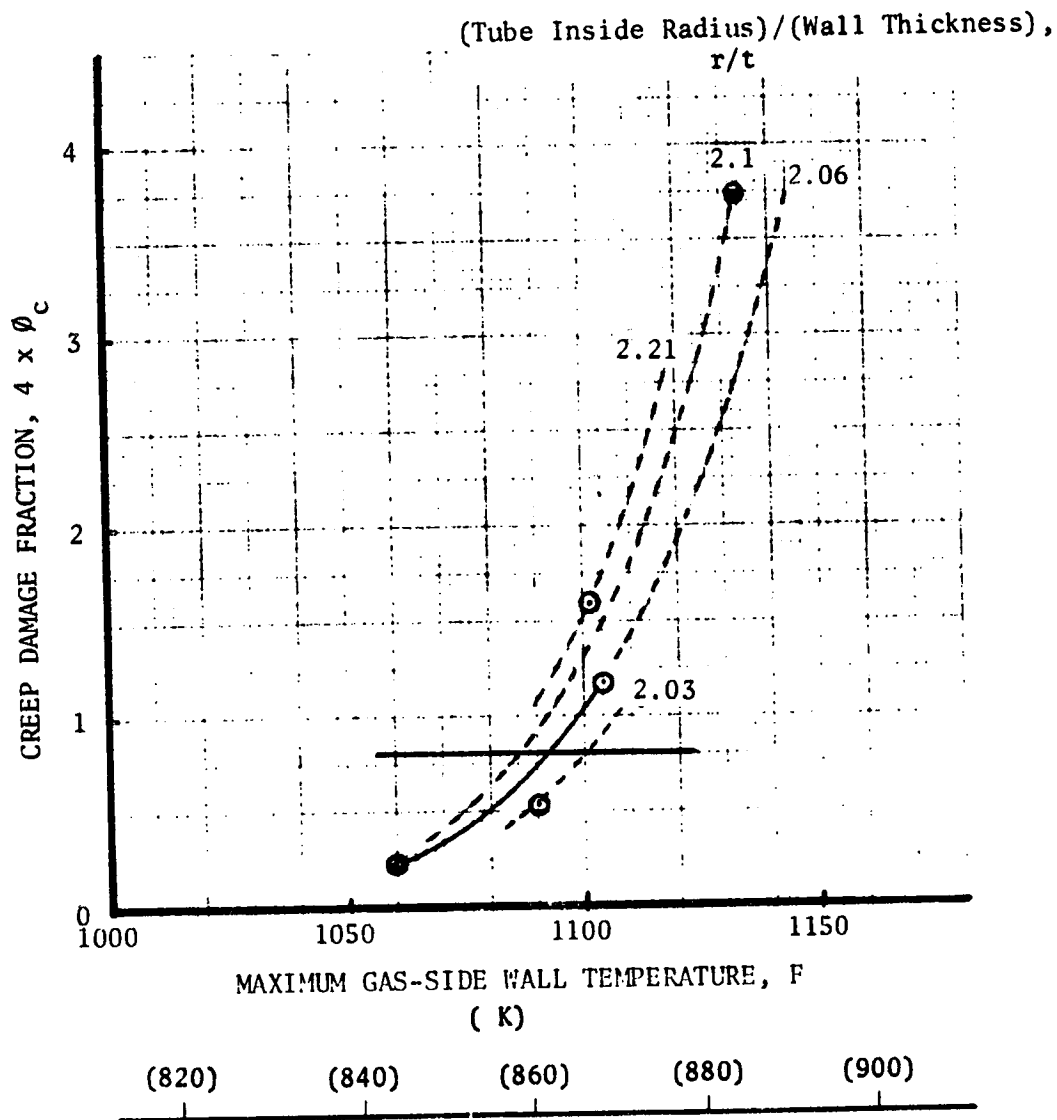


Figure 26. Creep Damage Fraction for the NARloy-Z Tubular Configuration

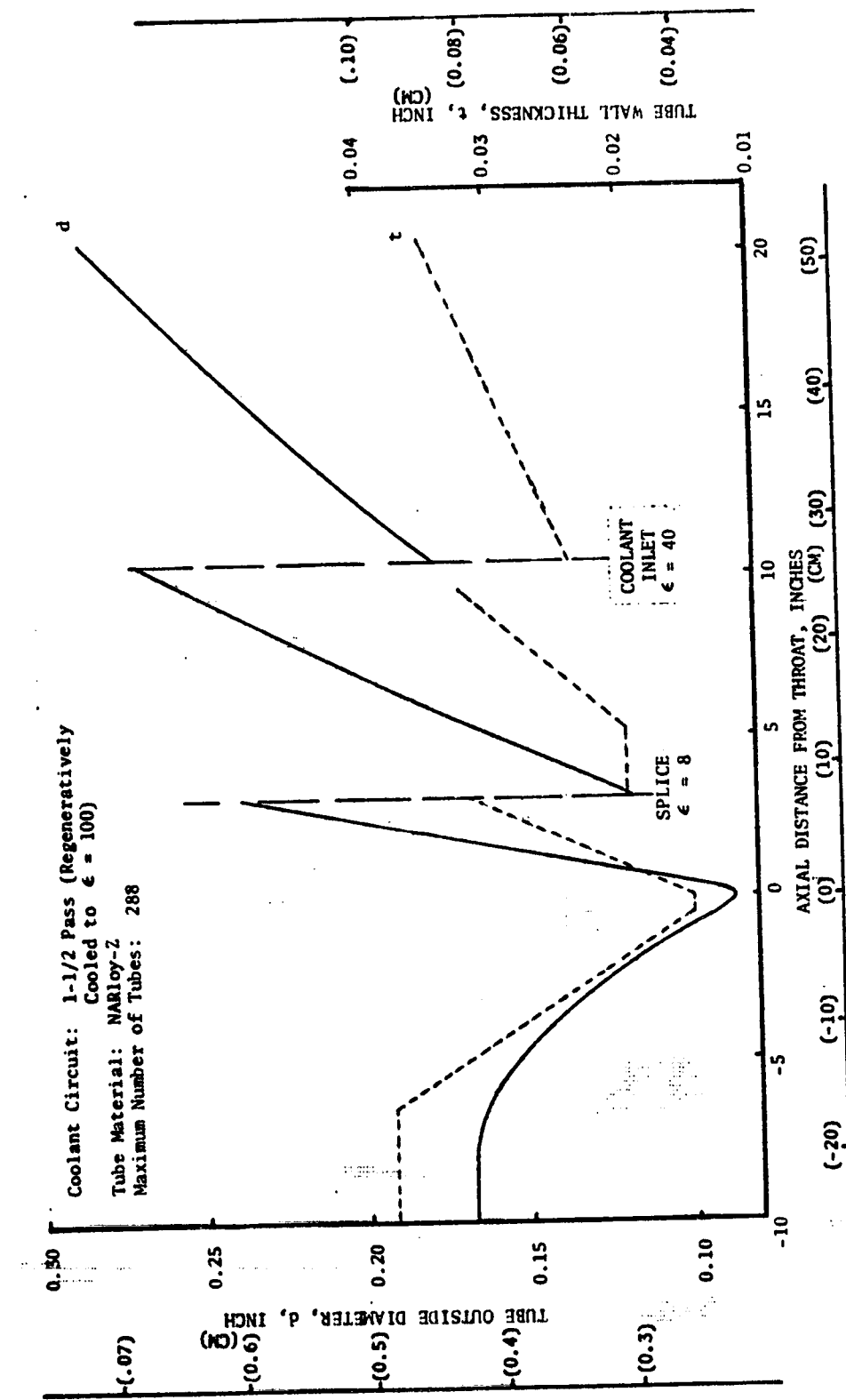


Figure 27. Selected NARLOY-Z Tubular Configuration

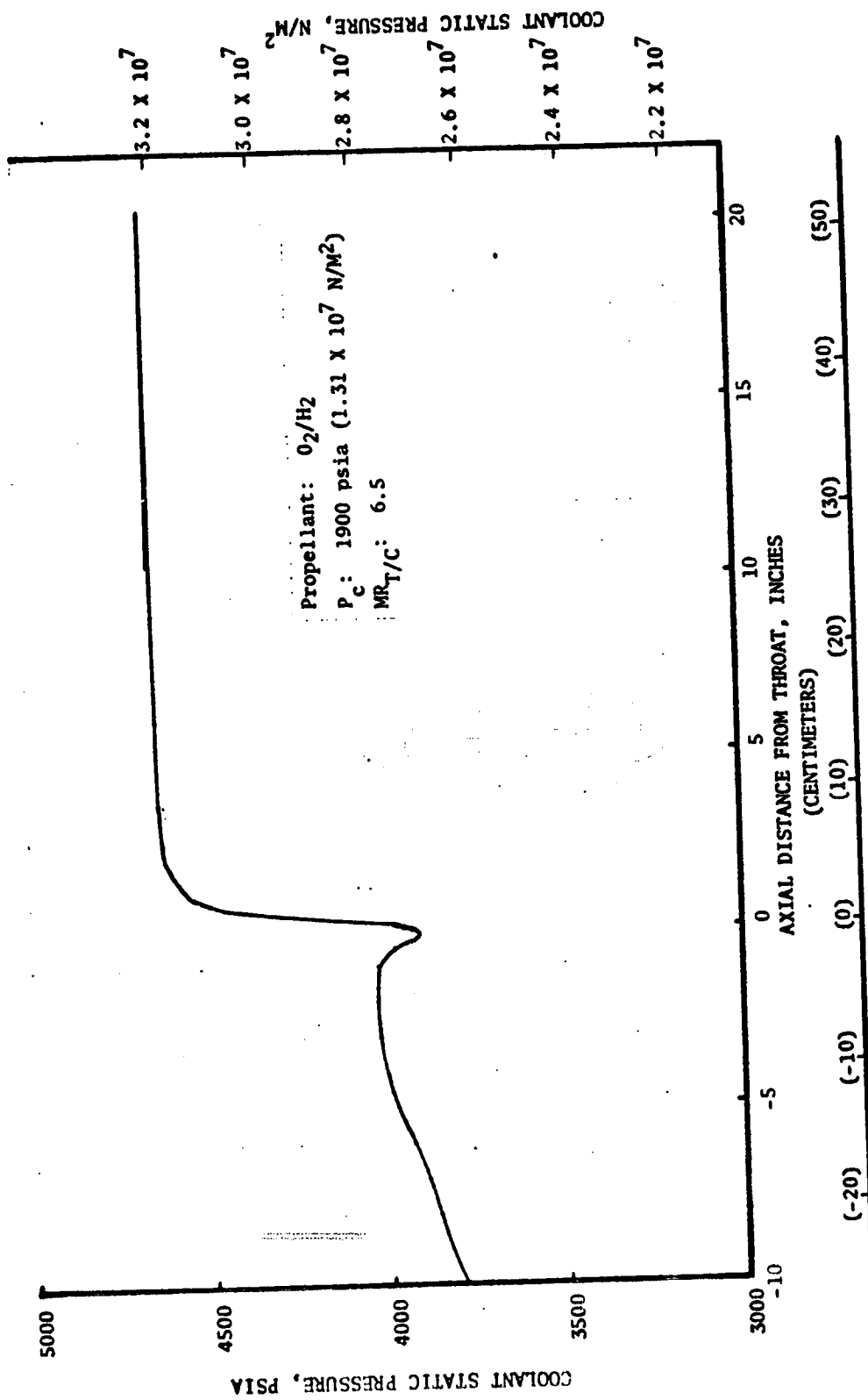


Figure 28. Coolant Static Pressure Distribution for the Selected NARloy Tubular Configuration

Coolant Circuit: 1-1/2 Pass (Regeneratively Cooled to $\epsilon = 100$)
 Tube Material: NARLOY-Z
 Maximum Number of Tubes: 288

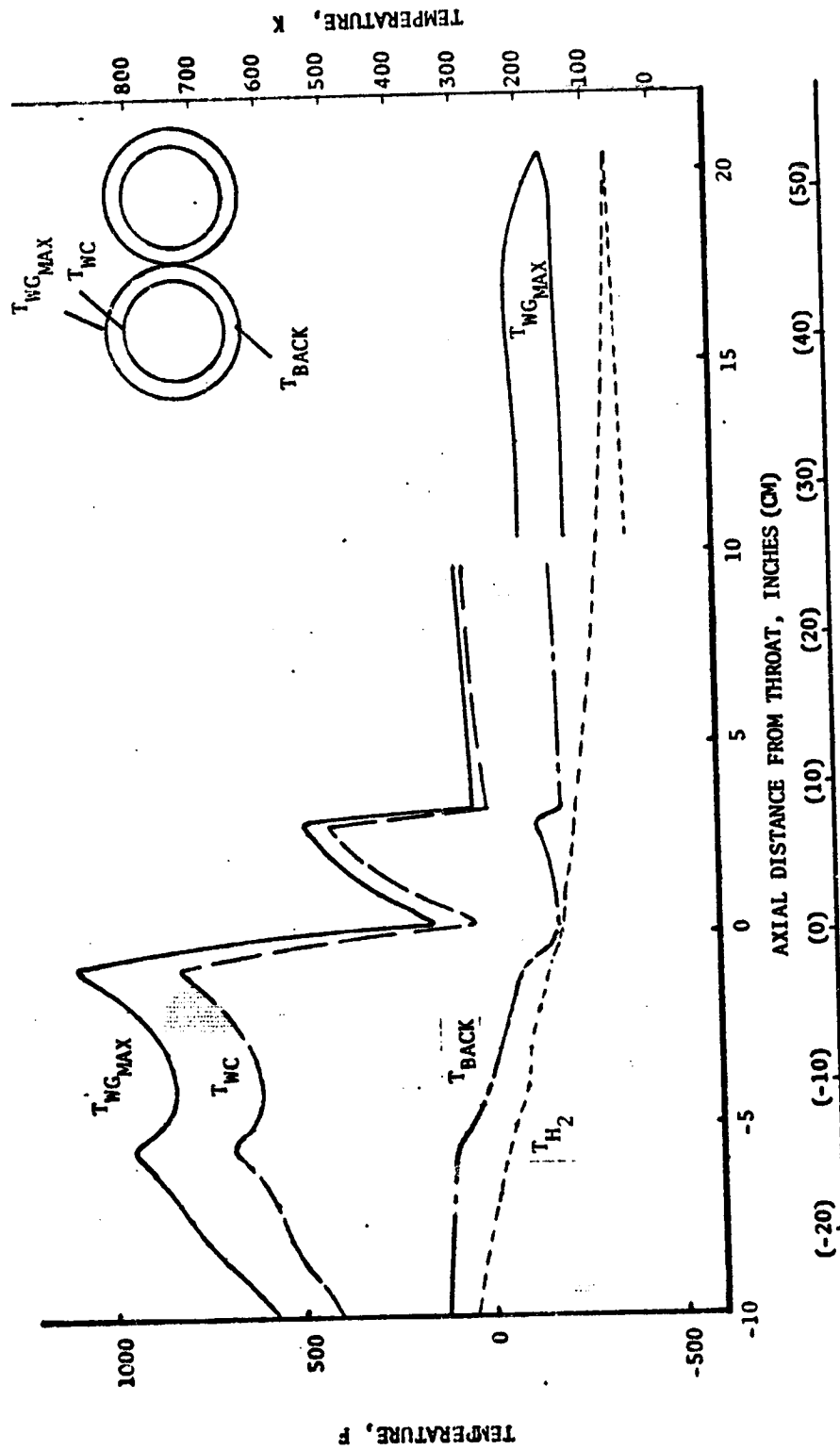
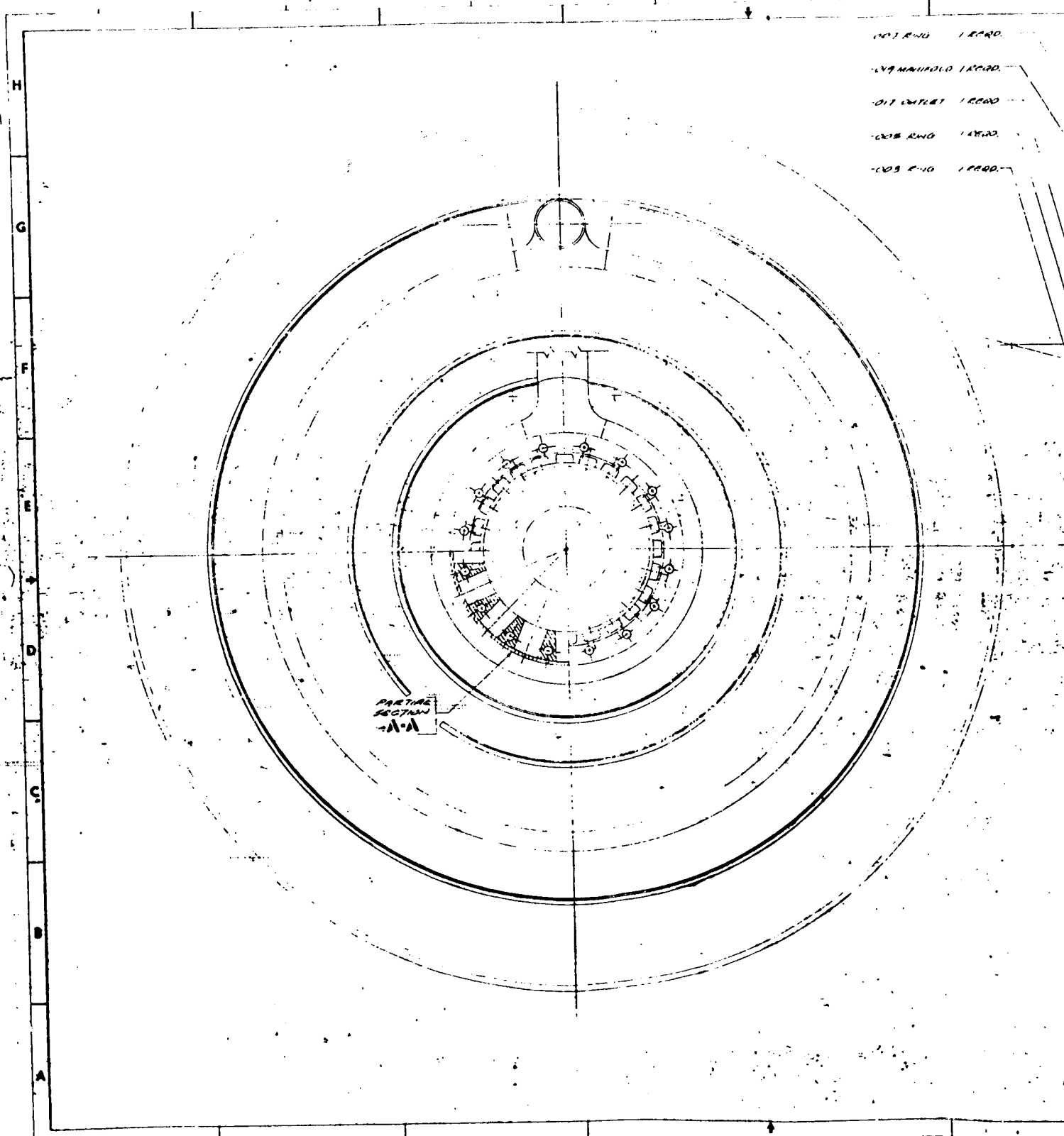


Figure 29. Temperature Distribution for the Selected NARLOY-Z Tubular Configuration

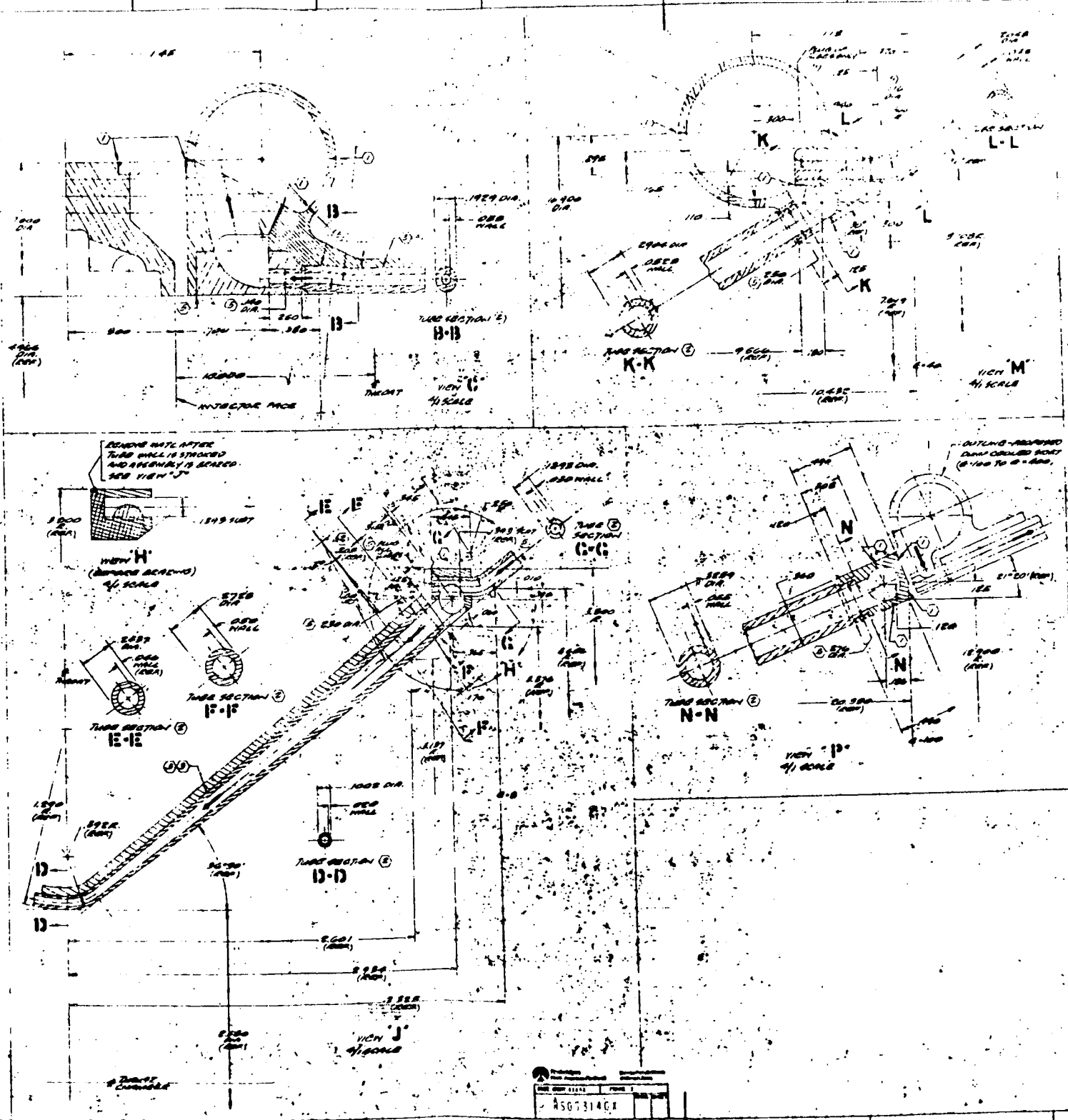
TABLE III. SELECTED TUBULAR CONFIGURATIONS

	Zr-Cu	NARloy-Z
Maximum Number of Tubes	252	68
Coolant Inlet Area Ratio	40	5
Tube Splice Area Ratio	8	8
Minimum Tube Outside Diameter, inch	0.1002 (0.2545 cm)	0.0873 (0.2215 cm)
Minimum Tube Wall Thickness, inch	0.02 (0.0508 cm)	0.015 (0.381 cm)
Maximum Gas-Side Wall Temperature, F	1149 (894 K)	1090 (861 K)
Coolant Pressure Drop, psi	996 (6.86 x 10 ⁶ N/m ²)	854 (5.88 x 10 ⁶ N/m ²)
Coolant Tube Weight, pounds	46.2 (20.9 Kg)	32.2 (14.6 Kg)
Critical Location Stress and Life Parameters:		
Yield	1.22	1.44
Ultimate	1.57	2.16
Damage Fraction	4(0.01 + 0.091) = 0.40	4(0.133 + 0.0477) = 0.724
$4(\phi_c + \phi_f)$		



FOLDOUT FRAME

NO.	DESCRIPTION	AMOUNT
1	X	
2		
3		
4		
5		
6		
7		
8		
9		
10		
11		
12		
13		
14		
15		
16		
17		
18		
19		
20		
21		
22		
23		
24		
25		
26		
27		
28		
29		
30		
31		
32		
33		
34		
35		
36		
37		
38		
39		
40		
41		
42		
43		
44		
45		
46		
47		
48		
49		
50		
51		
52		
53		
54		
55		
56		
57		
58		
59		
60		
61		
62		
63		
64		
65		
66		
67		
68		
69		
70		
71		
72		
73		
74		
75		
76		
77		
78		
79		
80		
81		
82		
83		
84		
85		
86		
87		
88		
89		
90		
91		
92		
93		
94		
95		
96		
97		
98		
99		
100		



CHAMBER (NOT ONE WALL, CONSTANT AREA - 1-1/2 PASS)

NO.	X	Y	WALL THICKNESS	INSTR. NO.
1	1000	2488	1000	058
2	1000	2478	1000	
3	1000	2468	1000	
4	1000	2458	1000	
5	1000	2448	1000	
6	1000	2438	1000	
7	1000	2428	1000	
8	1000	2418	1000	
9	1000	2408	1000	
10	1000	2398	1000	
11	1000	2388	1000	
12	1000	2378	1000	
13	1000	2368	1000	
14	1000	2358	1000	
15	1000	2348	1000	
16	1000	2338	1000	
17	1000	2328	1000	
18	1000	2318	1000	
19	1000	2308	1000	
20	1000	2298	1000	
21	1000	2288	1000	
22	1000	2278	1000	
23	1000	2268	1000	
24	1000	2258	1000	
25	1000	2248	1000	
26	1000	2238	1000	
27	1000	2228	1000	
28	1000	2218	1000	
29	1000	2208	1000	
30	1000	2198	1000	
31	1000	2188	1000	
32	1000	2178	1000	
33	1000	2168	1000	
34	1000	2158	1000	
35	1000	2148	1000	
36	1000	2138	1000	
37	1000	2128	1000	
38	1000	2118	1000	
39	1000	2108	1000	
40	1000	2098	1000	
41	1000	2088	1000	
42	1000	2078	1000	
43	1000	2068	1000	
44	1000	2058	1000	
45	1000	2048	1000	
46	1000	2038	1000	
47	1000	2028	1000	
48	1000	2018	1000	
49	1000	2008	1000	
50	1000	1998	1000	
51	1000	1988	1000	
52	1000	1978	1000	
53	1000	1968	1000	
54	1000	1958	1000	
55	1000	1948	1000	
56	1000	1938	1000	
57	1000	1928	1000	
58	1000	1918	1000	
59	1000	1908	1000	
60	1000	1898	1000	
61	1000	1888	1000	
62	1000	1878	1000	
63	1000	1868	1000	
64	1000	1858	1000	
65	1000	1848	1000	
66	1000	1838	1000	
67	1000	1828	1000	
68	1000	1818	1000	
69	1000	1808	1000	
70	1000	1798	1000	
71	1000	1788	1000	
72	1000	1778	1000	
73	1000	1768	1000	
74	1000	1758	1000	
75	1000	1748	1000	
76	1000	1738	1000	
77	1000	1728	1000	
78	1000	1718	1000	
79	1000	1708	1000	
80	1000	1698	1000	
81	1000	1688	1000	
82	1000	1678	1000	
83	1000	1668	1000	
84	1000	1658	1000	
85	1000	1648	1000	
86	1000	1638	1000	
87	1000	1628	1000	
88	1000	1618	1000	
89	1000	1608	1000	
90	1000	1598	1000	
91	1000	1588	1000	
92	1000	1578	1000	
93	1000	1568	1000	
94	1000	1558	1000	
95	1000	1548	1000	
96	1000	1538	1000	
97	1000	1528	1000	
98	1000	1518	1000	
99	1000	1508	1000	
100	1000	1498	1000	

CHAMBER (NOT ONE WALL, CONSTANT AREA - 1-1/2 PASS)

NO.	X	Y	WALL THICKNESS	INSTR. NO.
16	1888	3088	1000	058
17	1888	3078	1000	
18	1888	3068	1000	
19	1888	3058	1000	
20	1888	3048	1000	
21	1888	3038	1000	
22	1888	3028	1000	
23	1888	3018	1000	
24	1888	3008	1000	
25	1888	2998	1000	
26	1888	2988	1000	
27	1888	2978	1000	
28	1888	2968	1000	
29	1888	2958	1000	
30	1888	2948	1000	
31	1888	2938	1000	
32	1888	2928	1000	
33	1888	2918	1000	
34	1888	2908	1000	
35	1888	2898	1000	
36	1888	2888	1000	
37	1888	2878	1000	
38	1888	2868	1000	
39	1888	2858	1000	
40	1888	2848	1000	
41	1888	2838	1000	
42	1888	2828	1000	
43	1888	2818	1000	
44	1888	2808	1000	
45	1888	2798	1000	
46	1888	2788	1000	
47	1888	2778	1000	
48	1888	2768	1000	
49	1888	2758	1000	
50	1888	2748	1000	
51	1888	2738	1000	
52	1888	2728	1000	
53	1888	2718	1000	
54	1888	2708	1000	
55	1888	2698	1000	
56	1888	2688	1000	
57	1888	2678	1000	
58	1888	2668	1000	
59	1888	2658	1000	
60	1888	2648	1000	
61	1888	2638	1000	
62	1888	2628	1000	
63	1888	2618	1000	
64	1888	2608	1000	
65	1888	2598	1000	
66	1888	2588	1000	
67	1888	2578	1000	
68	1888	2568	1000	
69	1888	2558	1000	
70	1888	2548	1000	
71	1888	2538	1000	
72	1888	2528	1000	
73	1888	2518	1000	
74	1888	2508	1000	
75	1888	2498	1000	
76	1888	2488	1000	
77	1888	2478	1000	
78	1888	2468	1000	
79	1888	2458	1000	
80	1888	2448	1000	
81	1888	2438	1000	
82	1888	2428	1000	
83	1888	2418	1000	
84	1888	2408	1000	
85	1888	2398	1000	
86	1888	2388	1000	
87	1888	2378	1000	
88	1888	2368	1000	
89	1888	2358	1000	
90	1888	2348	1000	
91	1888	2338	1000	
92	1888	2328	1000	
93	1888	2318	1000	
94	1888	2308	1000	
95	1888	2298	1000	
96	1888	2288	1000	
97	1888	2278	1000	
98	1888	2268	1000	
99	1888	2258	1000	
100	1888	2248	1000	

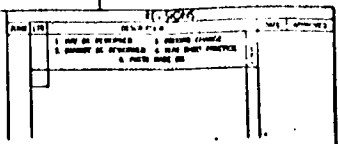


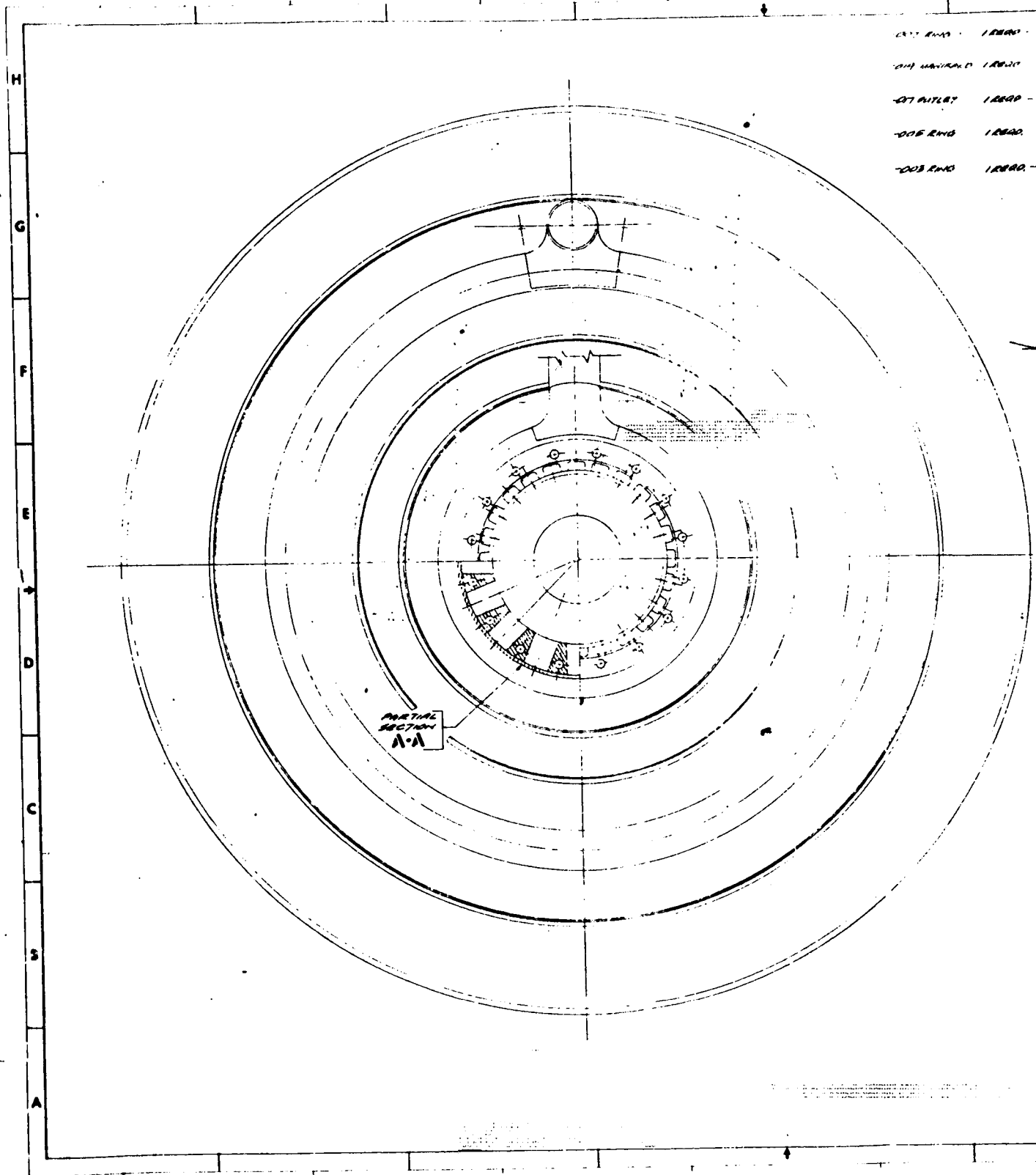
Figure 30. Zr-Cu Tubular Wall Configuration (1-1/2 Pass Cooling Circuit)

43

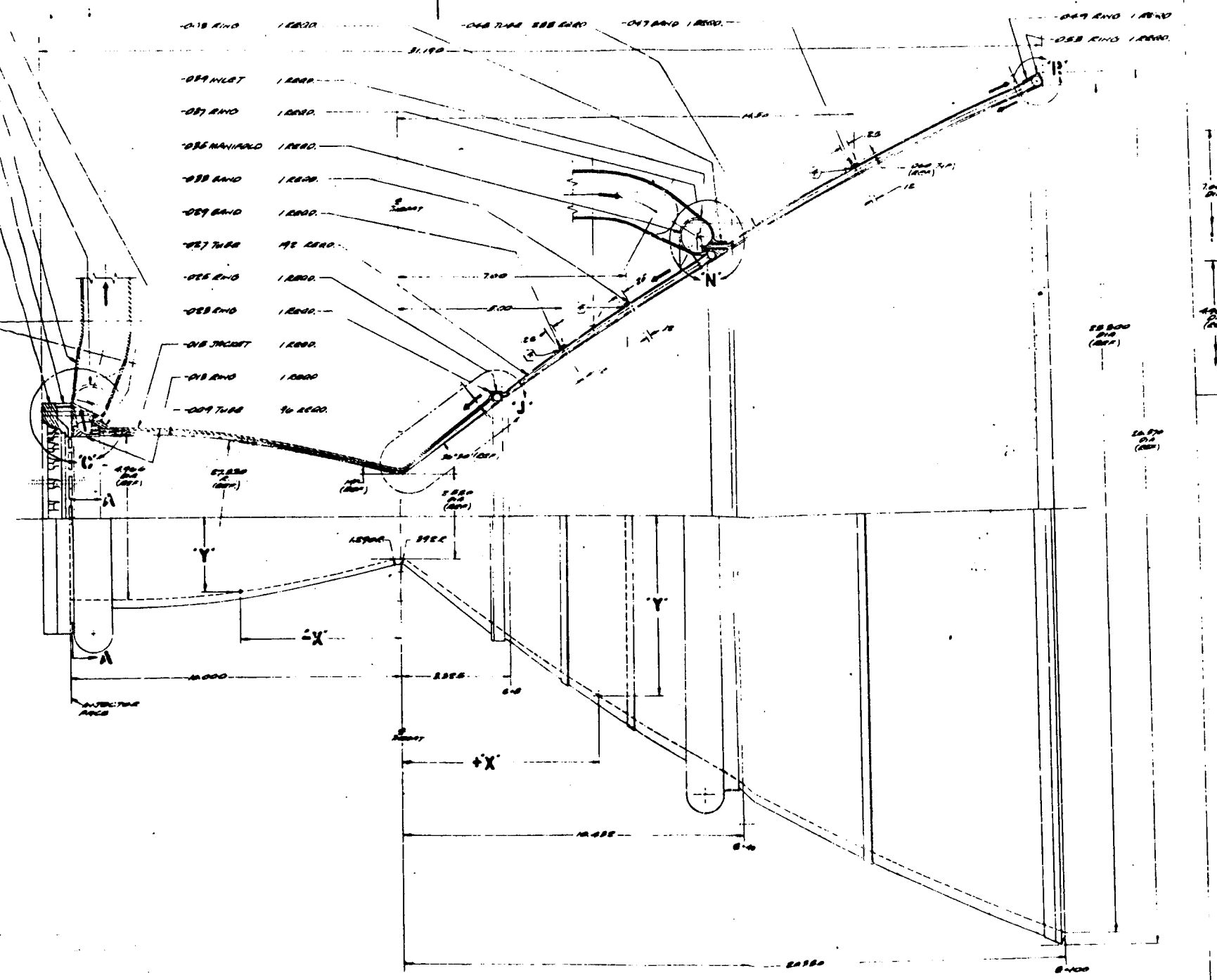
1001	INSUL TUB WALL	220170-101
1002	INSUL TUB WALL	220170-101
1003	INSUL TUB WALL	220170-059
1004	INSUL TUB WALL	780
1005	INSUL TUB WALL	220170-101
1006	INSUL TUB WALL	780
1007	INSUL TUB WALL	220170-101
1008	INSUL TUB WALL	780
1009	INSUL TUB WALL	220170-059
1010	INSUL TUB WALL	220170-059
1011	INSUL TUB WALL	780
1012	INSUL TUB WALL	220170-101
1013	INSUL TUB WALL	780
1014	INSUL TUB WALL	220170-059
1015	INSUL TUB WALL	780
1016	INSUL TUB WALL	220170-101
1017	INSUL TUB WALL	780
1018	INSUL TUB WALL	220170-059
1019	INSUL TUB WALL	220170-059
1020	INSUL TUB WALL	780
1021	INSUL TUB WALL	220170-101
1022	INSUL TUB WALL	780
1023	INSUL TUB WALL	220170-059
1024	INSUL TUB WALL	220170-059
1025	INSUL TUB WALL	780
1026	INSUL TUB WALL	220170-101
1027	INSUL TUB WALL	780
1028	INSUL TUB WALL	220170-059
1029	INSUL TUB WALL	220170-059
1030	INSUL TUB WALL	780

- ① FINISHED SURF AS SHOWN BY DETAIL.
- ② WALLS ON THIS DRAWING TO BE CONSIDERED AS TUBULAR WALL WITH INSULATION ON THE INSIDE AT LOCATION B WITH INSULATION ON THE OUTSIDE AT LOCATION C.
- ③ CORROSION PROTECTION SHALL BE AS SHOWN BY DETAIL C-10.
- ④ INSULATION SHALL BE AS SHOWN BY DETAIL C-10.
- ⑤ WALLS ON THIS DRAWING TO BE CONSIDERED AS TUBULAR WALL WITH INSULATION ON THE INSIDE AT LOCATION B WITH INSULATION ON THE OUTSIDE AT LOCATION C.
- ⑥ WALLS ON THIS DRAWING TO BE CONSIDERED AS TUBULAR WALL WITH INSULATION ON THE INSIDE AT LOCATION B WITH INSULATION ON THE OUTSIDE AT LOCATION C.
- ⑦ WALLS ON THIS DRAWING TO BE CONSIDERED AS TUBULAR WALL WITH INSULATION ON THE INSIDE AT LOCATION B WITH INSULATION ON THE OUTSIDE AT LOCATION C.
- ⑧ WALLS ON THIS DRAWING TO BE CONSIDERED AS TUBULAR WALL WITH INSULATION ON THE INSIDE AT LOCATION B WITH INSULATION ON THE OUTSIDE AT LOCATION C.

NO.	DESCRIPTION	QUANTITY	UNIT	REMARKS
1	INSULATION	1	sq ft	
2	INSULATION	1	sq ft	
3	INSULATION	1	sq ft	
4	INSULATION	1	sq ft	
5	INSULATION	1	sq ft	
6	INSULATION	1	sq ft	
7	INSULATION	1	sq ft	
8	INSULATION	1	sq ft	
9	INSULATION	1	sq ft	
10	INSULATION	1	sq ft	
11	INSULATION	1	sq ft	
12	INSULATION	1	sq ft	
13	INSULATION	1	sq ft	
14	INSULATION	1	sq ft	
15	INSULATION	1	sq ft	
16	INSULATION	1	sq ft	
17	INSULATION	1	sq ft	
18	INSULATION	1	sq ft	
19	INSULATION	1	sq ft	
20	INSULATION	1	sq ft	
21	INSULATION	1	sq ft	
22	INSULATION	1	sq ft	
23	INSULATION	1	sq ft	
24	INSULATION	1	sq ft	
25	INSULATION	1	sq ft	
26	INSULATION	1	sq ft	
27	INSULATION	1	sq ft	
28	INSULATION	1	sq ft	
29	INSULATION	1	sq ft	
30	INSULATION	1	sq ft	
31	INSULATION	1	sq ft	
32	INSULATION	1	sq ft	
33	INSULATION	1	sq ft	
34	INSULATION	1	sq ft	
35	INSULATION	1	sq ft	
36	INSULATION	1	sq ft	
37	INSULATION	1	sq ft	
38	INSULATION	1	sq ft	
39	INSULATION	1	sq ft	
40	INSULATION	1	sq ft	
41	INSULATION	1	sq ft	
42	INSULATION	1	sq ft	
43	INSULATION	1	sq ft	
44	INSULATION	1	sq ft	
45	INSULATION	1	sq ft	
46	INSULATION	1	sq ft	
47	INSULATION	1	sq ft	
48	INSULATION	1	sq ft	
49	INSULATION	1	sq ft	
50	INSULATION	1	sq ft	
51	INSULATION	1	sq ft	
52	INSULATION	1	sq ft	
53	INSULATION	1	sq ft	
54	INSULATION	1	sq ft	
55	INSULATION	1	sq ft	
56	INSULATION	1	sq ft	
57	INSULATION	1	sq ft	
58	INSULATION	1	sq ft	
59	INSULATION	1	sq ft	
60	INSULATION	1	sq ft	
61	INSULATION	1	sq ft	
62	INSULATION	1	sq ft	
63	INSULATION	1	sq ft	
64	INSULATION	1	sq ft	
65	INSULATION	1	sq ft	
66	INSULATION	1	sq ft	
67	INSULATION	1	sq ft	
68	INSULATION	1</		



FOLDOUT FRAME



RSJ031391

CHANGE (NOT TO SCALE) - SEE DRAWING FOR DETAILS

STN	X	Y	CHG. NO.	DATE	BY
18	10.000	2.481			
17	8.800	2.481	1680	039	
16	8.000	2.476	1674		
15	7.500	2.471	1671		
14	7.000	2.450			
13	6.500	2.450	1668	039	
12	6.000	2.385	1664		
11	5.500	2.340	1661		
10	5.000	2.318	1659		
9	4.500	2.220	1602		
8	4.000	2.180	1601		
7	3.500	2.000	1598		
6	3.000	1.970	1595		
5	2.500	1.860	1589		
4	2.000	1.750	1584		
3	1.500	1.680	1583		
2	1.000	1.570	1578		
1	0	1.520	1577	015	2/20/07
0	0	1.527			
1	0.500	1.600	1598		
2	1.000	1.674			
3	1.500	1.668	1596		
4	2.000	1.702			
5	2.500	1.710	1601		
6	3.000	2.020			
7	3.500	2.148			
8	4.000	2.274	1599		
9	4.500	2.423			
10	5.000	2.566			
11	5.500	2.785	1600		
12	6.000	2.950			
13	6.500	3.187	2122	028	
14	7.000	3.374	2284	042	
15	7.500	3.680			

(TOTAL OF 90 TUBES)

CHANGE (NOT TO SCALE) - SEE DRAWING FOR DETAILS

STN	X	Y	CHG. NO.	DATE	BY
16	3.225	1.140	1576	020	C-8
17	3.545	2.011			
18	3.700	2.750			
19	4.000	4.000	1592		
20	4.400	5.000	1591		
21	4.800	7.000	1588	042	C-8
22	5.000	8.100			

CHANGE (NOT TO SCALE) - SEE DRAWING FOR DETAILS

STN	X	Y	CHG. NO.	DATE	BY
22	10.850	2.200	1589	024	C-10
23	10.950	2.400	1588		
24	10.980	2.500	1587		
25	10.985	2.600			
26	11.105	1.400	1584		
27	11.100	1.400	1585		
28	11.071	12.025	1586		
29	12.000	12.000	1585	010	C-10

(TOTAL OF 208 TUBES
150 DOWN TUBES,
158 UP TUBES)

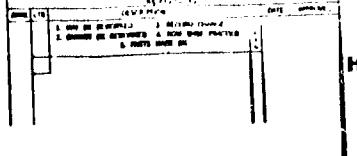


Figure 31. NARloy-Z Tubular Wall Configuration (1-1/2 Pass Cooling Circuit)

-001	INCO TUB SAC	280170-101
-002	INCO TUB SAC	280170-101
-003	INCO TUB SAC	280170-089
-004	NARLOY Z TUBING	280170-109
-005	INCO TUB SAC	280170-101
-006	INCO TUB TUBING	780
-007	INCO TUB SAC	280170-101
-008	INCO TUB TUBING	780
-009	INCO TUB SAC	280170-089
-010	INCO TUB SAC	280170-089
-011	NARLOY Z TUBING	280170-109
-012	INCO TUB SAC	280170-101
-013	INCO TUB SAC	280170-101
-014	INCO TUB TUBING	780
-015	INCO TUB SAC	280170-089
-016	INCO TUB TUBING	780
-017	INCO TUB SAC	280170-101
-018	INCO TUB SAC	280170-101
-019	NARLOY Z TUBING	280170-109
-020	INCO TUB SAC	280170-101
-021	INCO TUB SAC	280170-089
-022	INCO TUB SAC	280170-101

- ① INCO TUBING APPROXIMATE MATCH UP TO CENTER LINE OF TUBULAR WALL. IF TUBING IS NOT MATCHING UP TO CENTER LINE, THE WALL SHOULD BE ADJUSTED TO MATCH UP TO CENTER LINE.
- ② NARLOY Z TUBING APPROXIMATE MATCH UP TO CENTER LINE OF TUBULAR WALL. IF TUBING IS NOT MATCHING UP TO CENTER LINE, THE WALL SHOULD BE ADJUSTED TO MATCH UP TO CENTER LINE.
- ③ TUBING APPROXIMATE MATCH UP TO CENTER LINE OF TUBULAR WALL. IF TUBING IS NOT MATCHING UP TO CENTER LINE, THE WALL SHOULD BE ADJUSTED TO MATCH UP TO CENTER LINE.
- ④ TUBING APPROXIMATE MATCH UP TO CENTER LINE OF TUBULAR WALL. IF TUBING IS NOT MATCHING UP TO CENTER LINE, THE WALL SHOULD BE ADJUSTED TO MATCH UP TO CENTER LINE.

UNION PACIFIC CORPORATION

PROJECT: NARLOY-Z TUBULAR WALL CONFIGURATION

DATE: 02/20/07

BY: [Signature]

REVISIONS:

NO.	DESCRIPTION	DATE
1	ISSUED FOR CONSTRUCTION	02/20/07

UNION PACIFIC CORPORATION

102602

ratio of 8. For the specified design criteria, the jacket thickness profile shown in Fig. 32 was determined. Again, to provide reasonable thickness for fabrication, a 0.06-inch (0.1524 cm) constant thickness was used. This constant thickness would allow the jacket to be spun for fabrication. The Zr-Cu or NARloy-Z tubes would be stacked in the spun jacket and brazed. To maintain desirable material properties, the thrust chamber would be heat treated after brazing. The inlet and return manifolds would be EB or TIG welded. The 2 tubes-to-1 tube splice at an area ratio of 8-to-1 with the thick wall tubes necessitated a manifold-type splice.

CHANNEL WALL COMBUSTOR/TUBULAR NOZZLE CONFIGURATION (1-1/2 PASS COOLING CIRCUIT)

Tubular A-286 Nozzle

As for the all tubular design, parametric heat transfer data were generated by varying the number of tubes using both a 0.005-inch (0.0127 cm) and 0.007-inch (0.0178 cm) constant tube wall thickness. Because of the high yield strength of A-286, the tube wall thickness was fabrication-limited rather than design-limited. The 0.007-inch (0.0178 cm) wall thickness increased the coolant pressure drop and the tube weight slightly, but was selected since it provided the most realistic wall thickness from a fabrication standpoint. Similar trends of increasing coolant pressure drop and decreasing wall temperature with an increase in the number of tubes were obtained.

In addition to achieving a satisfactory wall temperature distribution for A-286 and low coolant pressure drop, the A-286 tubular nozzle must be designed to provide reasonable wall temperatures at the joint between the copper alloy channel wall combustor and the tubular nozzle, as well as, providing tube sizes that can be manufactured.

An evaluation of the influence of combustor-nozzle joint area ratio on coolant pressure drop indicated, as shown in Fig. 33, that an increase in the joint area ratio significantly reduced coolant pressure drop for designs having 300 or more tubes. As shown in Fig. 33, these nozzle pressure drops ranged from 10 psi ($6.895 \times 10^4 \text{ N/m}^2$) to 120 psi ($8.28 \times 10^5 \text{ N/m}^2$). For the round tube configuration with 240 to 360 tubes (approximate 600 F or 589 K maximum wall temperature), an increase in the coolant inlet area ratio was detrimental, since no significant pressure drop reduction resulted and both the tube weight and the wall temperature increased just upstream of the coolant inlet.

The round tube configuration offered low coolant tube weights; however, this configuration resulted in extremely low wall temperatures at the high nozzle area ratios so that satisfactory wall temperatures can be obtained at low area ratios. The end result was a relatively high nozzle coolant pressure drop. Therefore, to minimize the pressure drop and yet achieve satisfactory cooling, a nozzle configuration was evaluated with a large number of tubes that are round at the inlet ($\epsilon = 100$) and become booked (not round) as the low area ratio locations are approached. The designs evaluated consisted of 400 tubes with the coolant inlet at an area ratio of 100-to-1. For the booked tube configuration, an increase in the combustor-nozzle joint area ratio significantly reduced

Coolant Circuit: 1-1/2 Pass (Regeneratively Cooled to $\epsilon = 100$)

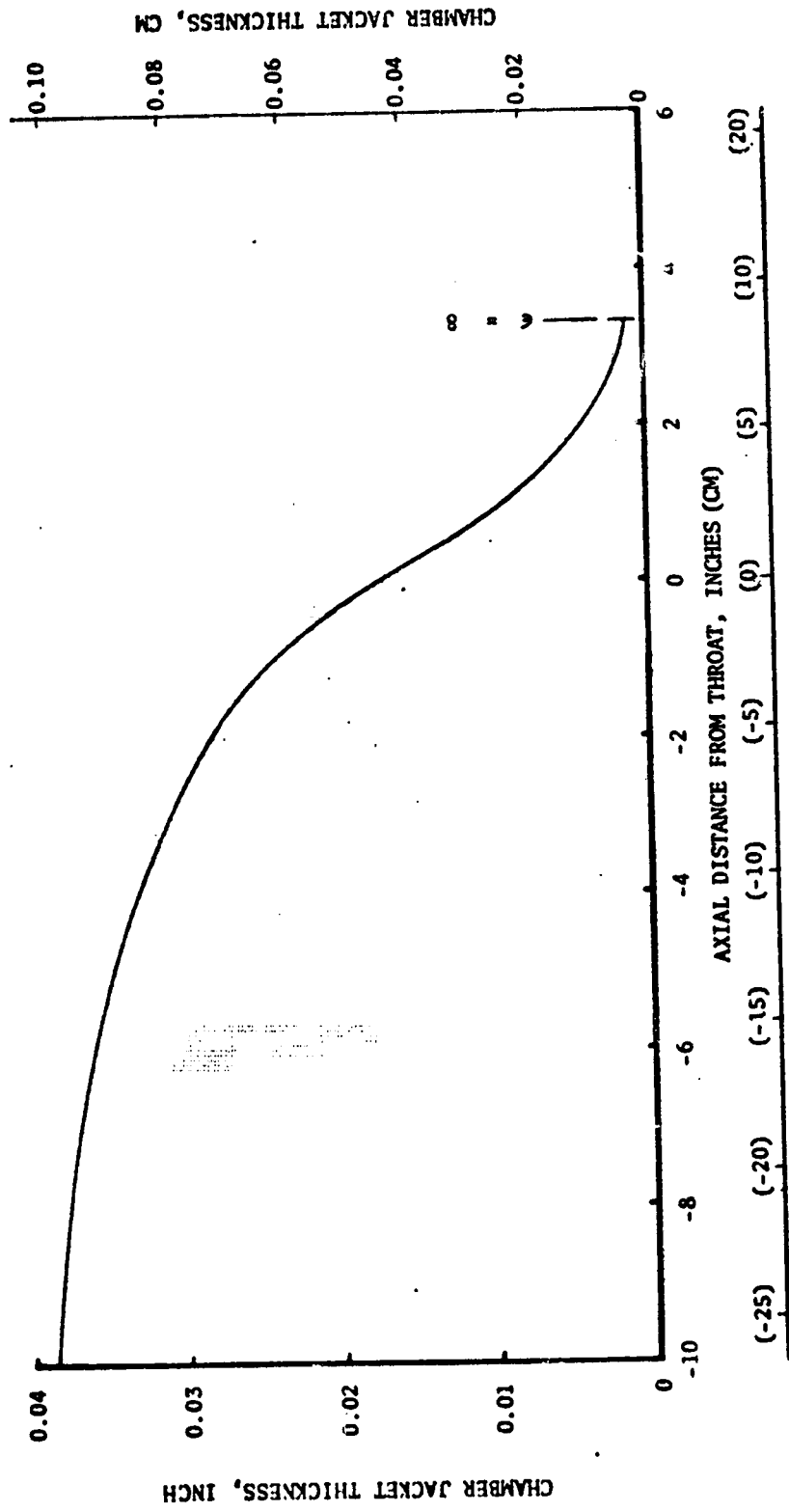


Figure 32. Chamber Jacket Thickness Distribution for the Tubular Wall Configuration (1-1/2 Pass Cooling Circuit)

Coolant Circuit: 1-1/2 Pass (Regeneratively Cooled to $\epsilon = 100$)
 Tube Material: A-286
 Coolant Inlet: $\epsilon = 20$
 Minimum Tube Wall Thickness = 0.007-inch (0.01778 CM)

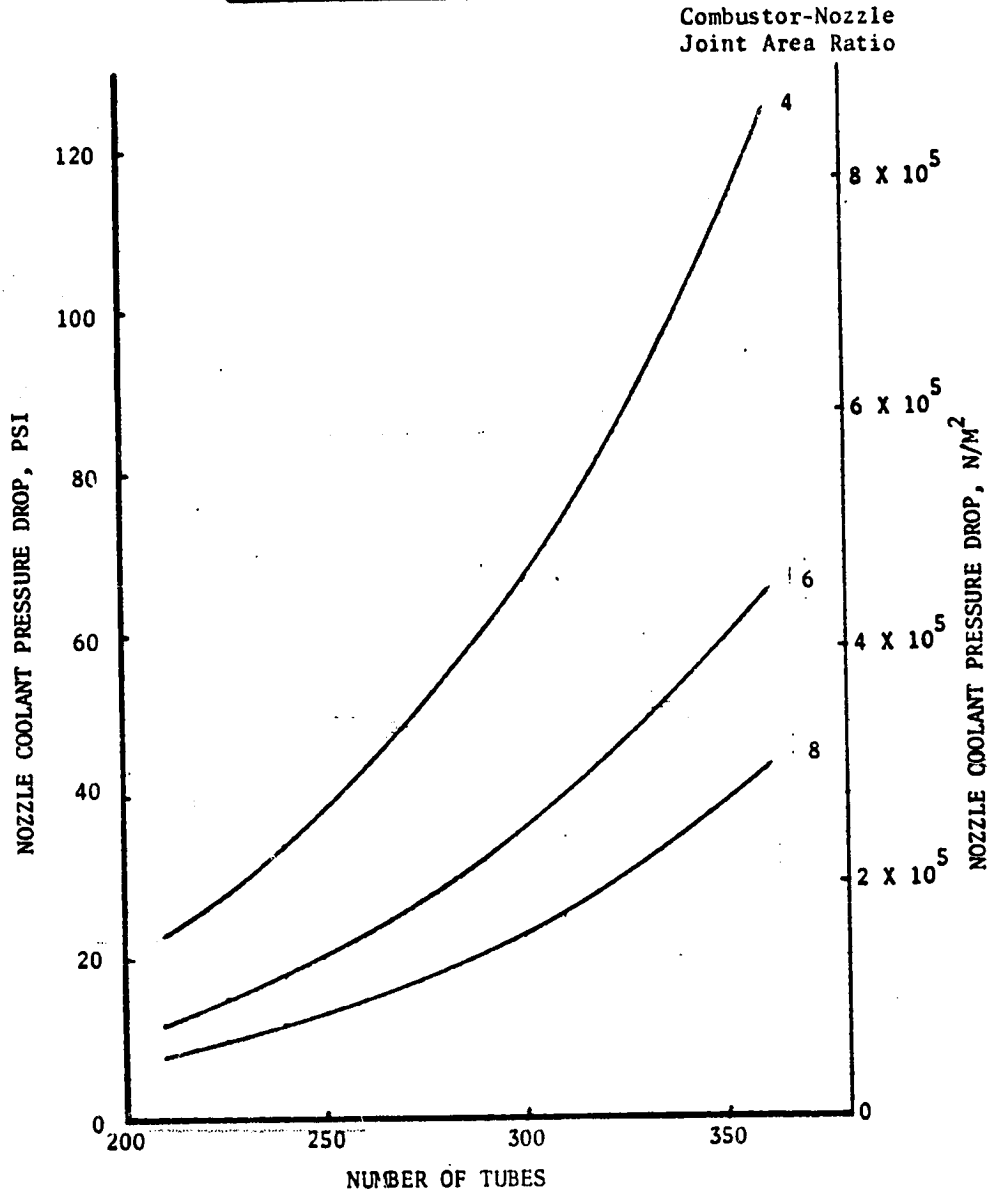


Figure 33. A-286 Nozzle (Round Tube Configuration) Coolant Pressure Drop Variation With Number of Tubes and Combustor-Nozzle Joint Area Ratio

(approximately 35 psi or $2.41 \times 10^4 \text{ N/m}^2$) the nozzle coolant pressure drop. As shown by the comparisons presented in Fig. 34 and Table IV, the booked tube configuration (Design E) achieved the lower nozzle coolant pressure drop, tube weight, and wall temperature distribution at low area ratios. Also, with a nozzle coolant pressure drop of 22 psi ($1.517 \times 10^4 \text{ N/m}^2$), any further pressure drop reduction would not be significant from an engine system standpoint; therefore, the booked tube configuration, Design E, was selected as the 1-1/2 pass A-286 tubular nozzle design.

TABLE IV. A-286 NOZZLE (1-1/2 PASS COOLING CIRCUIT) COMPARISON

	Round Tube Configuration	Booked Tube Configuration (Design E)
Maximum Number of Tubes	320	400
Coolant Inlet Area Ratio	20	100
Combustor-Nozzle Joint Area Ratio	8	8
Minimum Tube Unformed Diameter, inch	0.109 (0.277 CM)	0.075 (0.1905 CM)
Minimum Tube Wall Thickness, inch	0.007 (0.01778 CM)	0.007 (0.01778 CM)
Nozzle Coolant Pressure Drop, psi	28.8 ($1.987 \times 10^5 \text{ N/m}^2$)	22 ($1.518 \times 10^5 \text{ N/m}^2$)
Nozzle Coolant Tube Weight, pounds	7.5 (3.4 kg)	6.8 (3.08 kg)
Maximum Gas-Side Wall Temperature at $\epsilon = 8$, F	~550 (561 K)	525 (547 K)
Maximum Gas-Side Wall Temperature at $\epsilon = 20$, F	625 (603 K)	388 (472 K)

The tube dimensions, static coolant pressure distribution, and wall temperature distribution for the selected A-286 nozzle design are presented in Fig. 35 through 37. As shown in Fig. 37, the nozzle resulted in a maximum gas-side wall temperature of 525 F (547 K).

Channel Wall Combustor

Using the stress criteria presented in Appendix A, parametric curves of allowable pressure versus channel width-to-wall thickness ratio (a/t) were generated for the candidate channel wall materials, Zr-Cu and NARloy-Z (Fig. 38 and 39). As shown by these data, NARloy-Z has a higher allowable coolant pressure than Zr-Cu, because of a higher yield strength.

Coolant Circuit: 1-1/2 Pass (Regeneratively Cooled to $\epsilon = 100$)
 Tube Material: A-286
 Minimum Tube Wall Thickness: 0.007-inch (0.01778 CM)

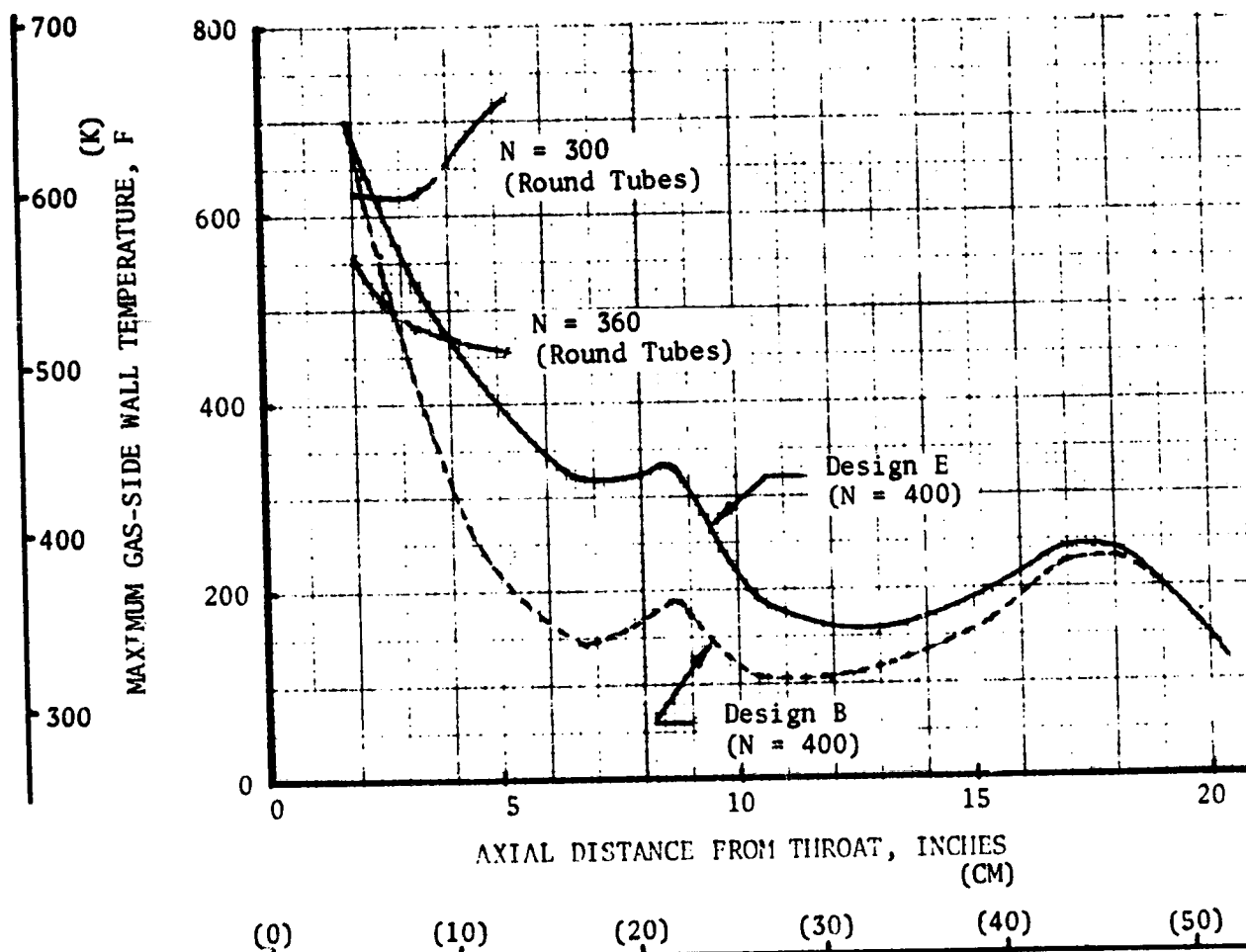


Figure 34. A-286 Nozzle (Hooked Tube Configurations) Gas-Side Wall Temperature Distributions

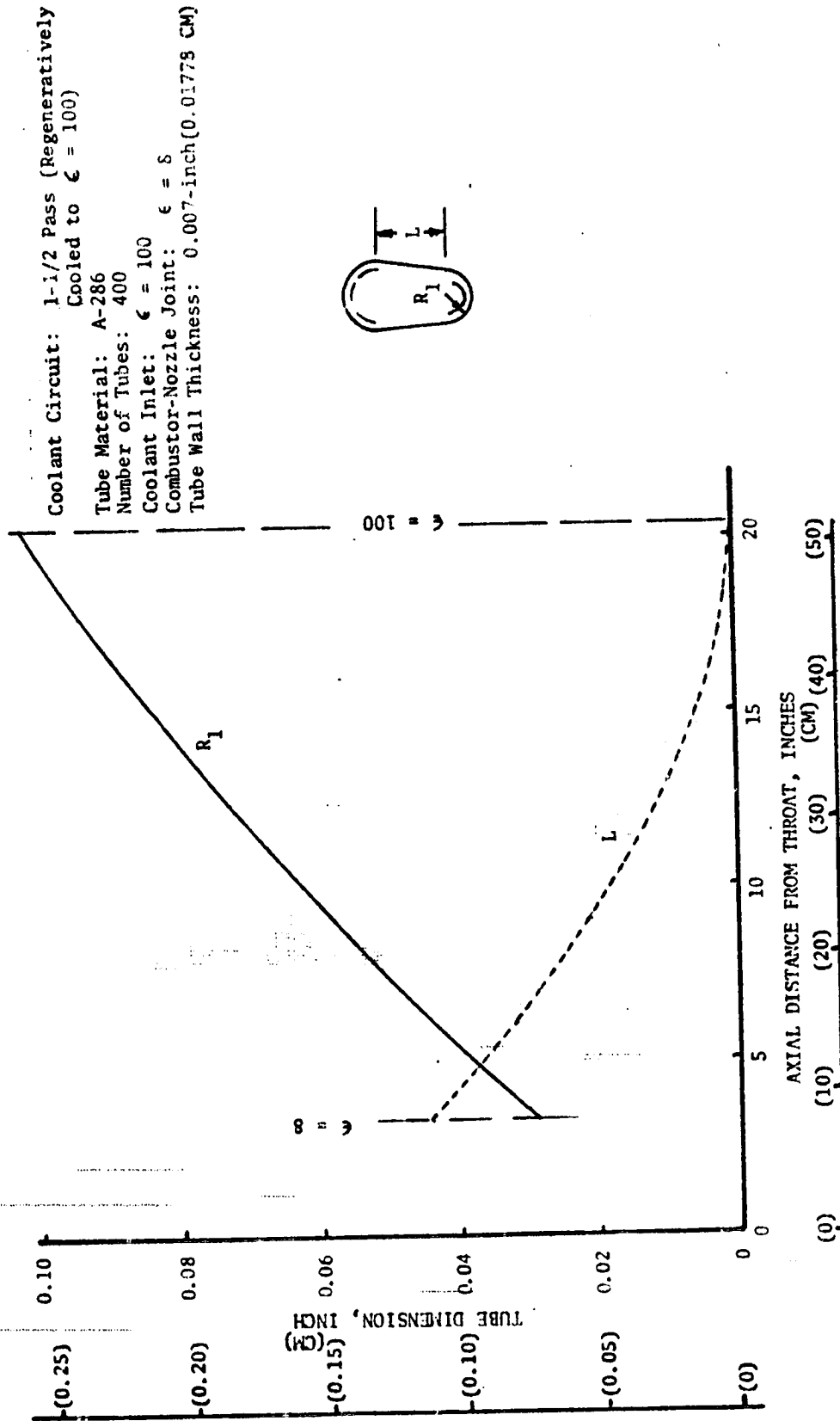


Figure 35. Selected A-286 Nozzle Configuration (1-1/2 Pass Cooling Circuit)

Cooling Circuit: 1-1/2 Pass (Regeneratively
 Cooled to $\epsilon = 100$)
 Coolant Inlet: $\epsilon = 100$

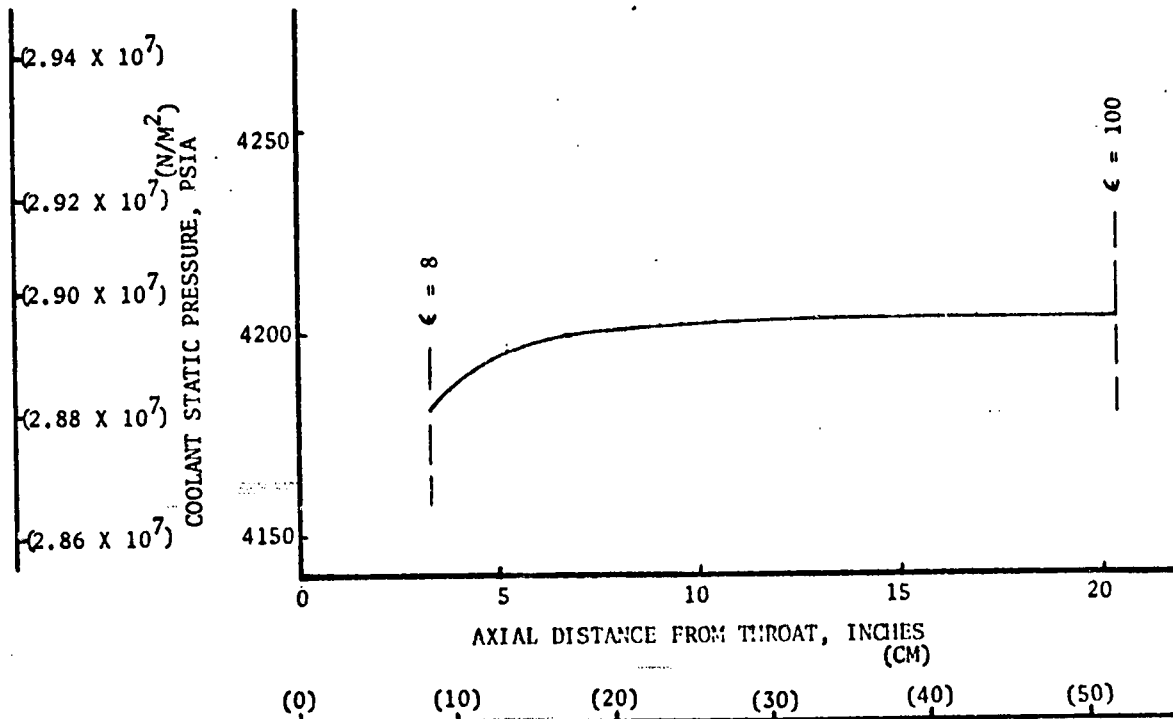


Figure 36. Coolant Static Pressure Distribution for the Selected A-286 Nozzle (1-1/2 Pass Cooling Circuit)

Coolant Circuit: 1-1/2 Pass (Regeneratively Cooled to $\epsilon = 100$)
 Tube Material: A-286
 Number of Tubes: 400
 Coolant Inlet: $\epsilon = 100$
 Tube Wall Thickness: 0.007-inch (0.01778 CM)

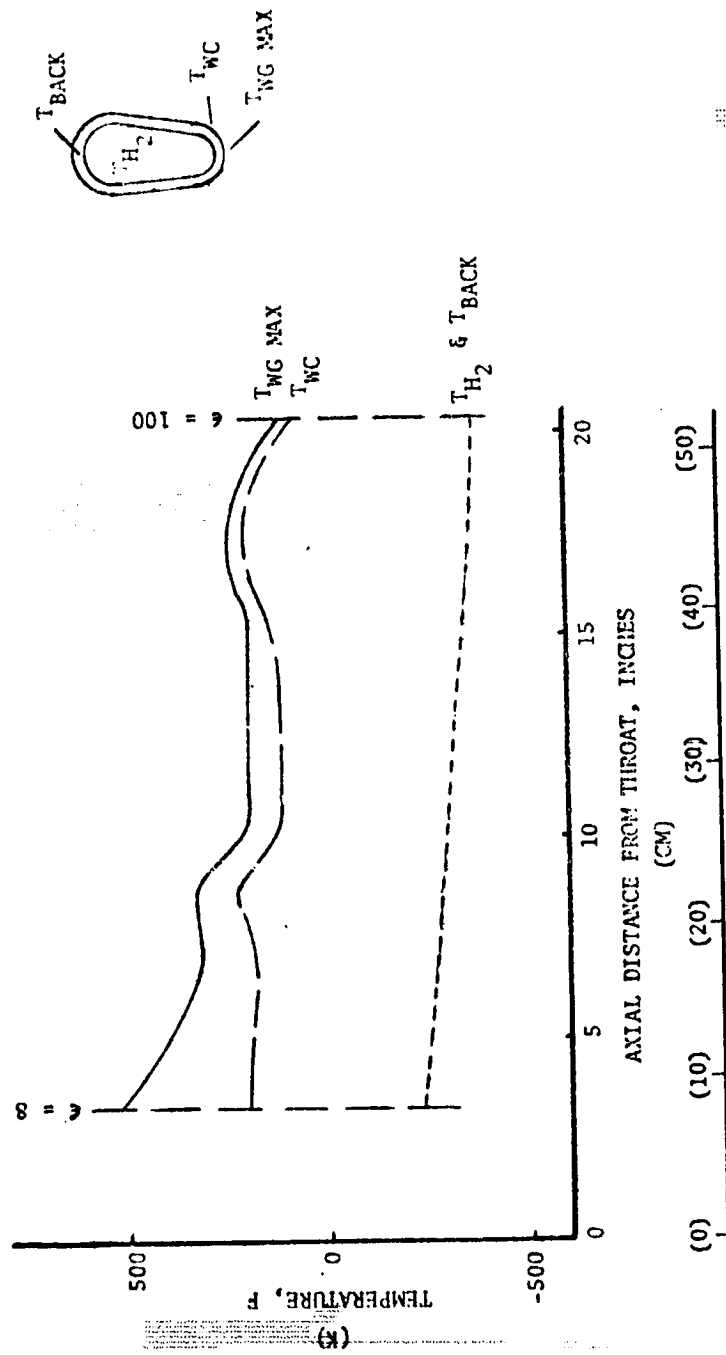


Figure 37. Temperature Distributions for the Selected A-286 Nozzle (1-1/2 Pass Cooling Circuit)

NOTE: $P = \frac{1.62 \tau}{(a/t)^2}$; $\sigma = \frac{F_{ty}}{1.2}$

P = Allowable Coolant Pressure
 σ = Maximum Fixed End Beam Bending Stress
 a = Channel Width
 t = Nominal Hot Wall Thickness
 F_{ty} = Minimum Yield Strength at Average Temperature Through the Hot Wall

$P = \frac{1.2 \tau}{a/t}$; $\tau = 0.6 \frac{F_{ty}}{1.2}$

τ = Maximum Hot Wall Shear Stress

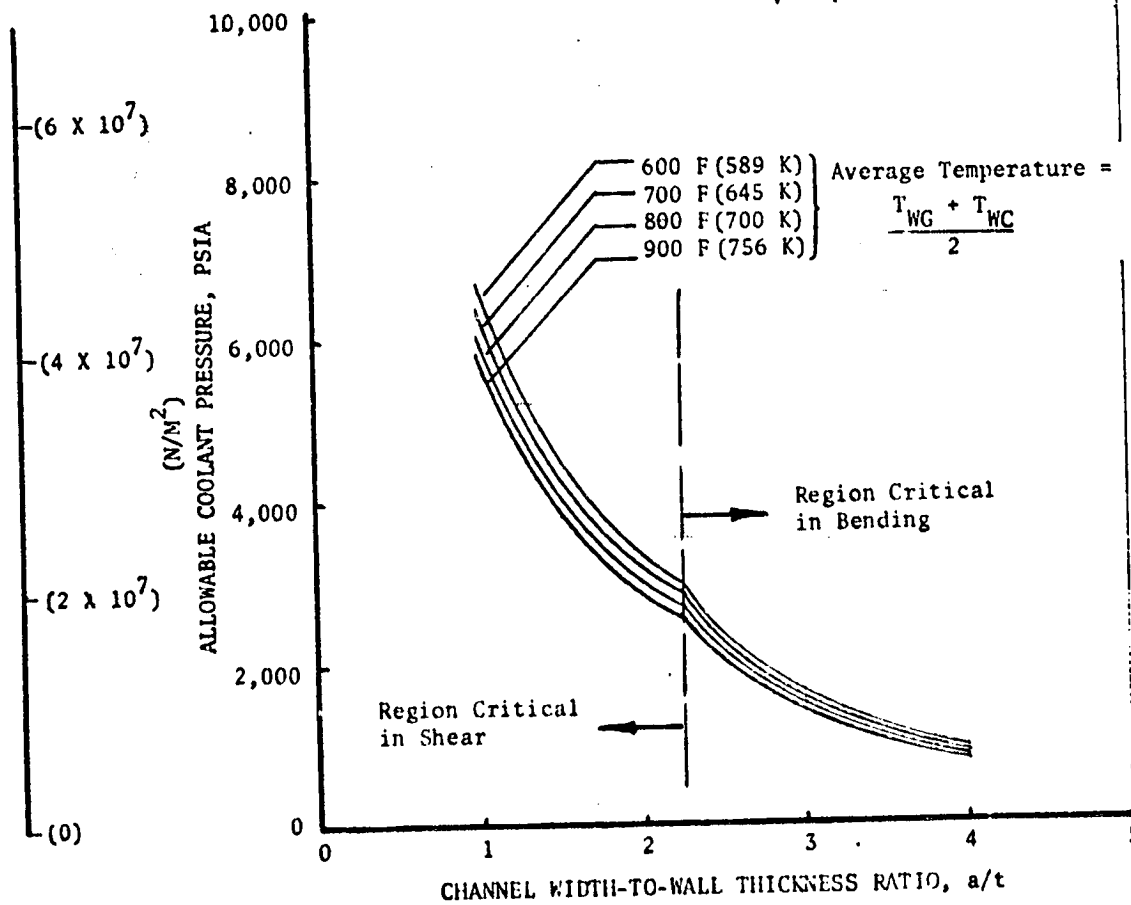
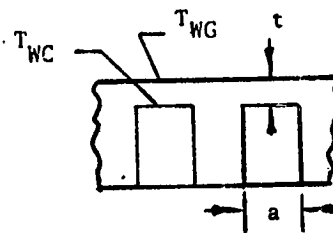


Figure 38. Basic Structural Criteria for Zirconium-Copper

NOTE: $P = \frac{1.62}{(a/t)^2} ; \sigma = \frac{F_{ty}}{1.2}$
 $P = \text{Allowable Coolant Pressure}$
 $\sigma = \text{Maximum Fixed End Beam Bending Stress}$
 $a = \text{Channel Width}$
 $t = \text{Nominal Hot Wall Thickness}$
 $F_{ty} = \text{Minimum Yield Strength at Average Temperature Through the Hot Wall}$

$P = \frac{1.2 \tau}{a/t} ; \tau = 0.6 \frac{F_{ty}}{1.2}$
 $\tau = \text{Maximum Hot Wall Shear Stress}$

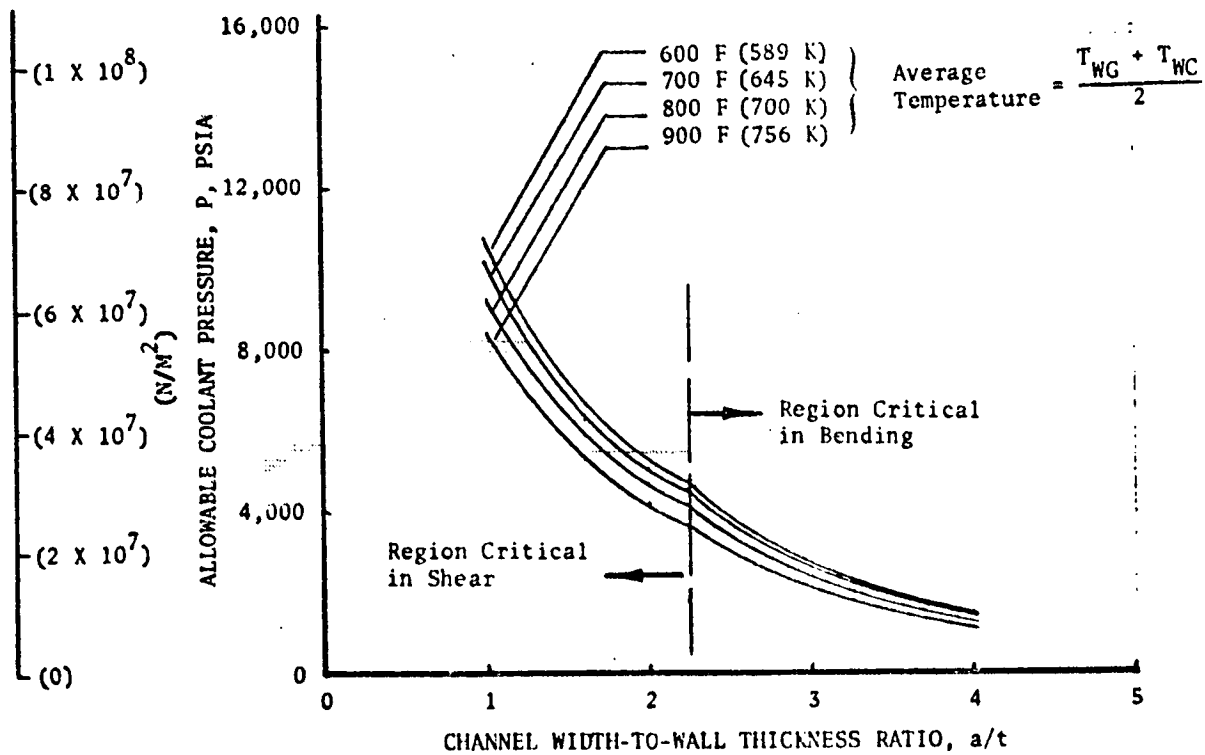
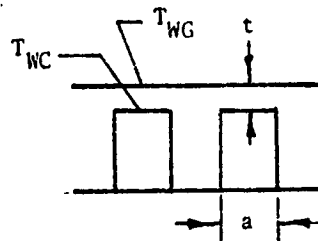


Figure 39. Basic Structural Criteria for NARloy-Z

In general, for Zr-Cu the damage fraction was limited by the fatigue damage fraction and the creep damage fraction was less than 0.01. Therefore, if the creep damage fraction is set equal to 0.01 (time to rupture of 1000 hours) and the backwall temperature is fixed at a reasonable design value, the fatigue damage fraction, θ_f , is dependent only on the gas-side wall temperature as shown in Fig. 40. For a θ_c of 0.01 the θ_f must be equal to or less than 0.24; therefore, from Fig. 40 a gas-side wall temperature limit of approximately 1020 F (822 K) exists¹. The optimum channel design may be determined by comparing designs resulting in a wall temperature of approximately 1020 F (822 K), which was done in Fig. 41. The designs shown all have a yield safety factor slightly greater than the required 1.2 (channel width-to-wall thickness ratio of approximately 1.5) and the designs with a channel width of 0.040-inch (0.1016 cm) and greater have a total damage fraction between 0.92 and 1.0.

As shown in Fig. 41, an optimum channel width of 0.040-inch (0.1016 cm) resulted for the Zr-Cu combustor. Basically, for a fixed channel-to-wall thickness ratio (a/t), the optimum channel width is the value at which the channel depth is approximately three times the channel width. Since this is the fabrication restriction placed on the designs, any smaller value of channel width will only result in a lower wall temperature, and therefore, a higher coolant pressure drop. Also, the 0.040-inch (0.1016 cm) channel width represents a reasonable minimum from a fabrication standpoint.

For the Zr-Cu channel wall combustor, an increase in the combustor-nozzle joint area ratio did not significantly influence the combustor coolant pressure drop; however, the combustor liner weight increased approximately 2 pounds (0.906 kg) for an increase in the joint area ratio from 4 to 8. Using the selected A-286 nozzle and Zr-Cu combustor designs, the optimum combustor-nozzle joint area ratio was determined from a total chamber coolant pressure drop and a combined combustor liner and nozzle tube weight. The results, presented in Fig. 42, indicated that the coolant pressure drop achieve a minimum at a joint area ratio of 8-to-1 with only a 2-pound (0.906 kg) increase in liner and tube weight; therefore, a combustor-nozzle joint area ratio of 8-to-1 was selected. The channel sizes and resulting wall temperature distributions for the selected Zr-Cu design are shown in Fig. 43 and 44. The minimum channel size was 0.040 by 0.112-inch (0.1017 by 0.2845 cm) with a minimum hot-gas wall thickness of 0.027-inch (0.686 cm). The maximum gas-side wall temperature of 1021 F (823 K) occurred 0.5-inch (1.27 cm) upstream of the geometric throat.

For the Zr-Cu channel wall combustor the basic structural requirements limited the channel width-to-wall thickness ratio (a/t) to approximately 1.5. Also, as discussed previously, the Zr-Cu design was limited because of the fatigue damage fraction. The NARloy-Z combustor was limited because of the creep damage fraction, which is a function of a/t . With certain assumptions, parametric life-cycle data to describe this influence were generated and resulted in the limit curve presented in Fig. 45. For Zr-Cu, at the assumed conditions shown in Fig. 45, the maximum allowable gas-side wall temperature limited because of the fatigue damage

¹ Subsequent finite stress element analysis indicated that the maximum wall allowable for the 300 cycle life for Zr-Cu was approximately 900 F (755 K).

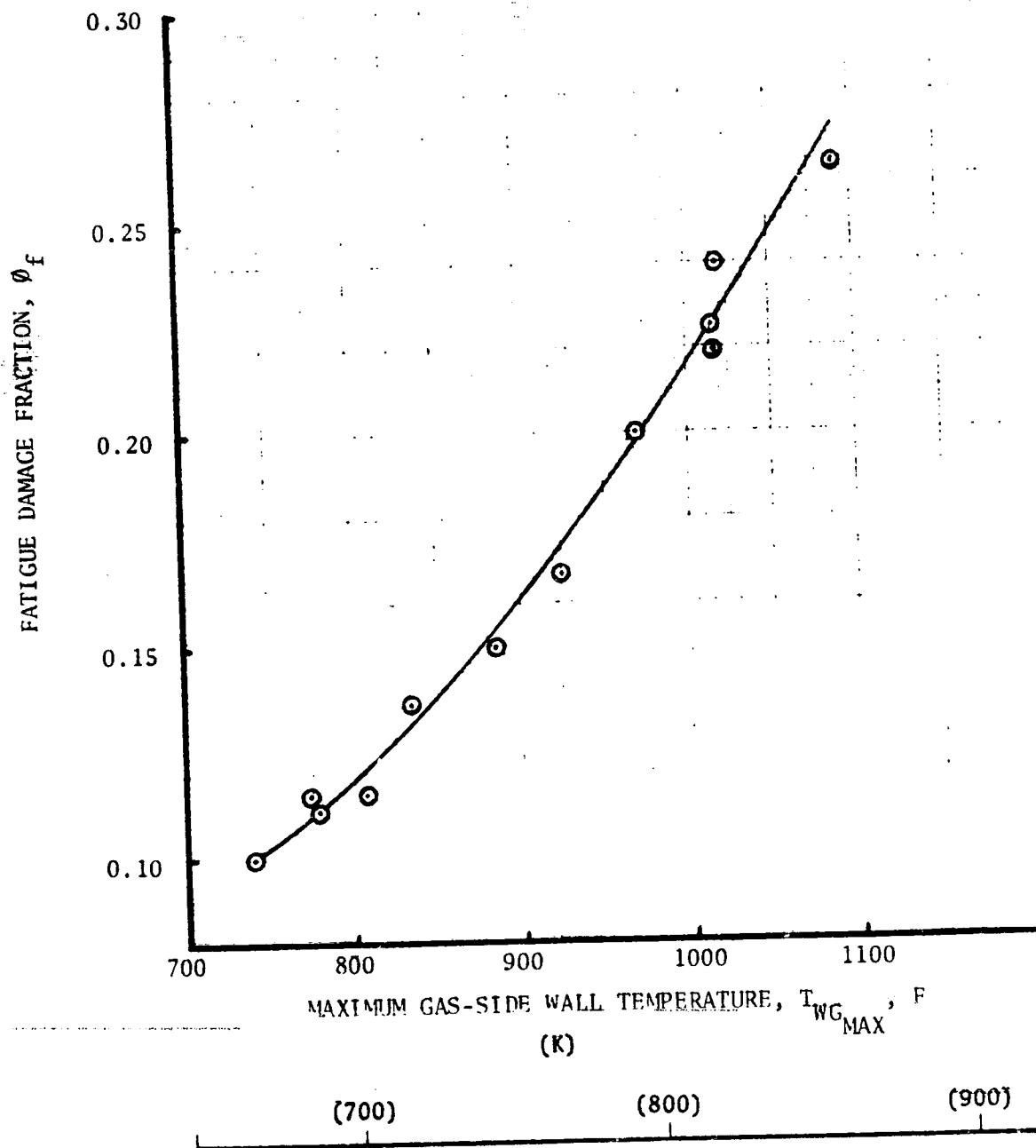


Figure 40. Fatigue Damage Fraction Variation With Wall Temperature for Zr-Cu Channel Configuration (1-1/2 Pass Cooling Circuit)

Coolant Circuit: 1-1/2 Pass (Regeneratively Cooled to $\epsilon = 100$)
 Material: Zr-Cu
 Channel Width-to-Wall Thickness Ratio: ~ 1.5

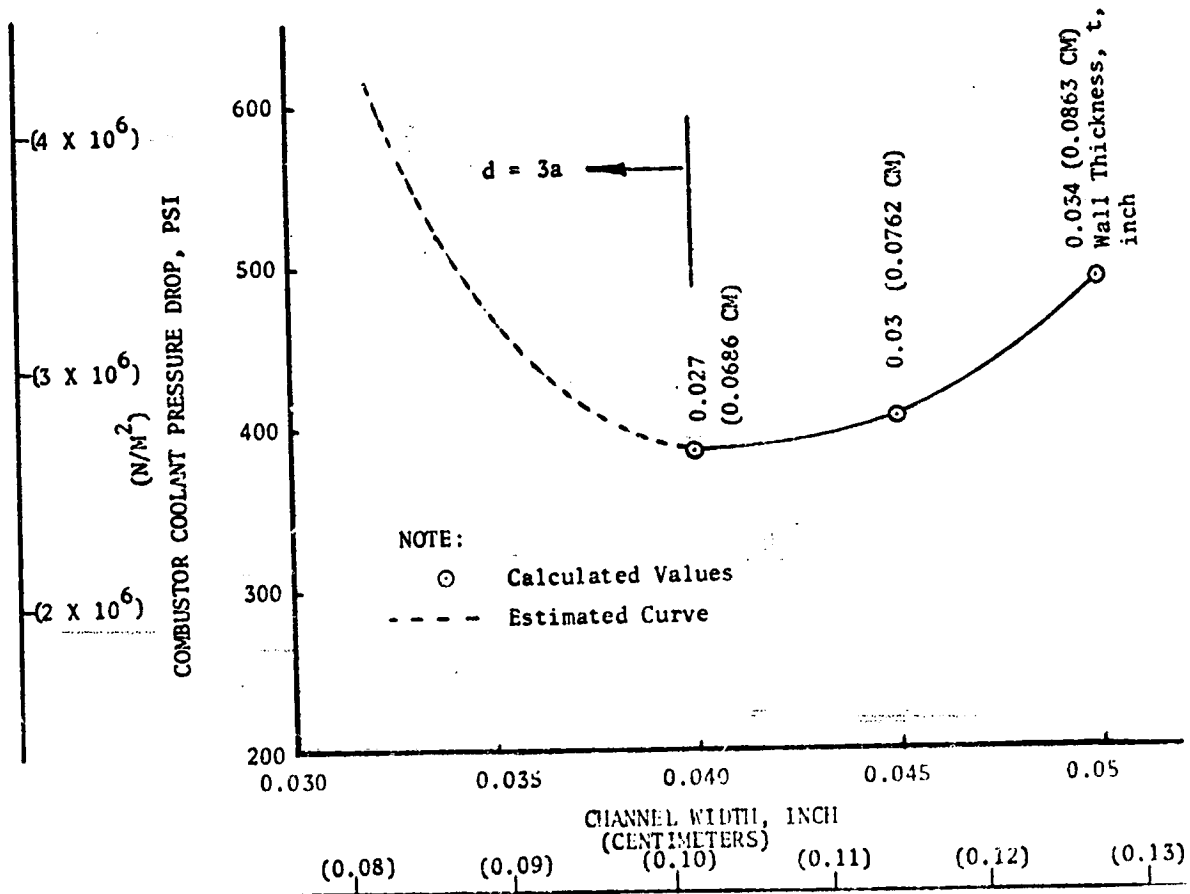
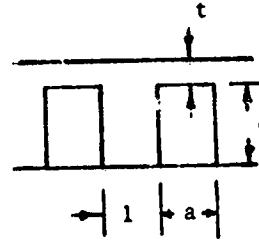


Figure 41. Zr-Cu Combustor (1-1/2 Pass Cooling Circuit) Channel Width Influence on Coolant Pressure Drop

Cooling Circuit: 1-1/2 Pass (Regeneratively Cooled to $\epsilon = 100$)
 Nozzle: 400 A-286 Booked Tubes
 Coolant Inlet: $\epsilon = 100$
 Combustor: Zr-Cu
 Minimum Channel Width = 0.040-inch (0.1016 CM)

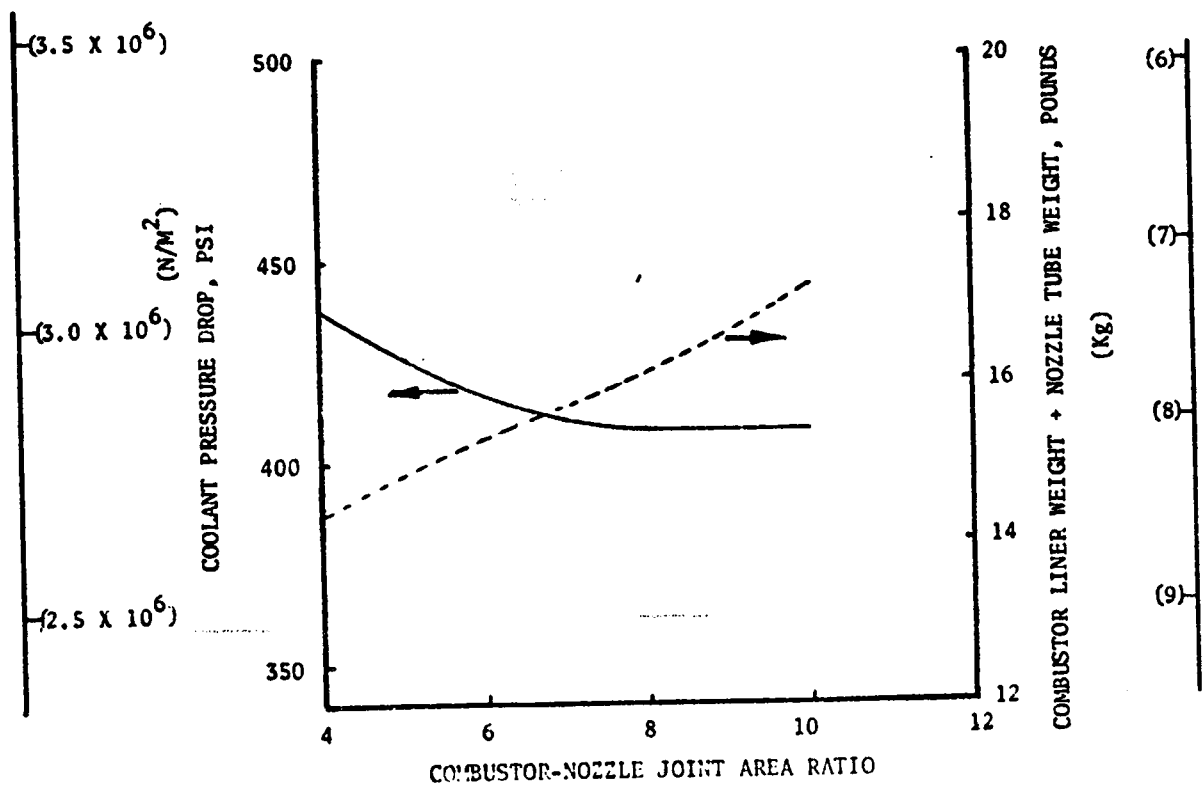


Figure 42. Chamber Coolant Pressure Drop and Weight Variation With Combustor-Nozzle Joint Area Ratio for Zr-Cu Combustor/A-286 Nozzle (1-1/2 Pass Cooling Circuit)

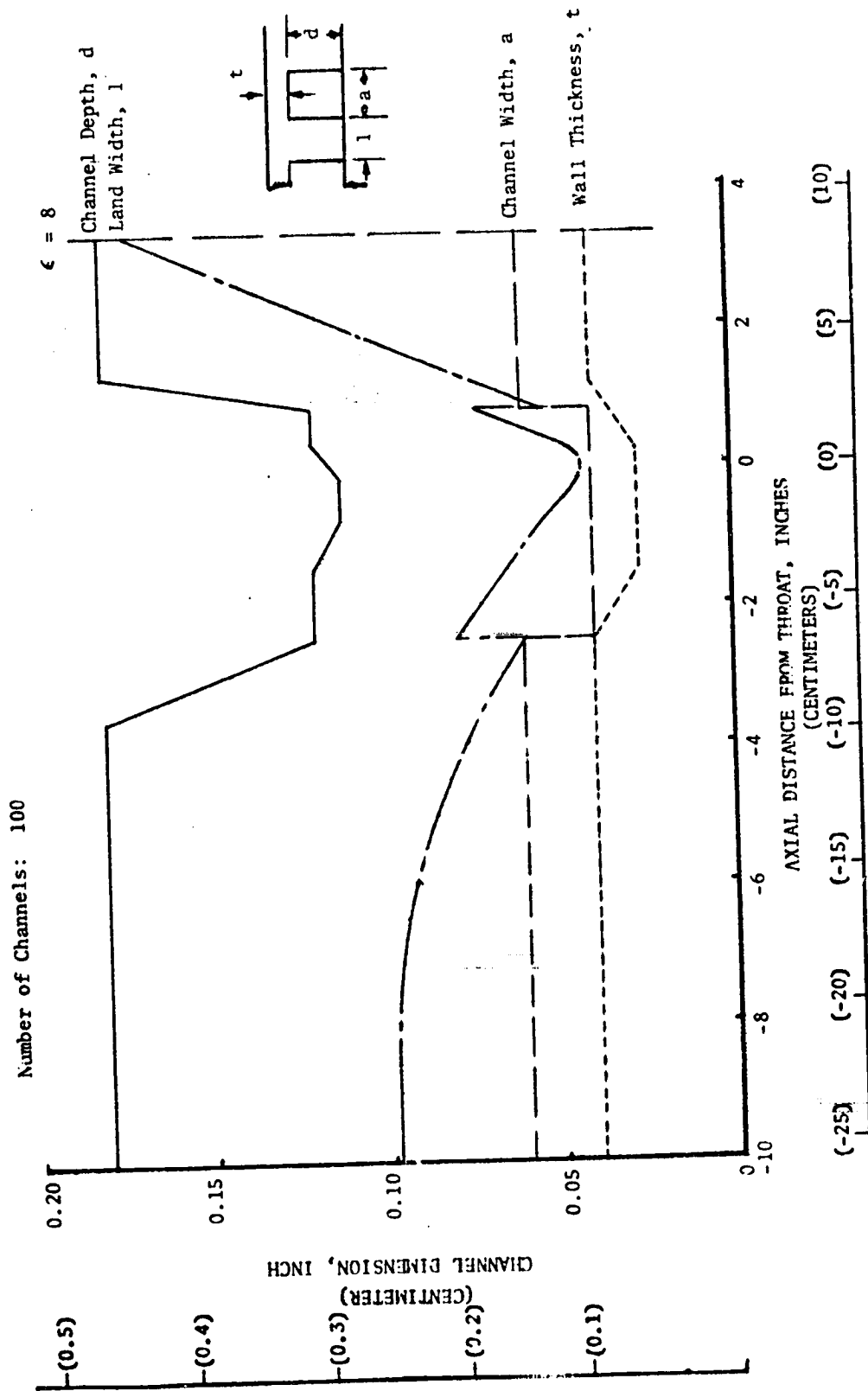


Figure 43. Channel Dimensions of the Selected Zr-Cu Channel Wall Combustor Configuration (1-1/2 Pass Cooling Circuit)

Coolant Circuit: 1-1/2 Pass (Regeneratively Cooled to $\epsilon = 100$)
 Combustor Liner Material: Zr-Cu
 Number of Channels: 100

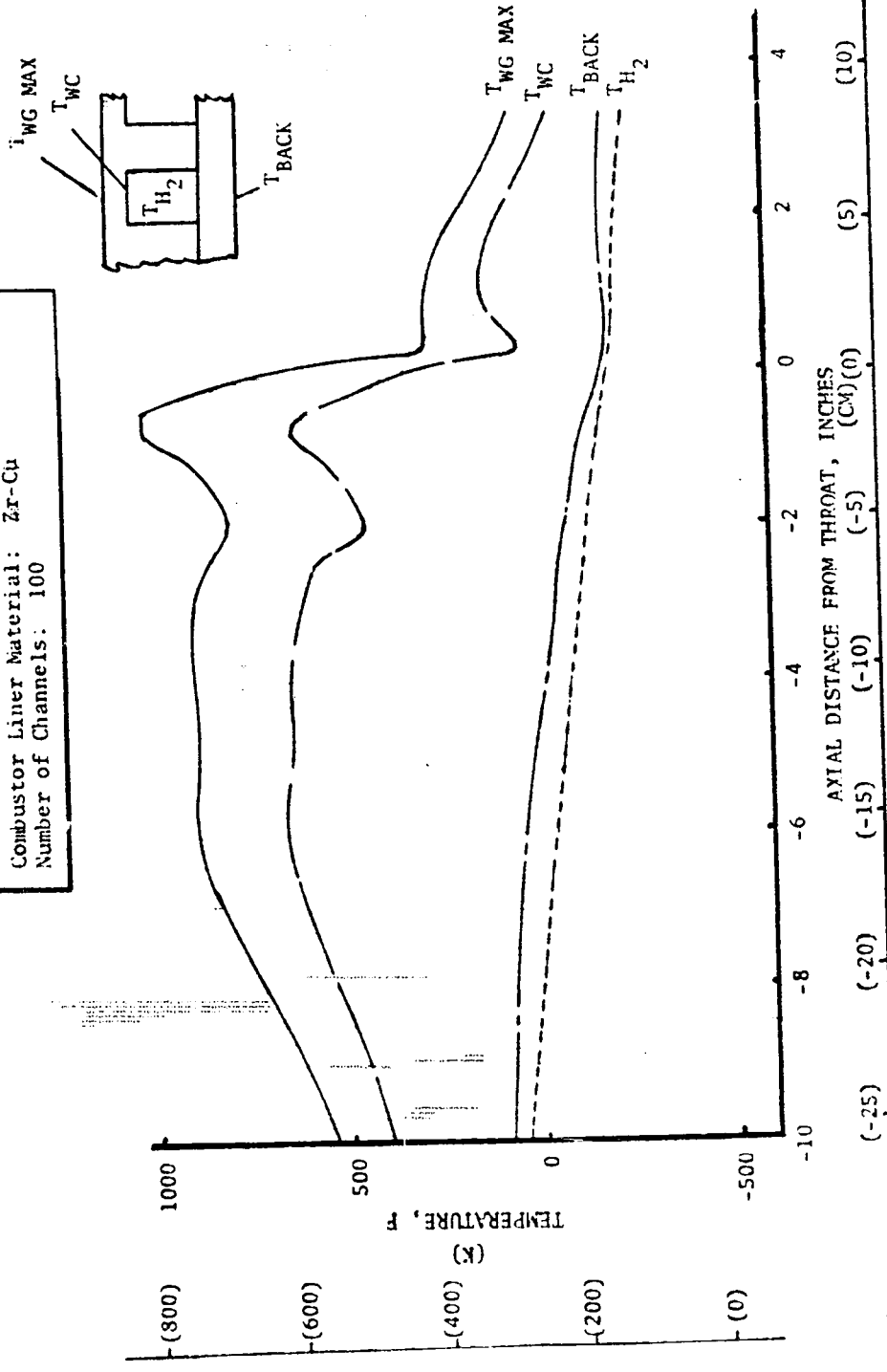


Figure 44. Temperature Distributions for the Selected Zr-Cu Channel Wall Combustor Configuration (1-1/2 Pass Cooling Circuit)

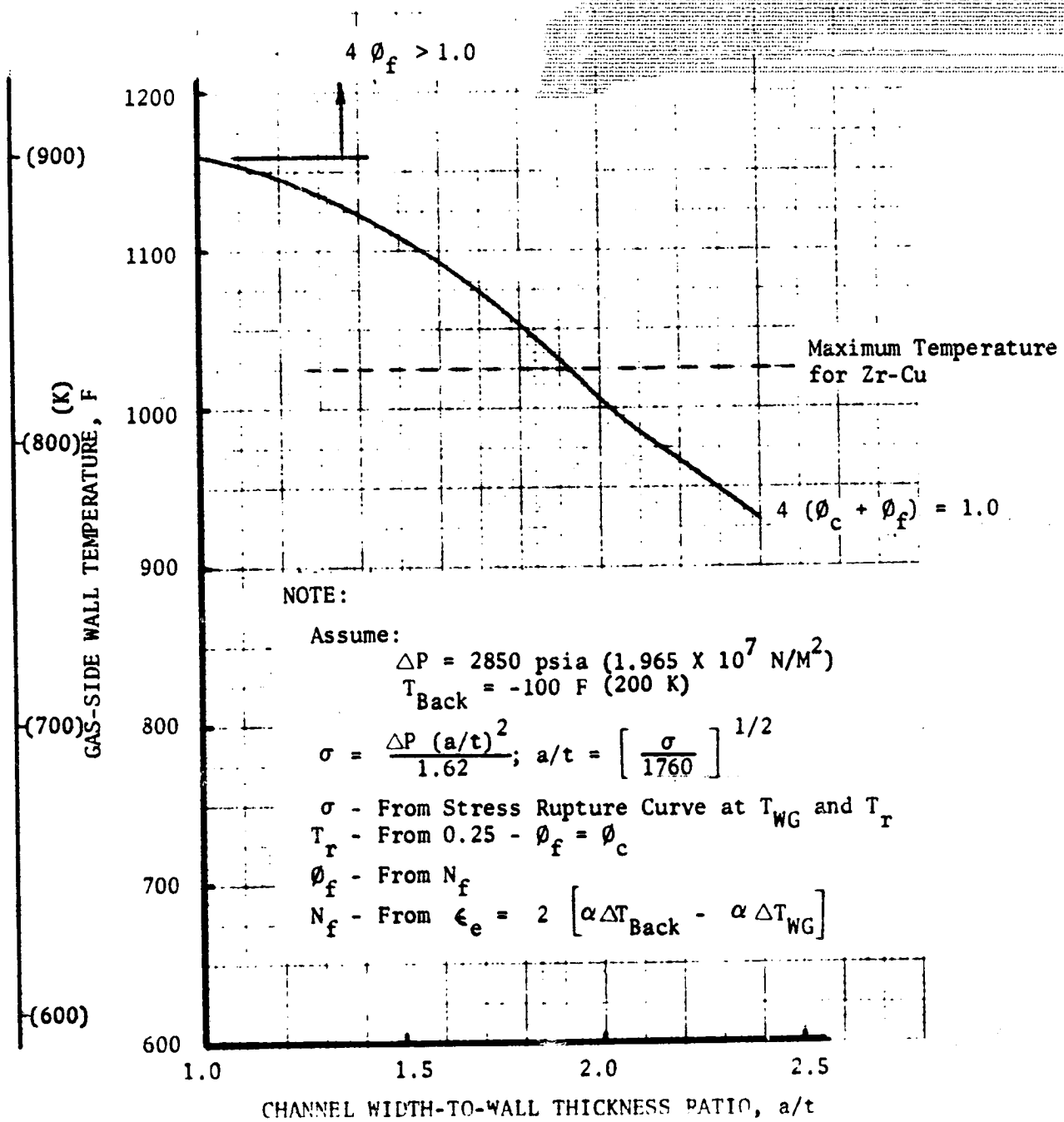


Figure 45. Maximum Allowable Wall Temperature to Meet Life Cycle Requirements (NARloy-2)

was approximately 1025 F (825 K). Therefore, NARloy-Z can achieve a higher allowable wall temperature than with Zr-Cu for a a/t less than 1.9. The higher allowable wall temperatures result in lower coolant pressure drops with the same cycle life.

As shown in Fig. 45, for NARloy-Z, low values of a/t resulted in higher allowable wall temperatures. For a fixed channel width low values of a/t means a thick wall; conversely a high value of a/t results in a thin wall. Now a thick wall (low a/t) will require a higher coolant mass velocity to achieve the same wall temperature, but a higher wall temperature is allowed to achieve the same cycle life so the result may be a lower coolant mass velocity. However, if the wall thickness becomes too large, an increased mass velocity will be required; therefore, there will be an a/t that will result in a minimum coolant pressure drop.

An analysis was performed for the NARloy-Z combustor in which the channel width and the channel width-to-wall thickness ratio were varied as shown in Fig. 46. An a/t of approximately 1.8 was optimum. A channel width of 0.045-inch (0.1143 cm) represented the optimum channel width for NARloy-Z, which was the result of the high strength and the higher cycle-life capability of NARloy-Z. These factors resulted in a higher allowable wall temperature (1050 F or 838 K versus 1020 F or 822 K), which resulted in larger coolant channels (larger channel width) and lower combustor coolant pressure drops. The channel dimensions and wall temperature distribution for the selected NARloy-Z channel combustor (minimum channel width = 0.045-inch (0.1142 cm) and minimum wall thickness = 0.025-inch (0.0635 cm), (a/t = 1.8) are presented in Fig. 47 and 48.

A comparison of the Zr-Cu and NARloy-Z 1-1/2 pass cooling circuit channel wall combustors is presented in Table V. An overall comparison of the two configurations is shown in Table VI. Both channel wall combustors resulted in narrow, tall coolant channels, which tend to increase thrust chamber weight. As shown in Table VI, the higher allowable channel width-to-wall thickness ratio (a/t) for the NARloy-Z combustor resulted in a slightly thinner wall thickness. Because of this thinner wall and the higher allowed wall temperatures (resulting from its better thermal fatigue characteristics), the NARloy-Z design achieved a 101 psi ($6.96 \times 10^5 \text{ N/m}^2$) coolant pressure drop reduction.

For the selected A-286 tubular nozzle (1-1/2 pass cooling circuit), three hatbands of 0.00208 in² (0.01342 cm²) minimum cross-sectional area would be sufficient to meet the structural requirements. However, to facilitate accurate nozzle contour control in brazing the tubes, an additional hatband was added as shown in Fig. 49 and 50. The 400 A-285 nozzle tubes are beveled and tapered tubes with a constant 0.007-inch (0.01778 cm) tube wall thickness. The joint between the channel wall combustor and the tubular nozzle is at an area ratio of 8-to-1.

The combustor coolant channels are milled and closed out with electroformed nickel with an INCO 818 structural jacket (Fig. 49 and 50). As for the tubular configurations, the minimum calculated jacket thicknesses (Fig. 51) were increased to a constant 0.06-inch (0.1524 cm) for fabrication simplicity. If deemed necessary for a reduced chamber weight, a thinner structural jacket could be fabricated.

Coolant Circuit: 1-1/2 Pass (Regeneratively Cooled to $\epsilon = 100$)
 Material: NARloy-Z
 Combustor-Nozzle Joint: $\epsilon = 8$

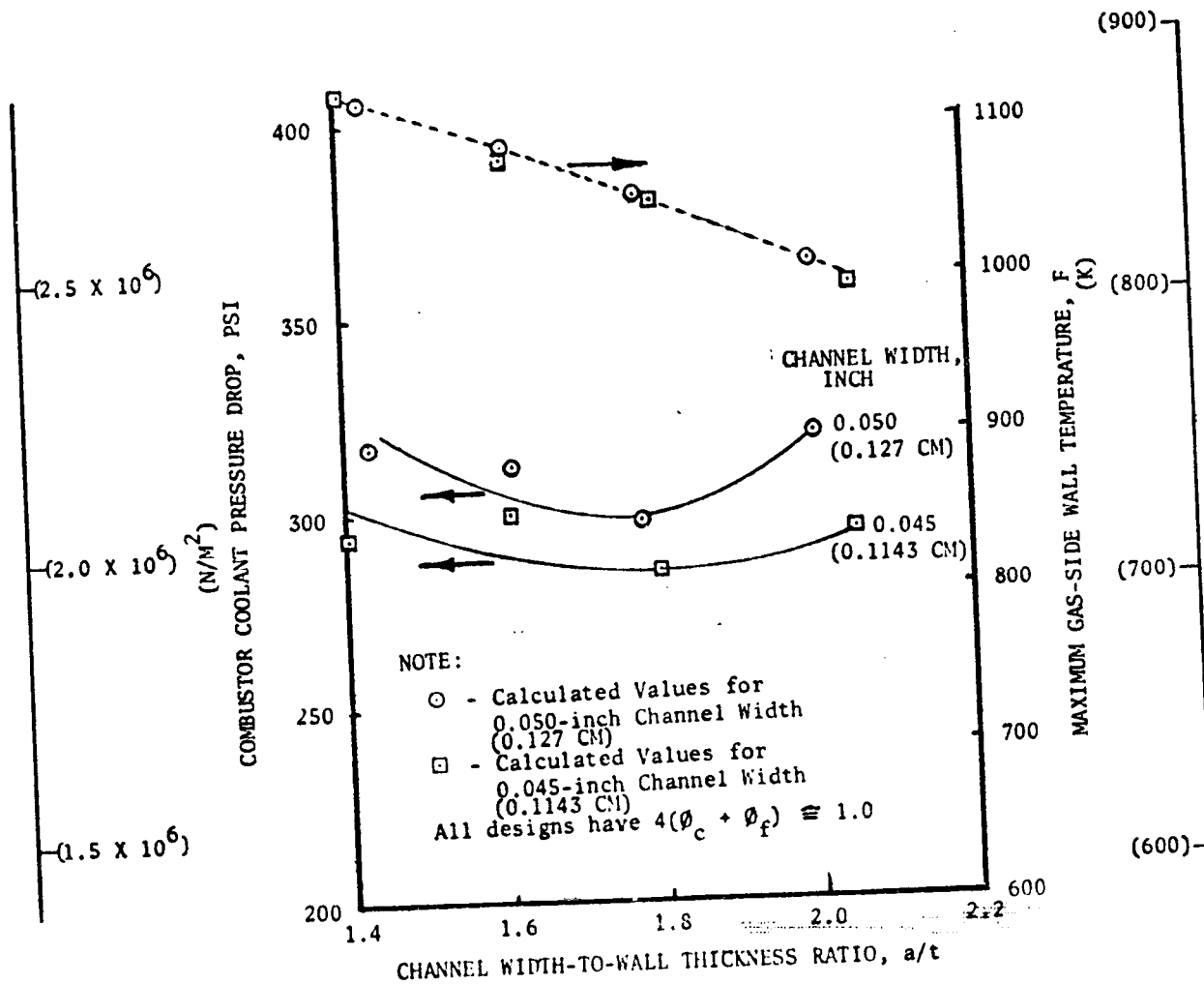


Figure 46. NARloy-Z Combustor (1-1/2 Pass Cooling Circuit) Channel Width-to-Wall Thickness Ratio Influence

Number of Channels: 95

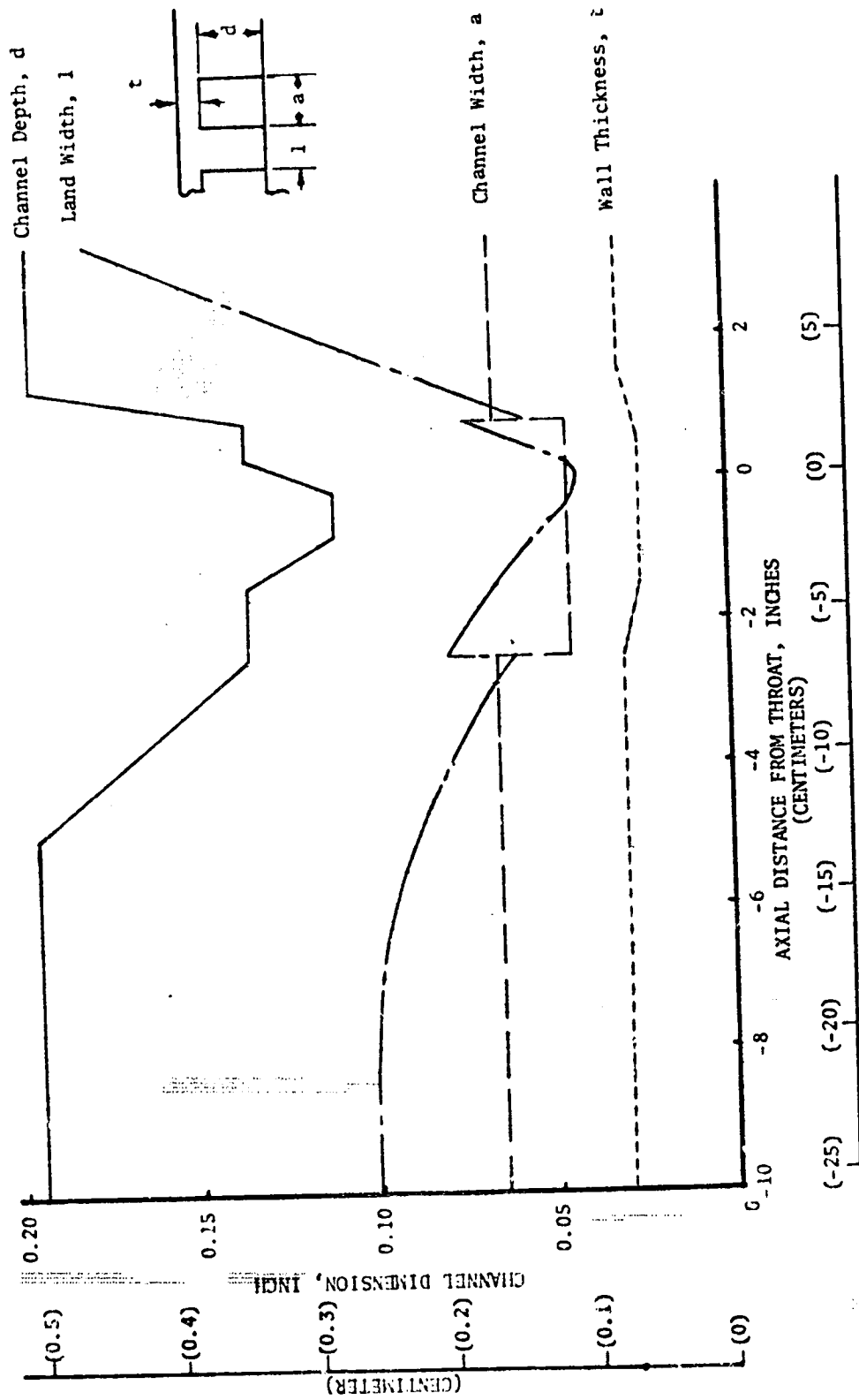


Figure 47. Channel Dimensions of the Selected NARLOY-Z Channel Wall Combustor Configuration (1-1/2 Pass Cooling Circuit)

Cooling Circuit: 1-1/2 Pass (Regeneratively Cooled to $\epsilon = 100$)
 Combustor Liner Material: NARLOY-Z
 Number of Channels: 95

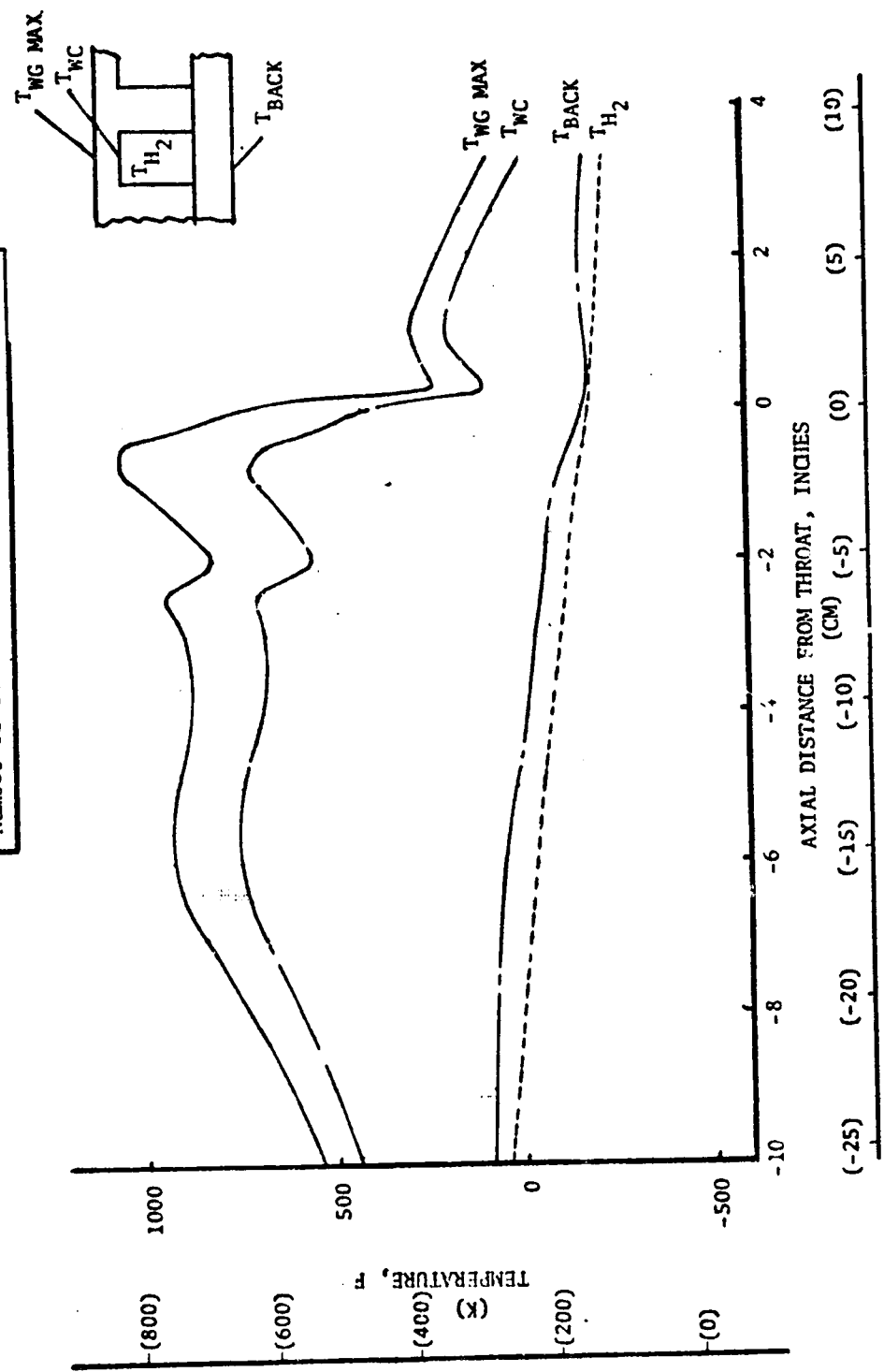


Figure 48. Temperature Distributions for the Selected NARLOY-Z Channel Wall Combustor Configuration (1-1/2 Pass Cooling Circuit)

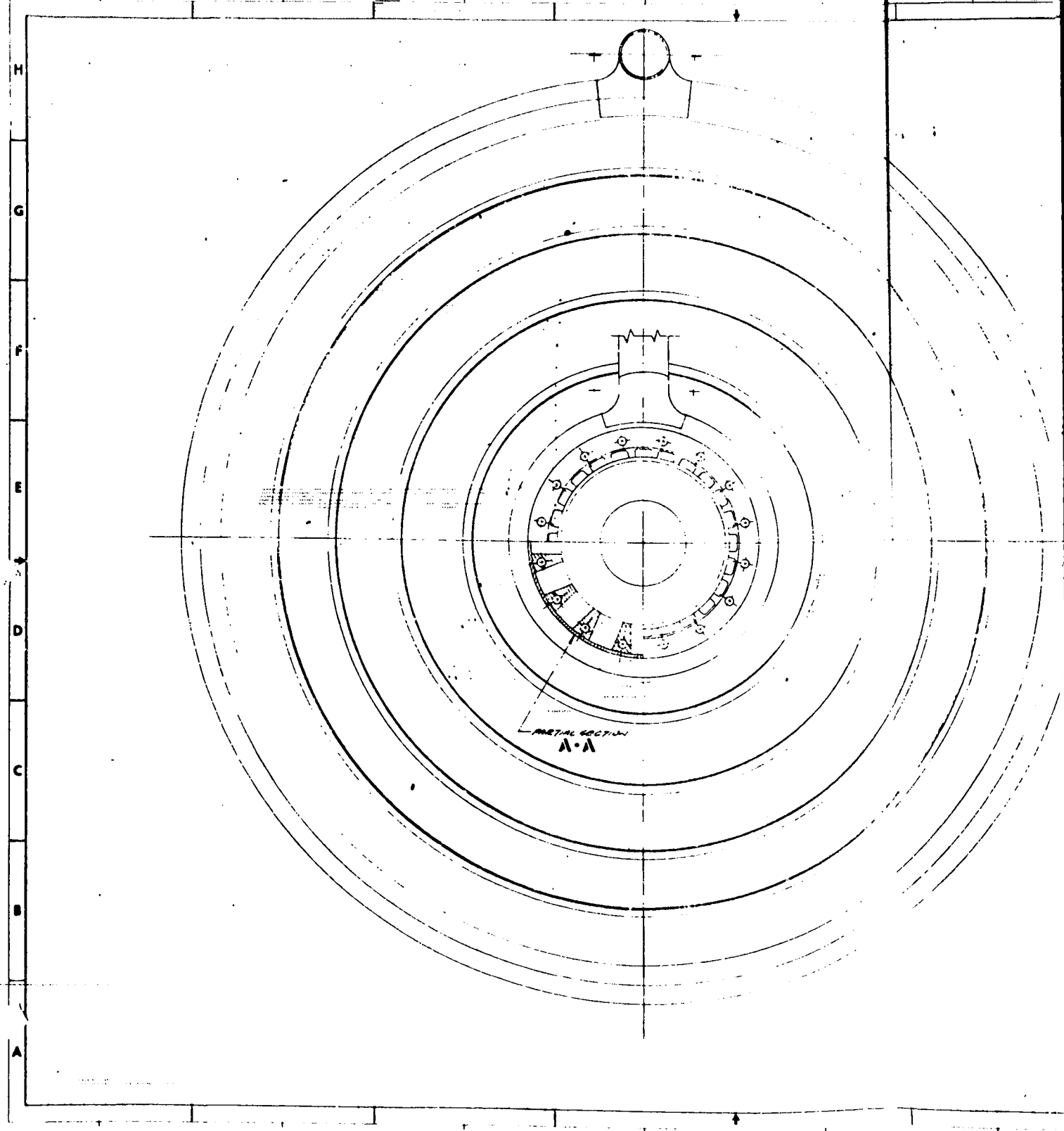
TABLE V. COMPARISON OF SELECTED 1-1/2 PASS COOLING CIRCUIT CHANNEL WALL COMBUSTORS

	Zr-Cu	NARloy-Z
Number of Channels	100	95
Combustor-Nozzle Joint Area Ratio	8	8
Channel Dimensions at the Critical Stress/Life Location:		
Location, inch	-0.50 (-1.28 CM)	-0.80 (-2.032 CM)
Width, inch	0.040 (0.1016 CM)	0.045 (0.1143 CM)
Depth, inch	0.112 (0.2845 CM)	0.110 (0.2775 CM)
Land, inch	0.0478 (0.1215 CM)	0.0532 (0.135 CM)
Hot-Gas Wall Thickness, inch	0.027 (0.0686 CM)	0.025 (0.0635 CM)
Maximum Gas-Side Wall Temperature, F	1022 (823 K)	1051 (840 K)
Combustor Coolant Pressure Drop, psi	386 (2.66 x 10 ⁶ N/m ²)	285 (1.962 x 10 ⁶ N/m ²)
Combustor Liner Weight, pounds	9.3 (4.22 Kg)	9.2 (4.17 Kg)
Critical Location Stress and Life Parameters:		
Yield Safety Factor	1.25	1.50
Ultimate Safety Factor	1.93	2.37
Damage Fraction	4 (0.01 + 0.24) = 1.00	4 (0.0451 + 0.182) = 0.912
4 ($\phi_c + \phi_f$)		

TABLE VI. SELECTED A-286 TUBULAR NOZZLE/CHANNEL WALL COMBUSTOR CONFIGURATION (1-1/2 PASS COOLING CIRCUIT)

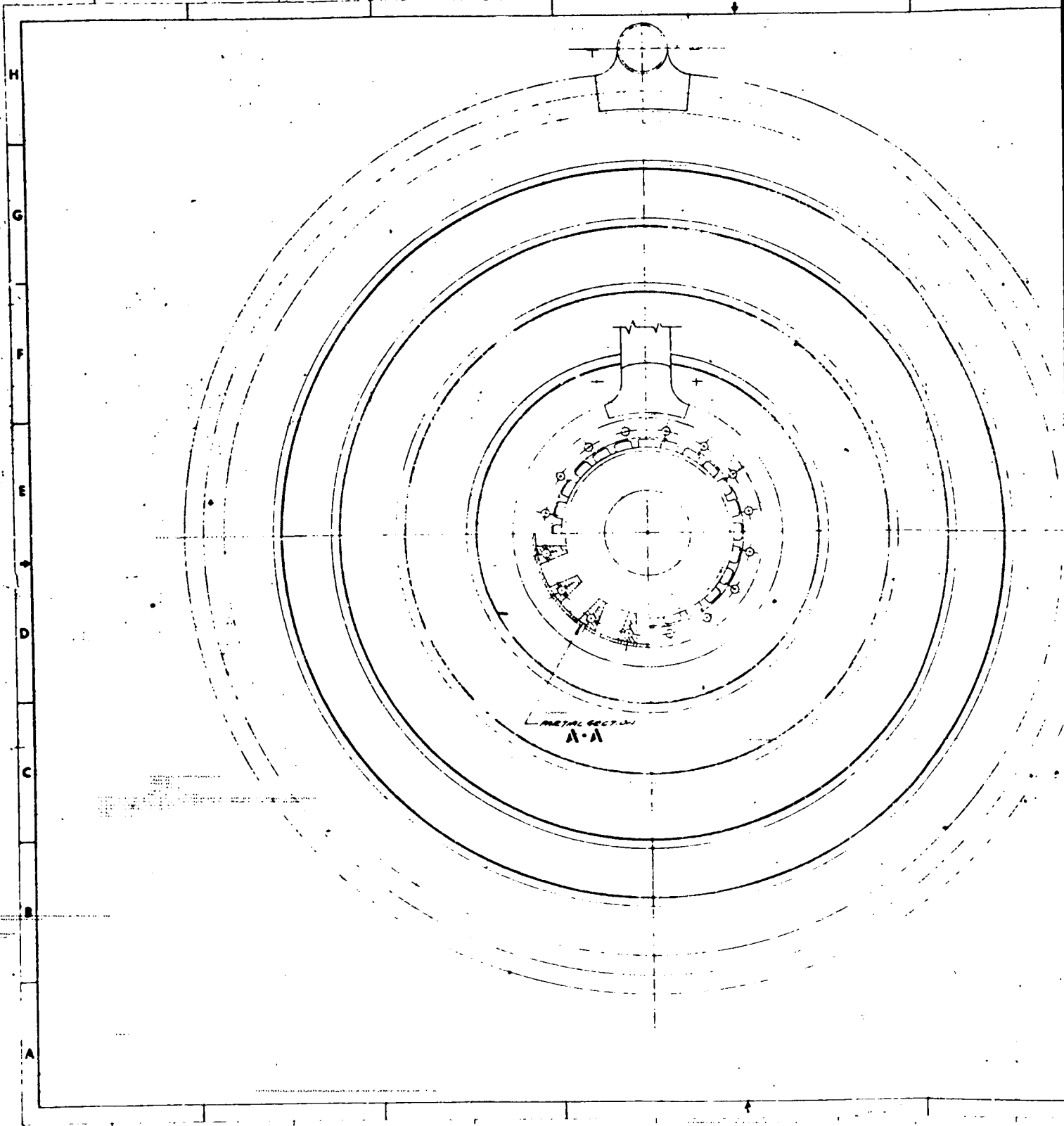
<u>Nozzle:</u>			
Material		A-286	
Number of Tubes		400	
Tube Wall Thickness, inch		0.007 (0.01778 CM)	
Coolant Inlet Area Ratio		100	
Combustor-Nozzle Joint Area Ratio		8	
Nozzle Coolant Tube Weight, pounds		6.8 (3.085 Kg)	
Maximum Gas-Side Wall Temperature, F		525 (547 K)	
Nozzle Coolant Pressure Drop, psi		24 for NARLOY-Z Combustor ($1.655 \times 10^5 \text{ N/m}^2$)	
		22 for Zr-Cu Combustor ($1.518 \times 10^5 \text{ N/m}^2$)	
<u>Combustor:</u>			
Material		Zr-Cu	NARLOY-Z
Number of Channels		100	95
Minimum Channel Width, inch		0.040 (0.1016 CM)	0.045 (0.1143 CM)
Minimum Channel Depth, inch		0.112 (0.2845 CM)	0.110 (0.2795 CM)
Minimum Channel Land, inch		0.0427 (0.1083 CM)	0.042 (0.1067 CM)
Minimum Hot-Gas Wall Thickness, inch		0.027 (0.0686 CM)	0.025 (0.0635 CM)
Combustor Liner Weight, pounds		9.3 (4.22 Kg)	9.2 (4.17 Kg)
Maximum Gas-Side Wall Temperature, F		1022 (823 K)	1051 (840 K)
Combustor Coolant Pressure Drop, psi		386 ($2.66 \times 10^6 \text{ N/m}^2$)	285 ($1.962 \times 10^6 \text{ N/m}^2$)
<u>Chamber:</u>			
Coolant Pressure Drop, psi		408 ($2.82 \times 10^6 \text{ N/m}^2$)	309 ($2.132 \times 10^6 \text{ N/m}^2$)
Combustor Liner Plus Nozzle Tube Weight, pounds		16.1 (7.3 Kg)	16.0 (7.26 Kg)

42021381



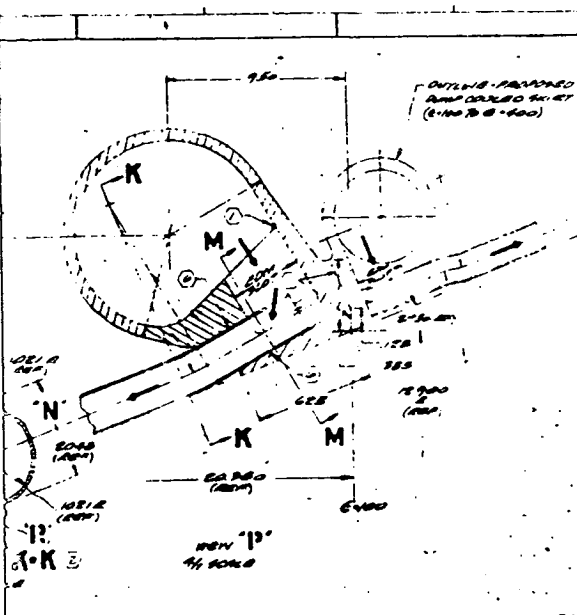
FOLDOUT FRAME

FOLDOUT



FOLDOUT BE AMT

FOLDOUT IN



Coolant Circuit: 1-1/2 Pass (Regeneratively Cooled to $\epsilon = 100$)

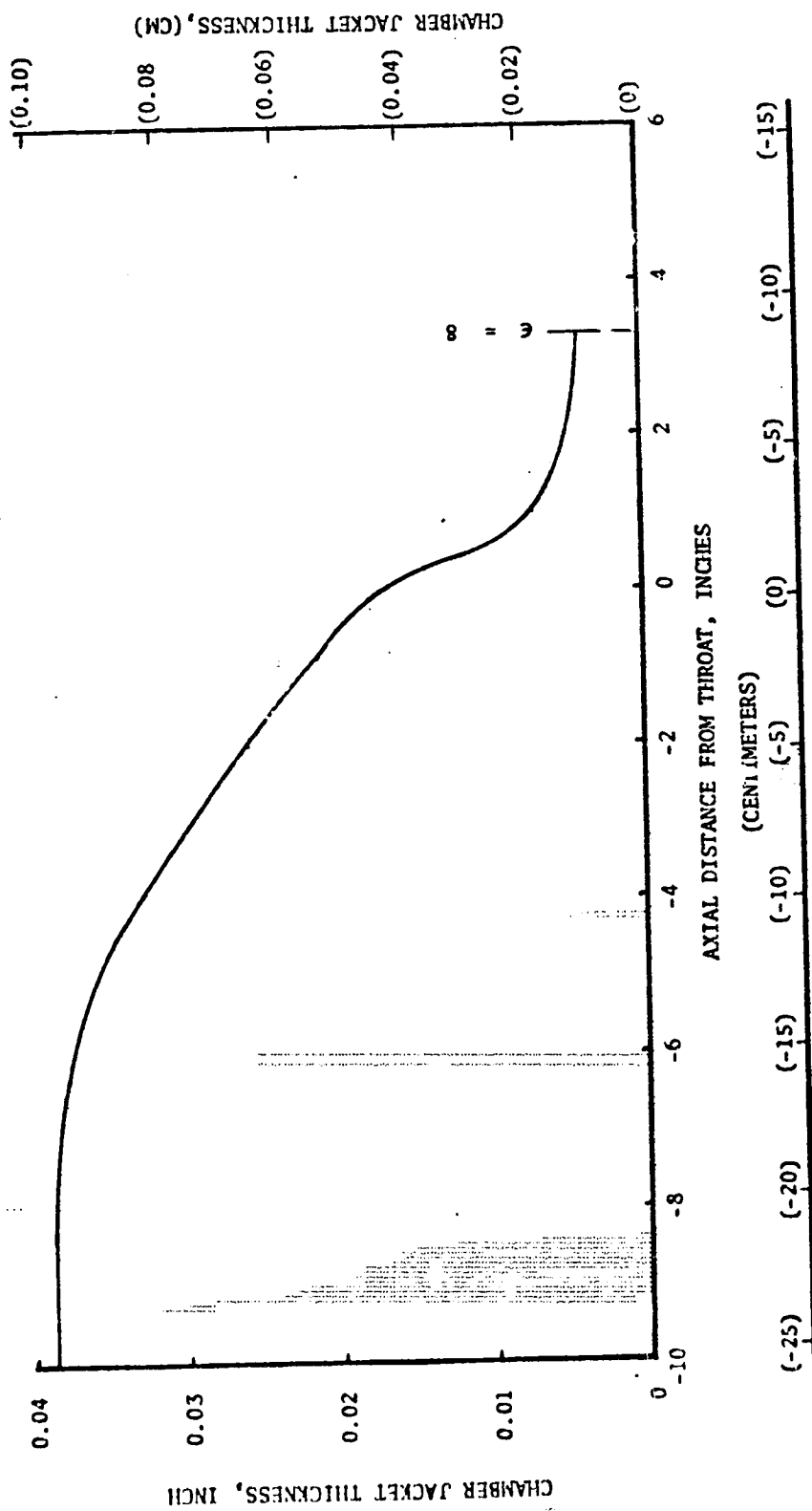


Figure 51. Chamber Jacket Thickness Distribution for the Channel Wall Combustor/Tubular Nozzle Configuration (1-1/2 Pass Cooling Circuit)

CHANNEL WALL COMBUSTOR/TUBULAR NOZZLE
(SPLIT-FLOW COOLING CIRCUIT)

Tubular A-286 Nozzle

As shown in Table I, the flow split for the split-flow cooling circuit was 68 percent for the combustor and 32 percent for the nozzle (to $\epsilon = 100$). These percentages were of the 5.6 lb/sec (2.54 Kg/sec) of hydrogen available for regenerative cooling. As previously discussed, these quantities were obtained from initial engine system analyses performed as part of the Advanced O_2/H_2 Engine Preliminary Design Program (Contract NAS3-16751).

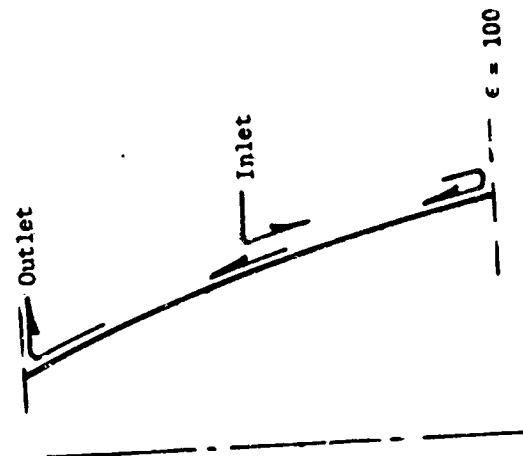
For the split-flow circuit, the nozzle may be cooled in three basic configurations, which are illustrated in Fig. 52. These include:

1. 1-1/2 pass cooling circuit
2. Reverse 1-1/2 pass cooling circuit
3. Modified reverse 1-1/2 pass cooling circuit

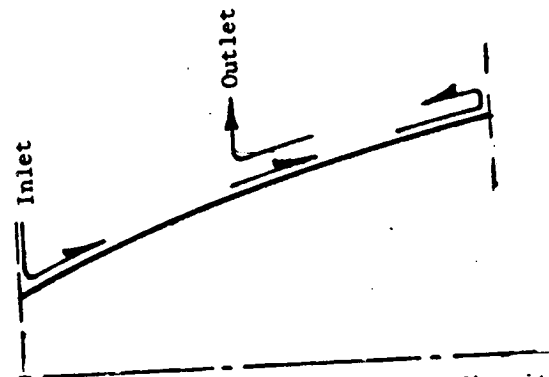
The last configuration had a large disadvantage in that the coolant at the exit ($\epsilon = 100$) would require a large manifold on a large diameter and a long large diameter return line. Both of these features represent additional chamber weight; therefore, design and analysis for the split-flow circuit evaluated the first two configurations and also evaluated the up-pass circuit, which is a degenerate case of the 1-1/2-pass coolant circuit with the inlet at the 100-to-1 area ratio.

Evaluation of the reversed 1-1/2 pass cooling circuit revealed that a degenerate case (a down-pass circuit) achieves a low nozzle coolant pressure drop (15 psi or $1.034 \times 10^4 \text{ N/m}^2$), but would have the longest coolant return line and also a large manifold on a large diameter. Both of these features increase chamber weight, therefore, the booked tube up-pass circuit was analyzed.

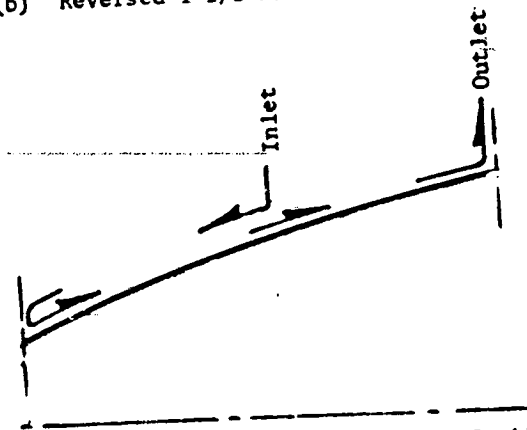
For the uppass cooling circuit, parametric heat transfer data for the A-286 nozzle, shown in Fig. 53 through 55, were generated for round tubes. These data indicated a trend seen previously, that an increase in number of tubes resulted in an increase in nozzle coolant pressure drop, a decrease in wall temperature, and slight decrease in coolant tube weight. As shown in Fig. 55, the inside tube diameter becomes less than 0.03-inch (0.0762 cm) for greater than 525 tubes. The results of the booked tube, up-pass nozzle cooling circuit are presented in Fig. 56 and 57. As shown in Fig. 56, various booked tube configurations were analyzed. Results (Fig. 57) indicated that a gas-side wall temperature of less than 700 F (389 K) could be achieved with less than 40 psi ($2.76 \times 10^5 \text{ N/m}^2$) nozzle coolant pressure drop. This design (Design B) represents the most significant pressure drop reduction from the round tube configuration and therefore was selected for the split-flow cooling circuit. This design also should minimize coolant outlet manifold and coolant return line weight. The tube dimensions, coolant static pressure distribution, and wall temperature distribution for the selected nozzle are presented in Fig. 58 through 60.



(a) 1-1/2 Pass Cooling Circuit



(b) Reversed 1-1/2 Pass Cooling Circuit



(c) Modified Reversed 1-1/2 Pass Cooling Circuit

Figure 52. Candidate A-286 Nozzle Split-Flow-Cooling Circuits

Coolant Circuit: Split-Flow
 Tube Material: A-286
 Coolant Inlet: $\epsilon = 100$
 Combustor-Nozzle Joint: $\epsilon = 8$
 Tube Wall Thickness: 0.007-inch (0.01778 CM)
 (Constant)

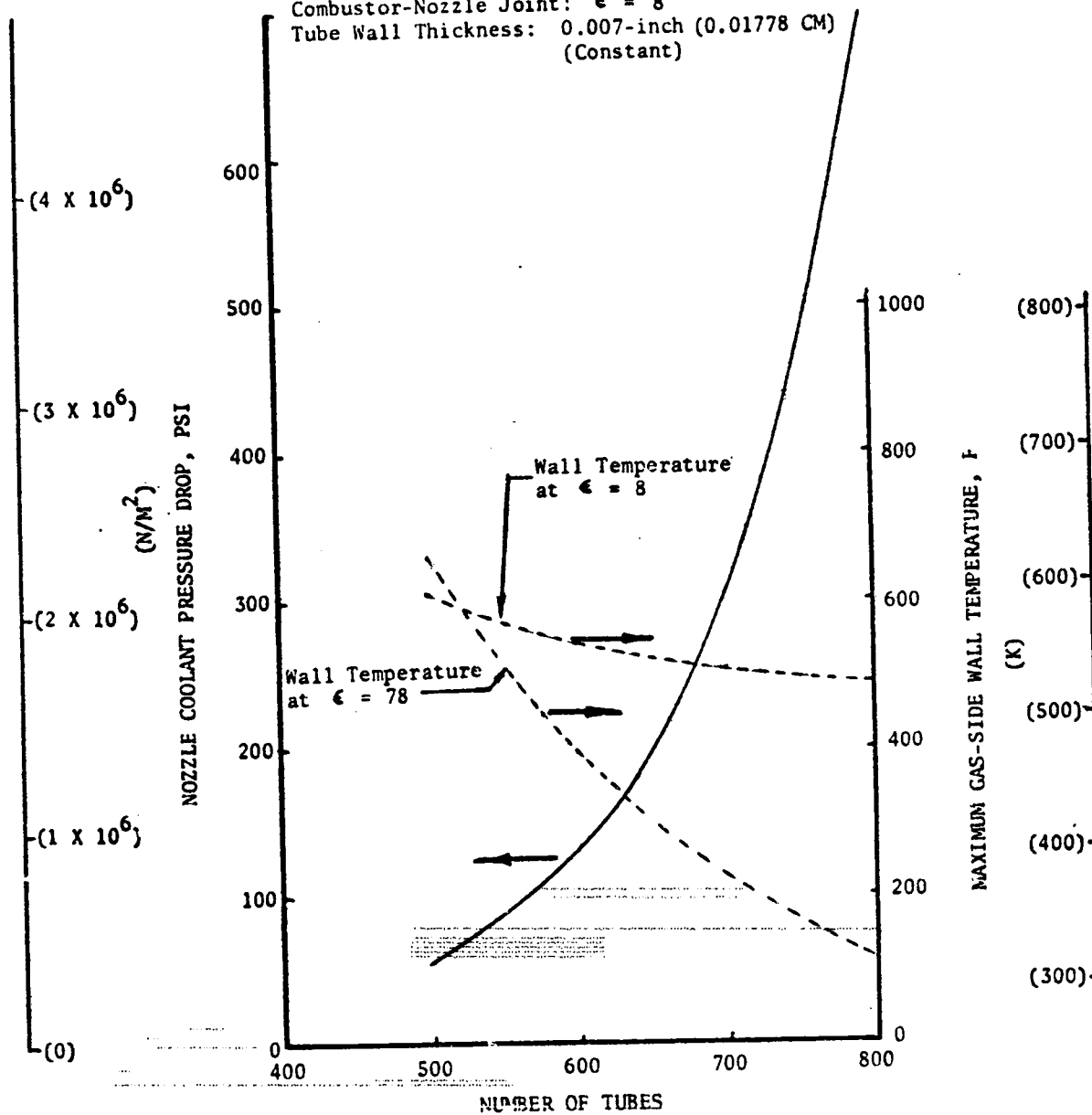


Figure 53. A-286 Nozzle Split-Flow Circuit (Round Tube Configuration) Coolant Pressure Drop and Wall Temperature Variation With Number of Tubes

Coolant Circuit: Split-Flow
 Tube Material: A-286
 Coolant Inlet: $\epsilon = 100$
 Combustor-Nozzle Joint: $\epsilon = 8$
 Tube Wall Thickness: 0.007-inch (0.01778 CM)

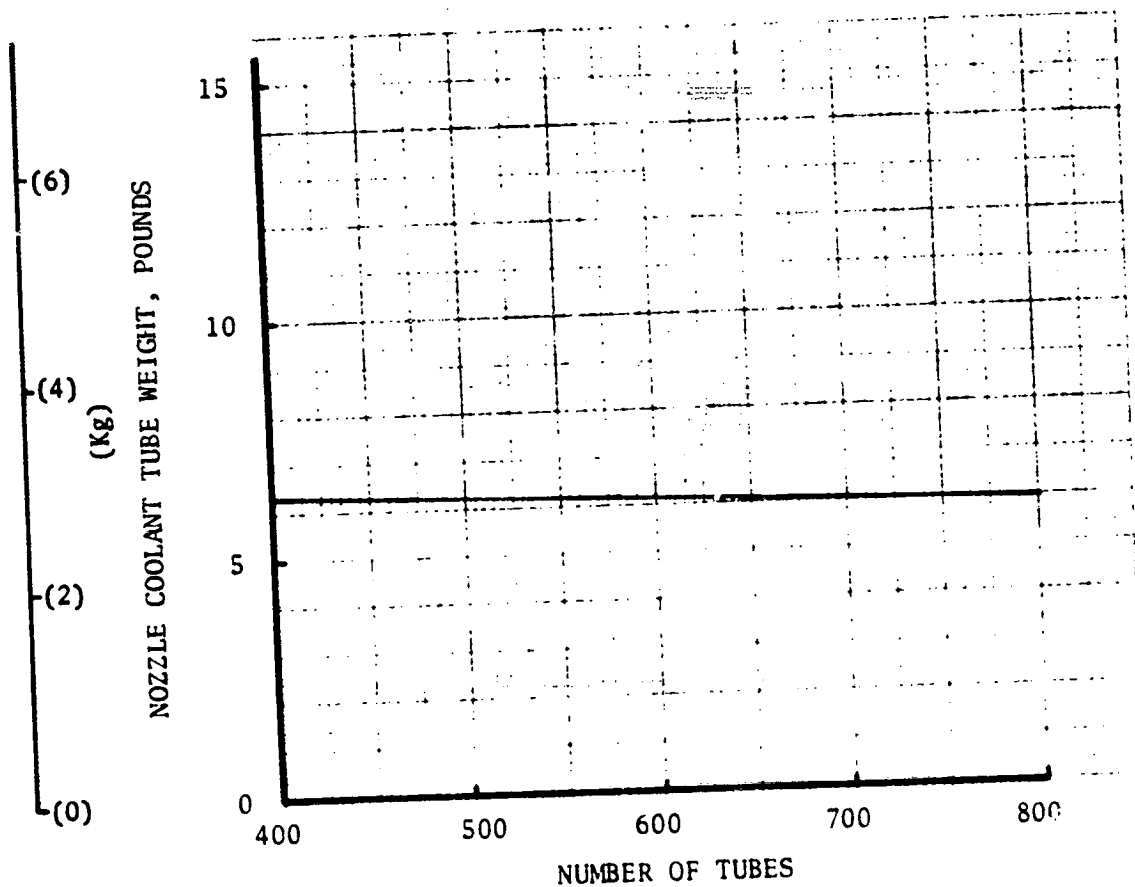


Figure 54. A-286 Nozzle (Round Tube Configuration)
 Tube Weight Variation With Number of
 Tubes (Uppass Coolant Circuit)

Coolant Circuit: Split-Flow
 Coolant Inlet: $\epsilon = 100$
 Combustor-Nozzle Joint: $\epsilon = 8$
 Tube Wall Thickness: 0.007-inch (0.01778 CM)
 (Constant)

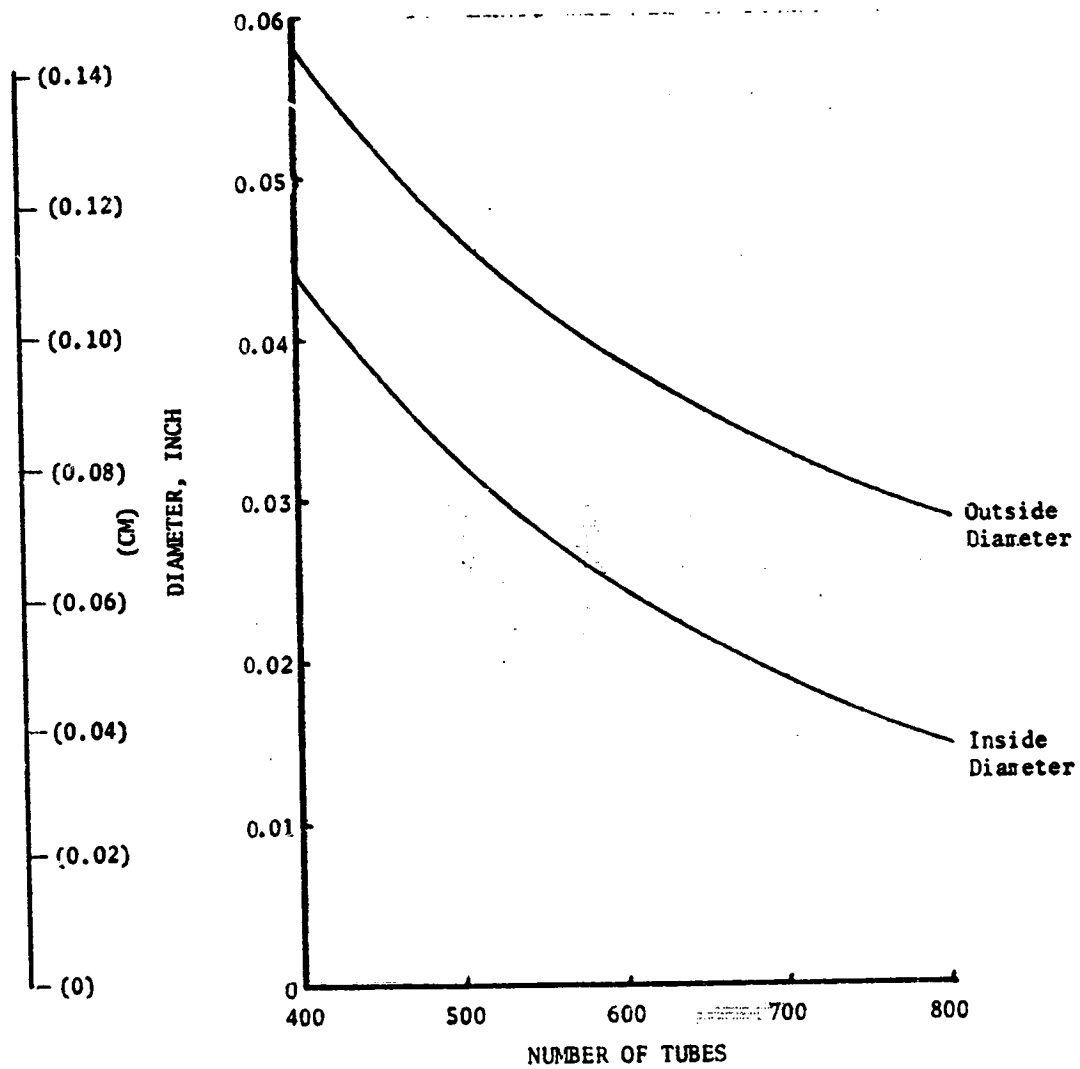


Figure 55. A-286 Nozzle Split-Flow Circuit (Round Tubes)
 Tube Diameter Variation With Number of Tubes

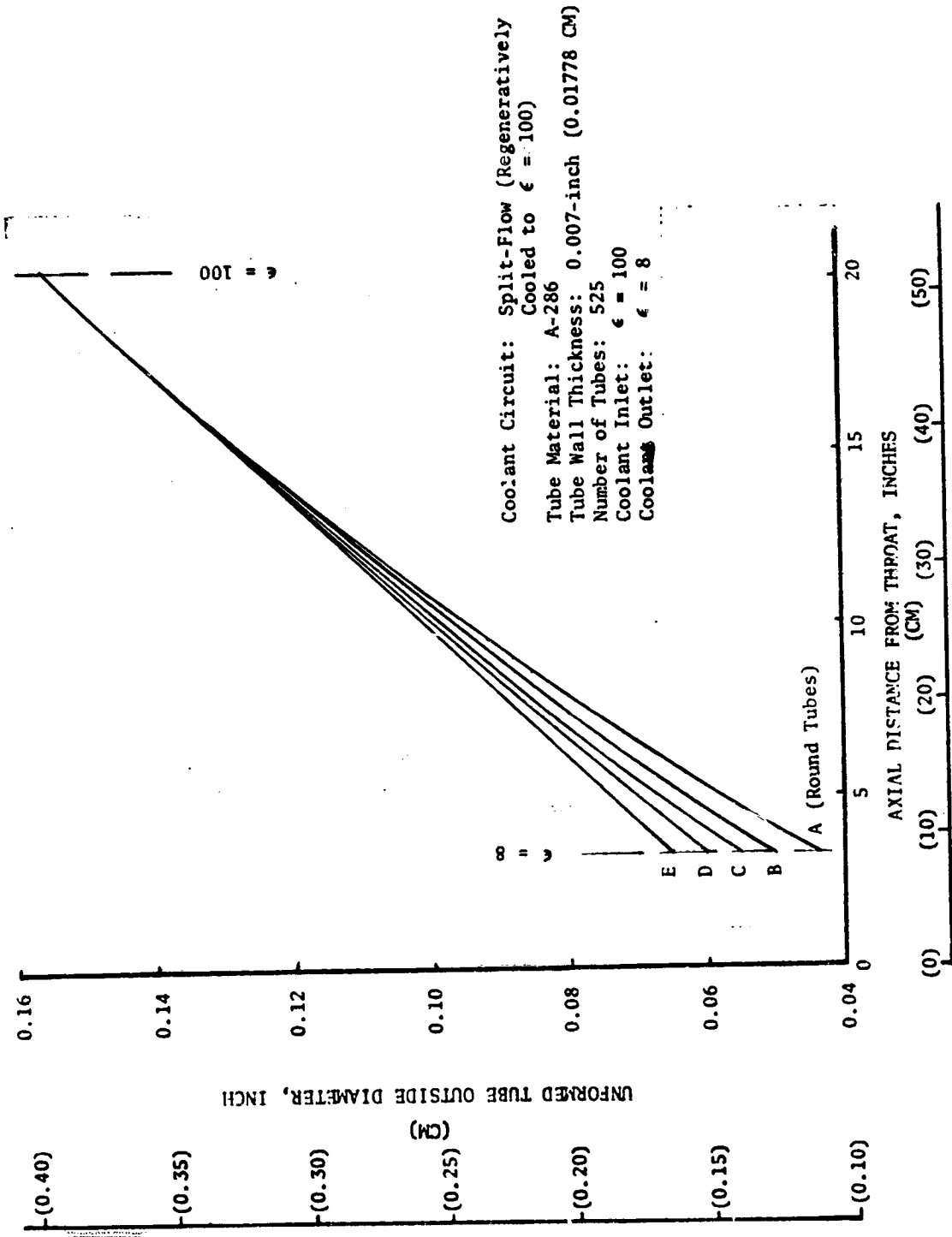


Figure 56. Uppass Booked A-286 Nozzle Configurations (Split-Flow Cooling Circuit)

Coolant Circuit: Split-Flow (Uppass)
 Tube Material: A-286
 Tube Wall Thickness: 0.007-inch (0.01778 CM)
 Number of Tubes: 525
 Coolant Inlet: $\epsilon = 100$
 Coolant Outlet: $\epsilon = 8$

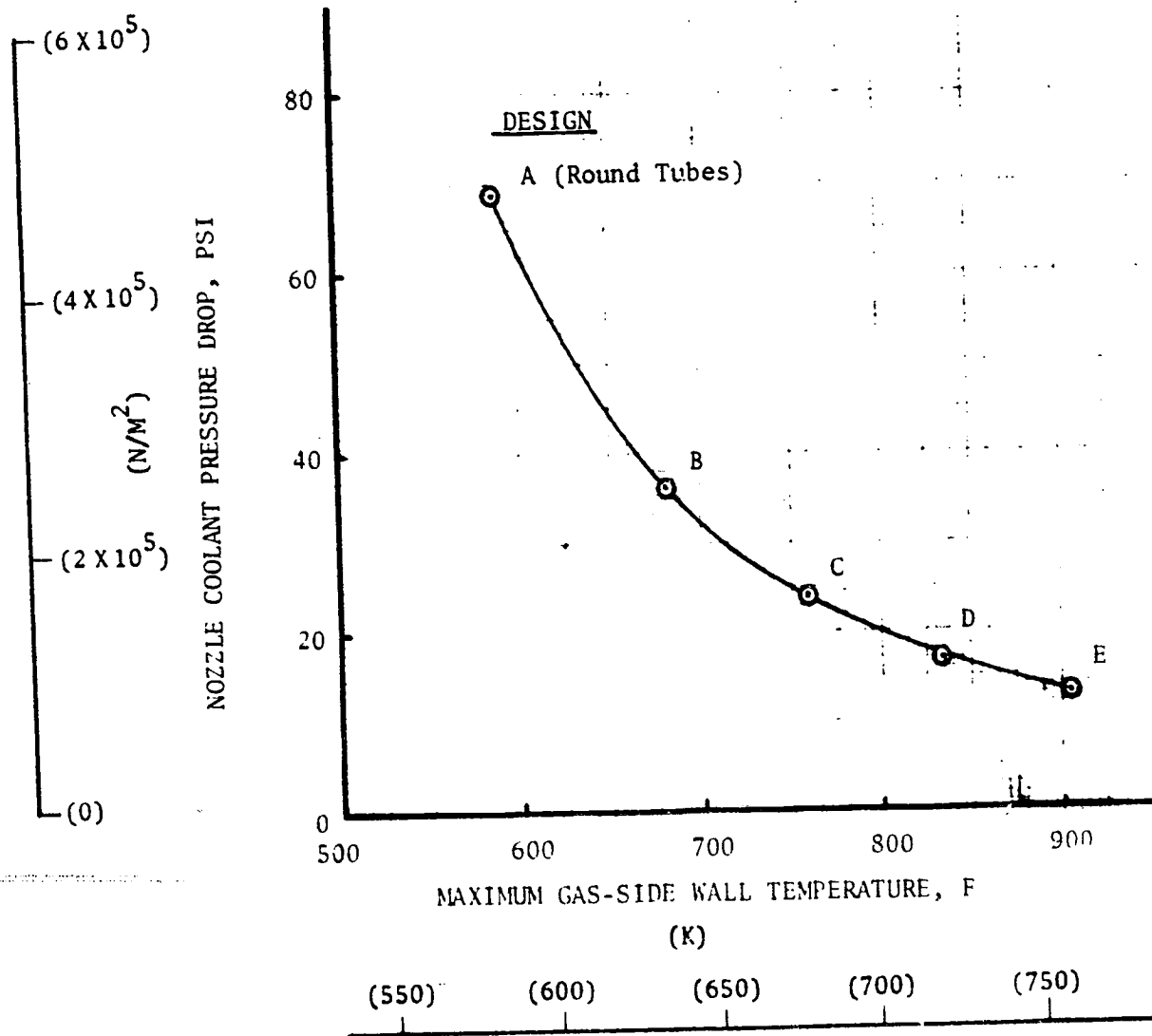


Figure 57. Nozzle Coolant Pressure Drop Influence on Maximum Wall Temperature for Uppass A-286 Nozzle (Split-Flow Cooling Circuit)

Coolant Circuit: Split-Flow (Regeneratively Cooled to $\epsilon = 100$)
 Tube Material: A-286
 Number of Tubes: 525
 Coolant Inlet: $\epsilon = 100$
 Combustor-Nozzle Joint: $\epsilon = 8$
 Tube Wall Thickness: 0.007-inch (0.01778 CM)

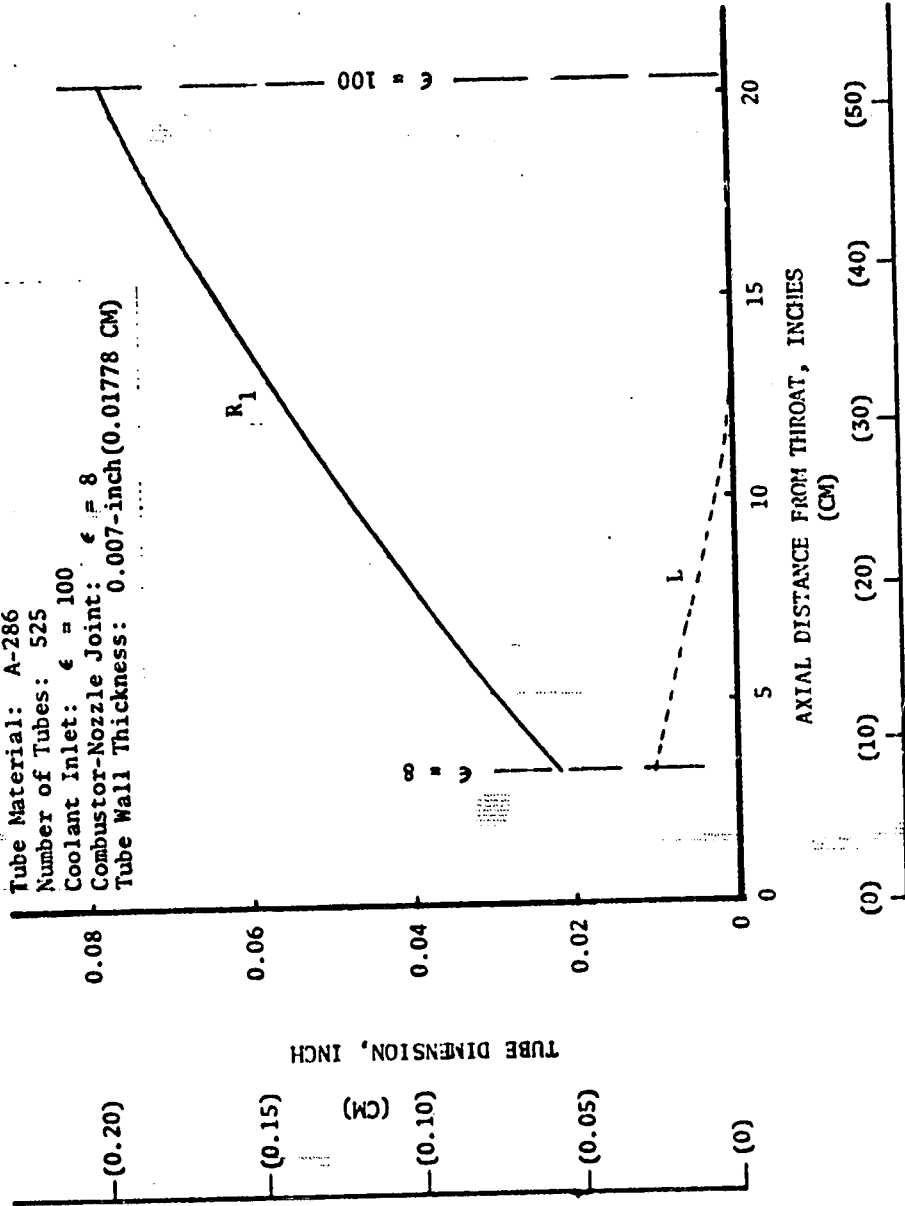


Figure 58. Selected A-286 Nozzle Configuration (Split-Flow Cooling Circuit)

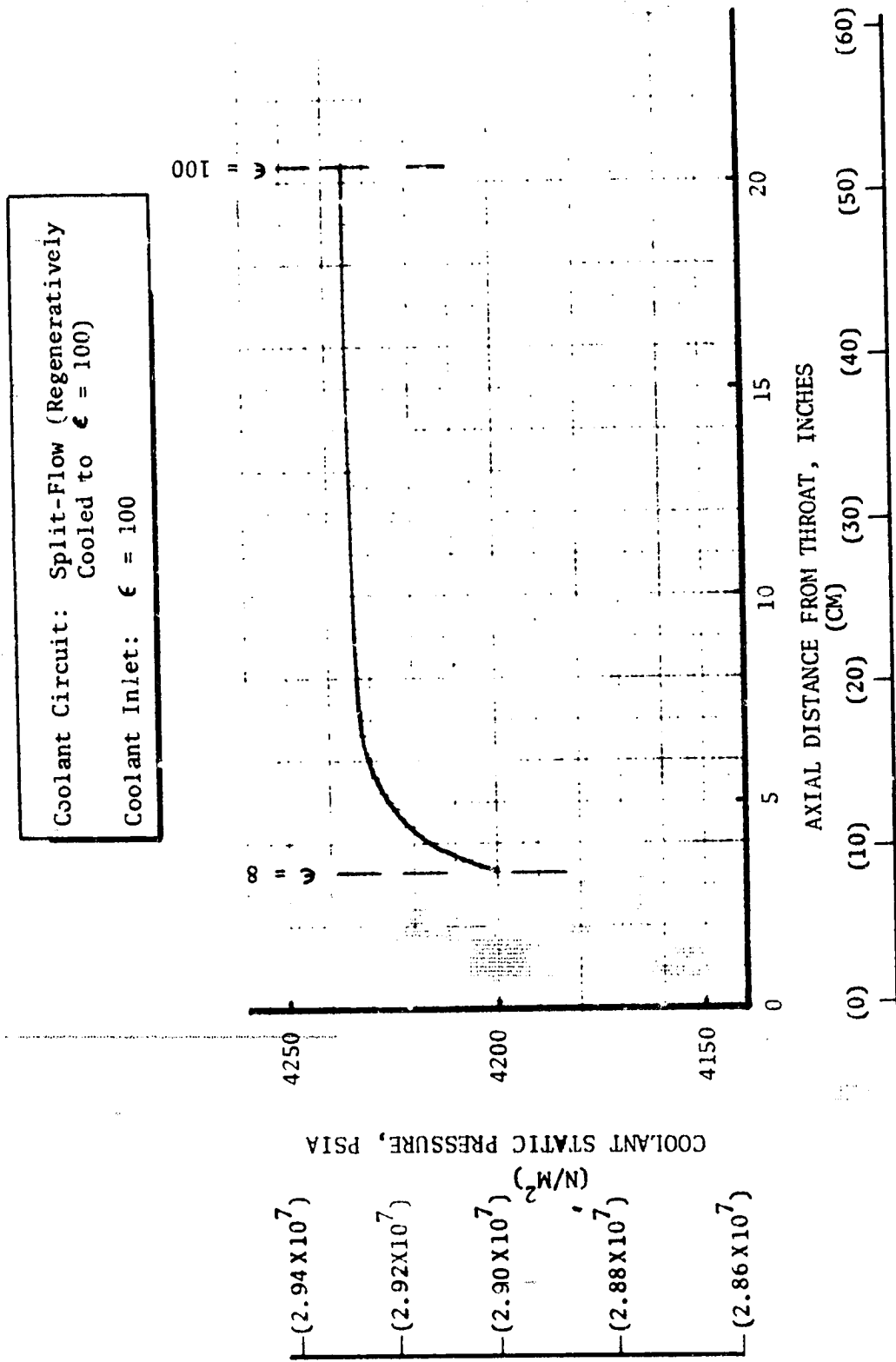


Figure 59. Coolant Static Pressure Distribution for the Selected A-286 Nozzle (Split-Flow Cooling Circuit)

Coolant Circuit: Split-Flow (Regeneratively Cooled to $\epsilon = 100$)
 Tube Material: A-286
 Number of Tubes: 525
 Coolant Inlet: $\epsilon = 100$
 Tube Wall Thickness: 0.007-inch (0.01778 CM)

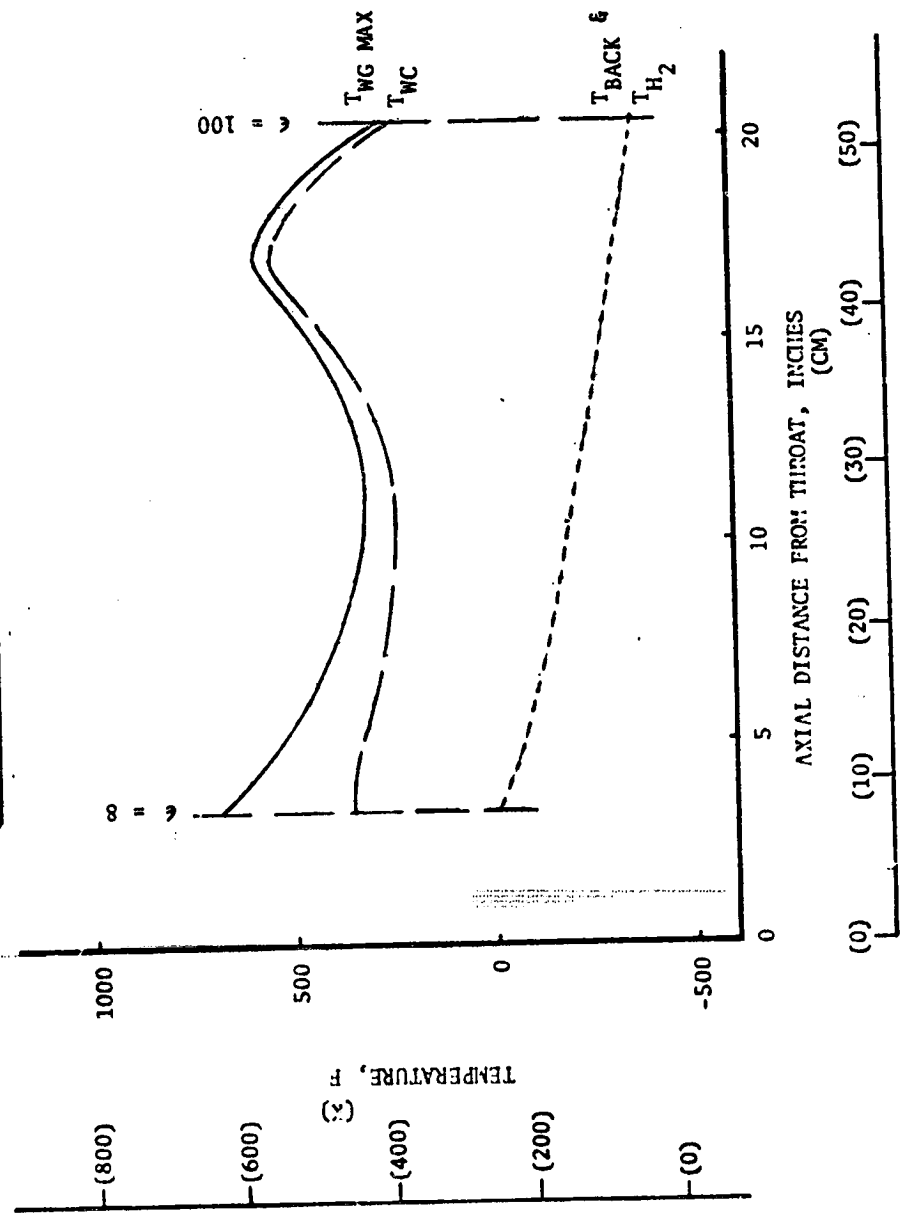
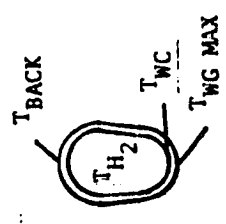


Figure 60. Temperature Distributions for the Selected A-286 Nozzle (Split-Flow Cooling Circuit)

Channel Wall Combustor

Parametric heat transfer/stress data generated for the 1-1/2 pass cooling circuit channel wall configuration were used to design the critical locations of the Zr-Cu and NARloy-Z combustor.

For the NARloy-Z channel wall combustor with a total damage fraction of approximately 1.0, the smallest channel width of 0.035-inch (0.0888 cm) offered the lowest combustor coolant pressure drop as shown in Fig. 61. However, as previously discussed, a 0.040-inch (0.1016 cm) channel width represented a reasonable minimum from a fabrication standpoint. Therefore, a channel width of 0.040-inch (0.1016 cm) was selected. For the selected channel width, a channel width-to-wall thickness ratio (a/t) of approximately 1.74 resulted in the minimum coolant pressure drop (Fig. 61). Using this design, the combustor-nozzle joint area ratio was varied to investigate the influence on the combustor and nozzle coolant pressure drops. As shown in Fig. 62, a joint area ratio of 8-to-1 achieved the minimum combustor pressure drop (299 psi or $2.06 \times 10^6 \text{ N/m}^2$). Moving the joint from an area ratio of 6 to 8, increased the combined combustor liner and nozzle tube weight by 0.8 pounds or 0.363 kg (Fig. 63). However, the joint area ratio of 6-to-1 would result in a 100-percent increase in the nozzle coolant pressure drop (36 psi or $2.48 \times 10^5 \text{ N/m}^2$ to more than 60 psi or $4.14 \times 10^5 \text{ N/m}^2$). Therefore, the combustor-nozzle joint area ratio of 8-to-1 was selected. The channel dimensions and wall temperature distributions for the selected NARloy-Z channel wall combustor are presented in Fig. 64 through 65. The maximum gas-side wall temperature of 1059 F (844 K) occurred 0.5-inch (1.27 cm) upstream of the geometric throat.

Designing the Zr-Cu combustor to a gas-side wall temperature of approximately 1020 F (822 K), the variation of combustor coolant pressure drop for the Zr-Cu channel wall combustor with channel width indicates that the small channel widths have a significantly lower pressure drop (Fig. 66). However, as for the NARloy-Z channel wall combustor, a 0.040-inch (0.1016 cm) minimum channel width was selected as a reasonable minimum for fabrication. The channel dimensions for the selected bi-width design of the Zr-Cu channel wall combustor are presented in Fig. 67. The wall temperature distribution for this design is shown in Fig. 68. As illustrated in Fig. 68, the maximum gas-side wall temperature of 1021 F (822 K) occurs 0.5-inch (1.27 cm) upstream of the throat.

A comparison of the two split-flow cooling circuit channel wall combustors is presented in Table VII and VIII, and each design with a minimum channel width of 0.040-inch has 100 channels. The higher channel width-to-wall thickness ratio (a/t) allowed for the NARloy-Z combustor resulted in a slightly thinner wall thickness. Also, the better thermal fatigue characteristics allowed a higher maximum gas-side wall temperature for the NARloy-Z. Therefore, the thinner wall and the higher allowable wall temperature resulted in substantially lower combustor coolant pressure drop (124 psi or $8.55 \times 10^5 \text{ N/m}^2$) for the NARloy-Z channel wall combustor, but a slightly higher combustor liner weight.

The design drawings for the two split-flow cooling circuit configurations are presented in Fig. 69 and 70. The combustor designs are similar to those of the

Coolant Circuit: Split-Flow (Regeneratively Cooled to $t = 100$)

Material: NARloy-Z

Combustor-Nozzle Joint: $\epsilon = 8$

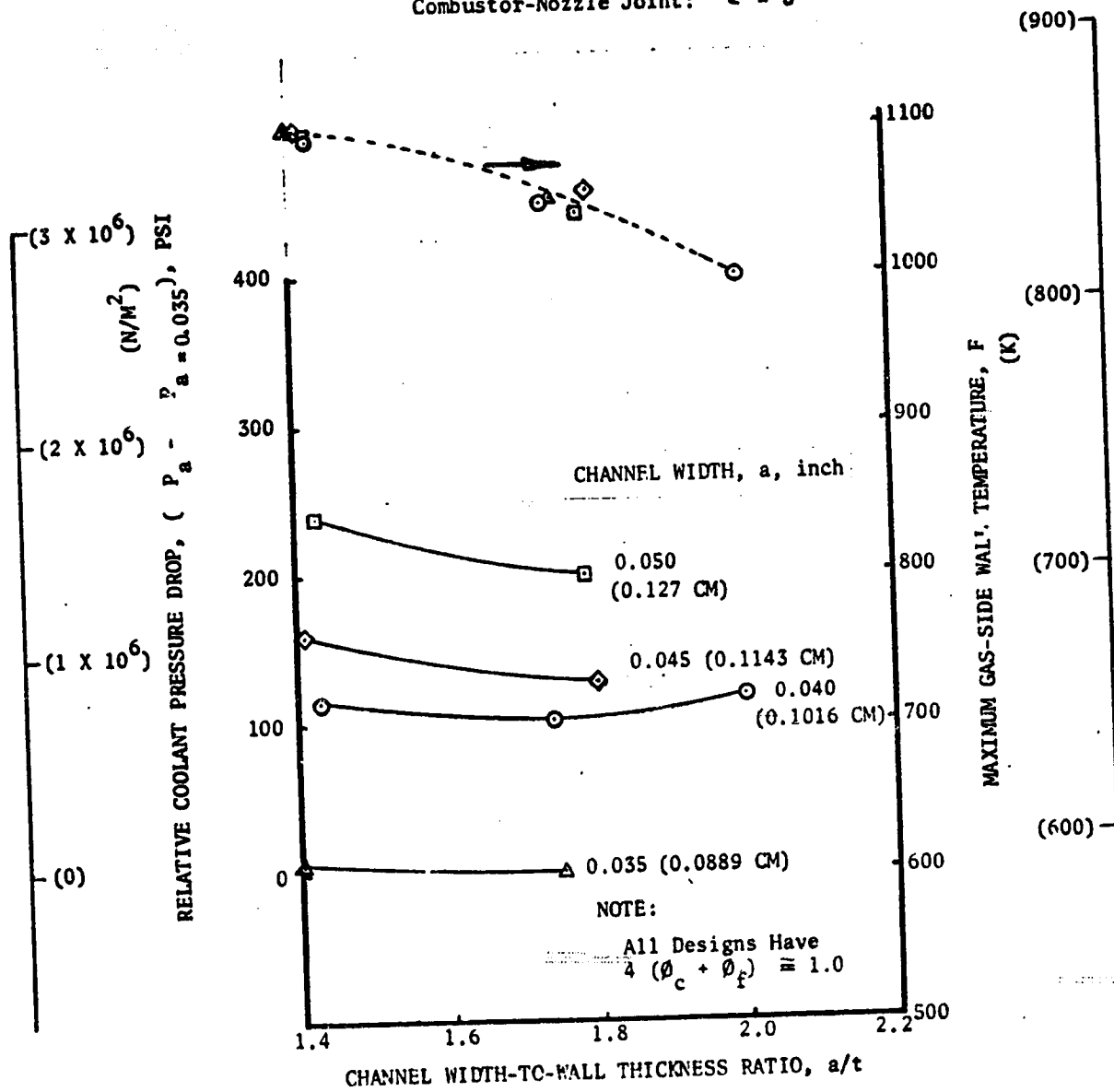


Figure 61. NARloy-Z Combustor (Split-Flow Cooling Circuit) Channel Width-to-Wall Thickness Ratio Influence

Coolant Circuit: Split-Flow (Regeneratively Cooled to $\epsilon = 100$)
 Combustor - Uppass
 Nozzle - Uppass

Materials:

Combustor Liner - NARloy-Z
 Nozzle Tubes - A-286

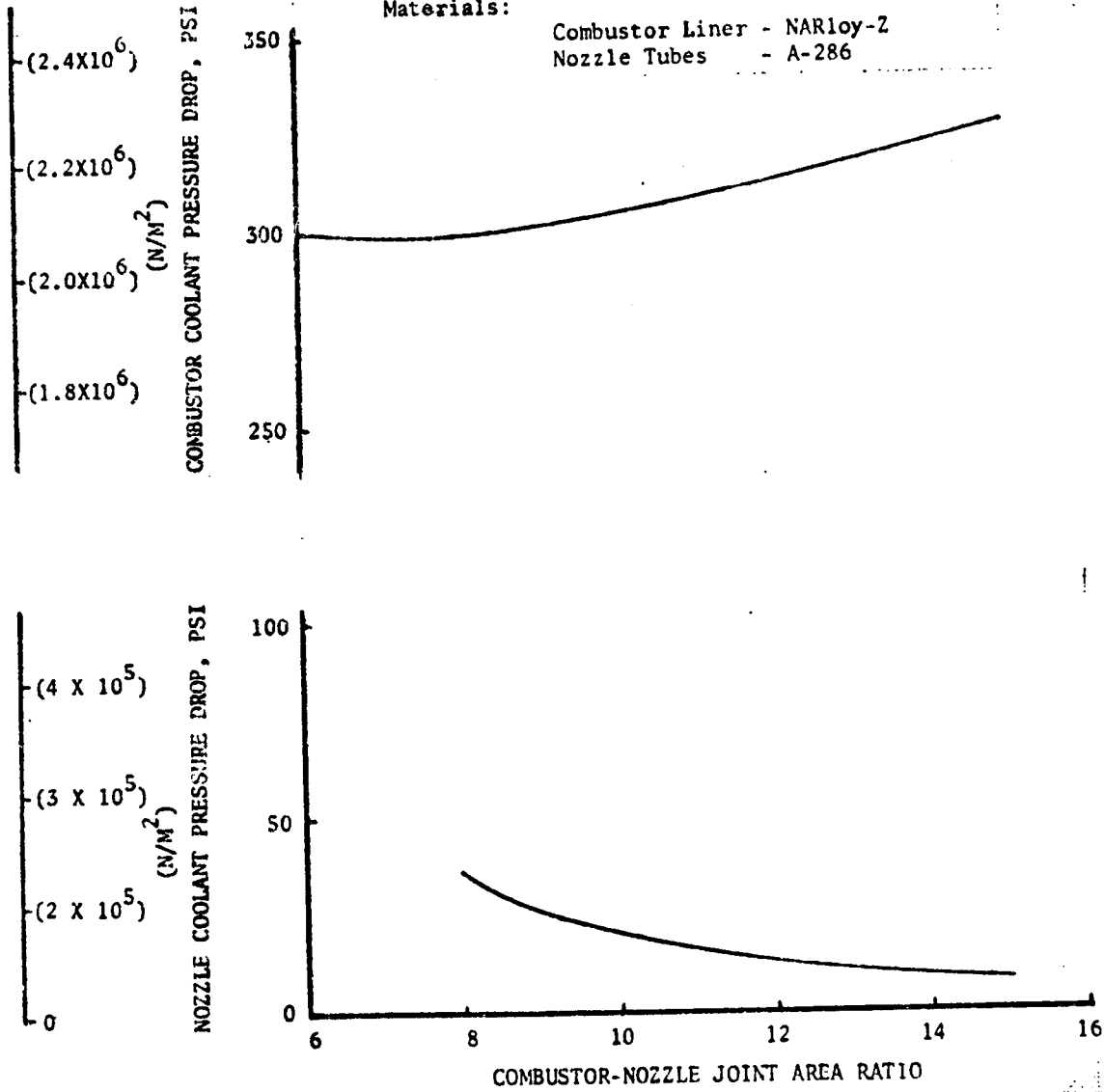


Figure 62. Combustor and Nozzle Coolant Pressure Variation With Joint Area Ratio (Split-Flow Cooling Circuit)

Cooling Circuit: Split-Flow (Regeneratively Cooled to $\epsilon = 100$)
 Combustor - Uppass
 Nozzle - Uppass
 Materials:
 Combustor Liner - NARloy-Z
 Nozzle Tubes - A-286

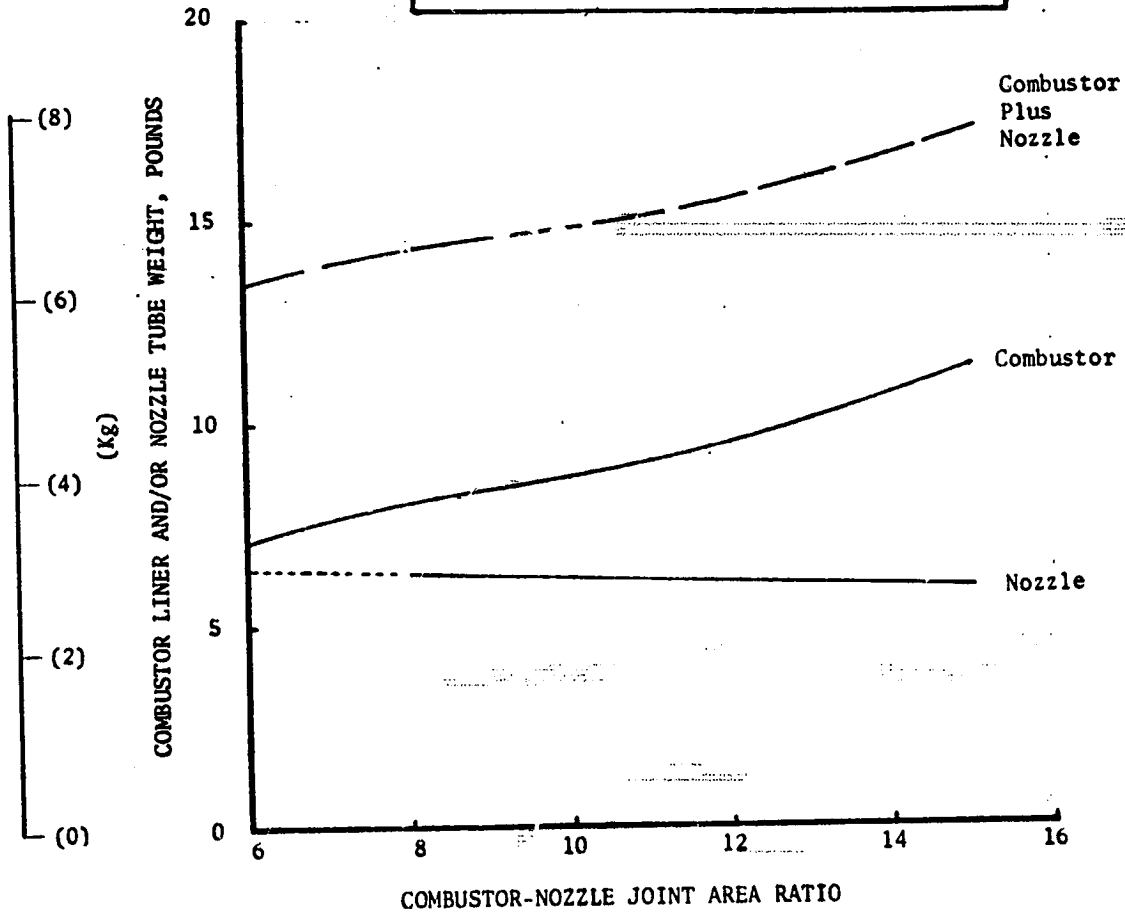


Figure 63. Combustor Liner and/or Nozzle Tube Weight Variation With Joint Area Ratio (Split-Flow Cooling Circuit)

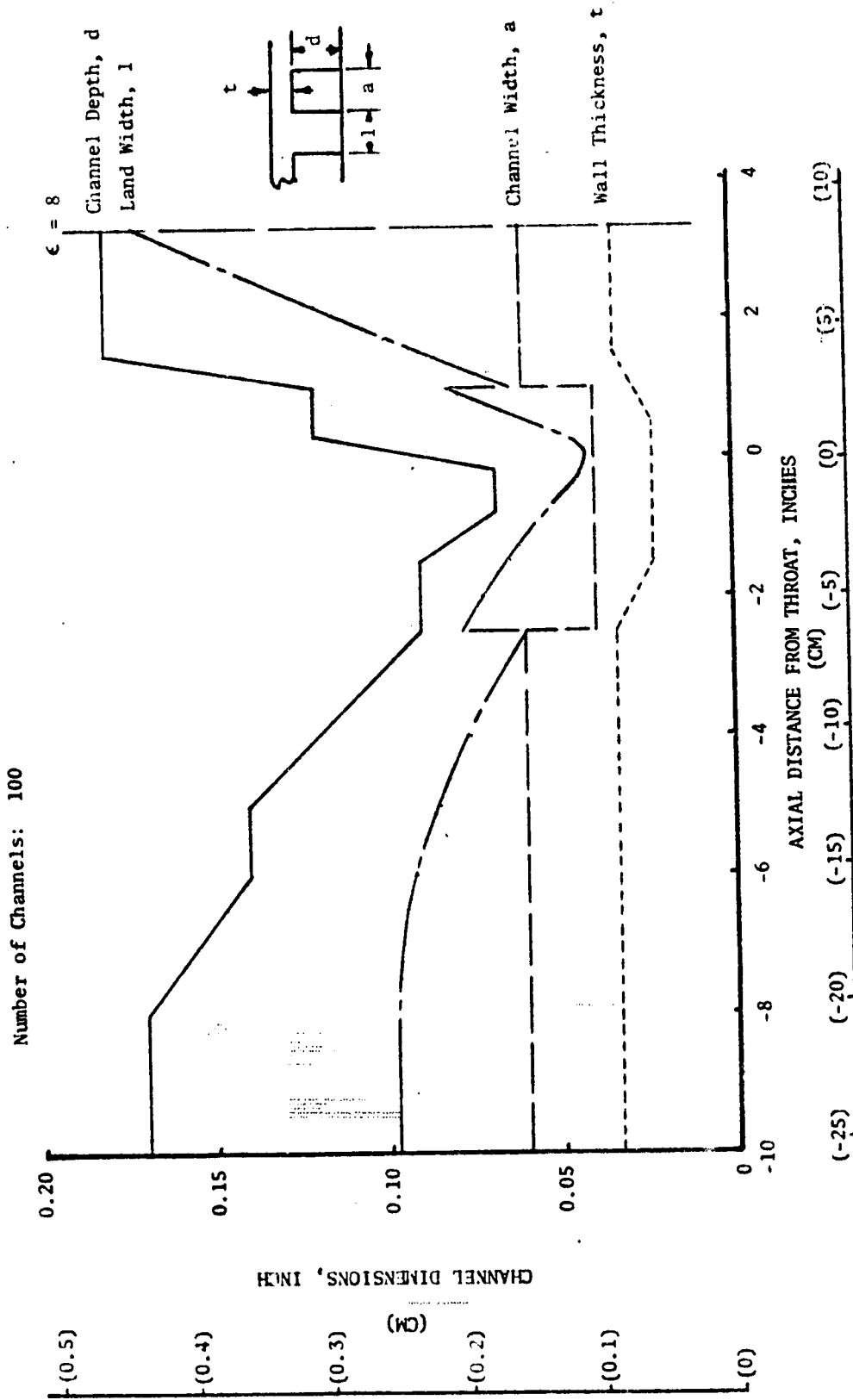


Figure 64. Channel Dimensions of the Selected NARLOY-Z Channel Wall Combustor Configuration (Split-Flow Cooling Circuit)

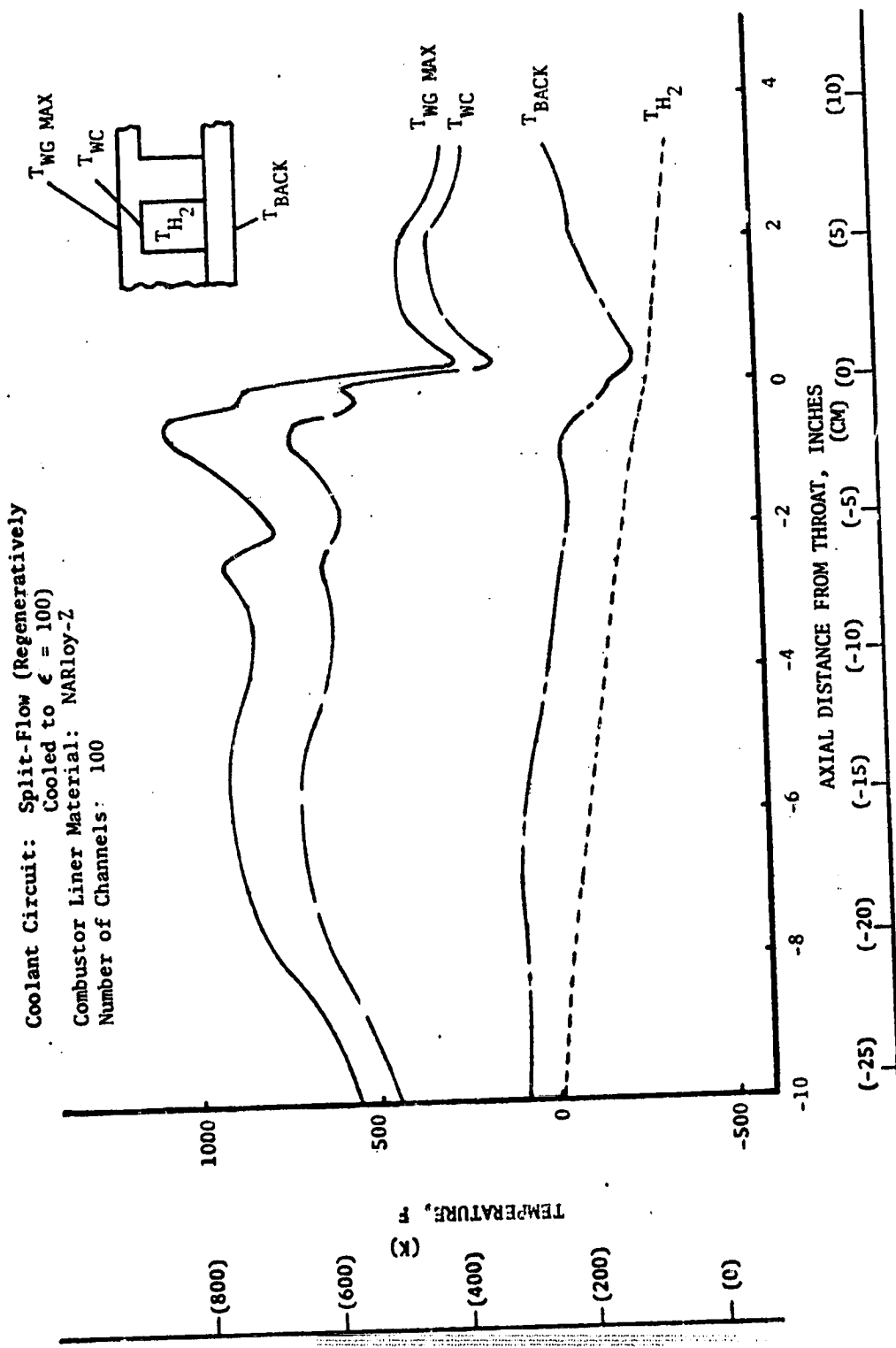


Figure 65. Temperature Distributions for the Selected NARLOY-Z Channel Wall Combustor Configuration (Split-Flow Cooling Circuit)

Coolant Circuit: Split-Flow (Regeneratively Cooled to $\epsilon = 100$)
 Material: Zr-Cu
 Combustor-Nozzle Joint: $\epsilon = 8$
 Channel Width-To-Wall Thickness Ratio: ~ 1.5

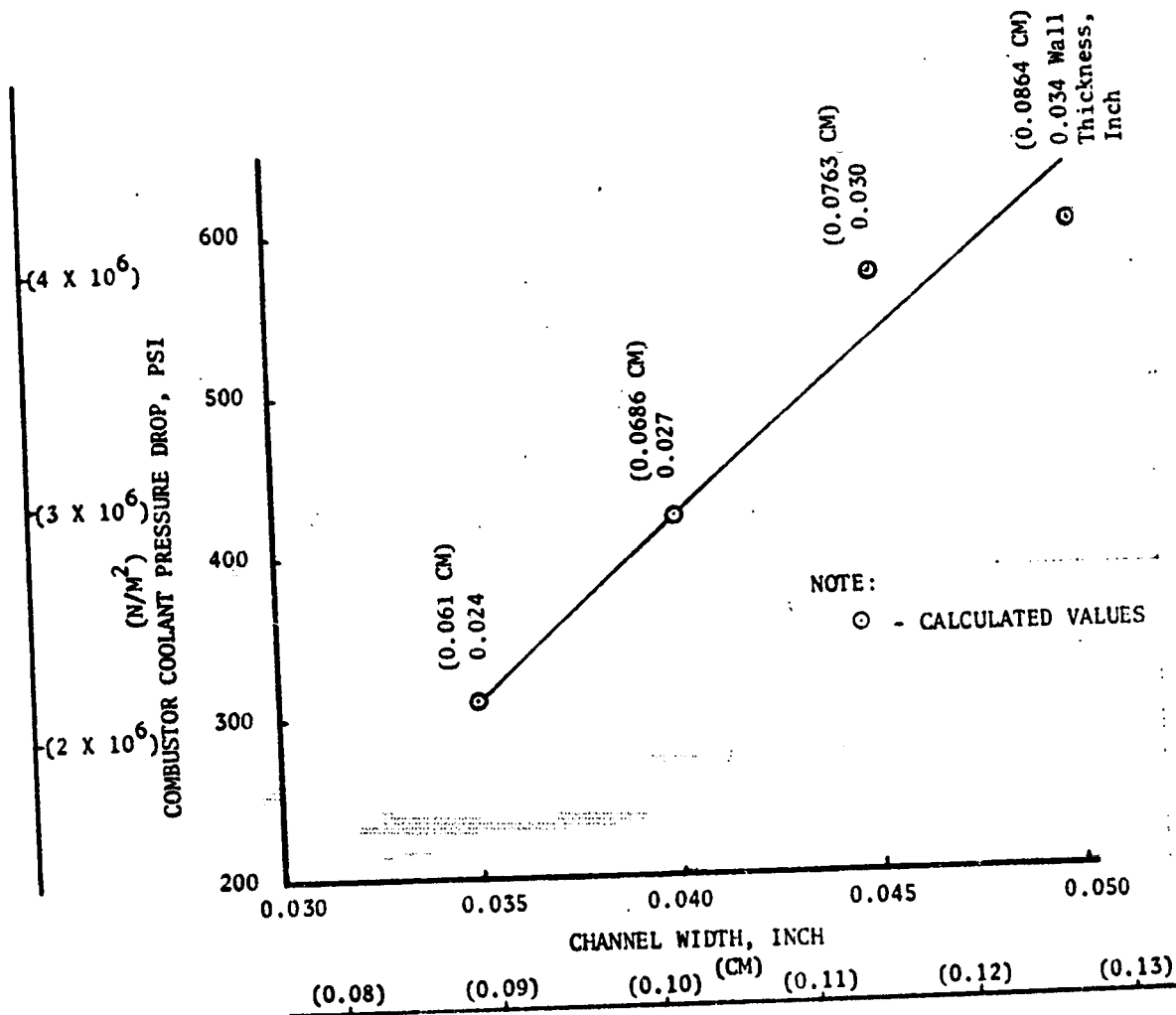


Figure 66. Influence of Channel Width on Combustor Coolant Pressure Drop on the Zr-Cu Combustor (Split-Flow Cooling Circuit)

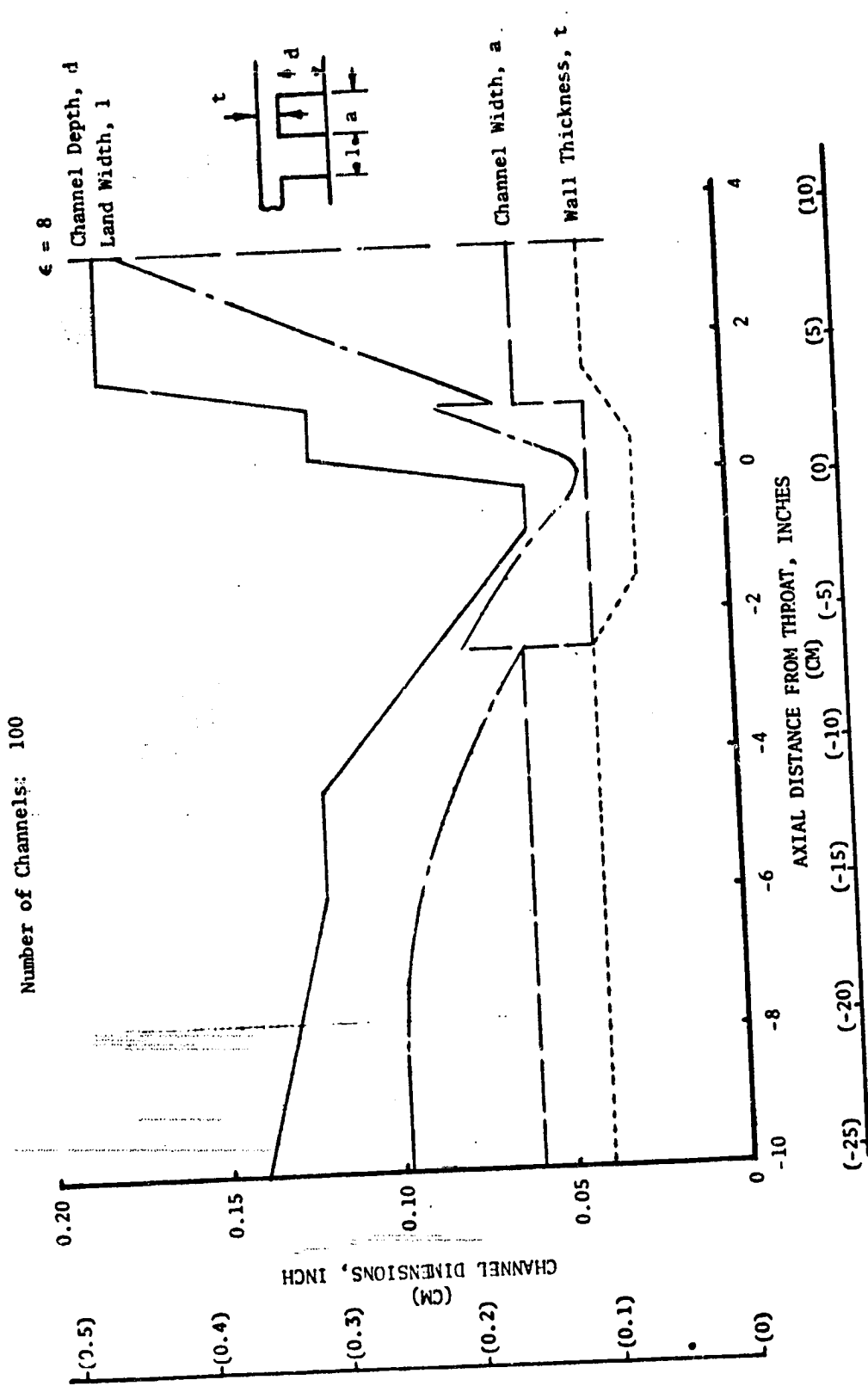


Figure 67. Channel Dimensions of the Selected Zr-Cu Channel Wall Combustor Configuration (Split-Flow Cooling Circuit)

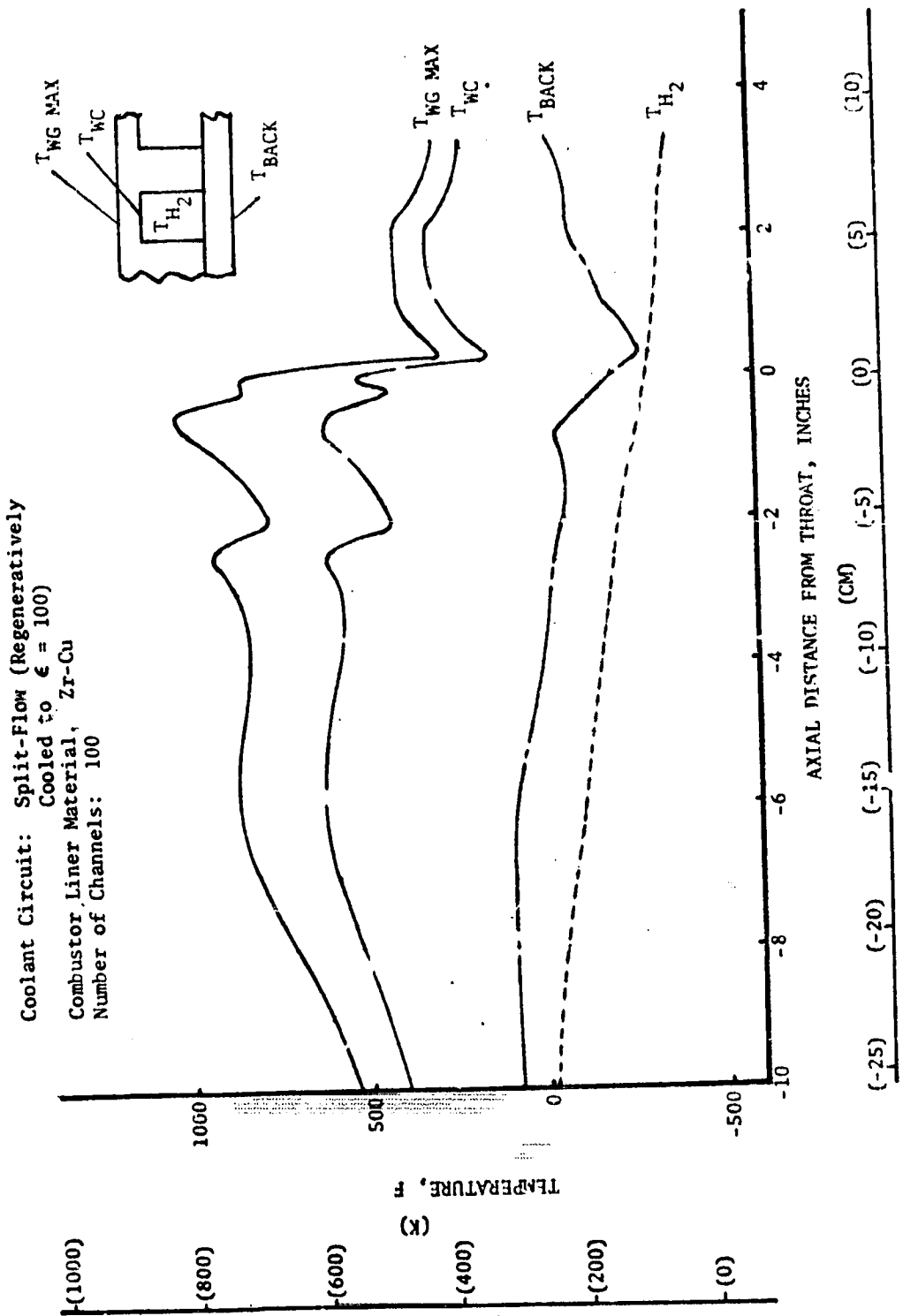


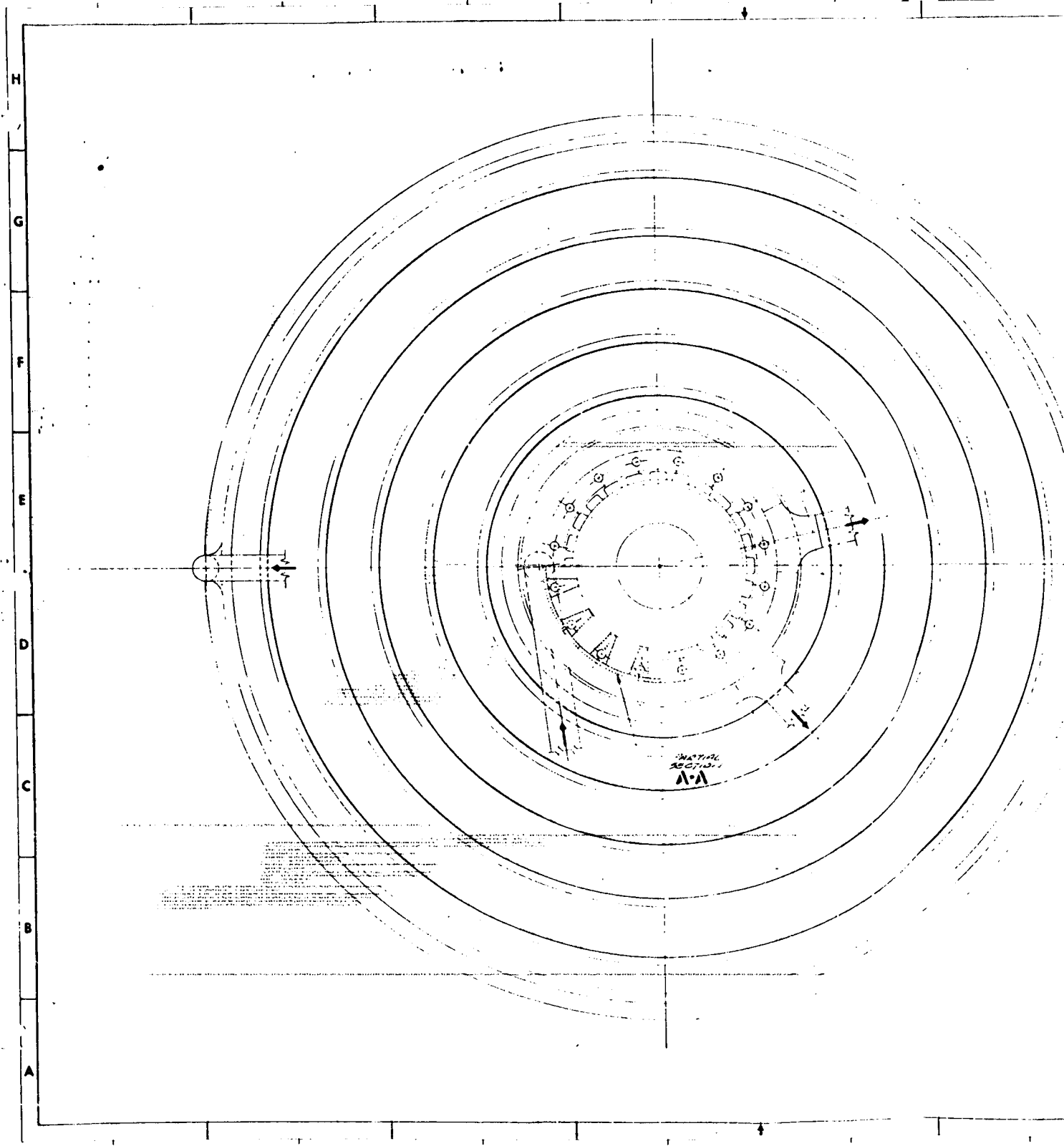
Figure 68. Temperature Distributions for the Selected Zr-Cu Channel Wall Combustor Configuration (Split-Flow Cooling Circuit)

TABLE VII. COMPARISON OF SELECTED SPLIT-FLOW COOLING
CIRCUIT CHANNEL WALL COMBUSTORS

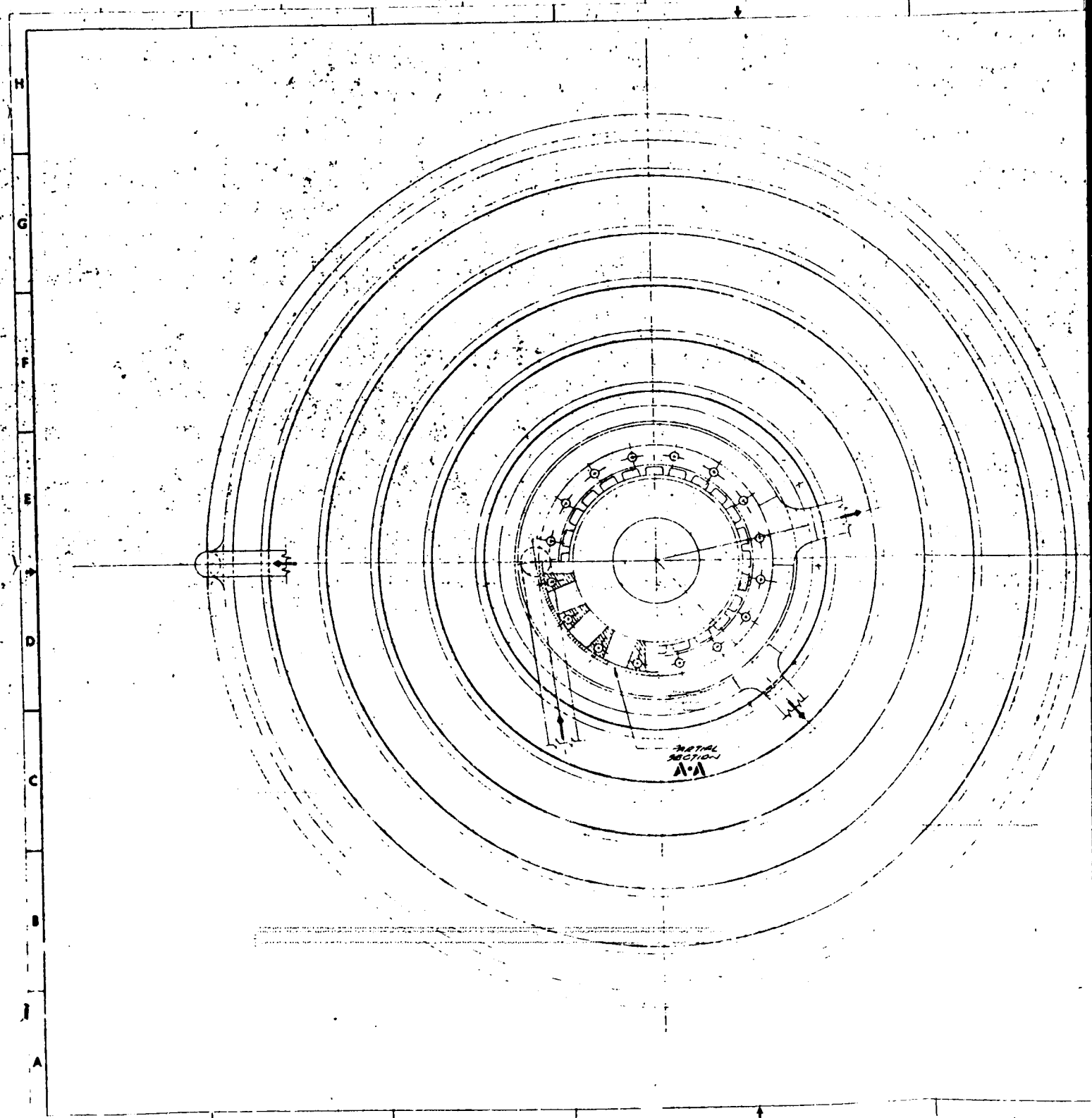
	Zr-Cu	NARloy-Z
Number of Channels	100	100
Combustor-Nozzle Joint Area Ratio	-0.5 (-1.27 cm)	-0.5 (-1.27 cm)
Channel Dimensions at the Critical Stress/Life Location:		
Location, inch	0.040 (0.1016 cm)	0.040 (0.1016 cm)
Width, inch	0.058 (0.1472 cm)	0.068 (0.1728 cm)
Depth, inch	0.0475 (0.1207 cm)	0.0475 (0.1207 cm)
Land, inch	0.027 (0.0686 cm)	0.023 (0.0584 cm)
Hot-Gas Wall Thickness, inch	1021 (823 K)	1059 (844 K)
Maximum Gas-Side Wall Temperature, F	423 (2.915 x 10 ⁶ N/m ²)	299 (2.06 x 10 ⁶ N/m ²)
Combustor Coolant Pressure Drop, psi	7.8 (3.54 Kg)	8.0 (3.63 Kg)
Combustor Liner Weight, pounds		
Critical Location Stress and Life Parameters:		
Yield Safety Factor	1.33	1.64
Ultimate Safety Factor	2.09	2.60
Damage Fraction	4 (0.01 + 0.214) = 0.896	4 (0.05 + 0.1875) = 0.95
4 ($\phi_c + \phi_f$)		

TABLE VIII. SELECTED A-286 TUBULAR NOZZLE/CHANNEL WALL COMBUSTOR CONFIGURATIONS (SPLIT-FLOW COOLING CIRCUIT)

<u>Nozzle:</u>		
Material	A-286	
Number of Tubes	525	
Tube Wall Thickness, inch	0.007 (0.01778 cm)	
Coolant Inlet Area Ratio	100	
Combustor-Nozzle Joint Area Ratio	8	
Nozzle Coolant Tube Weight, pounds	6.3 (2.86 Kg)	
Maximum Gas-Side Wall Temperature, F	685 (635 K)	
Nozzle Coolant Pressure Drop, psi	36 (2.48 x 10 ⁵ N/m ²)	
<u>Combustor:</u>		
Material	Zr-Cu	NARLOY-Z
Number of Channels	100	100
Minimum Channel Width, inch	0.040 (0.1016 cm)	0.040 (0.1016 cm)
Minimum Channel Depth, in	0.058 (0.1472 cm)	0.068 (0.1728 cm)
Minimum Channel Land, i.	0.0427 (0.1083 cm)	0.0427 (0.1083 cm)
Minimum Hot-Gas Wall Thickness, Inch	0.027 (0.0686 cm)	0.023 (0.0584 cm)
Combustor Liner Weight, pounds	7.8 (3.54 Kg)	8.0 (3.63 Kg)
Maximum Gas-Side Wall Temperature, F	1021 (823 K)	1059 (844 K)
Combustor Coolant Pressure Drop, psi	423 (2.915 x 10 ⁶ N/m ²)	299 (2.06 x 10 ⁶ N/m ²)
<u>Chamber:</u>		
Coolant Pressure Drop, psi	423 (2.915 x 10 ⁶ N/m ²)	299 (2.06 x 10 ⁶ N/m ²)
Combustor Liner Plus Nozzle Tube Weight, pounds	14.1 (6.39 Kg)	14.3 (6.49 Kg)



FOLDOUT FRAME



FOLDBOUT FRAME

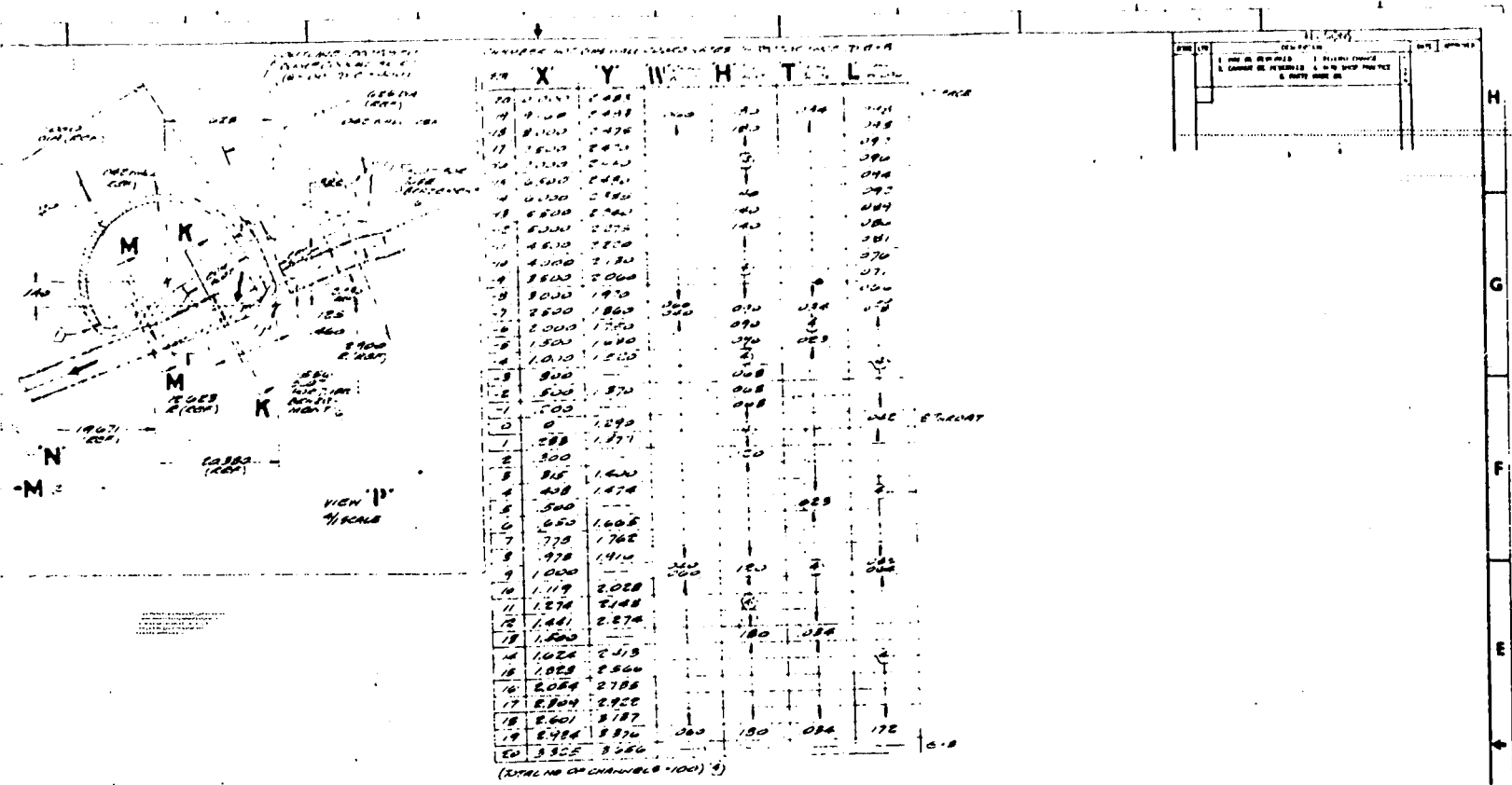


Figure 70. NARloy-Z Channel Wall Combustor A-286 Tubular Configuration (Split-Flow Cooling Circuit)

CHANNEL (NOT USED) IN THE COOLING CIRCUIT - C.B. 70-1100

NO	X	Y	Z	H	T	L
21	1000	1000	1000	100	100	100
22	1000	1000	1000	100	100	100
23	1000	1000	1000	100	100	100
24	1000	1000	1000	100	100	100
25	1000	1000	1000	100	100	100
26	1000	1000	1000	100	100	100
27	1000	1000	1000	100	100	100
28	1000	1000	1000	100	100	100
29	1000	1000	1000	100	100	100
30	1000	1000	1000	100	100	100
31	1000	1000	1000	100	100	100
32	1000	1000	1000	100	100	100
33	1000	1000	1000	100	100	100
34	1000	1000	1000	100	100	100
35	1000	1000	1000	100	100	100
36	1000	1000	1000	100	100	100
37	1000	1000	1000	100	100	100
38	1000	1000	1000	100	100	100
39	1000	1000	1000	100	100	100
40	1000	1000	1000	100	100	100

41	1000	1000	1000	100	100	100
42	1000	1000	1000	100	100	100
43	1000	1000	1000	100	100	100
44	1000	1000	1000	100	100	100
45	1000	1000	1000	100	100	100
46	1000	1000	1000	100	100	100
47	1000	1000	1000	100	100	100
48	1000	1000	1000	100	100	100
49	1000	1000	1000	100	100	100
50	1000	1000	1000	100	100	100
51	1000	1000	1000	100	100	100
52	1000	1000	1000	100	100	100
53	1000	1000	1000	100	100	100
54	1000	1000	1000	100	100	100
55	1000	1000	1000	100	100	100
56	1000	1000	1000	100	100	100
57	1000	1000	1000	100	100	100
58	1000	1000	1000	100	100	100
59	1000	1000	1000	100	100	100
60	1000	1000	1000	100	100	100

J 02602

1-1/2 pass cooling circuit channel wall combustors. The combustor backup structure consists of an electroform nickel channel closeout of 0.03-inch (0.0762 cm) thickness with a 0.060-inch INCO 718 structural jacket. The backup structure of the A-286 tubular nozzle is formed by five flat hatbands. The split-flow circuit nozzle has one additional hatband because of the slightly smaller nozzle tubes.

CONFIGURATION SELECTION

Configuration Summary and Conclusions

Schematics of the three configurations are presented in Fig. 71. At an area ratio of 8-to-1, the tubular configuration has a tube splice and the channel wall combustor/tubular nozzle configurations have the combustor-nozzle joint at this area ratio. A detail comparison using the simplified cycle-life method is presented in Table IX and X for the three configurations. The tubular configuration had the highest coolant pressure drop, which was attributed to the two-dimensional analysis resulting in temperatures higher than one-dimensional (flat-plate) values. Also, this configuration had the highest tube weight because of the low strength of Zr-Cu and NARloy compared to A-286. The two channel wall combustor/tubular nozzle configurations resulted in comparable coolant pressure drops with the split-flow cooling circuit configuration having a slight weight advantage. This slightly lower weight is the result of the lower coolant channel depths of the split-flow cooling circuit configuration. Also, this configuration provides a separate fluid supply to drive the boost pumps and independent development of the combustor and the nozzle.

The overall conclusions of the Task I steady-state design and analysis were:

1. Zr-Cu and NARloy-Z required different designs because of differences in strength and life characteristics.
2. NARloy-Z design provided substantially lower coolant pressure drops and lower or equal chamber basic weights.
3. The all tubular configurations (1-1/2 pass cooling circuit) resulted in relatively high coolant pressure drops and tube weights because of the higher than one-dimensional (flat plate) gas-side wall temperatures and the low strength of the copper alloys.
4. For the all tubular configurations, the Zr-Cu design was limited because of the yield safety factor and the NARloy-Z design was limited because of the creep damage fraction.
5. For the tubular nozzle/channel wall combustor configurations, a booked tube up-pass circuit provided satisfactory cooling with low coolant pressure drops and tube weights.
6. The optimum channel width of the Zr-Cu and NARloy-Z channel wall combustors led to small channel widths (less than 0.040-inch or 0.1016 cm).
7. For the channel wall combustors, both the Zr-Cu and NARloy-Z designs were limited because of the fatigue damage fraction.

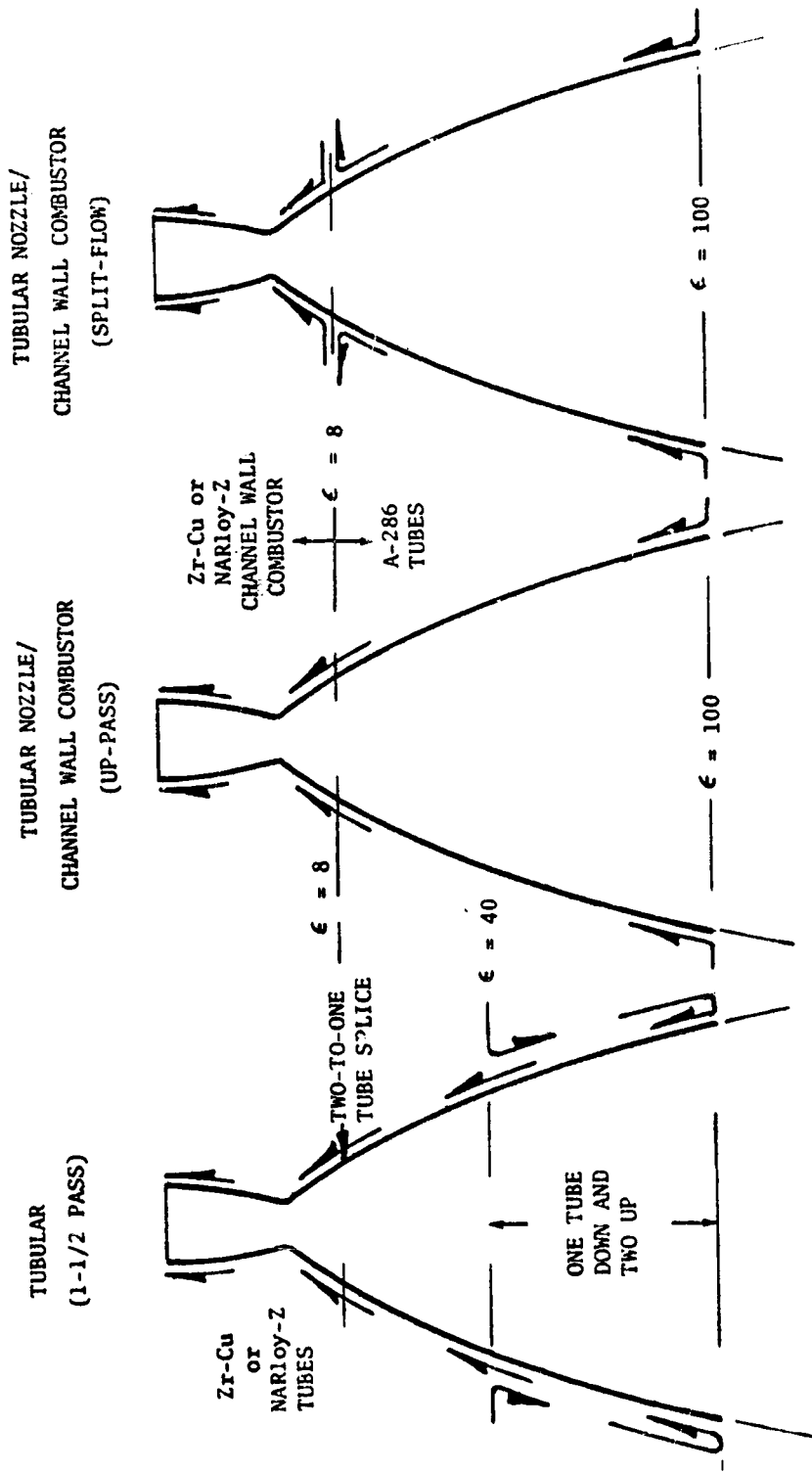


Figure 71. Selected Task I Configurations

TABLE IX. COOLANT CIRCUIT OVERALL COMPARISONS
(NARLOY-Z CONFIGURATIONS)

Coolant Circuit	1-1/2 Pass		Spit-Flow
<u>Nozzle</u>			
Tube Material	NARLOY-Z	A-286	A-286
Number of Tubes	288 (maximum)	400	525
Minimum Unformed Tube Outside Diameter, inch	0.119 (0.302 cm)	0.075 (0.1905 cm)	0.050 (0.127 cm)
Maximum Gas-Side Wall Temperature, F	485 (525 K)	525 (547 K)	685 (636 K)
<u>Combustor</u>			
Material	NARLOY-Z	NARLOY-Z	NARLOY-Z
Number of Channels (or Tubes)	96	95	100
Minimum Tube Outside Diameter, inch	0.0873 (0.2215 cm)	--	--
Minimum Channel Dimensions:			
Width, inch	--	0.045 (0.1143 cm)	0.040 (0.1016 cm)
Height, inch	--	0.110 (0.2795 cm)	0.068 (0.1728 cm)
Land, inch	--	0.042 (0.1068 cm)	0.0427 (0.1083 cm)
Maximum Gas-Side Wall Temperature, F	1090 (861 K)	1051 (839 K)	1059 (844 K)
Critical Location Stress and Life Parameters:			
Yield Safety Factor	1.44	1.50	1.64
Ultimate Safety Factor	2.16	2.37	2.60
Damage Fraction	4 (0.133 + 0.0477) = 0.724	4 (0.0461 + 0.182) = 0.912	4 (0.05 + 0.1875) = 0.951
4 ($\phi_c + \phi_f$)	854 (5.68 x 10 ⁶ N/m ²)	309 (2.13 x 10 ⁶ N/m ²)	299 (2.06 x 10 ⁶ N/m ²)
<u>Chamber</u>			
Coolant Pressure Drop, psi	32.2 (14.62 Kg)	16.0 (7.27 Kg)	14.3 (6.49 Kg)
Combustor Liner and Nozzle Tube Weight, pounds			

TABLE X. COOLANT CIRCUIT OVERALL COMPARISONS
(Zr-Cu CONFIGURATIONS)

Coolant Circuit	1-1/2 Pass		Split-Flow
<u>Nozzle</u>			
Tube Material	Zr-Cu	A-286	A-286
Number of Tubes	252 (maximum)	400	525
Minimum Unformed Tube Outside Diameter, inch	0.132 (0.335 cm)	0.075 (0.1905 cm)	0.050 (0.127 cm)
Maximum Gas-Side Wall Temperature, F	475 (530 K)	525 (547 K)	685 (636 K)
<u>Combustor</u>			
Material	Zr-Cu	Zr-Cu	Zr-Cu
Number of Channels (or Tubes)		100	100
Minimum Tube Outside Diameter, inch	0.1002 (0.2545 cm)	--	--
Minimum Channel Dimensions:			
Width, inch	--	0.040 (0.1016 cm)	0.040 (0.1016 cm)
Height, inch	--	0.112 (0.2845 cm)	0.058 (0.1472 cm)
Land, inch	--	0.0427 (0.1083 cm)	0.0427 (0.1083 cm)
Maximum Gas-Side Wall Temperature, F	1149 (894 K)	1021 (823 K)	1021 (823 K)
Critical Location Stress and Life Parameters:			
Yield Safety Factor	1.22	1.25	1.33
Ultimate Safety Factor	1.57	1.93	2.09
Damage Fraction	4 (0.01 + 0.091) = 0.040	4 (0.01 + 0.24) = 1.0	4 (0.01 + 0.213) = 0.896
4 ($\phi_c + \phi_f$)			
<u>Chamber</u>			
Coolant Pressure Drop, psi	966 (6.86×10^6 N/m ²)	408 (2.82×10^6 N/m ²)	299 (2.06×10^6 N/m ²)
Combustor Liner and Nozzle Tube Weight, pounds	46.2 (20.9 Kg)	16.1 (7.3 Kg)	14.3 (6.49 Kg)

Finite Element Stress Analysis

The finite element stress computer program was used to predict the maximum effective strain range of the selected split-flow cooling circuit channel wall NARloy-Z combustor and the NARloy-Z tubular configuration. A plane strain model of the thrust chamber wall was developed. This model considered the strain in the axial, or out of plane direction, as a constant value that was input into the computer program. In this type of analysis, the section is modeled by a system of quadrilateral plane elements (A mesh). The channel wall and tube wall cases consisted of a section of the thrust chamber wall composed of one half of a channel or tube (Fig. 72 and 73). Sliding boundaries were imposed on the mid-channel and mid-land planes as shown in Fig. 73.

The loads imposed on the model are a coolant pressure of 3666 psia (2.52×10^7 N/m²) for the channel case and 4020 psia (2.77×10^7 N/m²) for the tube case, a hot gas pressure of 850 psia (5.85×10^6 N/m²), an axial thrust load of 36.3 pounds (16.44 kg) and thermal loads. The temperature distribution obtained from the heat transfer analysis along with the pressure loads on their respective boundaries were input to the program.

The cycles to failure (N_f) were obtained from the maximum effective strain range (ϵ_{eff}) and the NARloy-Z thermal fatigue life (Appendix A). The hours of rupture (T_R) were determined using the hydraulic stress (σ_{hyd}) on the hot wall and the NARloy-Z stress rupture curve (Appendix A).

The results of the finite element and the simplified stress analysis are shown in Table XI. For the tubular case, the simplified analysis predicted a conservative cycle life. However, the channel case, the finite element analysis result predicted a total damage fraction exceeding the required limit of 1.0. This maximum effective strain range occurred at point "a" (Fig. 73). These results indicate that the maximum gas-side wall temperature of this case must be lowered to achieve a total damage fraction equal to or less than one. An allowable maximum wall temperature was estimated by ratioing the predicted effective strain range to the allowable effective strain range and accounted for the reduced creep damage fraction because of the lower temperatures. An allowable maximum gas-side wall temperature of 1000 F (812 K) was determined. For this NARloy-Z channel wall configuration, an additional 25 psi (1.724×10^5 N/m²) in coolant pressure drop would be required to achieve this lower temperature as shown in Fig. 74.

Steady-State Analyses Configuration Selection

A detail presentation of the steady-state analyses was given at NASA-Lewis Research Center on 20 December 1972. Based on these results and the knowledge that some modifications of the channel wall designs would be required because of differences in the simplified and finite element stress analyses, the two Zr-Cu channel wall combustor/A-286 tubular nozzle configurations were selected by the NASA-LeRC Project Manager as the two configurations to be evaluated in the transient analysis. The Zr-Cu was selected since it represented the more conservative approach.

288 TUBE NARloy-Z T/C DESIGN-COOLANT
PLUS HOT GAS PRESSURE AND TEMPERATURE

UNDEFORMED STRUCTURE

CYCLE NO. 1

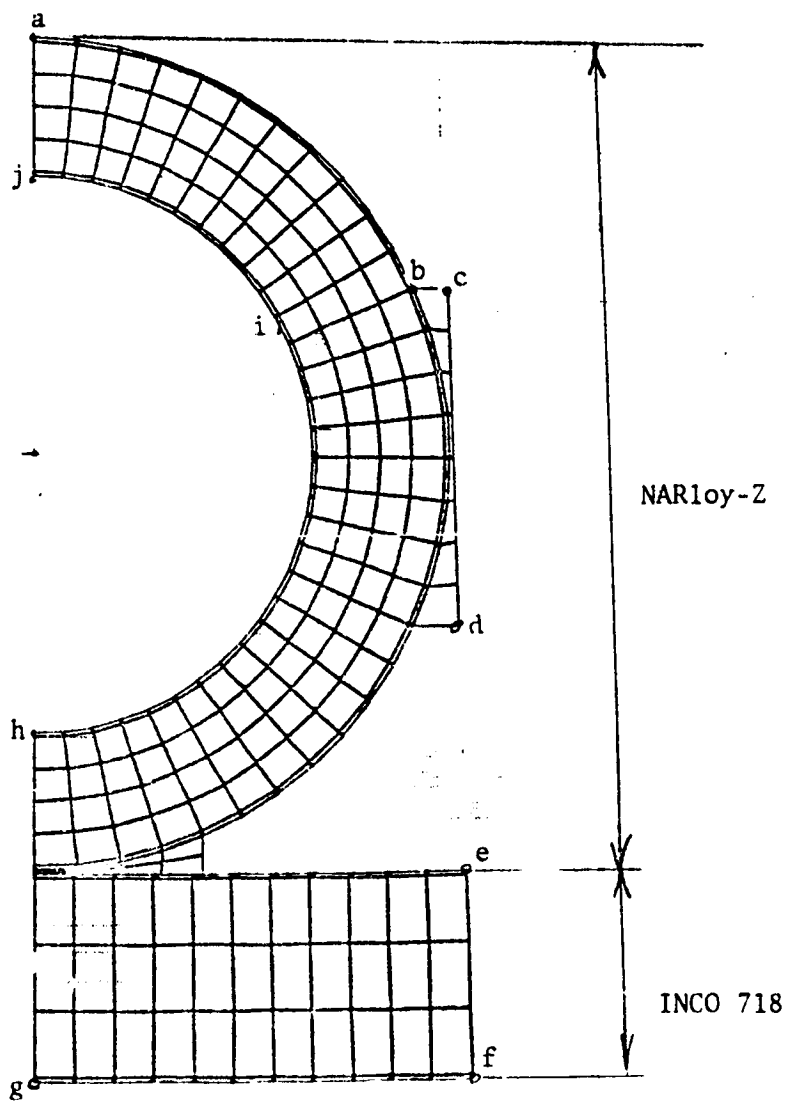


Figure 72. Finite Element Model (NARloy-Z Tubular Configuration
at $X = -0.8$ inch or -2.03 cm)

100 CHANNEL NARloy T/C DESIGN-COOLANT
PLUS HOT GAS PRESSURE AND TEMPERATURE

UNDEFORMED STRUCTURE

CYCLE NO. 1

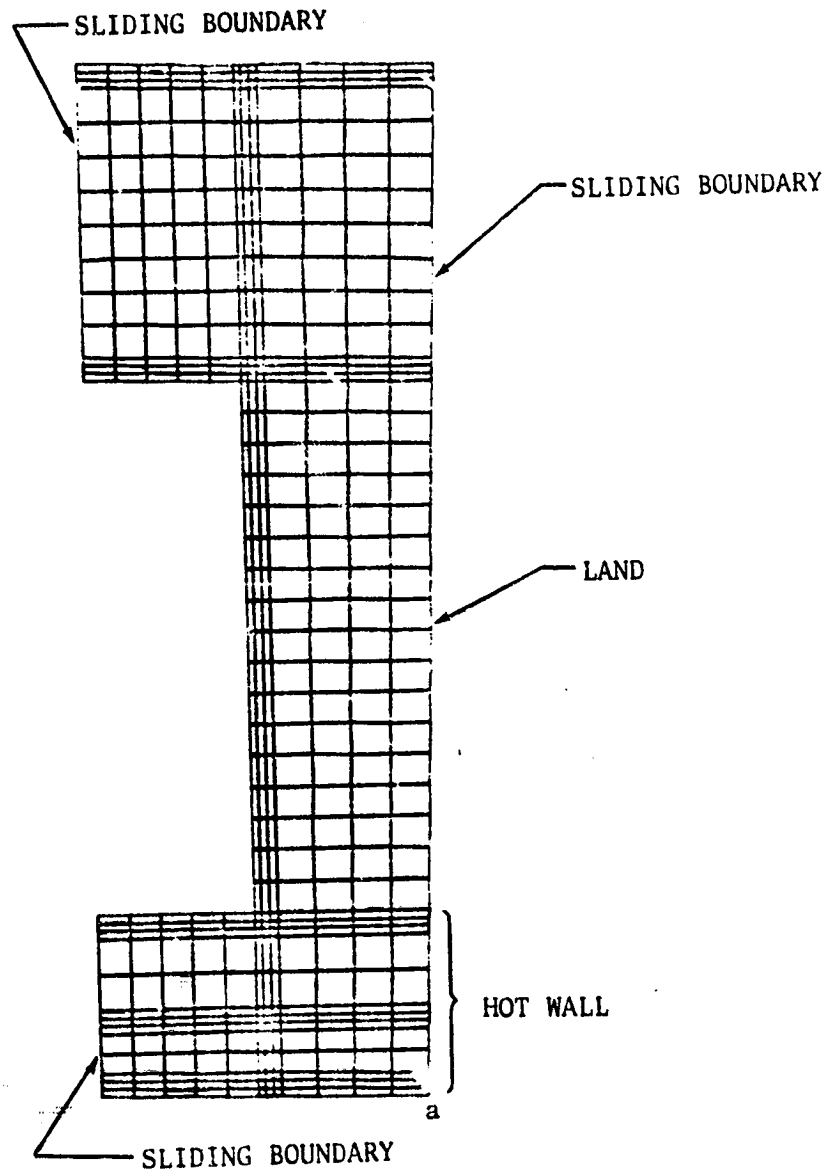


Figure 73. NARloy-2 Channel Wall Finite Element Stress Analysis Model

TABLE XI. NARLOY-Z CHANNEL WALL AND TUBULAR WALL
FINITE ELEMENT STRESS ANALYSIS RESULTS

Analysis Method	ϵ_{eff} (in/in)	N_f Cycles	ϕ_f	σ_{hyd} (psi)	T_R (hours)	ϕ_c	$4(\phi_f + \phi_c)$
Simplified	0.0216	1600	0.1875	5263 (3.63×10^7 N/m ²)	200	0.05	0.95
Finite Element	0.0245	1100	0.2727	5263 (3.63×10^7 N/m ²)	200	0.05	1.29
Simplified	0.01375	6300	0.0477	5240 (3.61×10^7 N/m ²)	75	0.133	0.723
Finite Element	0.01275	7900	0.038	5240 (3.61×10^7 N/m ²)	75	0.133	0.684

NARLOY-Z
Channel Wall
(Split-Flow
Cooling
Circuit)

NARLOY-Z
Tubular Wall
(1-1/2 Pass
Cooling
Circuit)

Coolant Circuit: Split-Flow (Regeneratively Cooled to $\epsilon = 100$)
 Material: NARloy-Z
 Combustor-Nozzle Joint: $\epsilon = 8$
 Minimum Channel Width: 0.040 inch (0.1016 cm)
 Minimum Hot-Gas Wall Thickness: 0.023 inch (0.0584 cm)

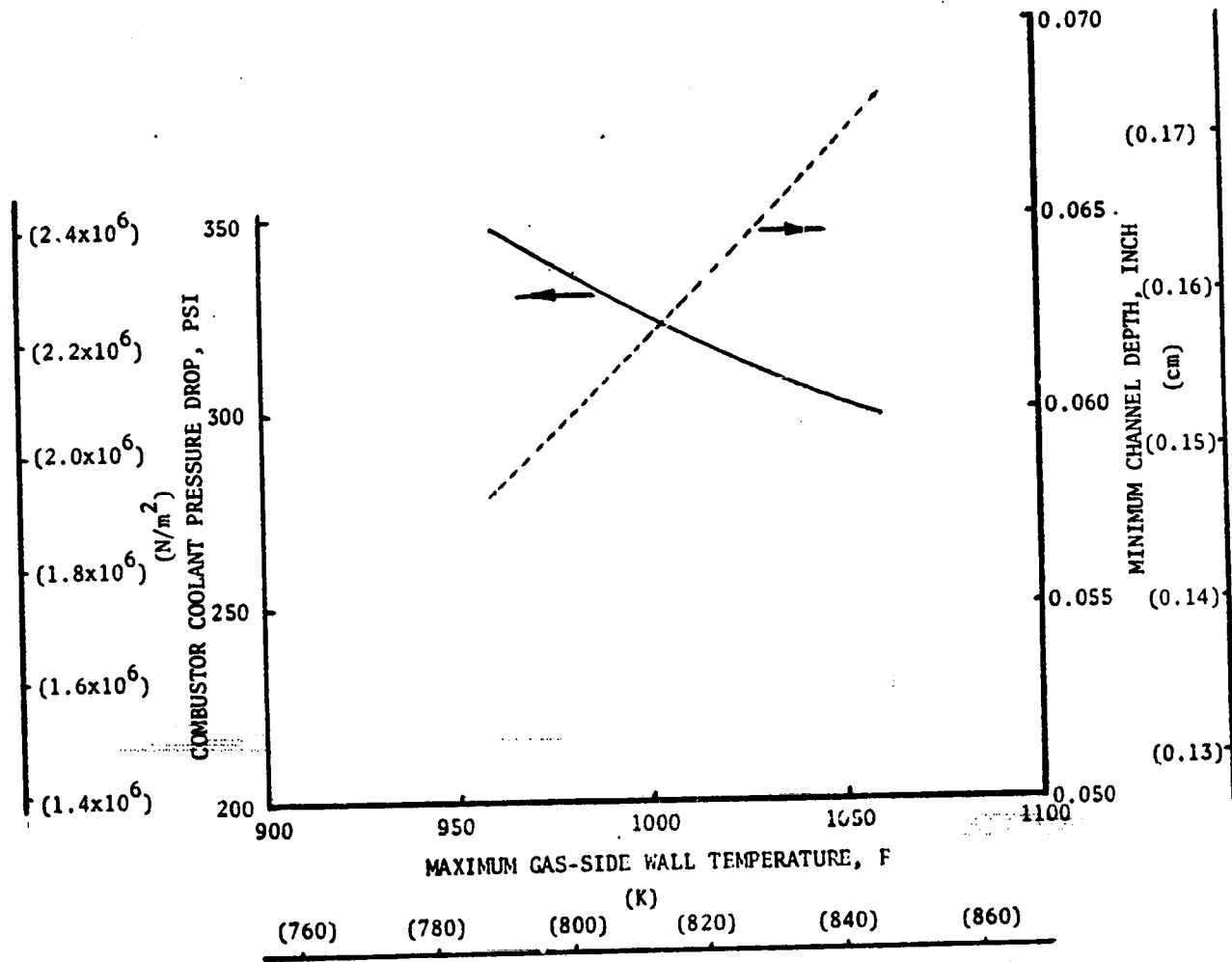


Figure 74. Variations of Combustor Coolant Pressure Drop and Channel Depth With Maximum Wall Temperature for Split-Flow Cooling Circuit NARloy-Z Combustor

Design Modifications of Selected Configurations

The finite element stress analysis results for the NARloy-Z channel wall configuration concluded that the selected designs must be modified to meet the required cycle life of 300 cycles. For these analyses, the stress determined thicknesses of the electroformed nickel closeout and the INCO 718 structural jacket of 0.01-inch (0.0254 cm) and 0.025-inch (0.0635 cm), respectively, were used. These values were different than the design drawing values of 0.030-inch (0.0762 cm) and 0.060-inch (0.1524 cm), respectively, which were termed "easily fabricated". At this time, the cycle life was believed to be insensitive to these thicknesses; however, subsequent analyses on the Zr-Cu channel wall designs indicated that the thicker closeout and jacket caused an increased restraint resulting in an increased strain on the gas-side wall. Because of this, the minimum reasonable fabrication thickness of 0.030-inch (0.0762 cm) for the electroform nickel and 0.032-inch (0.0813 cm) for the INCO 718 jacket were selected as a compromise.

The modifications to the two selected Zr-Cu channel wall designs resulted in a lower maximum gas-side wall temperature by 120 F (322 K) for the split-flow cooling circuit (Fig. 75) and by 140 F (333 K) for the 1-1/2 pass cooling circuit (Fig. 76). Approximately half of these temperature differences was due to the difference in the computed effective strain from the simplified and finite element stress analyses. The other half was the result of the increased electroform nickel and INCO 718 jacket thicknesses. All the pertinent information for the final split-flow cooling circuit design is presented in Fig. 77 through 80. Similar data for the 1-1/2 pass cooling circuit design are shown in Fig. 81 through 84.

The finite element stress analysis was performed using models (Fig. 85) similar to that previously described. The maximum effective strain occurred on the hot gas wall at mid-land. Results for the Zr-Cu channel wall cases (Table XII) indicated total damage fractions of 1.0 and 0.97 for the split-flow and 1-1/2 pass cooling circuits. As shown in Table XII, the fatigue damage fraction governed the design.

Various analytical and empirical modifications were investigated to modify the simplified cycle life analysis method for channels to more closely agree with the finite element stress analysis results. The combined thermal and pressure loads acting within a thrust chamber dictate the cycle life, are extremely complex, and cannot be merely superimposed. The modifications evaluated included:

1. Relating the coolant land height to the effective strain.
2. Combining axial and hoop loads in a simple manner to model the thermal and pressure effects.
3. Obtaining a ratio of the effective strains and applying this ratio.

The first modification yielded no significant influence of land height for the narrow range investigated. Evaluation of a combined axial and hoop load model reveal that a simple model does not exist.

Coolant Circuit: Split-Flow (Regeneratively Cooled to $\epsilon = 100$)

Material: Zr-Cu

Combustor-Nozzle Joint: $\epsilon = 8$

Minimum Channel Width: 0.040-inch (0.1016 CM)

Minimum Hot-Gas Wall Thickness: 0.027-inch (0.0686 CM)

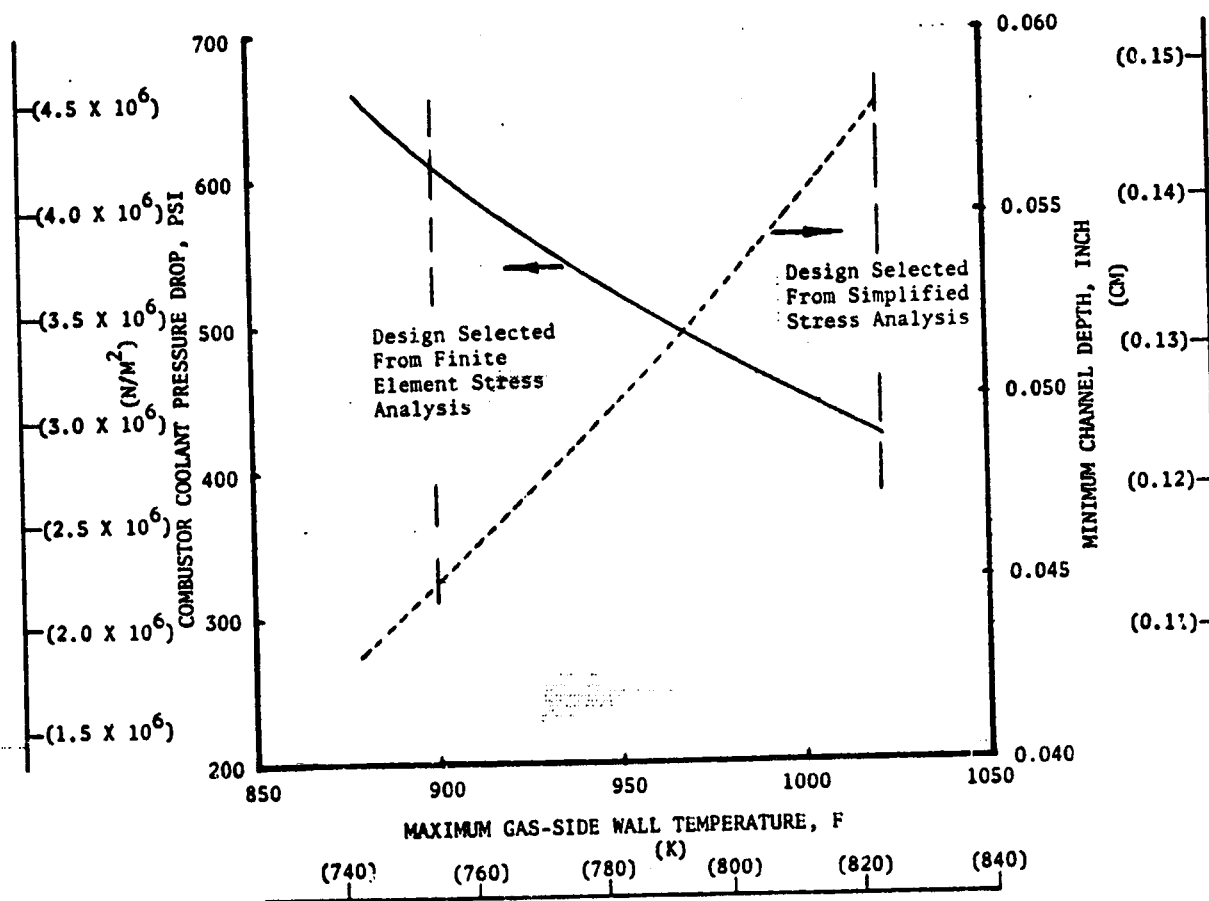


Figure 75. Variation of Combustor Coolant Pressure Drop and Minimum Channel Depth With Maximum Gas-Side Wall Temperature for Split-Flow Cooling Circuit Zr-Cu Combustor

Coolant Circuit: 1-1/2 Pass (Regeneratively Cooled to $\epsilon = 100$)

Material: Zr-Cu

Combustor-Nozzle Joint: $\epsilon = 8$

Minimum Channel Width: 0.040-Inch (0.1016 CM)

Maximum Hot-Gas Wall Thickness: 0.027-Inch (0.0686 CM)

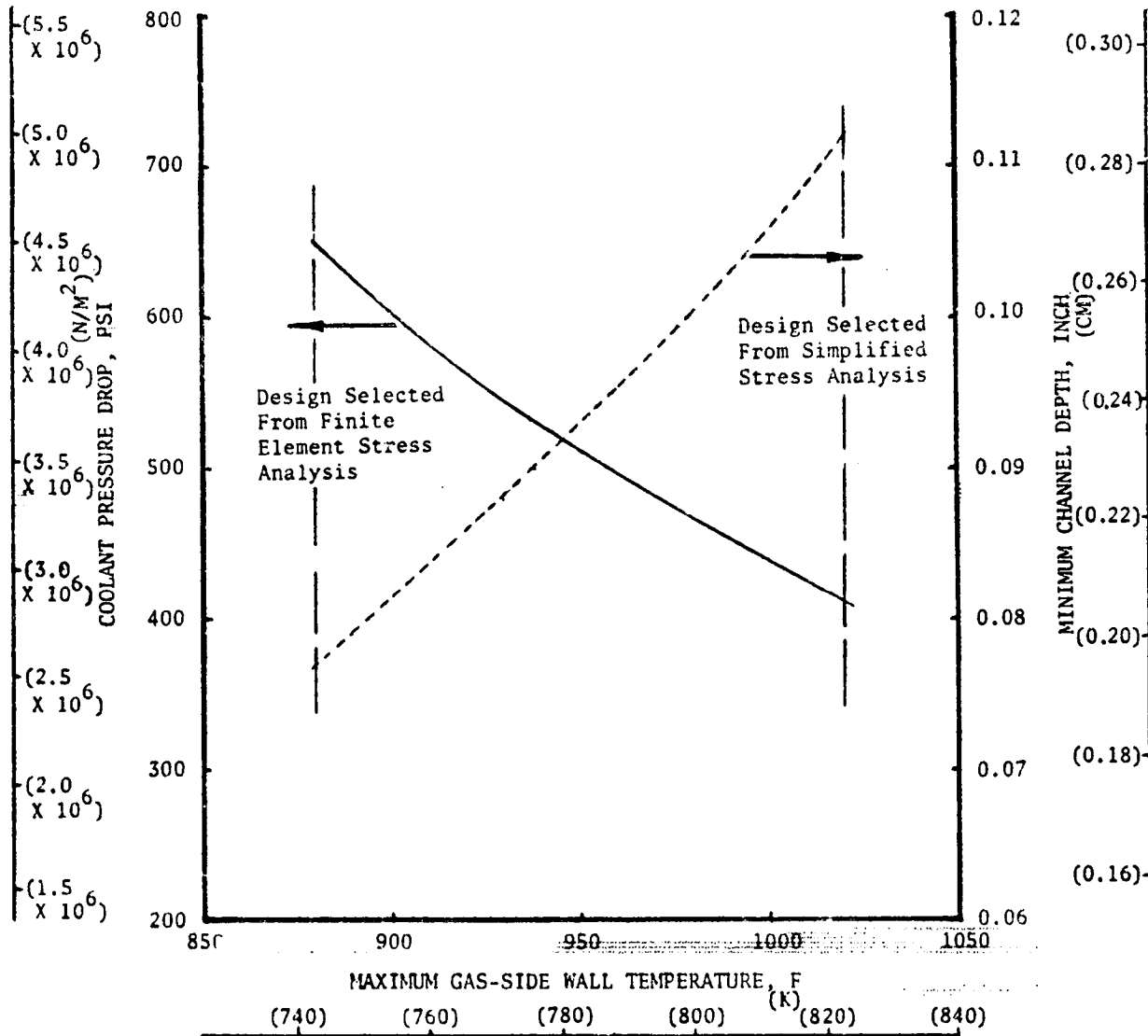


Figure 76. Variation of Combustor Coolant Pressure Drop and Minimum Channel Depth With Maximum Gas-Side Wall Temperature for 1-1/2 Pass Cooling Circuit Zr-Cu Combustor

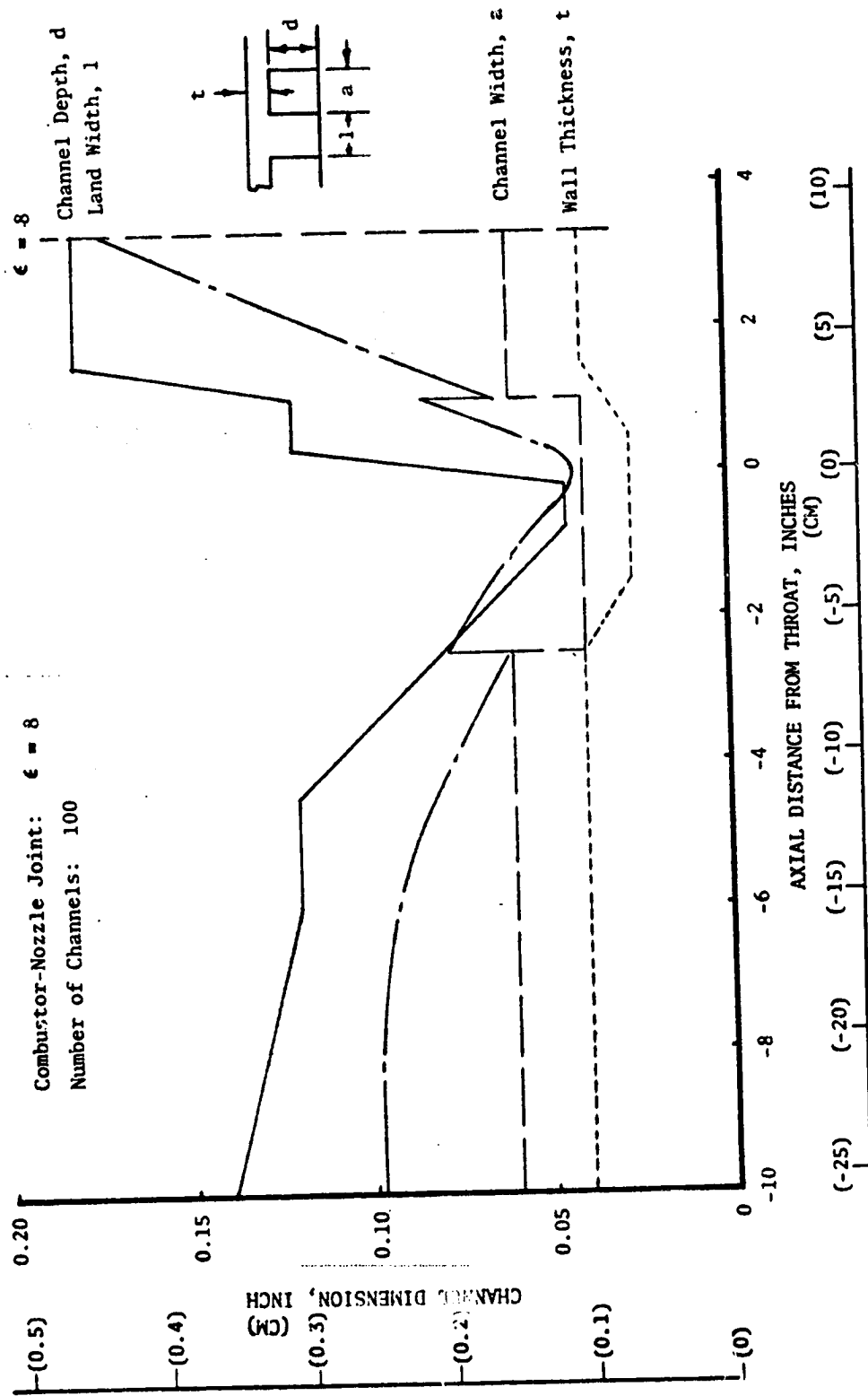


Figure 77. Channel Dimensions of the Final Zr-Cu Channel Wall Comburtor Configuration (Split-Flow Cooling Circuit)

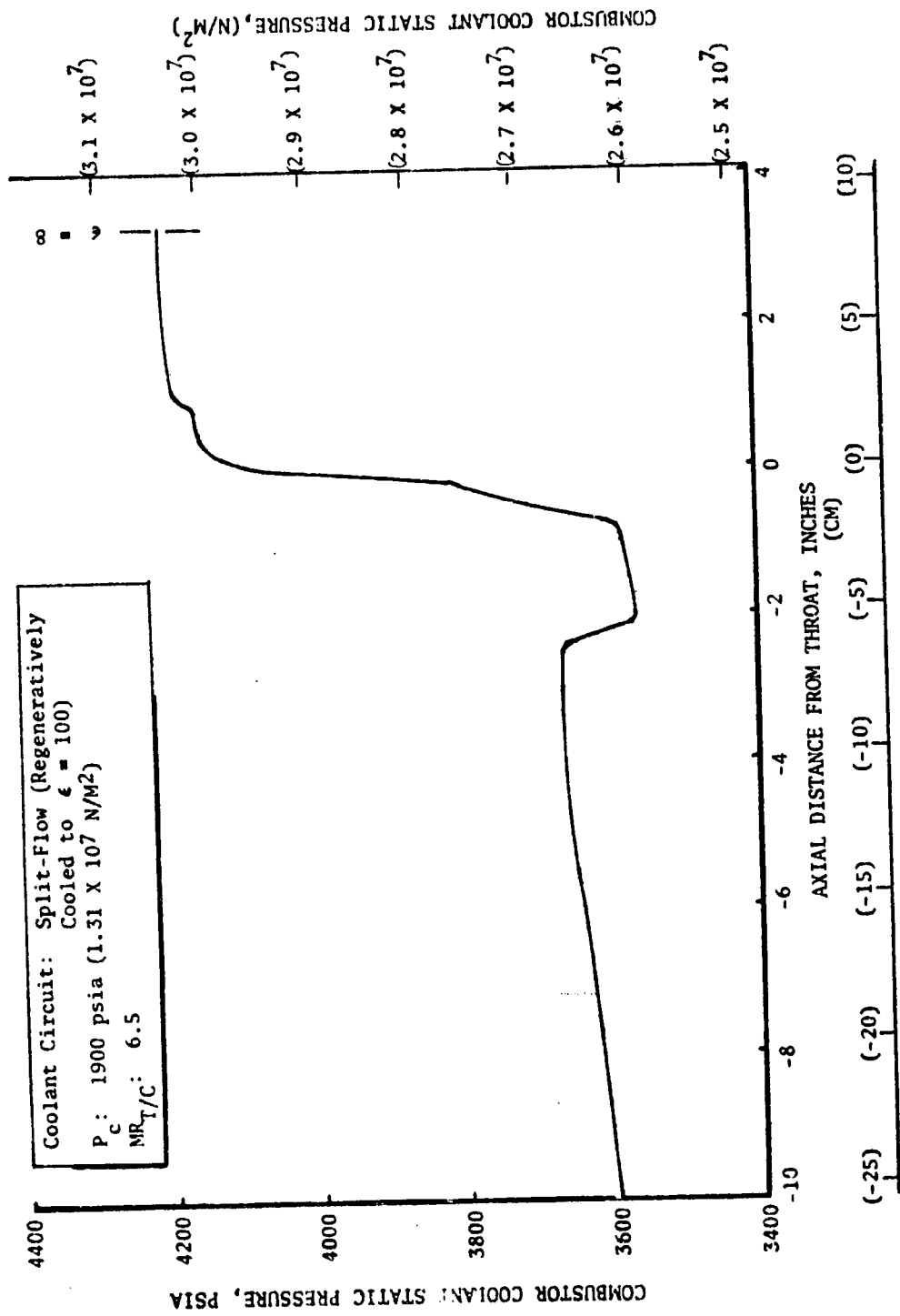


Figure 78. Coolant Static Pressure Distribution for the Final Zr-Cu Combustor Configuration (Split-Flow Cooling Circuit)

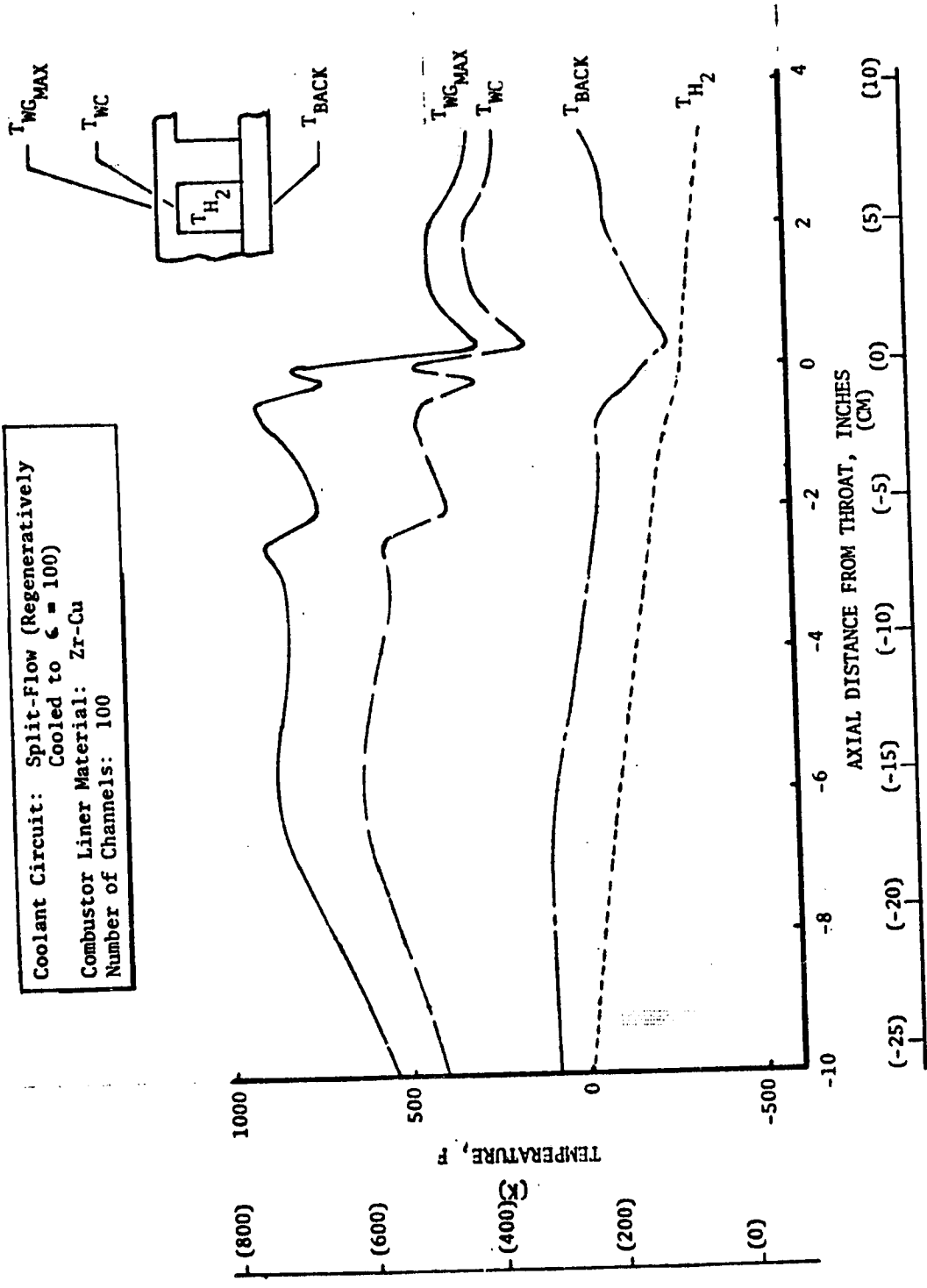


Figure 79. Temperature Distribution for the Final Zr-Cu Channel Wall Combustor Configuration (Split-Flow Cooling Circuit)

ZR-CU(SPLIT-FLOW)W=0.64-0.06IN T=627-0.04IN(A/T=1.482) N=100 DESIGN L

STATION NO. = 33
 X (INCHES) = -0.5000
 AREA RATIO = 1.1274

TWC(I-D) = 1942.06 F
 TWC(O-D) = 570.36 F
 HC(I-D) = 0.9141E-01

CHANNEL DIMENSIONS (IN.)
 WALL THICKNESS = 0.0270
 CHANNEL HEIGHT = 0.0450
 CHANNEL WIDTH = 0.0400
 LAND WIDTH = 0.0478
 CLOSURE THICK. = 0.1000

THERMAL CONDUCTIVITY
 (BTU/IN-SEC-F)

WALL = 0.4417E-02
 CLOSURE = 0.1000E-02

COMBUSTION-GAS
 PARAMETERS

TAW = 6195.75 F
 HG = 0.1500E-01
 (BTU/IN2-S-F)

COOLANT PARAMETERS

TAWLK = -273.71 F
 T3/TWC EXPONENT = 0.552
 MAX. CURVATURE = 1.247
 HC(PFF.) = 0.14/RE CO
 (BTU/IN2-S-F)

BETA = 1.814 AT ITERATION NUMBER 25

HEAT BALANCE = 0.3724E-34 CONVERGENCE SATISFIED AT ITERATION = 03
 MAXIMUM DT/T = 0.9233E-04 AT NODE 81

TEMPERATURES (F)

900.01	899.24	897.62	896.77	897.60	898.78	899.30
739.41	738.20	735.48	735.93	735.63	737.78	738.66
581.88	575.05	571.97	575.60	573.02	579.04	581.23
431.48	425.53	427.48	376.20	412.88	427.57	431.61
214.55	203.97	170.90	110.72			
72.74	62.17	30.57	-21.21	-165.69	-190.19	-204.34
5.91	-4.04	-34.12	-65.13	-103.09	-107.99	-109.72
-79.67	-81.77	-97.63	-85.99	-95.51	-86.14	-95.42
-92.21	-82.54	-93.42	-84.59	-94.63	-94.81	-94.49
-93.72	-93.82	-94.00	-94.38			

FINAL COOLANT FILM COEFFICIENTS

0.097460	0.100140	0.099229	0.099442
0.113979			
0.131710			
0.137762	0.146020	0.156066	0.159183

FIN FACTOR = 1.1233

Figure 80. Two-Dimensional Wall Temperature Distribution in Throat Region for Final Zr-Cu Combustor (Split-Flow Cooling Circuit)

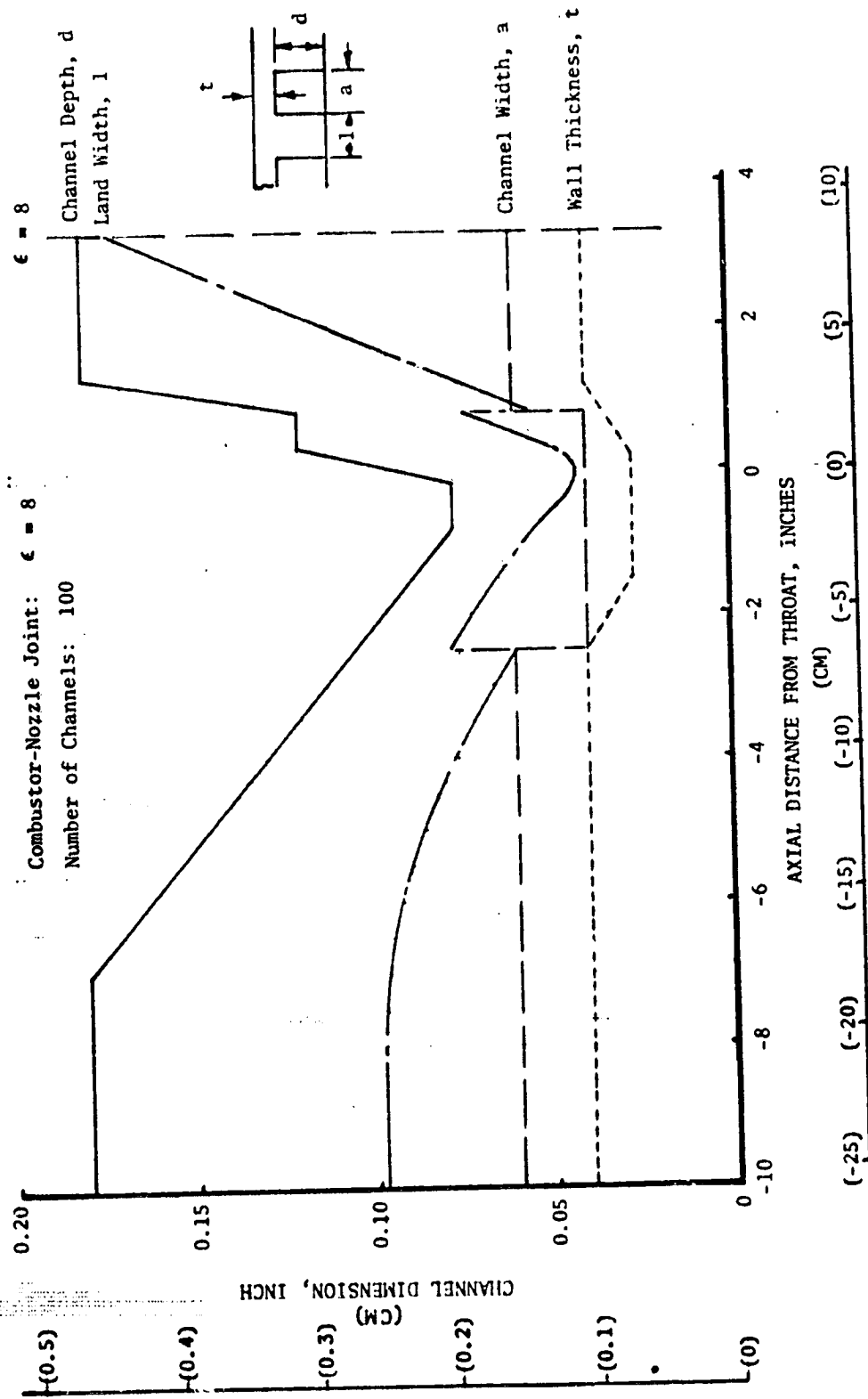


Figure 81. Channel Dimensions of the Final Zr-Cu Channel Wall Combustor Configuration (1-1/2 Pass Cooling Circuit)

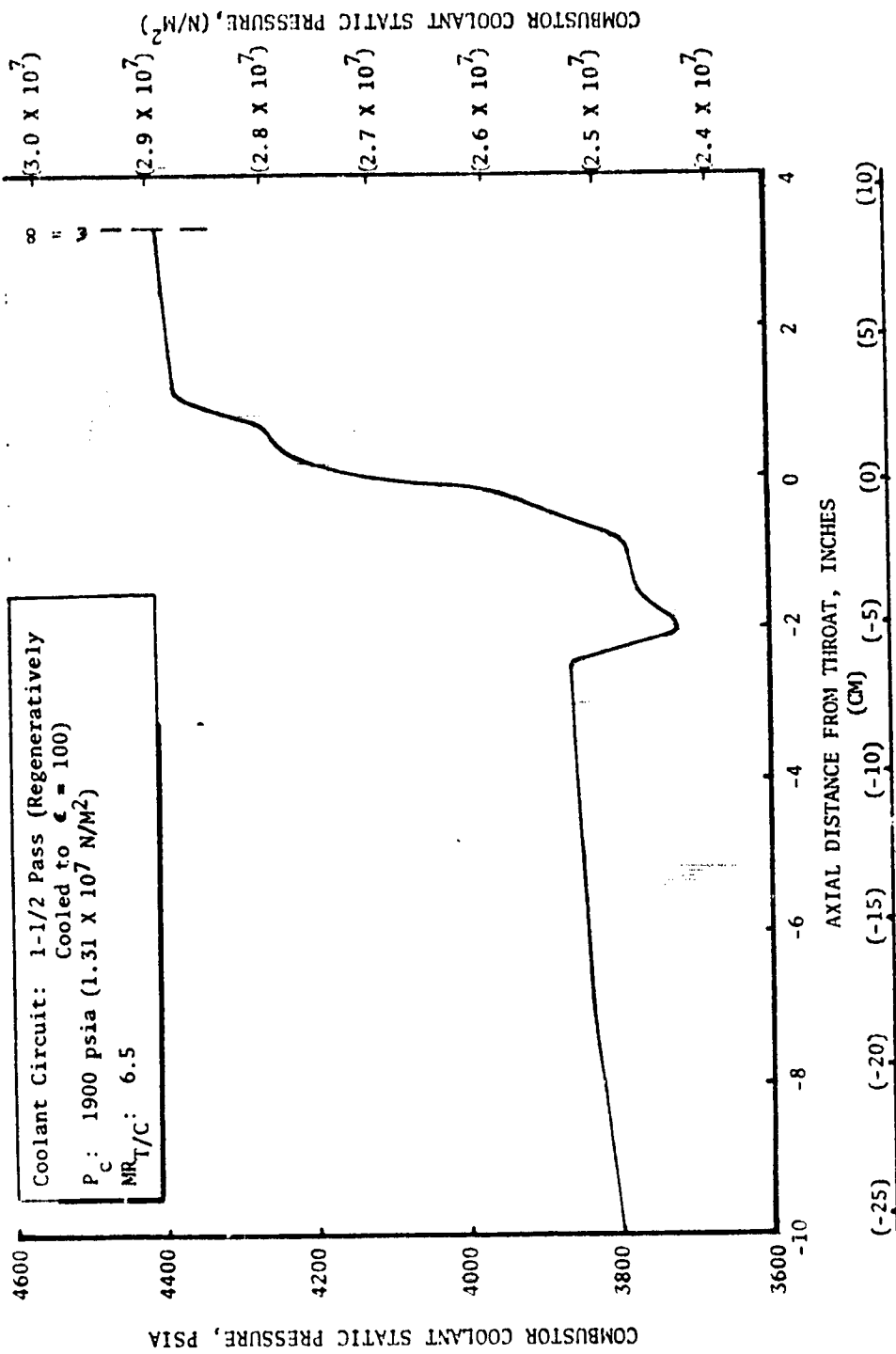


Figure 82. Coolant Static Pressure Distribution for the Final Er-Cu Combustor Configuration (1-1/2 Pass Cooling Circuit)

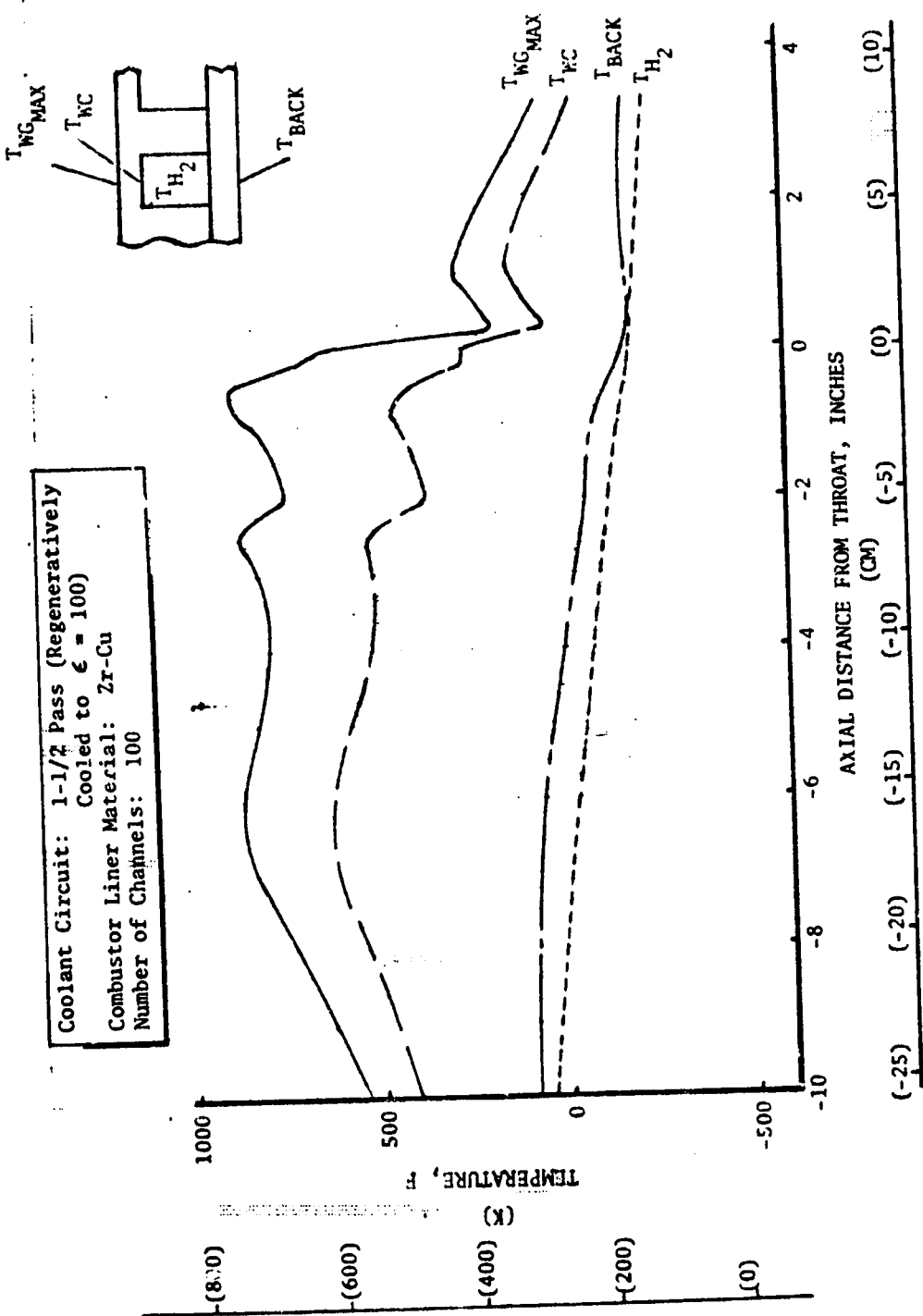


Figure 85. Temperature Distribution for the Final Zr-Cu Channel Wall Combustor Configuration (1-1/2 Pass Cooling Circuit)

4-26 IN T=0.07-0.04 IN (A/I=1.482) NE100 DESIGN H

STATION NO. = 23
 X (INCHES) = -0.5000
 AREA RATIO = 1.1271

TE (I-D) = 971.18 F
 TWC (I-O) = 502.00 F
 HC (I-U) = 0.1166 F

CHANNEL DIMENSIONS (IN.)
 WALL THICKNESS = 0.0270
 CHANNEL HEIGHT = 0.0770
 CHANNEL WIDTH = 0.0400
 LAP WIDTH = 0.0470
 CHANNEL THICKNESS = 0.1000

HEAT BALANCE = 0.4652E-04
 CONVERGENCE SATISFIED AT ITERATION = 80
 MAXIMUM DT/I = 0.0765E-04 AT NODE 91

COOLANT PARAMETERS
 TAUKE = -140.03 F
 TE/TWC PARAMENT = 0.510
 MAX. CURVATURE = 1.247
 HC (O/F) = 0.1001E 00
 (F/U/INC-S-F)

COMBUSTION GAS PARAMETERS
 TAMB = 5115.76 F
 FC = 0.1200E-01
 (O/F/I/INC-S-F)

PTG = 1.71 AT ITERATION NUMBER 25

TEMPERATURES (F)

870.12	878.91	876.08	873.78	873.72	874.39	874.74
720.00	718.22	713.84	710.31	711.16	712.12	710.54
544.42	540.74	550.90	540.57	547.16	542.92	544.66
418.25	411.12	311.49	345.47	384.65	380.78	403.12
101.48	92.24	68.27	75.17			
-45.25	-44.95	-173.54	-96.25			
-94.21	-97.65	-107.54	-103.60	-142.39	-150.62	-155.22
-118.27	-118.56	-110.71	-122.12	-124.85	-126.17	-127.64
-131.74	-131.26	-122.11	-122.44	-120.71	-122.89	-123.97
-122.14	-122.20	-122.22	-122.27	-122.45	-122.51	-122.54

FINAL COOLANT FILM COEFFICIENTS

0.122173	0.125224	0.124007	0.123666
0.143047			
0.176664			
0.176906	0.171968	0.174932	0.175282

FIN FACTOR = 1.1003

Figure 84. Two-Dimensional Wall Temperature Distribution in Throat Region for Final Zr-Cu Combustor (1-1/2 Pass Cooling Circuit)

TABLE XII. Zr-Cu CHANNEL WALL FINITE ELEMENT
STRESS ANALYSIS RESULTS

Cooling Circuit	ϵ eff (in/in)	N_f (cycles)	ϕ_f	σ_{hyp} (psi)	T_R (hours)	ϕ_c	$4(\phi_c + \phi_f)$
Split-Flow	0.022	1210	0.249	4105 (2.85×10^7 N/m ²)	10^4	10^{-3}	1.0
1-1/2 Pass	0.0217	1240	0.242	3872 (2.67×10^7 N/m ²)	10^4	10^{-3}	0.97

100 CHANNEL Zr-Cu T/C DESIGN NO. 4A

TEMPERATURE EFFECTS ONLY

UNDEFORMED STRUCTURE

CYCLE NO. 1

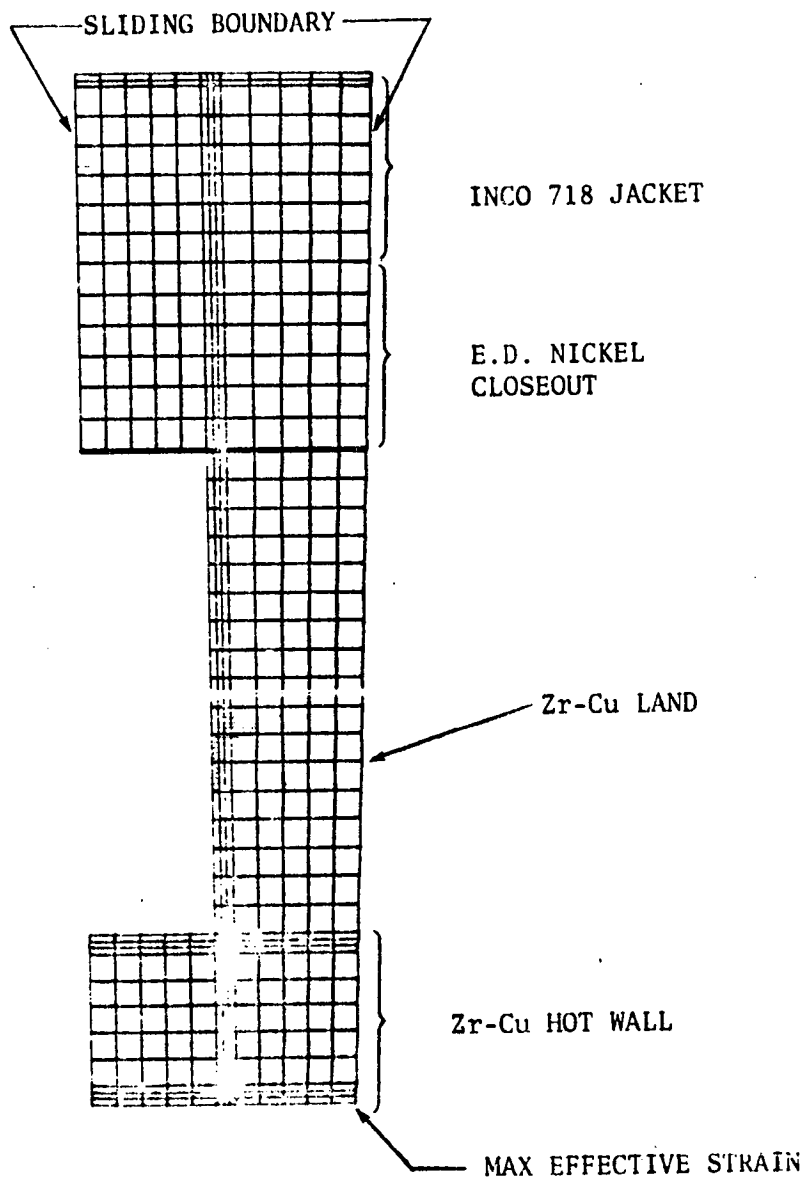


Figure 85. Zr-Cu Channel Wall Finite Element Stress Analysis Model

Of the modifications evaluated, the effective strain ratio method correlated the cases investigated with a ratio of 1.2¹ and also would be the simplest to apply. This modified method for channels would be:

$$\epsilon_{\text{eff}} = 1.2 (\epsilon_{\text{eff}}) \text{ simplified method}$$

An overall comparison of the two cooling circuits is shown in Table XIII. As shown in Table XIII, the split-flow cooling circuit achieved a 6-percent lower coolant pressure drop and a slight thrust chamber weight advantage. Both designs provide reasonable gas-side wall temperatures. From a thrust chamber development standpoint, the split-flow cooling circuit would enable independent development of the combustor and nozzle. Also, this circuit provides a separate fluid supply to drive the boost pumps. Design drawings for the two cooling circuits are presented in Fig. 86 and 87.

TRANSIENT ANALYSIS

For the transient analysis of the two Zr-Cu channel wall configurations, the engine start from the Advanced Space Engine Preliminary Design Program (NAS3-16751) was evaluated. As shown in Fig. 88, this engine start was a "cold" start with pumps at cryogenic temperatures and the thrust chamber initially at 0 F (255 K). The engine shutdown specified in the Work Statement (Fig. 89) was analyzed for the shutdown transient. For the transient analyses the following assumptions were made:

1. Pertinent dimensionless parameter distributions of $P_c/P_{c_{\text{design}}}$, $\dot{W}_{H_2}/\dot{W}_{H_2_{\text{design}}}$, and MR/MR_{design} were the same for both the 1-1/2 pass and split-flow cooling circuits.
2. $P_c \propto \dot{W}_{\text{total}}$ for the engine shutdown
3. $h_g \propto P_c^{0.8}$
4. $h_c \propto (\dot{W}_{H_2})^{0.8}$ and $h_c \propto (T_B/T_{WC})^{0.55}$

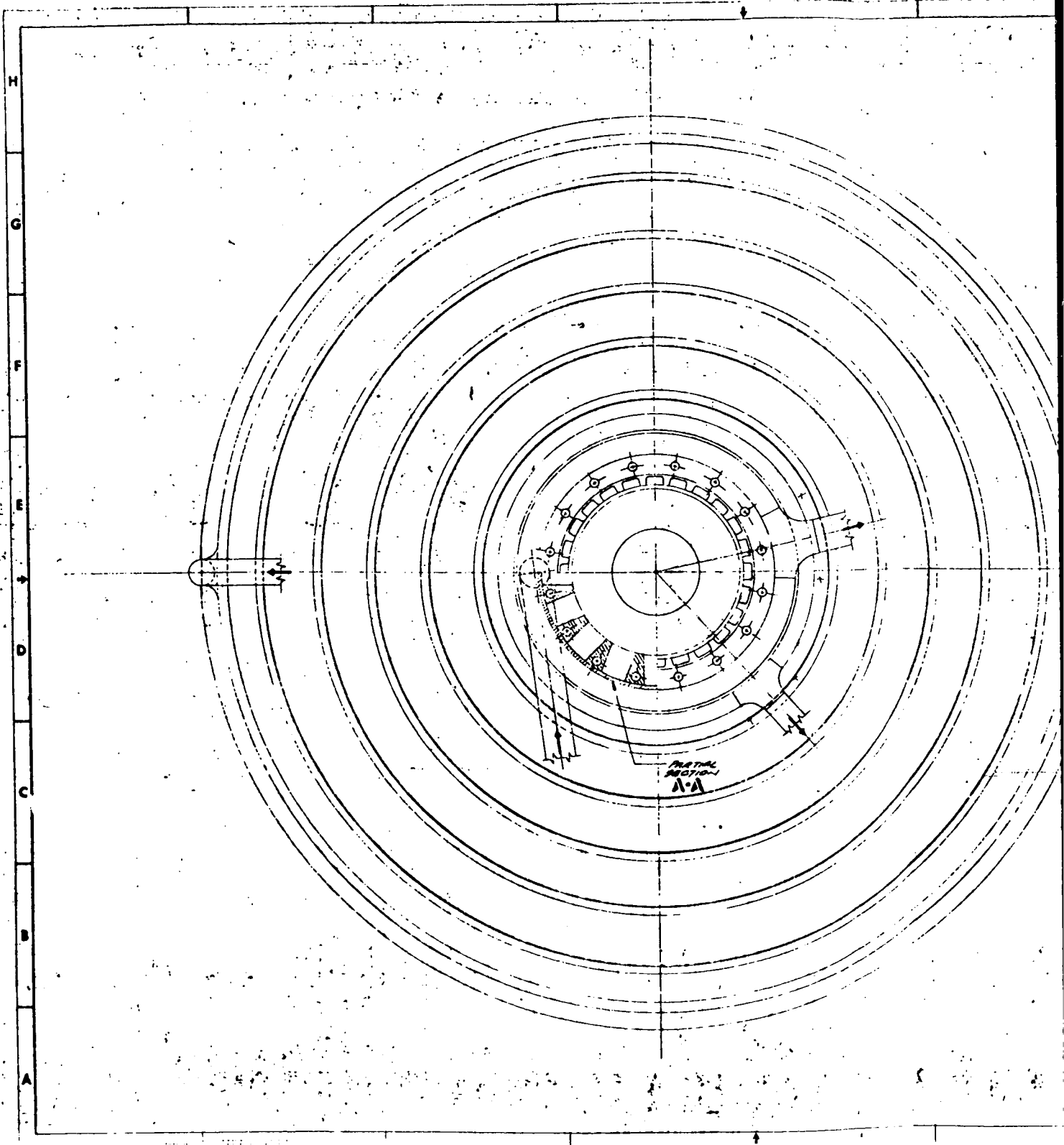
The thermal model used in this transient analysis was a 35-node two-dimensional model of a coolant channel. Initially, this analysis was to be performed using the 1-1/2 dimensional model incorporated in the regenerative-cooling design/analysis computer program. However, the incorporation of this model was not completed in time so the two-dimensional model was used. This model was set up for the Rocketdyne Differential Equation Analyzer Program (DEAP), which is capable of solving parabolic, hyperbolic, and elliptic problems in one, two, and

¹Subsequent finite element stress analysis indicated that this factor varied from 1.0 to 1.2

TABLE XIII. COOLANT CIRCUIT COMPARISON
(Zr-Cu CHANNEL WALL COMBUSTOR/A-286 TUBULAR NOZZLE)

Component	Coolant Circuit	1-1/2 Pass	Split-Flow
<u>Nozzle</u>			
Number of Tubes	400	525	525
Minimum Unformed Tube Outside Diameter, inch	0.075 (0.1905 cm)	0.050 (0.127 cm)	0.050 (0.127 cm)
Maximum Gas-Side Wall Temperature, F	525 (547 K)	685 (636 K)	685 (636 K)
<u>Combustor</u>			
Number of Channels	100	100	100
Minimum Channel Dimensions:			
Width, inch	0.040 (0.1016 cm)	0.040 (0.1016 cm)	0.040 (0.1016 cm)
Height, inch	0.077 (0.1955 cm)	0.045 (0.1143 cm)	0.045 (0.1143 cm)
Land, inch	0.0427 (0.1083 cm)	0.0427 (0.1083 cm)	0.0427 (0.1083 cm)
Minimum Hot-Gas Wall Thickness, inch	0.027 (0.0686 cm)	0.027 (0.0686 cm)	0.027 (0.0686 cm)
Maximum Gas-Side Wall Temperature, F	880 (745 K)	900 (756 K)	900 (756 K)
Critical Location Stress and Life Parameters:			
Yield Safety Factor	1.38	1.42	1.42
Ultimate Safety Factor	2.04	2.05	2.05
Damage Fraction*	4 (0.001 + 0.242) = 0.97	4 (0.001 + 0.242) = 0.97	4 (0.001 + 0.249) = 1.00
$4 (\phi_c + \phi_f)$			
<u>Chamber</u>			
Coolant Pressure Drop, psi	649 (4.48 x 10 ⁶ N/m ²)	608 (4.19 x 10 ⁶ N/m ²)	608 (4.19 x 10 ⁶ N/m ²)
Combustor Liner and Nozzle Tube Weight, pounds	15.6 (7.08 Kg)	(36) - Nozzle (2.48 x 10 ⁵ N/m ²)	14.0 (6.35 Kg)

*Obtained from finite element stress analysis



FOLDOUT FRAME

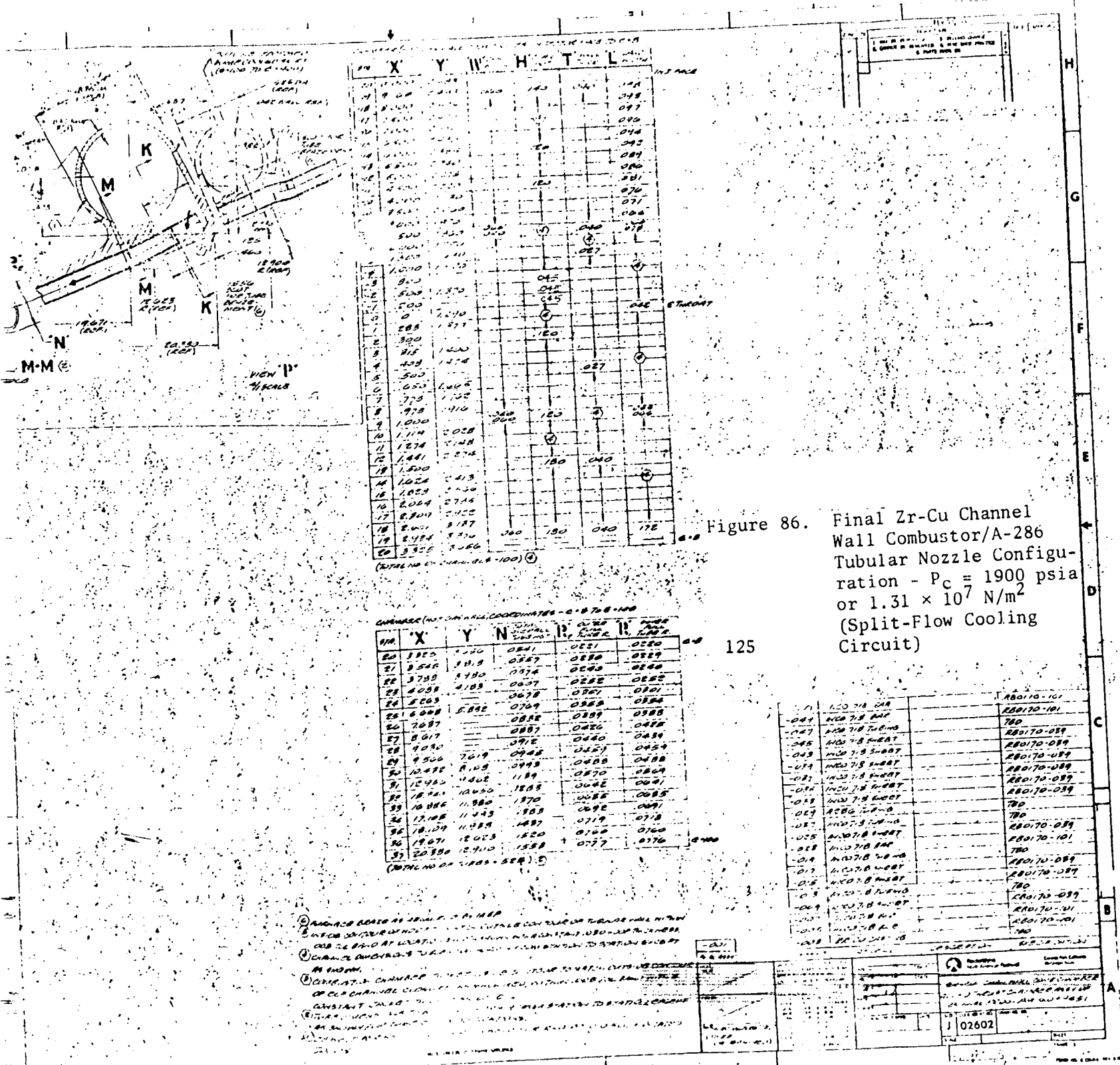


Figure 86. Final Zr-Cu Channel Wall Combustor/A-286 Tubular Nozzle Configuration - $P_C = 1900$ psia or 1.31×10^7 N/m² (Split-Flow Cooling Circuit)

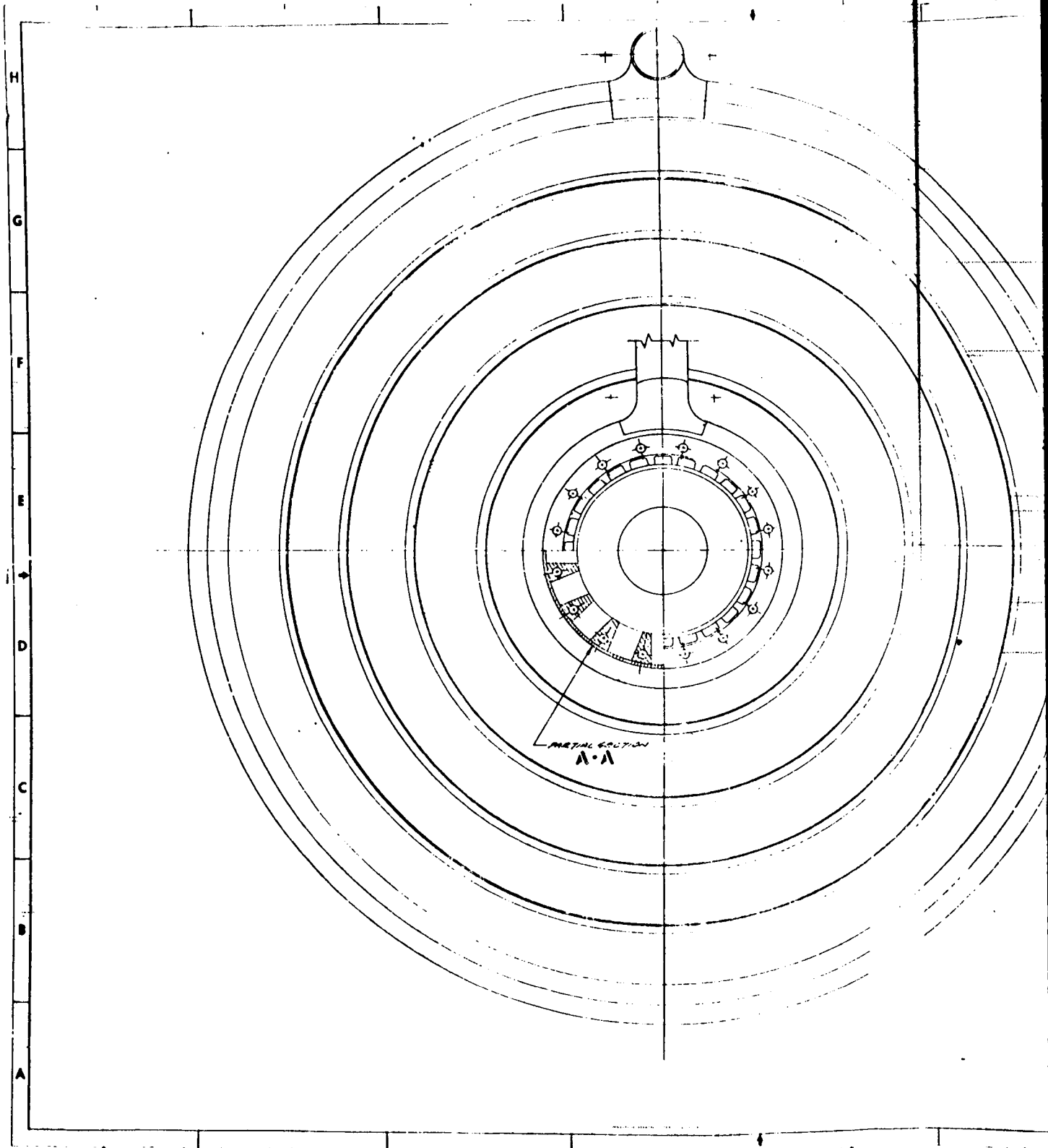
CHANNEL WALL COORDINATES - C-B 708-100

NO.	X	Y	N	H	T	L
20	3825	1000	0841	0851	0860	
21	3848	1018	0847	0856	0865	
22	3789	1080	0874	0883	0892	
23	4088	1108	0877	0886	0895	
24	3868		0878	0887	0896	
25	4088	5882	0709	0718	0727	
26	3887		0882	0891	0900	
27	3917		0887	0896	0905	
28	4010		0912	0921	0930	
29	4010	7019	0948	0957	0966	
30	4010	1108	0948	0957	0966	
31	12482	1108	1184	1193	1202	
32	12482	1000	1885	1894	1903	
33	12482	1188	1885	1894	1903	
34	12482	1108	1885	1894	1903	
35	12482	1108	1885	1894	1903	
36	12482	1108	1885	1894	1903	
37	12482	1108	1885	1894	1903	

045	NOZ 718 RMT	AB0170-101
046	NOZ 718 RMT	AB0170-101
047	NOZ 718 RMT	AB0170-089
048	NOZ 718 RMT	AB0170-089
049	NOZ 718 RMT	AB0170-089
050	NOZ 718 RMT	AB0170-089
051	NOZ 718 RMT	AB0170-089
052	NOZ 718 RMT	AB0170-089
053	NOZ 718 RMT	AB0170-089
054	NOZ 718 RMT	AB0170-089
055	NOZ 718 RMT	AB0170-089
056	NOZ 718 RMT	AB0170-089
057	NOZ 718 RMT	AB0170-089
058	NOZ 718 RMT	AB0170-089
059	NOZ 718 RMT	AB0170-089
060	NOZ 718 RMT	AB0170-089
061	NOZ 718 RMT	AB0170-089
062	NOZ 718 RMT	AB0170-089
063	NOZ 718 RMT	AB0170-089
064	NOZ 718 RMT	AB0170-089
065	NOZ 718 RMT	AB0170-089
066	NOZ 718 RMT	AB0170-089
067	NOZ 718 RMT	AB0170-089
068	NOZ 718 RMT	AB0170-089
069	NOZ 718 RMT	AB0170-089
070	NOZ 718 RMT	AB0170-089
071	NOZ 718 RMT	AB0170-089
072	NOZ 718 RMT	AB0170-089
073	NOZ 718 RMT	AB0170-089
074	NOZ 718 RMT	AB0170-089
075	NOZ 718 RMT	AB0170-089
076	NOZ 718 RMT	AB0170-089
077	NOZ 718 RMT	AB0170-089
078	NOZ 718 RMT	AB0170-089
079	NOZ 718 RMT	AB0170-089
080	NOZ 718 RMT	AB0170-089
081	NOZ 718 RMT	AB0170-089
082	NOZ 718 RMT	AB0170-089
083	NOZ 718 RMT	AB0170-089
084	NOZ 718 RMT	AB0170-089
085	NOZ 718 RMT	AB0170-089
086	NOZ 718 RMT	AB0170-089
087	NOZ 718 RMT	AB0170-089
088	NOZ 718 RMT	AB0170-089
089	NOZ 718 RMT	AB0170-089
090	NOZ 718 RMT	AB0170-089
091	NOZ 718 RMT	AB0170-089
092	NOZ 718 RMT	AB0170-089
093	NOZ 718 RMT	AB0170-089
094	NOZ 718 RMT	AB0170-089
095	NOZ 718 RMT	AB0170-089
096	NOZ 718 RMT	AB0170-089
097	NOZ 718 RMT	AB0170-089
098	NOZ 718 RMT	AB0170-089
099	NOZ 718 RMT	AB0170-089
100	NOZ 718 RMT	AB0170-089

① CHANNEL WALL COORDINATES - C-B 708-100
 ② CHANNEL WALL COORDINATES - C-B 708-100
 ③ CHANNEL WALL COORDINATES - C-B 708-100
 ④ CHANNEL WALL COORDINATES - C-B 708-100
 ⑤ CHANNEL WALL COORDINATES - C-B 708-100
 ⑥ CHANNEL WALL COORDINATES - C-B 708-100
 ⑦ CHANNEL WALL COORDINATES - C-B 708-100
 ⑧ CHANNEL WALL COORDINATES - C-B 708-100
 ⑨ CHANNEL WALL COORDINATES - C-B 708-100
 ⑩ CHANNEL WALL COORDINATES - C-B 708-100
 ⑪ CHANNEL WALL COORDINATES - C-B 708-100
 ⑫ CHANNEL WALL COORDINATES - C-B 708-100
 ⑬ CHANNEL WALL COORDINATES - C-B 708-100
 ⑭ CHANNEL WALL COORDINATES - C-B 708-100
 ⑮ CHANNEL WALL COORDINATES - C-B 708-100
 ⑯ CHANNEL WALL COORDINATES - C-B 708-100
 ⑰ CHANNEL WALL COORDINATES - C-B 708-100
 ⑱ CHANNEL WALL COORDINATES - C-B 708-100
 ⑲ CHANNEL WALL COORDINATES - C-B 708-100
 ⑳ CHANNEL WALL COORDINATES - C-B 708-100
 ㉑ CHANNEL WALL COORDINATES - C-B 708-100
 ㉒ CHANNEL WALL COORDINATES - C-B 708-100
 ㉓ CHANNEL WALL COORDINATES - C-B 708-100
 ㉔ CHANNEL WALL COORDINATES - C-B 708-100
 ㉕ CHANNEL WALL COORDINATES - C-B 708-100
 ㉖ CHANNEL WALL COORDINATES - C-B 708-100
 ㉗ CHANNEL WALL COORDINATES - C-B 708-100
 ㉘ CHANNEL WALL COORDINATES - C-B 708-100
 ㉙ CHANNEL WALL COORDINATES - C-B 708-100
 ㉚ CHANNEL WALL COORDINATES - C-B 708-100
 ㉛ CHANNEL WALL COORDINATES - C-B 708-100
 ㉜ CHANNEL WALL COORDINATES - C-B 708-100
 ㉝ CHANNEL WALL COORDINATES - C-B 708-100
 ㉞ CHANNEL WALL COORDINATES - C-B 708-100
 ㉟ CHANNEL WALL COORDINATES - C-B 708-100
 ㊱ CHANNEL WALL COORDINATES - C-B 708-100
 ㊲ CHANNEL WALL COORDINATES - C-B 708-100
 ㊳ CHANNEL WALL COORDINATES - C-B 708-100
 ㊴ CHANNEL WALL COORDINATES - C-B 708-100
 ㊵ CHANNEL WALL COORDINATES - C-B 708-100
 ㊶ CHANNEL WALL COORDINATES - C-B 708-100
 ㊷ CHANNEL WALL COORDINATES - C-B 708-100
 ㊸ CHANNEL WALL COORDINATES - C-B 708-100
 ㊹ CHANNEL WALL COORDINATES - C-B 708-100
 ㊺ CHANNEL WALL COORDINATES - C-B 708-100
 ㊻ CHANNEL WALL COORDINATES - C-B 708-100
 ㊼ CHANNEL WALL COORDINATES - C-B 708-100
 ㊽ CHANNEL WALL COORDINATES - C-B 708-100
 ㊾ CHANNEL WALL COORDINATES - C-B 708-100
 ㊿ CHANNEL WALL COORDINATES - C-B 708-100

02602



FOLDOUT FRAME

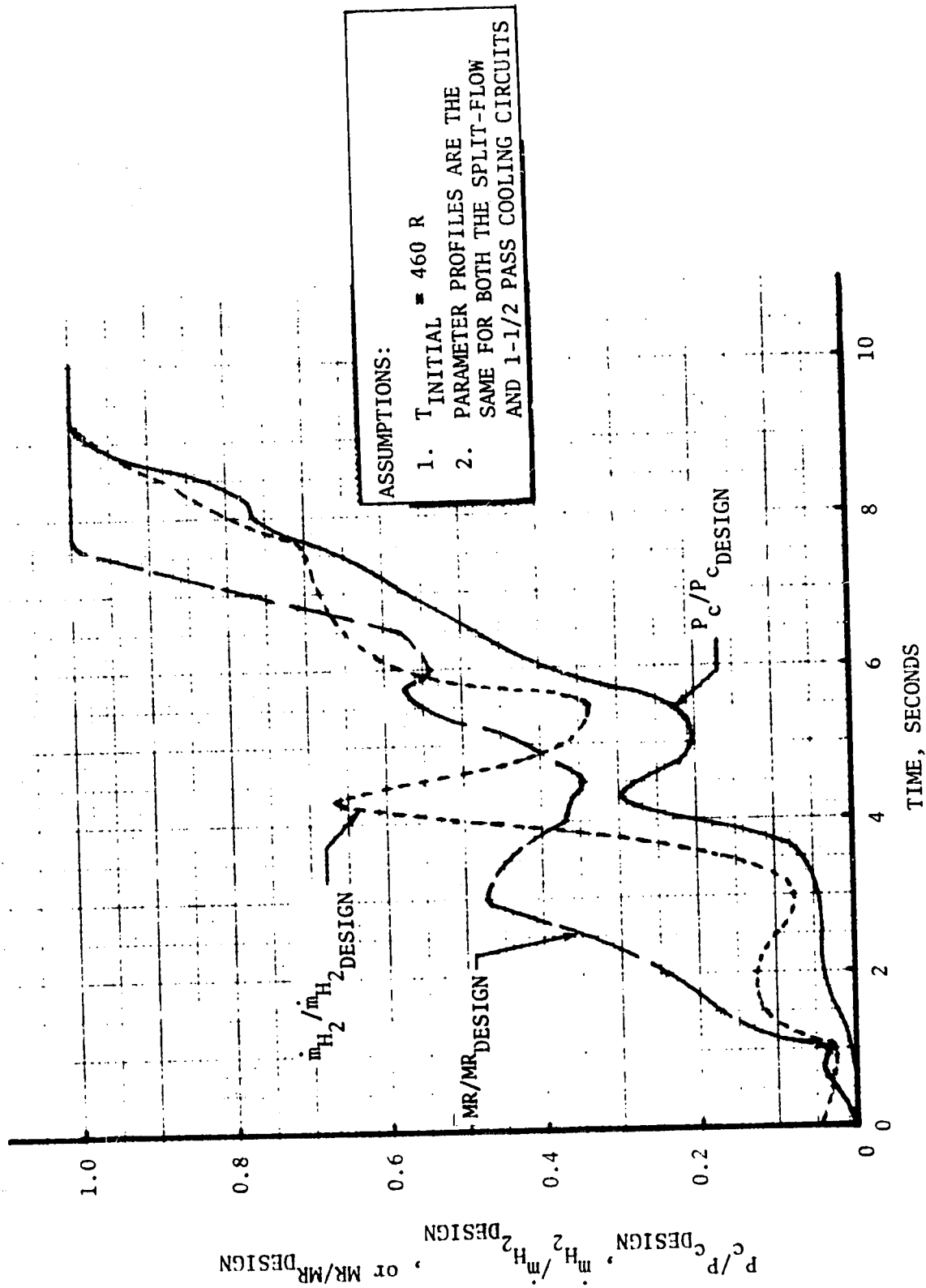


Figure 88. Engine Start Transients

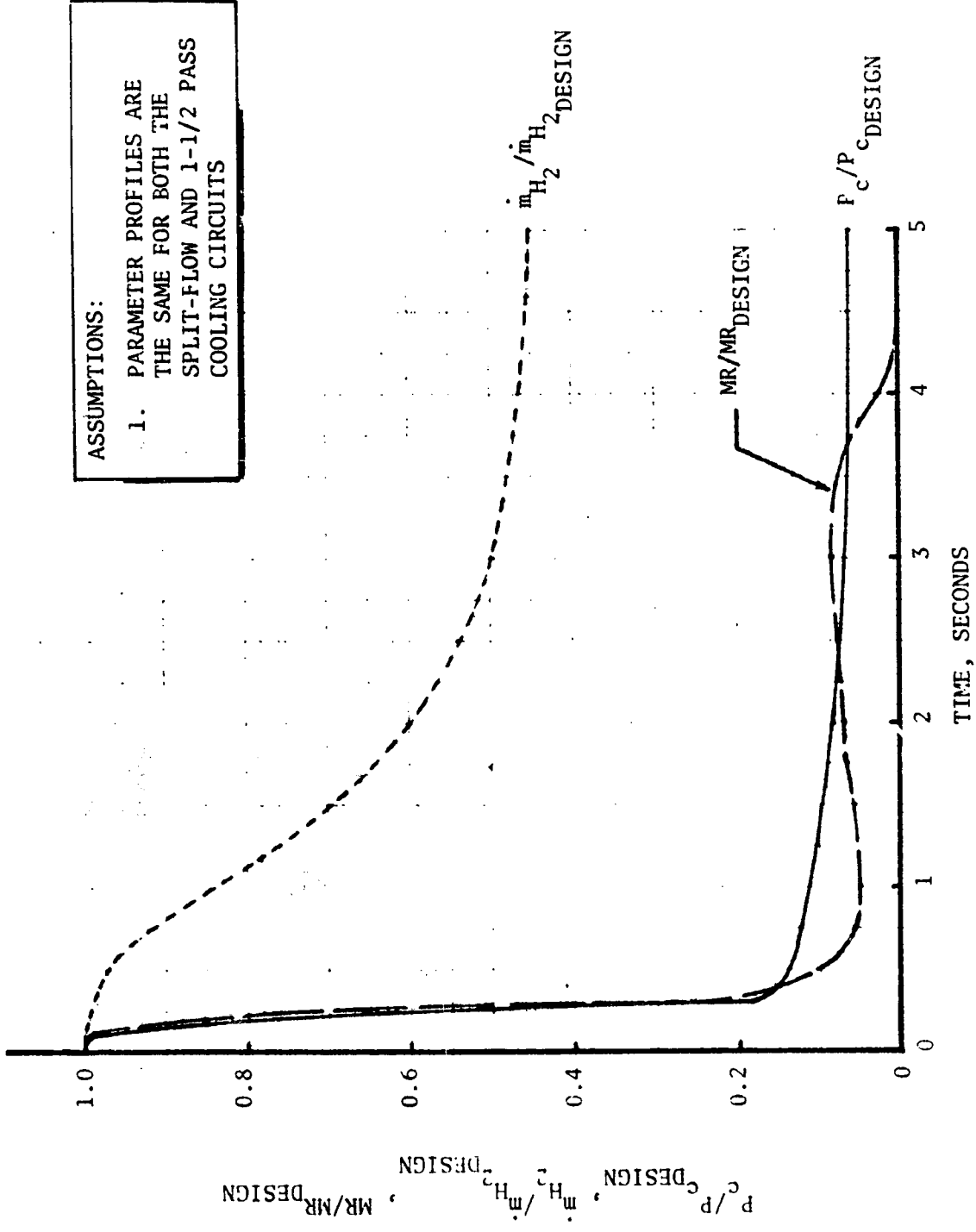


Figure 89. Engine Shutdown Transients

three dimensions. This digital computer program is primarily used to solve steady-state and transient heat transfer problems using finite difference methods.

Transient engine start temperature distributions for the two selected Zr-Cu channel wall combustor/A-286 tubular nozzle configurations are presented in Fig. 90 and 91. Similar distributions for the engine shutdown are shown in Fig. 92 and 93. The thrust chamber cycle life of a particular design is directly related to the gas-side to back-wall temperature differential and the internal coolant pressure. As shown in Fig. 90 through 93, the maximum thermal gradient occurs at the steady-state condition. Also, as indicated by the $P_c/P_{c_{design}}$ profiles, the coolant pressure would be the highest at the steady-state condition. Therefore, the cycle to steady-state operation governs the thrust chamber cycle life.

Reviewing the transient and steady-state analyses performed for the 1-1/2 pass and split-flow cooling circuits, the NASA-LeRC Project Manager selected the split-flow cooling circuit as the configuration to be further evaluated in Task II and III. This design was primarily selected because of the more difficult fabrication resulting from smaller coolant channel dimensions.

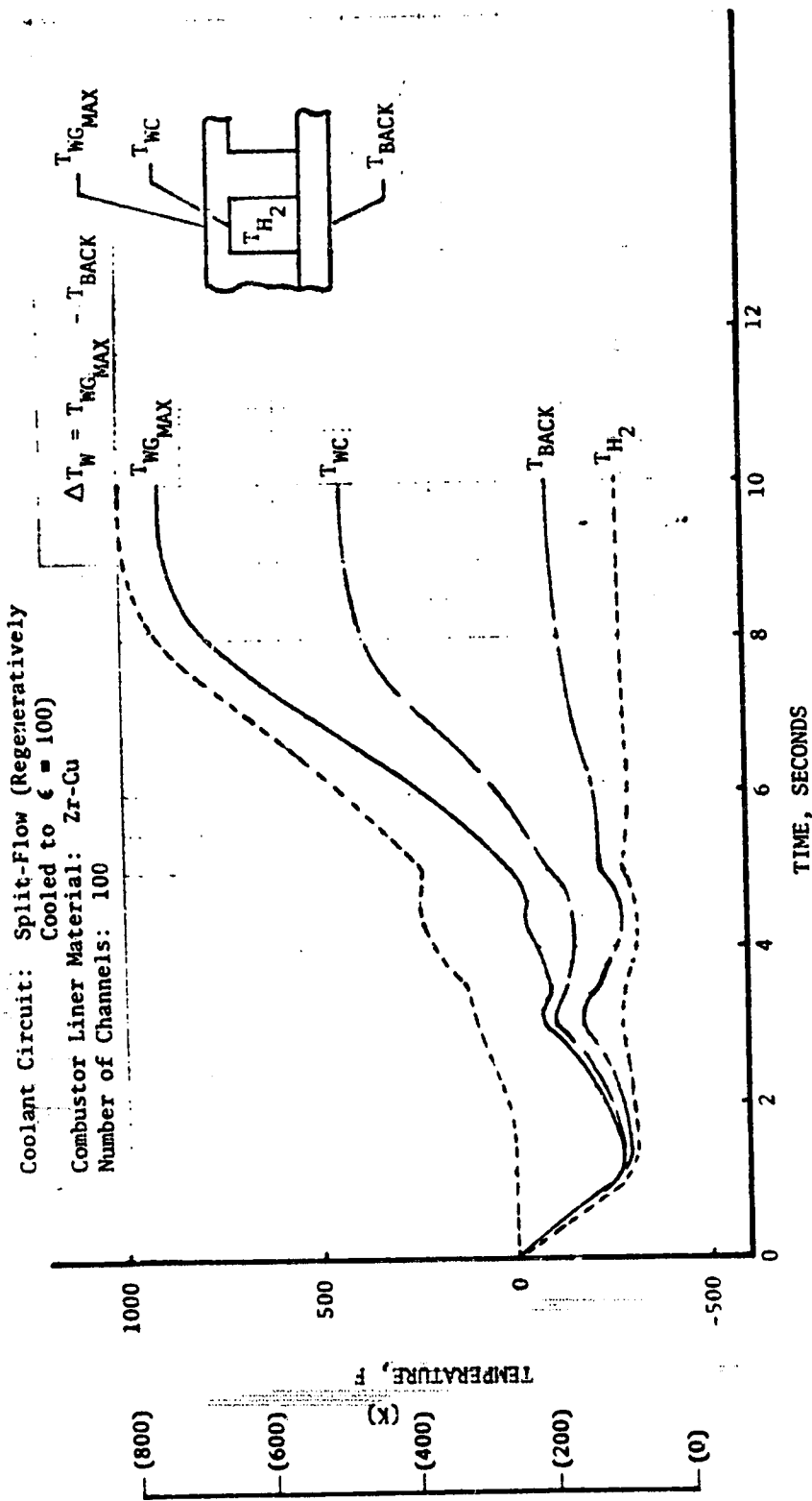


Figure 90. Zr-Cu Combustor Channel Wall Temperature Engine Start Transient at $X = -0.5$ Inch (-1.27 CM) (Split-Flow Cooling Circuit)

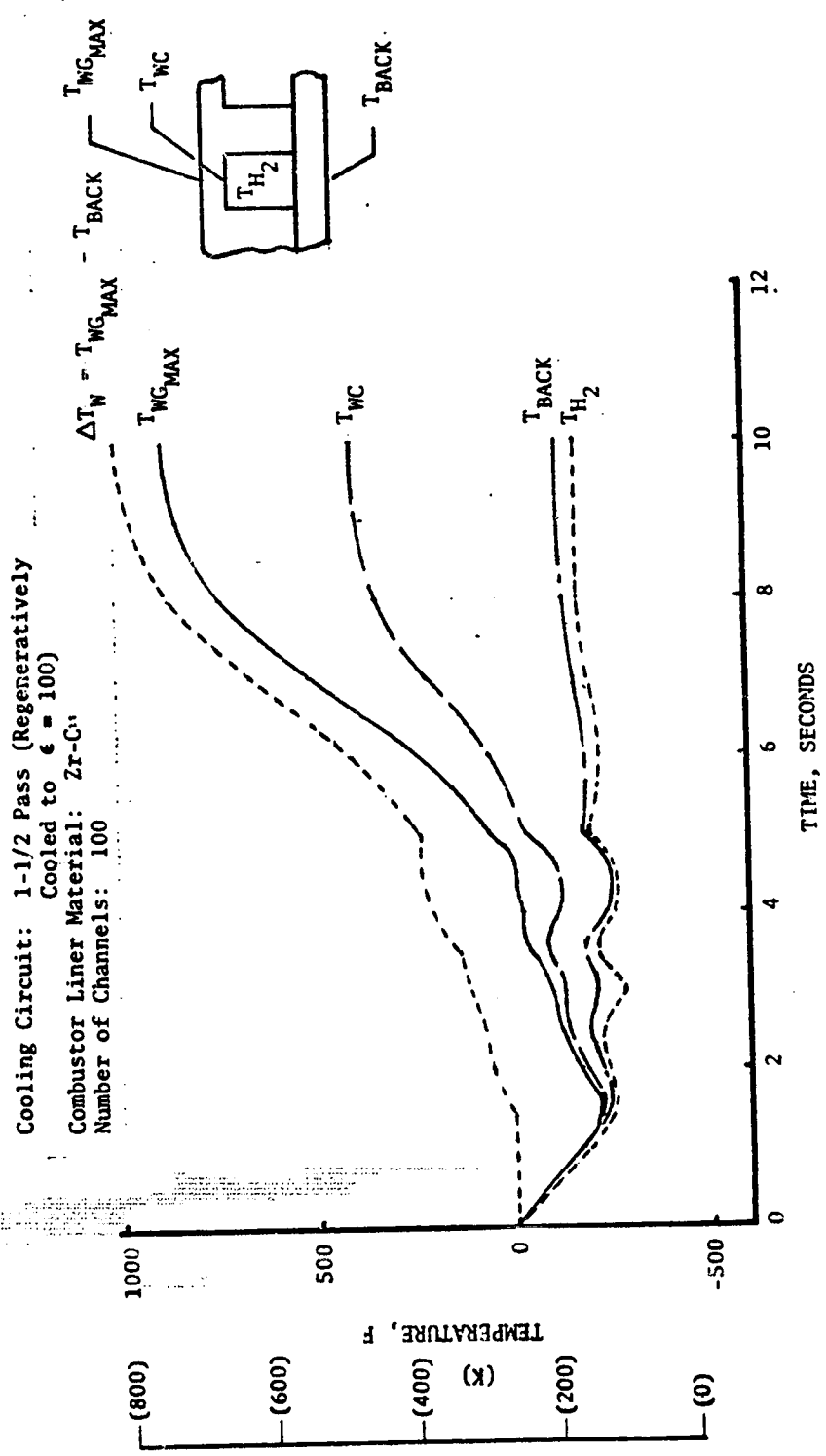


Figure 91. Zr-Cu Combustor Channel Wall Temperature Engine Start Transients at $X = -0.5$ Inch (-1.27 CM) (1-1/2 Pass Cooling Circuit)

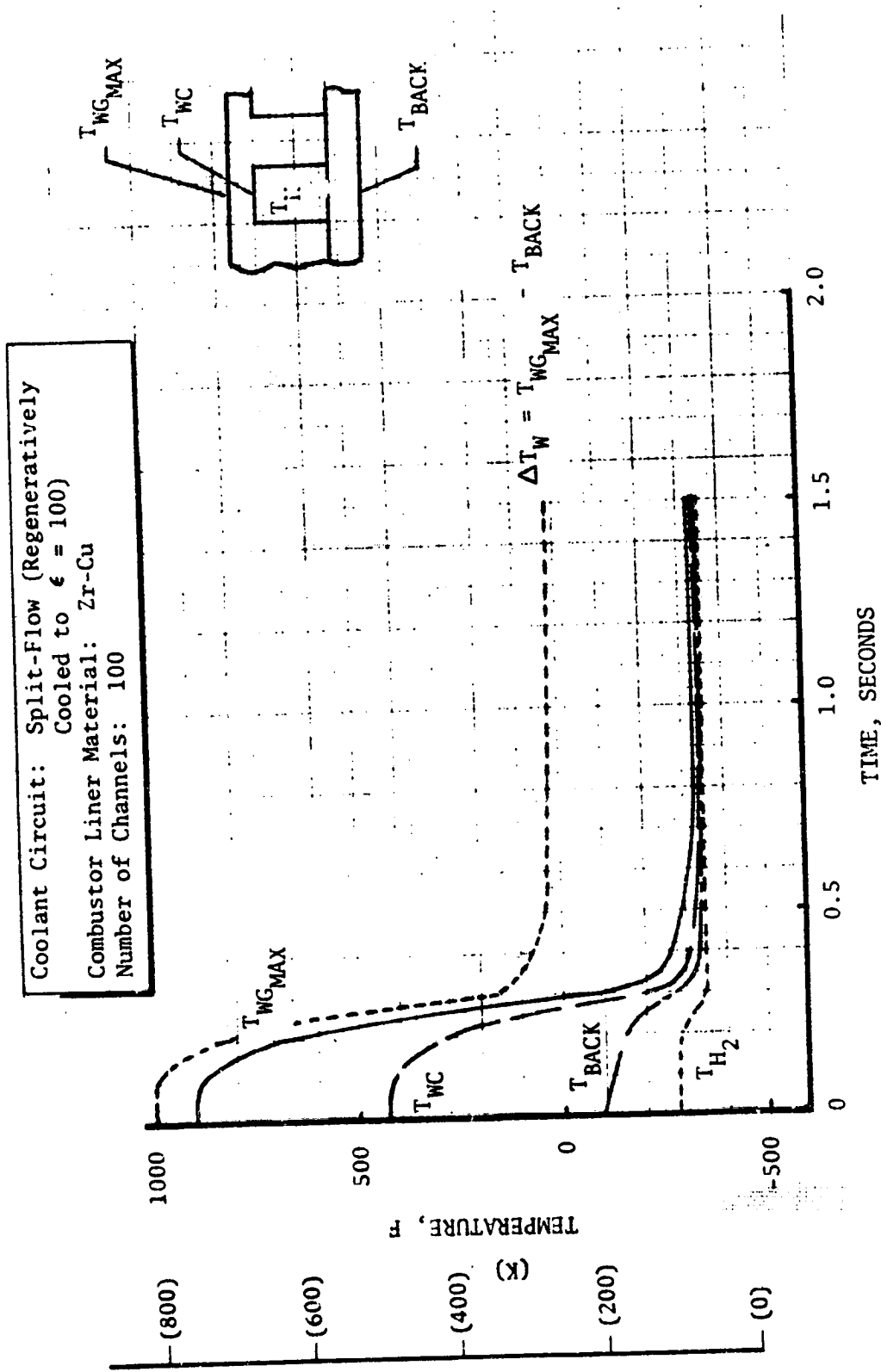


Figure 92. Zr-Cu Combustor Channel Wall Temperature Engine Shutdown Transients at $X = -0.5$ Inch (-1.27 CM) (Split-Flow Cooling Circuit)

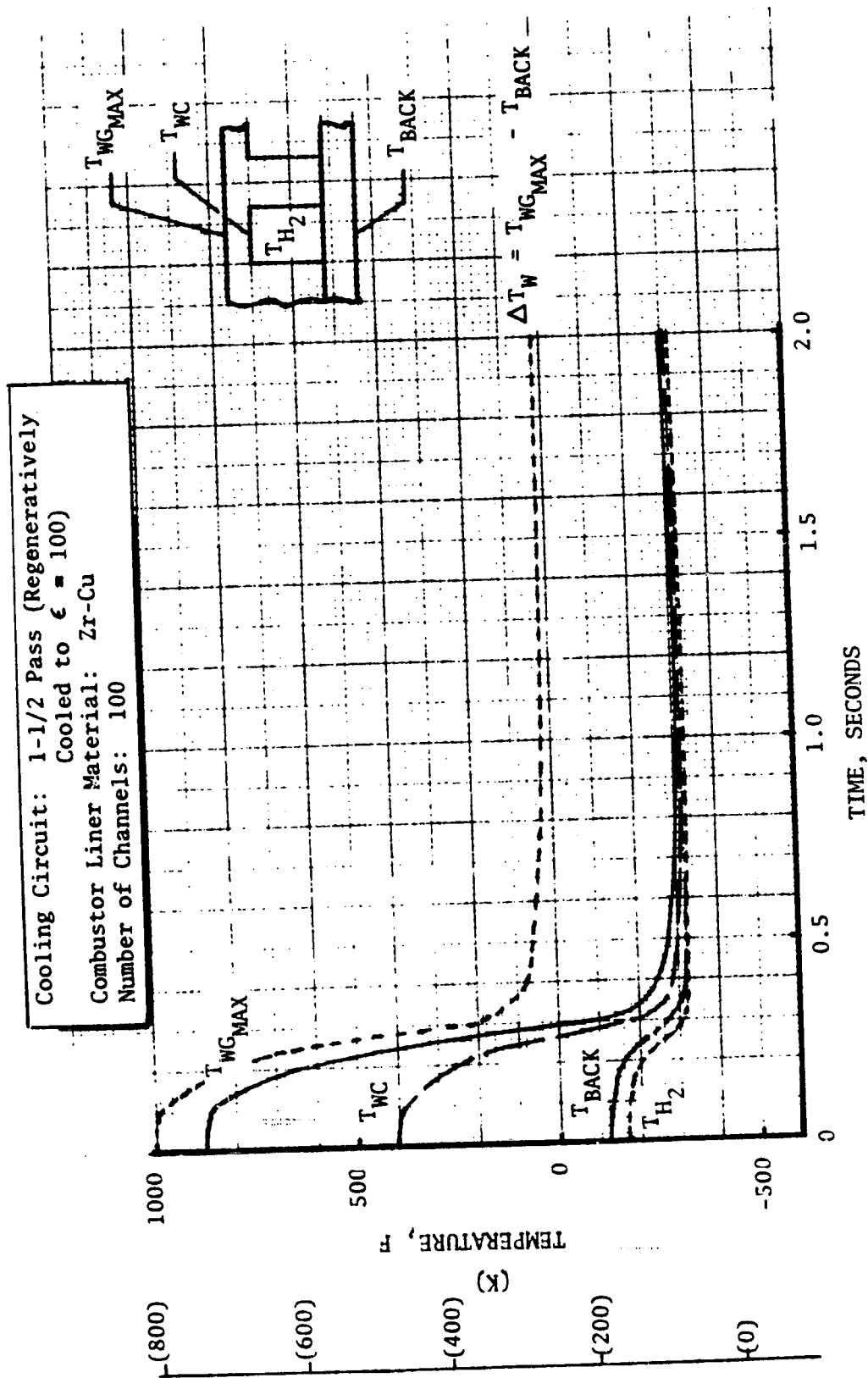


Figure 93. Zr-Cu Combustor Channel Wall Temperature Engine Shutdown Transients at $X = -0.5$ Inch (-1.27 CM) (1-1/2 Pass Cooling Circuit)

TASK II: OFF-DESIGN LIFE EVALUATION

OFF-DESIGN THRUST CHAMBER PARAMETERS

In Task II, the cycle life capability of the selected Task I configuration (Zr-Cu channel wall combustor/A-286 tubular nozzle with a split-flow cooling circuit) was evaluated for three operational duty cycles. These cycles, as shown in Fig. 94, included tank head idle, full and intermediate thrusts, and off-design mixture ratios.

A summary of pertinent off-design thrust chamber parameters is presented in Table XIV. The coolant outlet pressures were ratioed from the design point conditions through an evaluation of results presented in Ref. 1. Also the combustor-nozzle coolant flow split was assumed constant. Other assumptions included:

1. Hydrogen (coolant) flowrate

$$W_{H_2} \propto \frac{P_c}{c^*_{\text{theor}} (1 + MR)}$$

2. Gas-side heat transfer coefficient

$$H_g \propto P_c^{0.8}$$

3. Combustion temperature

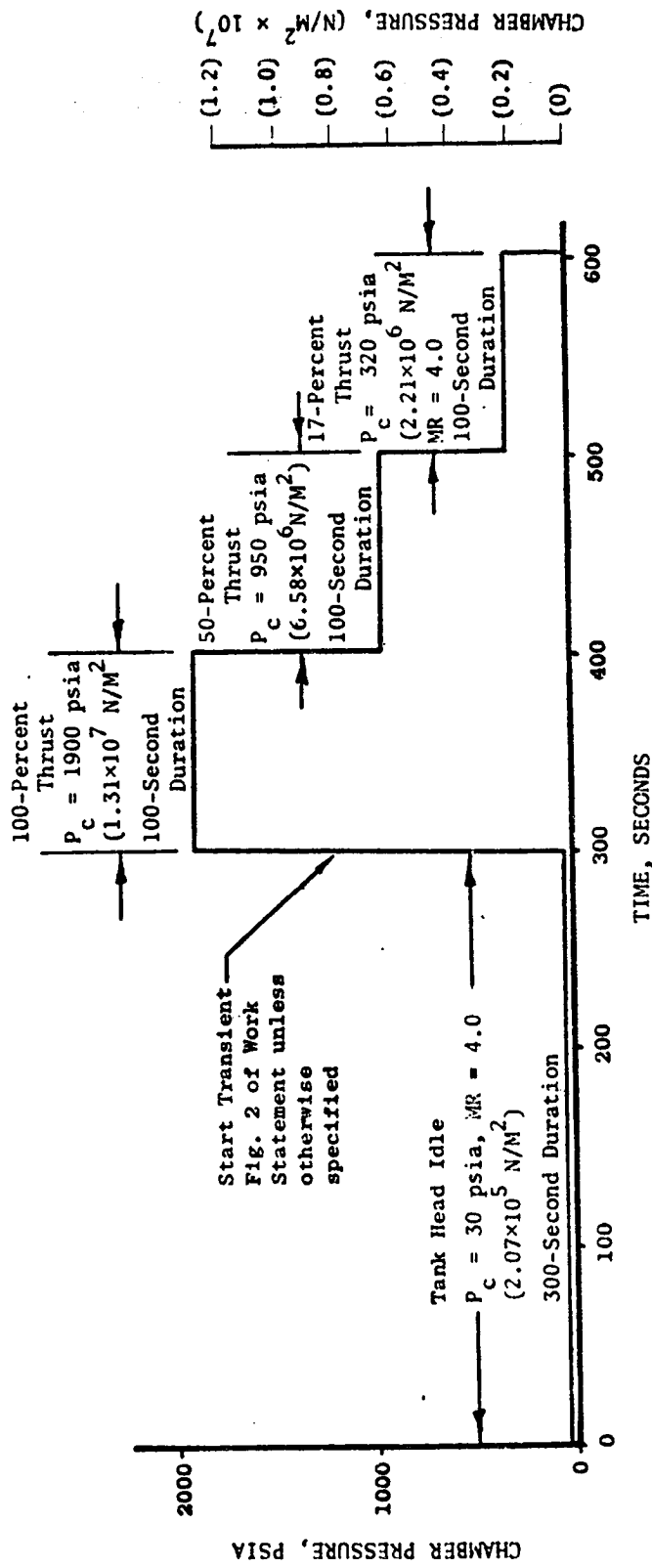
Theoretical

Two methods of duty cycle life evaluation were considered: (1) analyzing the individual chamber pressure steps as a half cycle and (2) treating the entire duty cycle as one cycle to full thrust. The method resulting in the more critical damage fraction determined the cycle life capability.

ANALYSIS AND RESULTS

Performing heat transfer analysis of the combustor and nozzle, the results presented in Fig. 95 and 96 and Table XV were determined. As shown in Fig. 95 and 96, the maximum temperature differential between the gas-side wall and the back wall and the maximum coolant pressure occurred at full thrust. The heat transfer summary presented in Table XV indicated that the location of the maximum gas-side wall temperature (combustor) progressed upstream toward the injector as the thrust chamber was throttled. This trend is due to the increased coolant bulk temperature rise as the chamber was throttled. However, the maximum wall temperature did decrease with a decrease in chamber pressure.

The results obtained from the step loading approach are presented in Table XVI and summarized in Table XVII. In analyzing the life cycle, the combustor



Case No.	MR at 100-Percent Thrust	MR at 50-Percent Thrust
1	6.5	6.0
2	7.0	6.5
3	6.0	5.5

Figure 94. Task II - Off-Design Life Evaluation

TABLE XIV. PERTINENT OFF-DESIGN THRUST CHAMBER PARAMETERS

Cooling Circuit: Split-Flow
(Regeneratively Cooled
to $\epsilon = 100\text{-to-1}$)

$F = 20,000$ Pounds (8.896×10^4 Newtons)

$P_c = 1900$ psia (1.31×10^7 N/m²)

$P_{c\text{design}} = 400\text{-to-1}$

$\epsilon = 3.7, L_c = 10\text{-inches}$ (25.4 centimeters)

$\epsilon_c = 3.7, L_c = 10\text{-inches}$ (25.4 centimeters)

P_c , psia (% Thrust)	$M_{R/T/C}$	T_o , (R)	h_g^* Factor	Combustor		Nozzle	
				\dot{W}_{H_2} , (lb/sec)	$P_{\text{coolant exit}}$ (psia)	\dot{W}_{H_2} , (lb/sec)	$P_{\text{coolant exit}}$ (psia)
1900 (1.31 x 10 ⁷ N/m ²) (100%)	6.0	6560 (3645 K)	1.0	4.006 (1.818 kg/sec)	3600 (2.48 x 10 ⁷ N/m ²)	1.885 (0.856 kg/sec)	4200 (2.895 x 10 ⁷ N/m ²)
950 (6.55 x 10 ⁶ N/m ²) (50%)	6.5	6658 (3700 K)	1.0	3.808 (1.729 kg/sec)	3600 (2.48 x 10 ⁷ N/m ²)	1.792 (0.814 kg/sec)	4200 (2.895 x 10 ⁷ N/m ²)
323 (2.22 x 10 ⁶ N/m ²) (17%)	7.0	6700 (3720 K)	1.0	3.637 (1.65 kg/sec)	3600 (2.48 x 10 ⁷ N/m ²)	1.712 (0.777 kg/sec)	4200 (2.895 x 10 ⁷ N/m ²)
	5.5	6290 (3495 K)	0.5744	2.13 (0.967 kg/sec)	2500 (1.724 x 10 ⁷ N/m ²)	1.002 (0.455 kg/sec)	2800 (1.93 x 10 ⁷ N/m ²)
	6.0	6410 (3560 K)	0.5744	2.014 (0.915 kg/sec)	2500 (1.724 x 10 ⁷ N/m ²)	0.948 (0.431 kg/sec)	2800 (1.93 x 10 ⁷ N/m ²)
	6.5	6490 (3605 K)	0.5744	1.914 (0.869 kg/sec)	2500 (1.724 x 10 ⁷ N/m ²)	0.901 (0.409 kg/sec)	2800 (1.93 x 10 ⁷ N/m ²)
	5.0	5940 (3300 K)	0.2425	0.778 (0.353 kg/sec)	1200 (8.27 x 10 ⁶ N/m ²)	0.366 (0.1663 kg/sec)	1250 (8.62 x 10 ⁶ N/m ²)
30 (2.07 x 10 ⁵ N/m ²) (1.578%) Idle Mode	4.0	5150 (2860 K)	0.0362	0.0847 (0.0384 kg/sec)	140 (9.65 x 10 ⁵ N/m ²)	0.0399 (0.0181 kg/sec)	150 (1.034 x 10 ⁶ N/m ²)

* Note: $h_{g_{p_c}} = (h_g \text{ FACTOR}) \left(h_{g_{p_c}} = 1900 \text{ psia } (1.31 \times 10^7 \text{ N/m}^2) \right)$

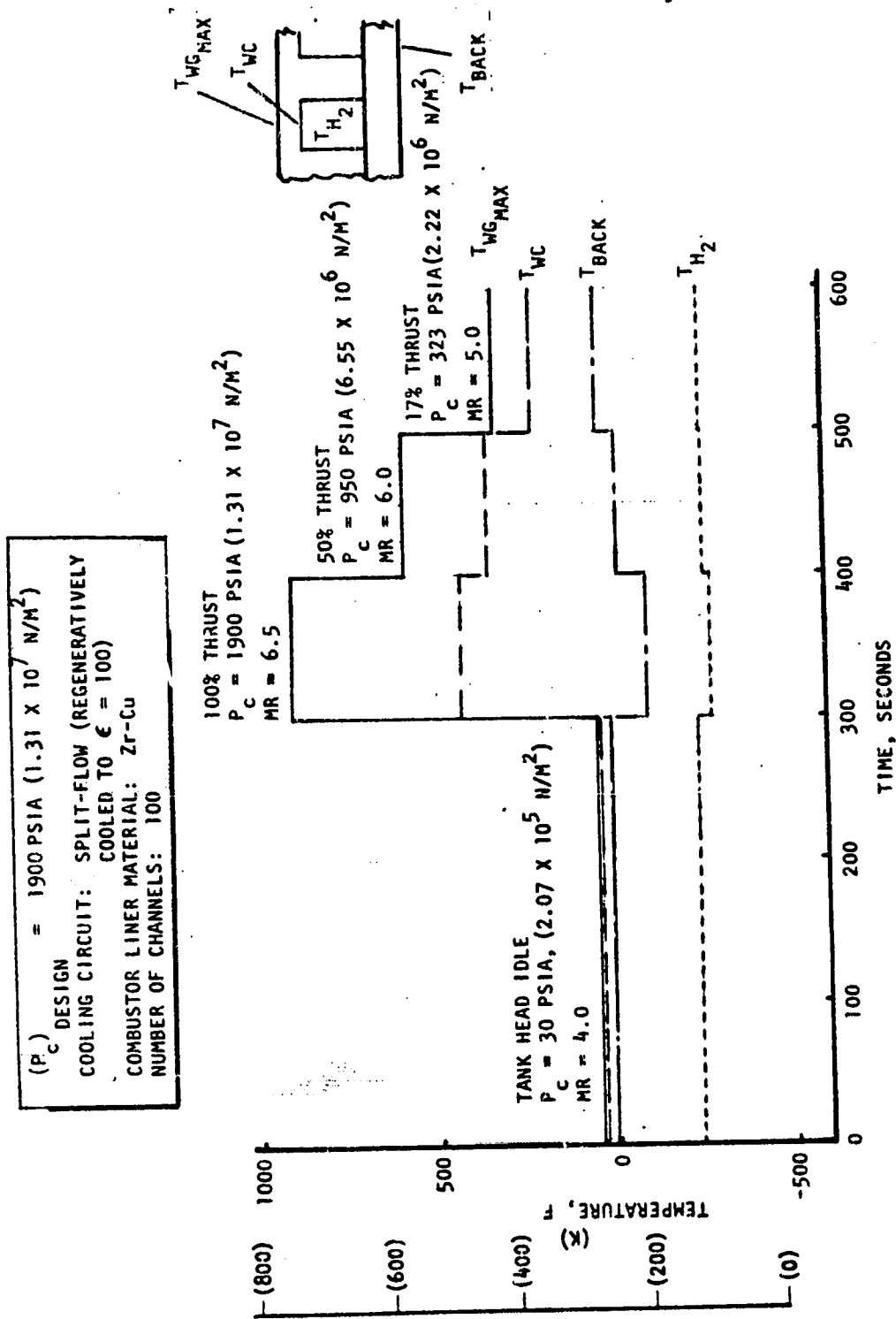


Figure 95. Duty Cycle Temperature Variation at Critical Location
 (X = -0.5 Inch or -1.27 CM) - Case No. 1

(P_c) DESIGN = 1900 PSIA (1.31×10^7 N/M²)
 COOLING CIRCUIT: SPLIT-FLOW (REGENERATIVELY COOLED TO $\epsilon = 100$)
 COMBUSTOR LINER MATERIAL: Zr-Cu
 NUMBER OF CHANNELS: 100

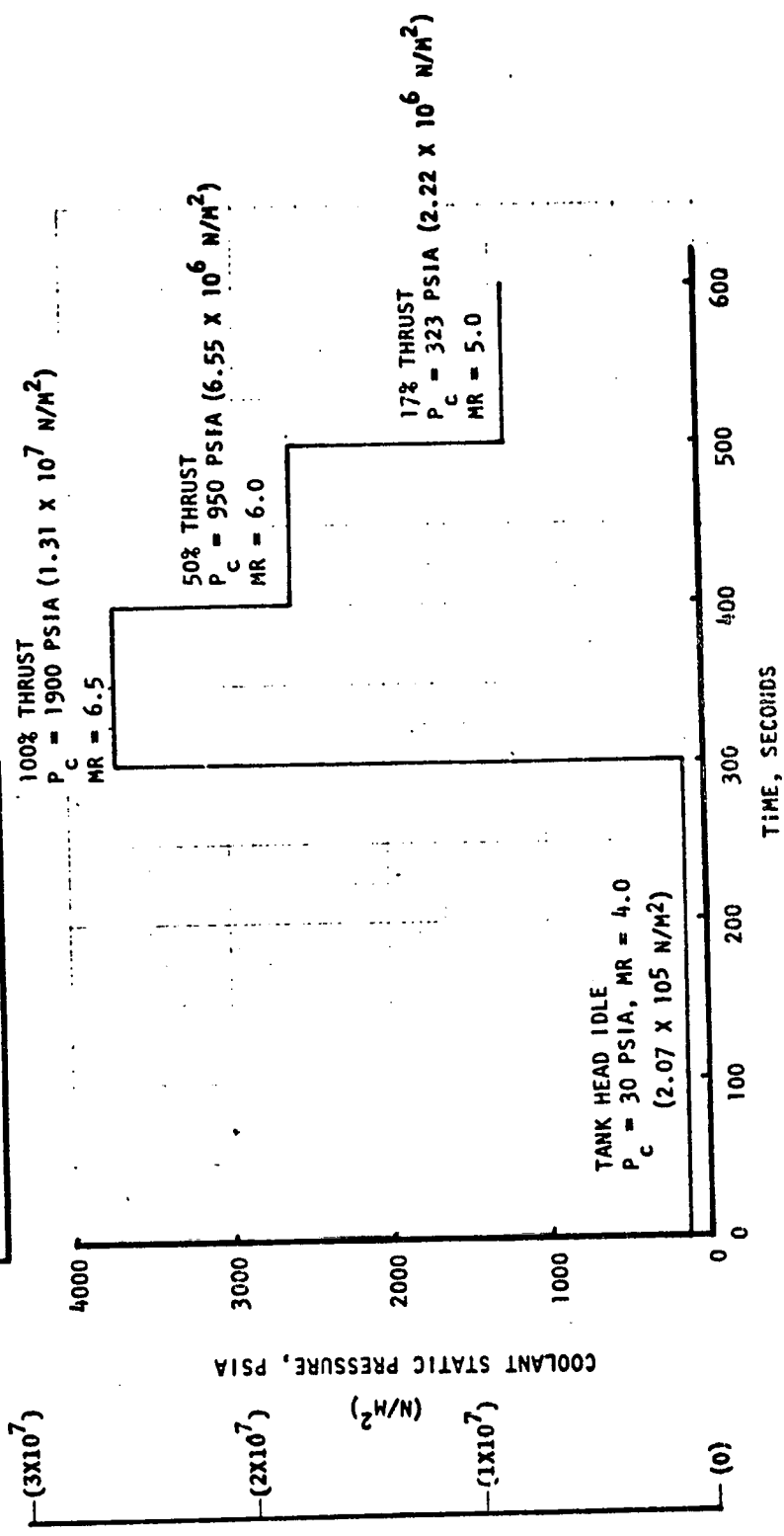


Figure 96. Duty Cycle Coolant Static Pressure Variation at Critical Location
 (X = -0.5 Inch or -1.27 cm) - Case No. 1

TABLE XV. OFF-DESIGN LIFE EVALUATION - HEAT TRANSFER SUMMARY

(P_c) design = 1900 psia (1.31 x 10⁷ N/m²)
 Cooling Circuit: Split-Flow (Regeneratively Cooled to ε = 100)

P _c (psia)	Percent Thrust	MR _{T/C}	Zr-Cu Combustor (100 Channels)				A-286 Nozzle (525 Tubes)			
			Location of T _{WG,MAX} (inch)	T _{WG,MAX} (F)	ΔP _{Cool} (psi)	T _{Cool,Exit} (R)	T _{WG,MAX} (F)	ΔP _{Cool} (psi)	T _{Cool,Exit} (R)	
1900 ⁷ (1.31 x 10 ⁷ N/m ²)	100	6.0		860 (733 K)	651.6 x 10 ⁶ N/m ²	439 (244 K)	636 (608 K)	38 (2.62 x 10 ⁵ N/m ²)	432 (240 K)	
		6.5	-0.5 (-1.27 cm)	900 (750 K)	608.6 x 10 ⁶ N/m ²	461 (256 K)	685 (636 K)	36 (2.48 x 10 ⁵ N/m ²)	453 (252 K)	
		7.0		925 (770 K)	571.6 x 10 ⁶ N/m ²	479 (266 K)	716 (653 K)	34 (2.345 x 10 ⁵ N/m ²)	471 (262 K)	
950 ⁶ (6.55 x 10 ⁶ N/m ²)	50	5.5		605 (591 K)	256 x 10 ⁶ N/m ²	462 (257 K)	471 (518 K)	16 (1.103 x 10 ⁵ N/m ²)	446 (248 K)	
		6.0	-6.0 (-15.23 cm)	660 (623 K)	239 x 10 ⁶ N/m ²	491 (273 K)	519 (544 K)	15 (1.034 x 10 ⁵ N/m ²)	472 (262 K)	
		6.5		714 (653 K)	229.6 x 10 ⁶ N/m ²	534 (297 K)	562 (568 K)	14 (9.65 x 10 ⁴ N/m ²)	496 (276 K)	
323 ⁶ (2.22 x 10 ⁶ N/m ²)	17	5.0	-6.0 (-15.23 cm)	428 (494 K)	71.5 x 10 ⁵ N/m ²	507 (282 K)	316 (432 K)	6 (4.14 x 10 ⁴ N/m ²)	484 (269 K)	
		4.0	-10.0 (-25.4 cm)	296 (420 K)	9.5 x 10 ⁴ N/m ²	634 (352 K)	244 (391 K)	0.7 (4.83 x 10 ³ N/m ²)	603 (335 K)	

TABLE XVI. OFF-DESIGN LIFE ANALYSIS SUMMARY
(STATION X = -0.5 INCH OR -1.27 CM)

Loading, (percent)	ϵ_{eff} (in./in.)	N_f' (cycles)	ϕ_f	ϕ_c^*
<u>Case 1</u>				
0 - Idle	0.0007	10^6	0.00015	0.00025
Idle - 100	0.0211	1,300	0.115	0.000083
100 - 50	0.0076	18,000	0.0083	0.000083
50 - 17	0.0078	17,000	0.0088	0.000083
17 - 0	0.0062	30,000	0.005	
Total			0.137	0.0005
<u>Case 2</u>				
0 - Idle	0.0007	10^6	0.00015	0.00025
Idle - 100	0.0214	1,260	0.119	0.000083
100 - 50	0.0077	17,500	0.0086	0.000083
50 - 17	0.0082	14,000	0.0107	0.000083
17 - 0	0.0062	30,000	0.005	
Total			0.143	0.0005
<u>Case 3</u>				
0 - Idle	0.0007	10^6	0.00015	0.00025
Idle - 100	0.0204	1,450	0.103	0.000083
100 - 50	0.0081	14,400	0.0104	0.000083
50 - 17	0.0068	24,000	0.00625	0.000083
17 - 0	0.0062	30,000	0.005	
			0.125	0.0005

* The predicted time to failure is 10^5 hours for the worst case at 100-percent thrust. Since this value is so large, it is used for all cases at every level of thrust.

TABLE XVII. OFF-DESIGN LIFE ANALYSIS RESULTS
(STATION X = -0.5 INCH OR -1.27 CM)

Loading	ϕ_f (Total)	ϕ_c (Total)	$4 (\phi_f \text{ (Total)} + \phi_c \text{ (Total)})$	(Number Thermal Cycles)/4	
Case 1	0.137	0.0005	0.55	545	Using Duty Cycle Life Evaluation Method
Case 2	0.143	0.0005	0.574	525	
Case 3	0.125	0.0005	0.502	600	
Case 1	0.249	0.001	1.0	300	Using 0-to 100-Percent Thrust Cycling
Case 2	0.25	0.001	1.004	299	
Case 3	0.234	0.001	0.94	319	

locations of $X = -0.5$ -inch (-1.27 cm), -6.0-inches (-15.22 cm), and -10.0-inches (-25.4 cm) were evaluated to determine the critical location. Although the locations of -6.0-inches (-15.22 cm) and -10.0-inches (-25.4 cm) resulted in higher wall temperatures than at $X = -0.5$ -inch (-1.27 cm) at throttled conditions, the thermal gradient and coolant pressure (Fig. 95) were the largest at design chamber pressure. As shown in Table XVI, most of the contribution to the total damage fraction occurs at design chamber pressure. Therefore, the critical location was determined to be at $X = -0.5$ -inch (-1.27 cm) as for steady-state full thrust cycling. As shown in Table XVII, the 0-100 percent -0 thrust cycle resulted in the more critical life. Therefore, the low mixture ratio duty cycle (Case 3) resulted in 19-cycle longer life than the nominal 300 cycles, and the high mixture ratio duty cycle (Case 2) is approximately the same as the nominal.

TASK III: PERTURBATION OF REFERENCE-POINT OPERATING CONDITIONS

To investigate the design impact of chamber pressure and cycle life, four design point perturbations at 20,000-pound (8.896×10^4 N) thrust, 400-to-1 area ratio, and 6.5 mixture ratio were evaluated. As shown in Table XVIII, these perturbations include two different chamber pressures at the 300-cycle nominal life and two different life cycles at the nominal 1900-psia (1.31×10^7 N/m²) chamber pressure. Using assumptions set forth in Task II (Off-Design Life Evaluation), pertinent thrust chamber parameters were defined (Table XIX). As shown in Fig. 97, the combustor chamber contours for the 1600-psia (1.103×10^7 N/m²) and 2100-psia (1.448×10^7 N/m²) chamber pressures were developed in the same manner as for the nominal 1900-psia (1.31×10^7 N/m²) chamber pressure contour. The injector-to-throat chamber length of 10.0-inches (25.4 cm), the 1.75-inch (4.45 cm) cylindrical section, and the 3.7-to-1 contraction ratio were all fixed.

CYCLE LIFE PERTURBATION ($P_c = 1900$ PSIA OR 1.31×10^7 N/m²)

The influence of cycle life was evaluated using the selected Zr-Cu channel wall combustor/A-286 tubular nozzle and varying the coolant channel heights to achieve desired maximum wall temperature. Thus, the influence of wall temperature on coolant pressure drop was determined. Using this generated thermal data, the cycle life capability was estimated using the modified simplified cycle life analysis method and finite element analysis (the latter only at lower wall temperatures). The A-286 tubular nozzles for these configurations were assumed to be of the same design as for the 300-cycle life thrust chamber with 525 booked tubes. For the desired 30-cycle thrust chamber, the design was dictated by the creep damage fraction so a finite element stress analysis was not performed. The low cycle requirement allowed high wall temperatures and resulted in low coolant pressure drops. Whereas, a high cycle requirement resulted in the opposite trend. As shown in Fig. 98 and 99, a 3000-cycle thrust chamber would require a maximum gas-side wall temperature of 430 F (494 K) with a combustor coolant pressure drop exceeding 4000 psi (2.76×10^7 N/m²), which is obviously an impractical engine system design.

Low Cycle Life Thrust Chamber ($P_c = 1900$ psia or 1.31×10^7 N/m²)

Analysis of several combustor designs to achieve the 30-cycle life resulted in the impossibility of achieving the required cycle life and meeting basic structural requirements simultaneously. As shown in Table XX, the design having approximately 30-cycle life resulted in a yield strength safety factor less than 1.2. Increasing the hot-wall thickness (from 0.027-inch or 0.0686 cm to 0.029-inch or 0.0737 cm) to increase the structural safety factor decreased the total damage fraction (increased cycle life). The thrust chamber must meet the structural safety factor, so the latter design, which was predicted to achieve 71 cycles, was selected. The 71 cycles were obtained using $[1/4 (\phi_c + \phi_f)]$ [30]. The coolant channel dimensions and wall temperature for distribution for this design are shown in Fig. 100 and 101. This 71-cycle thrust chamber design resulted in a 1271 F (962 K) maximum gas-side wall temperature, a combustor coolant pressure drop of 194 psi (1.487×10^6 N/m²), and a combustor liner weight of 9.2 pounds (4.18 kg). The design drawing for this configuration is shown in Fig. 102.

TABLE XVIII. TASK III: DESIGN PERTURBATIONS

Thrust = 20,000 Pounds (8.896×10^4 Newtons)	
Mixture Ratio (Thrust Chamber) = 6.5	
1. Chamber Pressure = 1600 psia (1.103×10^7 N/m ²)	} 300-Cycle Life
2. Chamber Pressure = 2100 psia (1.447×10^7 N/m ²)	
3. 30 Cycle Life	} Chamber Pressure = 1900 psia (1.31×10^7 N/m ²)
4. 3000 Cycle Life	

TABLE XIX. DESIGN PERTURBATION THRUST CHAMBER PARAMETERS

F = 20,000 pounds (8.896×10^4 Newtons)

$MR_{T/C} = 6.5$

$\epsilon = 400\text{-to-}1$

$\epsilon_c = 3.7$

$L_c = 10\text{-inches}$ (25.4 centimeters)

P_c (psia)	T_o (R)	R_T (inches)	h_g Factor	Combustor		Nozzle	
				\dot{W}_{H_2} (lb/sec)	$P_{Coolant'}$ Exit (psia)	\dot{W}_{H_2} (lb/sec)	$P_{Coolant'}$ Exit (psia)
1600^7 (1.103×10^7 N/m ²)	6617 (3680 K)	1.41 (3.58 cm)	0.8714	3.813 (1.732 kg/sec)	3300 (2.275×10^7 N/m ²)	1.794 (0.8138 kg/sec)	3900^7 (2.69×10^7 N/m ²)
1900^7 (1.31×10^7 N/m ²)	6658 (3700 K)	1.29 (3.275 cm)	1.0	3.808 (1.730 kg/sec)	3600 (2.485×10^7 N/m ²)	1.792 (0.8129 kg/sec)	4200^7 (2.895×10^7 N/m ²)
2100^7 (1.447×10^7 N/m ²)	6696 (3720 K)	1.23 (3.125 cm)	1.0834	3.804 (1.728 kg/sec)	3800^7 (2.62×10^7 N/m ²)	1.790 (0.8119 kg/sec)	4400^7 (3.032×10^7 N/m ²)

$F = 20,000 \text{ LBS } (8.896 \times 10^4 \text{ N})$
 $L_c = 10\text{-INCHES } (25.4 \text{ CM})$
 $\epsilon_c = 3.7$
 $P_c = 1600 \text{ PSIA } (1.103 \times 10^7 \text{ N/M}^2)$
 $P_c = 1900 \text{ PSIA } (1.31 \times 10^7 \text{ N/M}^2)$
 $P_c = 2100 \text{ PSIA } (1.447 \times 10^7 \text{ N/M}^2)$

NOTE:

--- $P_c = 1600 \text{ PSIA } (1.103 \times 10^7 \text{ N/M}^2)$
 --- $P_c = 1900 \text{ PSIA } (1.31 \times 10^7 \text{ N/M}^2)$
 - - - $P_c = 2100 \text{ PSIA } (1.447 \times 10^7 \text{ N/M}^2)$

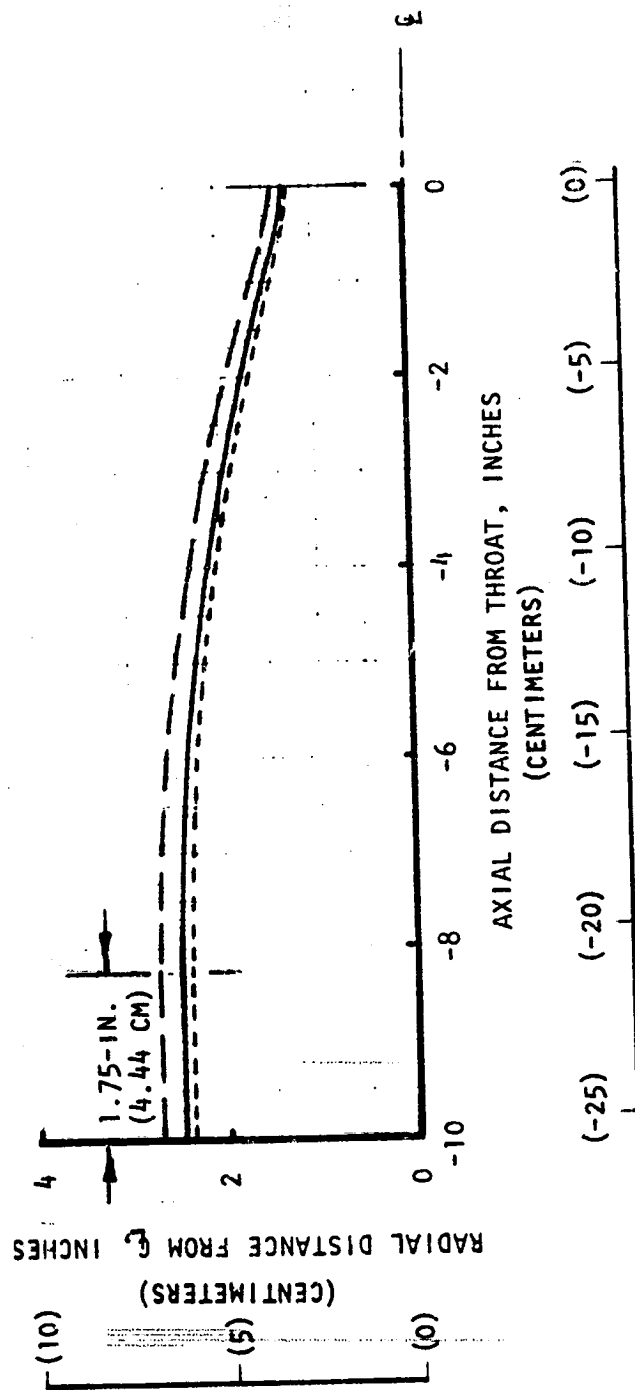


Figure 97. Task III - Combustion Chamber Contours

($P_c = 1900$ psia or 1.31×10^7 N/m², $MR_{T/C} = 6.5$)

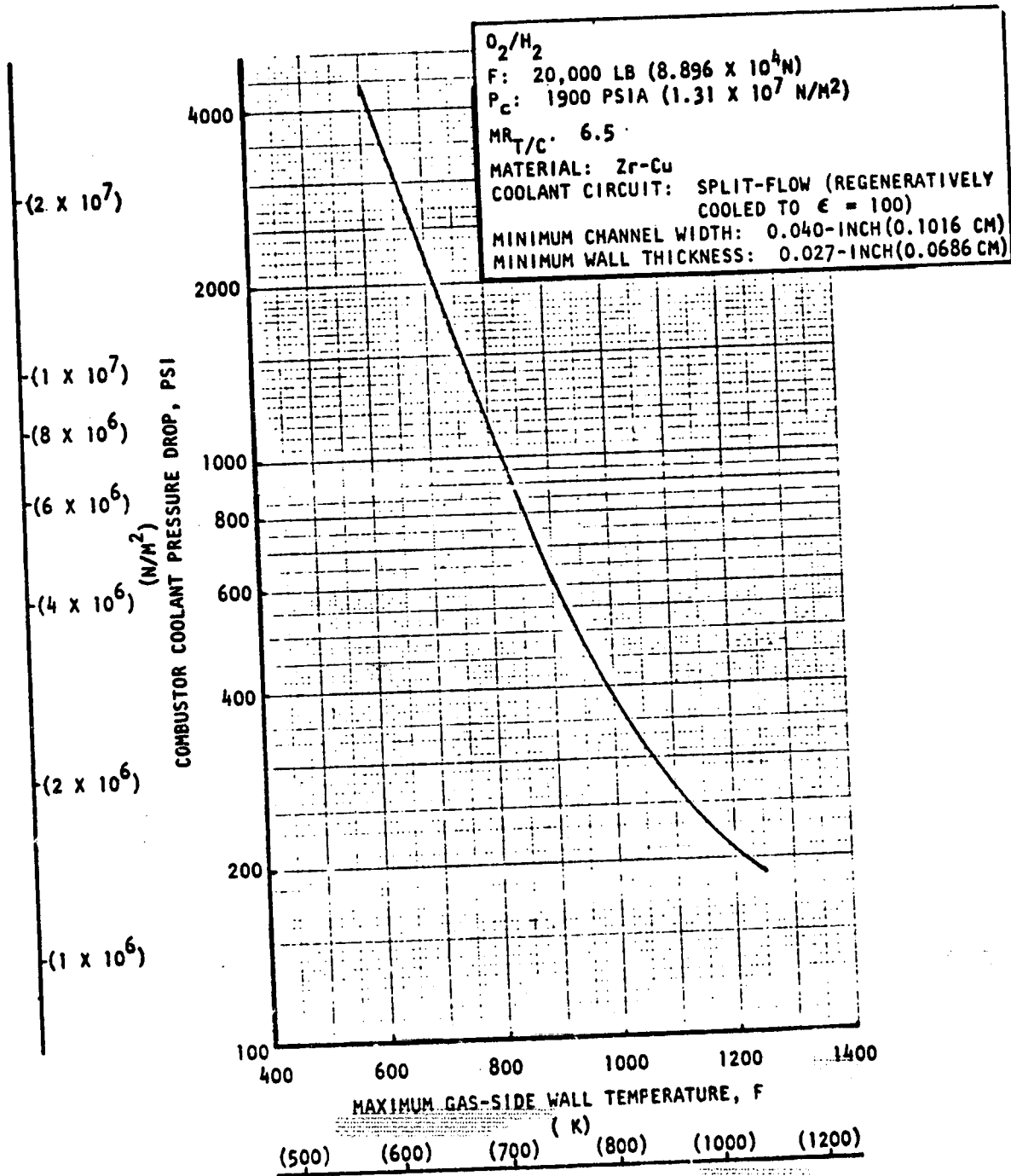
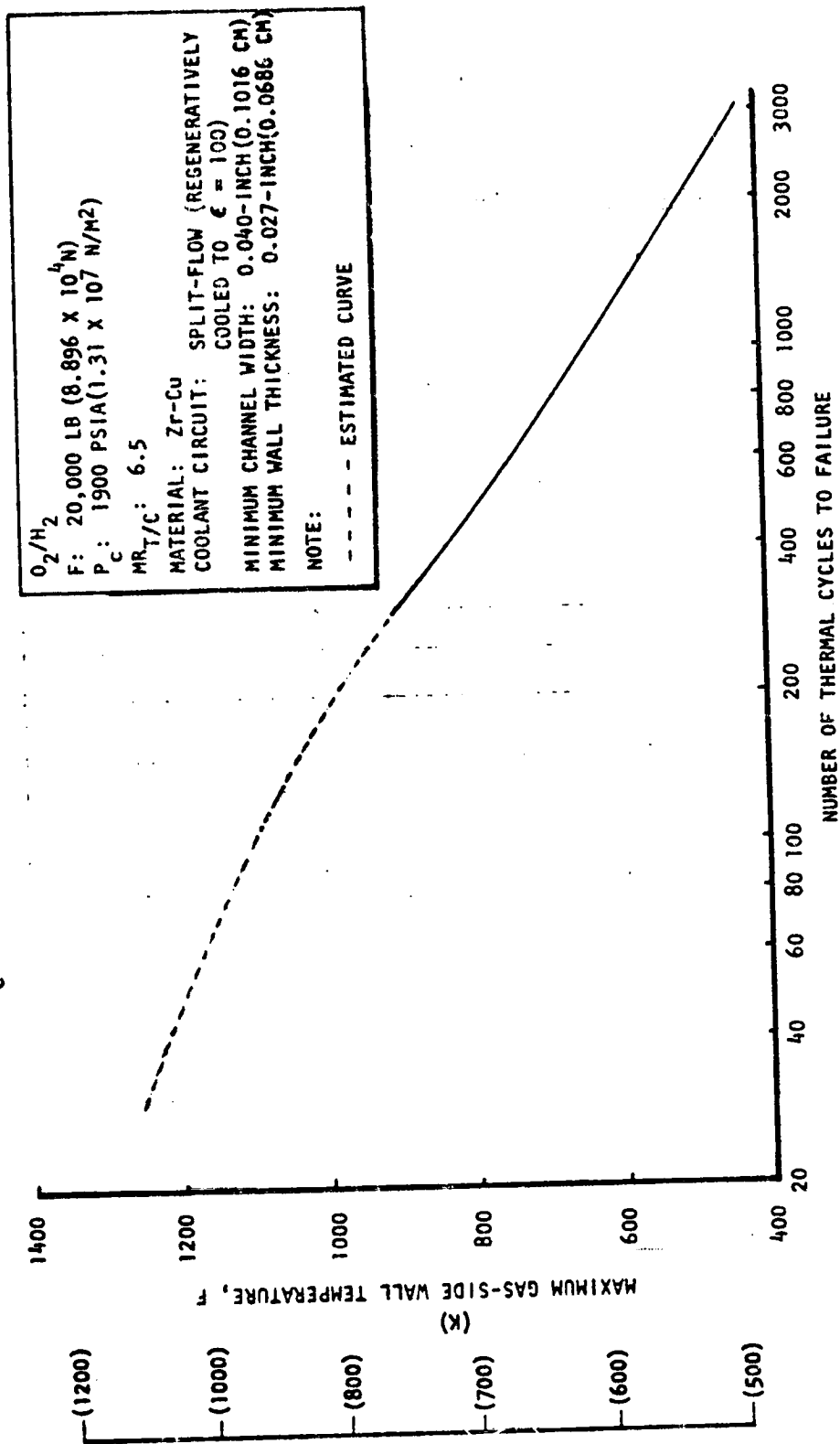


Figure 98. Approximate Variation of Combustor Coolant Pressure Drop With Maximum Wall Temperature

($P_c = 1900$ psia or 1.31×10^7 N/m², $MR_{T/C} = 6.5$)



O_2/H_2
 F: 20,000 LB (8.896 X 10⁴ N)
 P: 1900 PSIA (1.31 X 10⁷ N/M²)
 $MR_{T/C}$: 6.5
 MATERIAL: Zr-Cu
 COOLANT CIRCUIT: SPLIT-FLOW (REGENERATIVELY COOLED TO $\epsilon = 100$)
 MINIMUM CHANNEL WIDTH: 0.040-INCH (0.1016 CM)
 MINIMUM WALL THICKNESS: 0.027-INCH (0.0686 CM)
 NOTE: - - - - ESTIMATED CURVE

Figure 99. Approximate Variation of Maximum Wall Temperature With Number of Thermal Cycles

TABLE XX. LOW CYCLE LIFE THRUST CHAMBER STRESS/CYCLE LIFE RESULTS

P_c : 1900 psia ($1.31 \times 10^7 \text{ N/m}^2$)

$M_{T/C}$: 6.5

Comustor Liner Material: Zr-Cu

Critical Location: X = -0.5-Inch (-1.27 cm)

Channel Width (inch)	Gas-Side Wall Thickness (inch)	Coolant Pressure (psia)	Max Gas-Side Wall Temp, (F)	1.2 ϵ_{eff} (in/in)	N_f	ϕ_f	ϕ_c	$4(\phi_f + \phi_c)$	Yield Safety Factor
0.04	0.027 (0.0686 cm)	3661 (2.52 x 10 ⁷ N/m ²)	1249 (950 K)	0.0312	490	0.061	0.167	0.91	1.13
	0.027		1196 (920 K)	0.0296	560	0.054	0.0128	0.27	1.19
	0.029 (0.0736 cm)		1249 (950 K)	0.0312	490	0.061	0.033	0.377	1.23
	0.029		1260 (956 K)	0.0317	475	0.063	0.04	0.412	1.22
0.04 (0.1016 cm)	0.029	3661	1271 (962 K)	0.0319	460	0.065	0.04	0.421	1.21

N = 71
Cycles

Modified Simplified Stress/Cycle Life Analysis

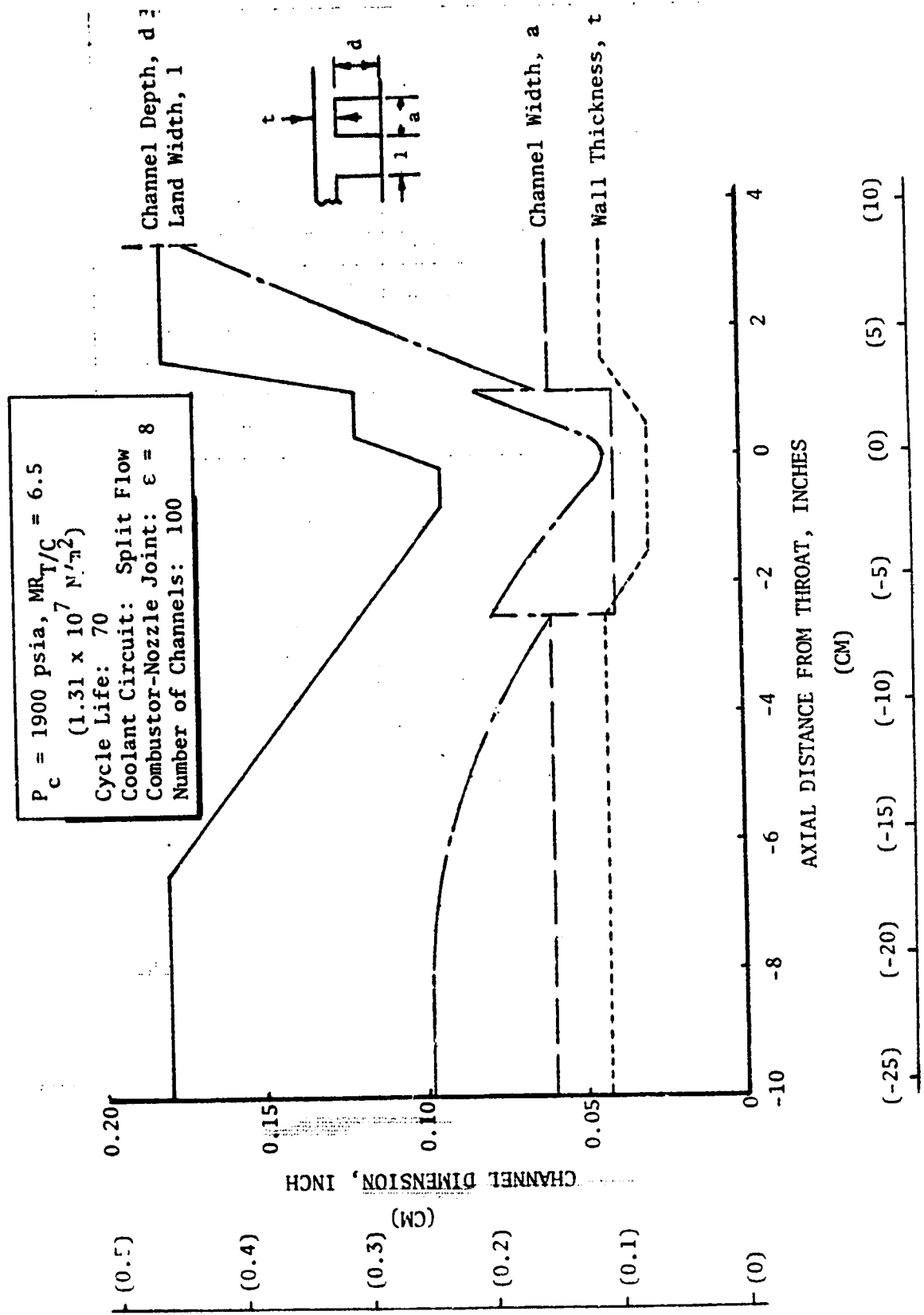


Figure 100. 70 Cycle Life Zr-Cu Combustor Channel Dimensions
 $(P_c = 1900$ psia or $1.31 \times 10^7 \text{ N/m}^2, MR_{T/C} = 6.5)$

$P_c = 1900$ psia, $MR_{T/C} = 6.5$

$(1.31 \times 10^7 \text{ N/M}^2)$

Coolant Circuit: Split-Flow (Regeneratively Cooled to $\xi = 100$)

Combustor Liner Material: Zr-Cu

Number of Channels: 100

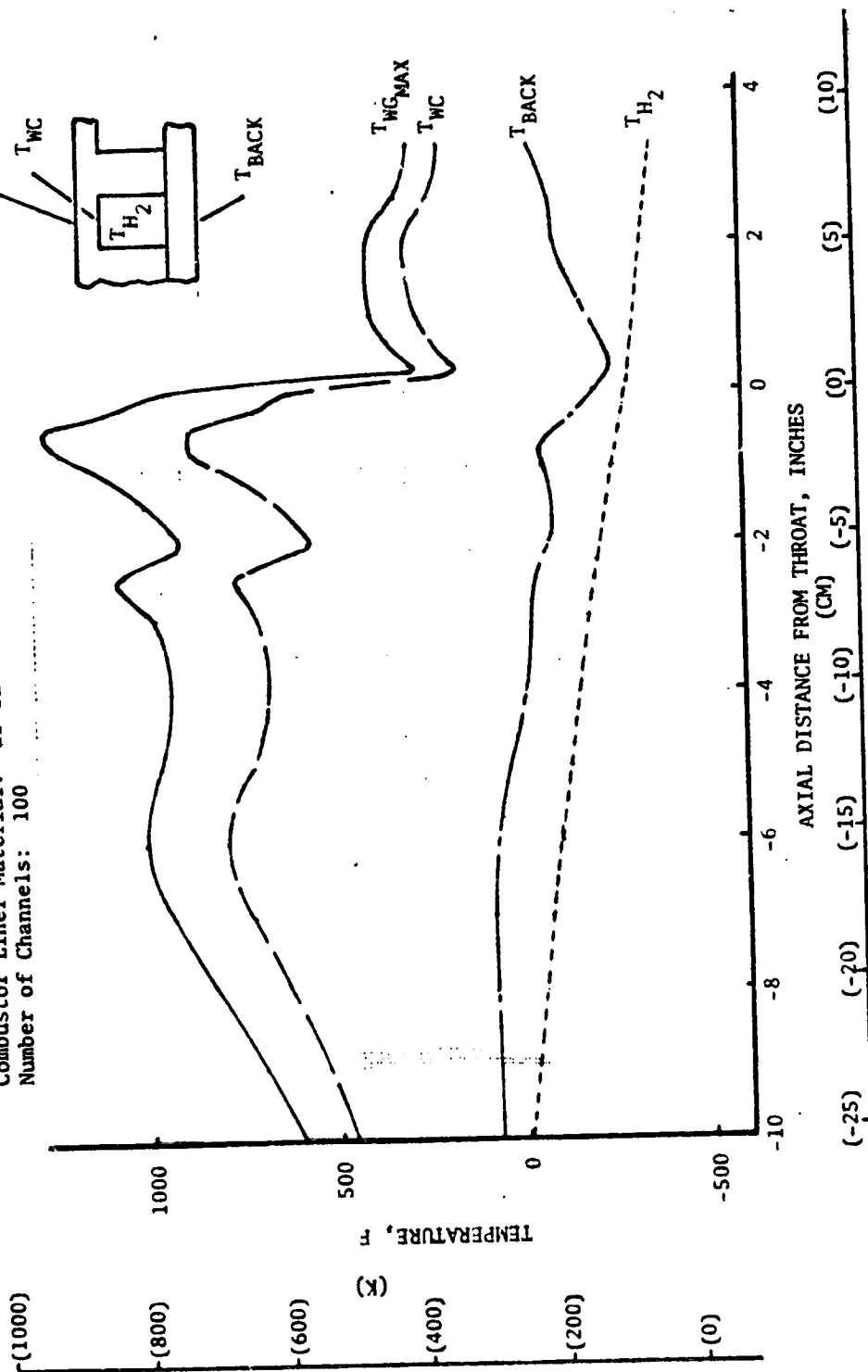
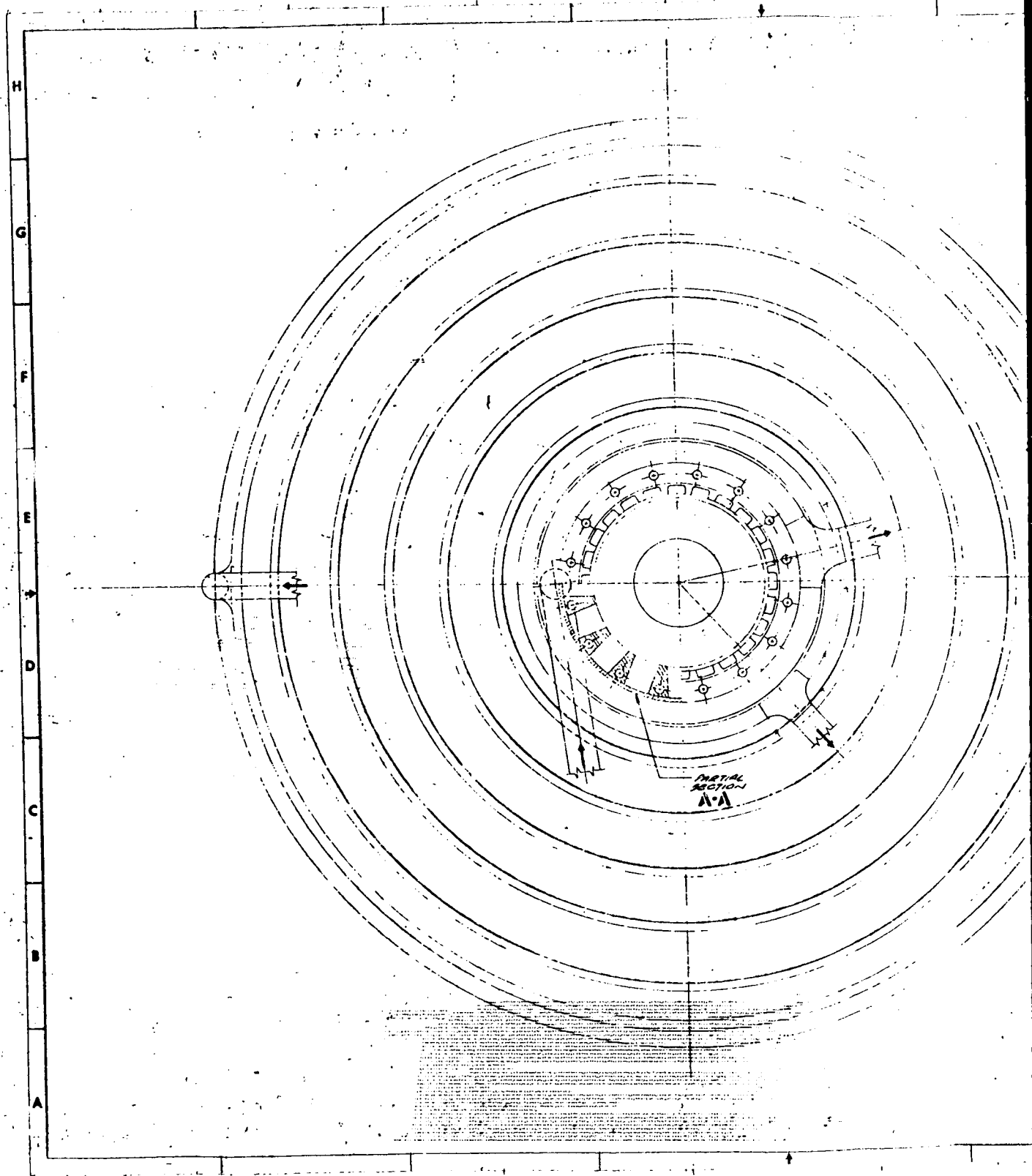


Figure 101. 70 Cycle Life Zr-Cu Combustor Wall Temperature Distribution

$(P_c = 1900$ psia or $1.31 \times 10^7 \text{ N/m}^2$, $MR_{T/C} = 6.5)$



FOLDOUT FRAME

High Cycle Life Thrust Chamber ($P_c = 1900$ psia or 1.31×10^7 N/m²)

As for the low cycle life thrust chamber, the basic structural requirements (yield safety factor) of the Zr-Cu combustor limited the design. The simplified and finite element stress analysis results presented in Table XXI indicated that a 700-cycle life could be achieved with a yield safety factor greater than 1.2. As noted in Table XXI, a factor of 1.1 resulted from the simplified analysis rather than the previously assumed value of 1.2. The selected chamber design had a minimum channel dimension of 0.040-by-0.028 inch (0.1016 cm-by-0.0712 cm), a maximum wall temperature of 698 F (644 K), a combustor coolant pressure drop of 2230 psi (1.538×10^7 N/m²), and a combustor liner weight of 6.3 pounds (2.86 kg). The coolant channel dimensions and wall temperature distributions for the selected high cycle life thrust chamber are presented in Fig. 103 and 104. The design drawing for this configuration is shown in Fig. 105.

Cycle Perturbation Summary

A summary of the life cycle perturbation analysis is presented in Table XXII. As shown in Table XXII, to design for low life cycle requirements, high gas-side wall temperatures result and the thrust chamber weight is increased. Also, the high wall temperatures make the design structurally limited; however a substantially lower combustor pressure drop is obtained. To achieve a high cycle life, the opposite is true. Low wall temperatures are required and result in extremely high coolant pressure drops. This coolant pressure drop requires high coolant pressures and, as for the low cycle thrust chamber, the design is structurally limited.

CHAMBER PRESSURE PERTURBATION (300-CYCLE LIFE)

1600-psia (1.103×10^7 N/m²) Chamber Pressure Thrust Chamber

In designing the A-286 tubular nozzle for the thrust chamber having a design chamber pressure of 1600 psi (1.103×10^7 N/m²), parametric heat transfer data were generated by assuming round tubes and varying the number of tubes. As in Task I, an 0.007-inch (0.01778 cm) tube wall thickness was used. As shown in Fig. 106, the coolant pressure drop increased and the wall temperature decreased with increase in the number of tubes. Also, the tube weight and tube inside diameter decreased as the number of tubes was increased (Fig. 107). A number of tubes that gave a design resulting in the highest wall temperature at an area ratio of 8-to-1 (combustor-nozzle joint) and not at high area ratios was selected ($N = 500$ tubes). To decrease the nozzle coolant pressure drop, various booked tube designs (Fig. 108 and 109) were analyzed, and design B was selected. This design resulted in a 25-psi (7.24×10^5 N/m²) coolant pressure drop, a 668 F (627 K) maximum wall temperature, and 7.5-pounds (3.405 kg) tube weight. The tube dimensions, coolant static pressure, and wall temperature distributions for the selected design are presented in Fig. 110 through 112.

The number of channels, channel width, and the combustor-nozzle joint area ratio were optimized for the 1600-psia (1.103×10^7 N/m²) thrust chamber Zr-Cu

TABLE XXI. HIGH CYCLE LIFE THRUST CHAMBER STRESS/CYCLE LIFE RESULTS

P_c : 1900 psia (1.31×10^7 N/m²)

$N_{T/C}$: 6.5

Combustor Liner Material: Zr-Cu

Critical Location: X = -0.5-Inch (-1.27 cm)

Channel Width, (inch)	Gas-Side Wall Thickness, (inch)	Coolant Pressure, (psia)	Max Gas-Side Wall Temp, (F)	1.1 ϵ_{eff} , (in/in)	N_f	ϕ_c	$N_f/4$	Yield Safety Factor
0.04 (0.1016 cm)	0.027 (0.0686 cm)	5109 (3.52×10^7 N/m ²)	661 (623 K)	0.0152	3000	10^{-4}	750	1.10
0.04	0.027	4652 (3.21×10^7 N/m ²)	698 (644 K)	0.0158	2800	10^{-4}	700	1.25
0.04 (0.1016 cm)	0.027 (0.0686 cm)	4652 (5.21×10^7 N/m ²)	698 (644 K)	0.0155	2800	10^{-4}	700	1.25

Modified
Simplified
Stress/
Cycle Life
Analysis

Finite
Element
Stress
Analysis

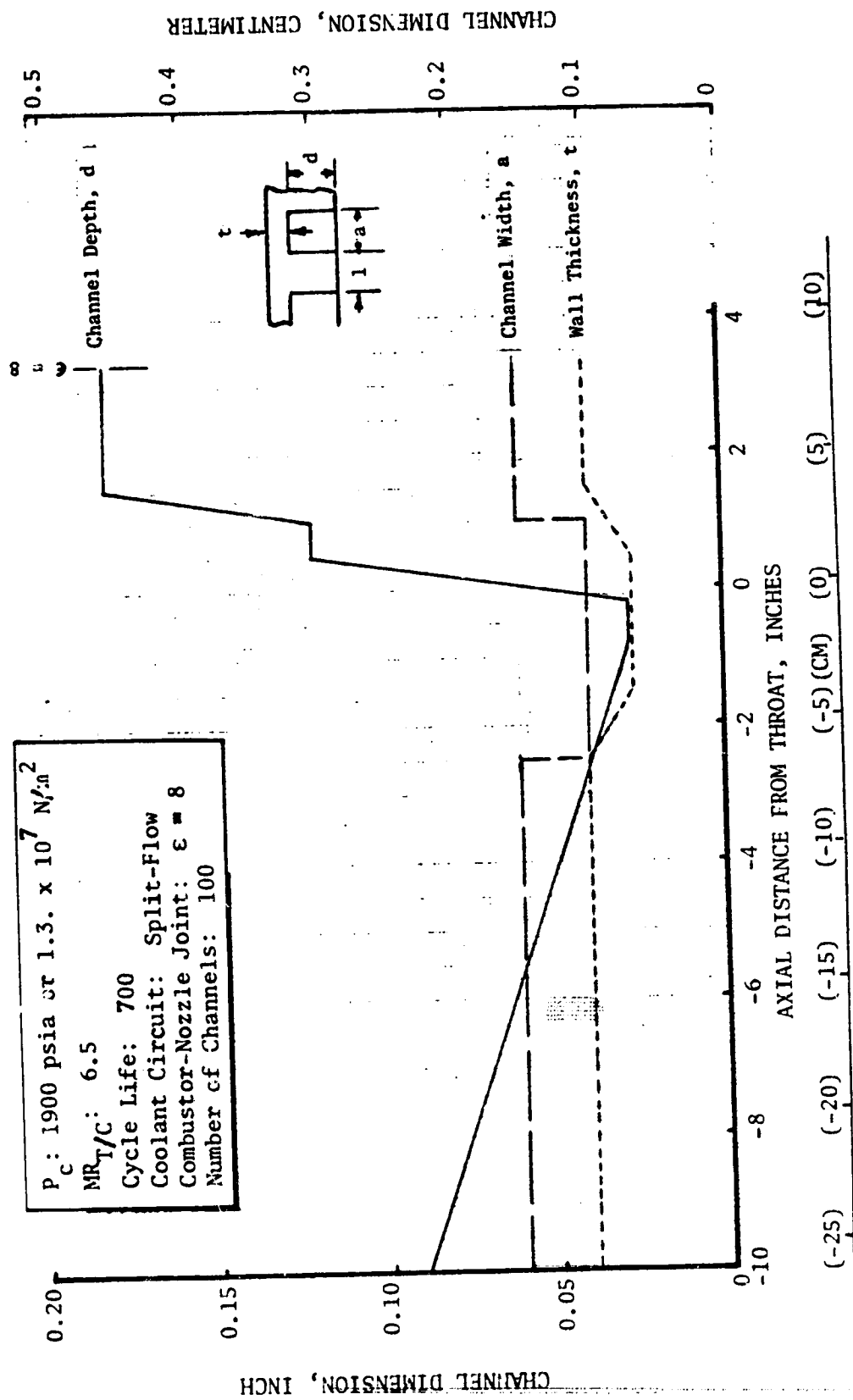


Figure 103. 700 Cycle Life Zr-Cu Combustor Channel Dimensions

($P_c = 1900 \text{ psia}$ or $1.31 \times 10^7 \text{ N/m}^2$, $MR_{T/C} = 6.5$)

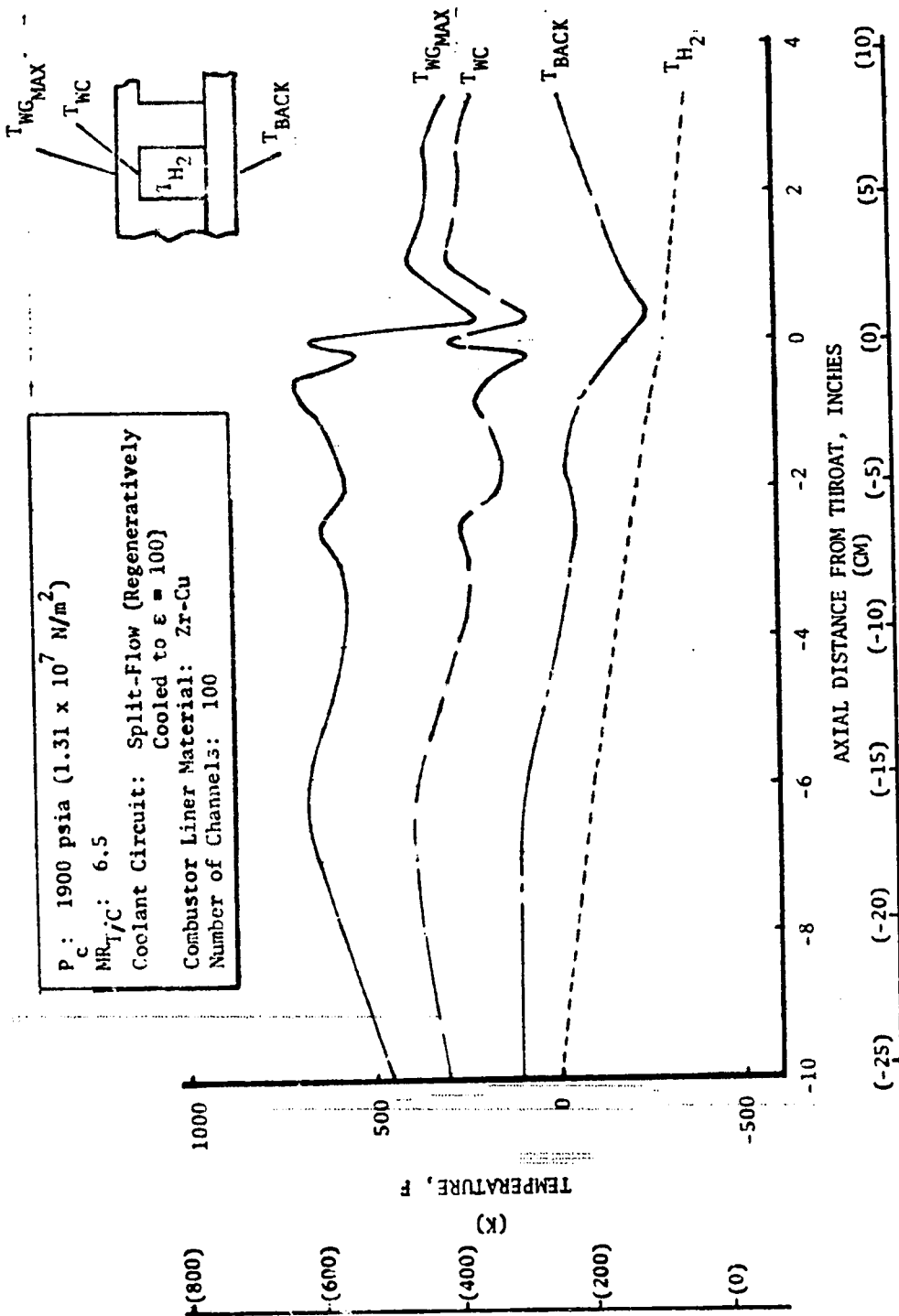
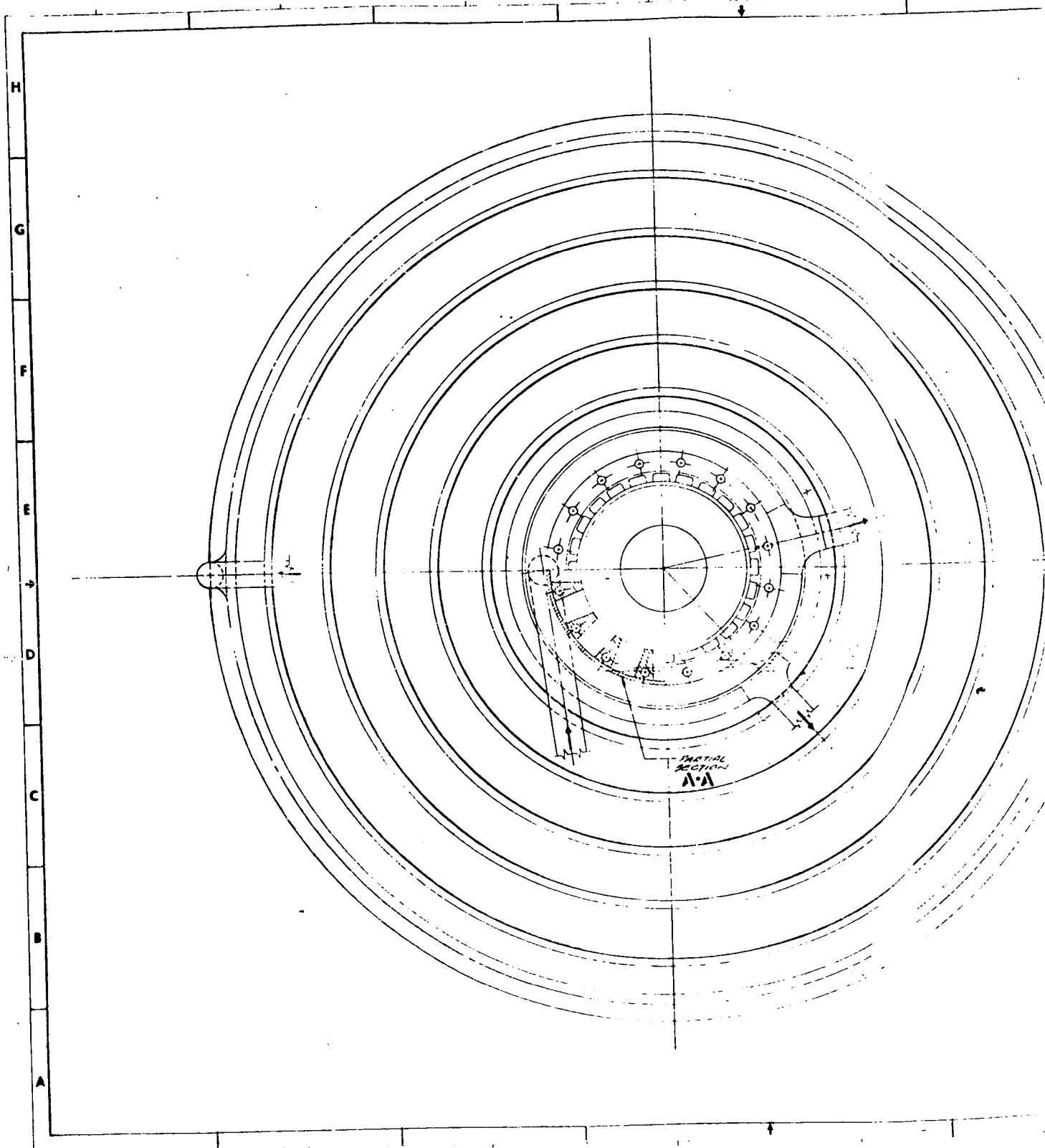
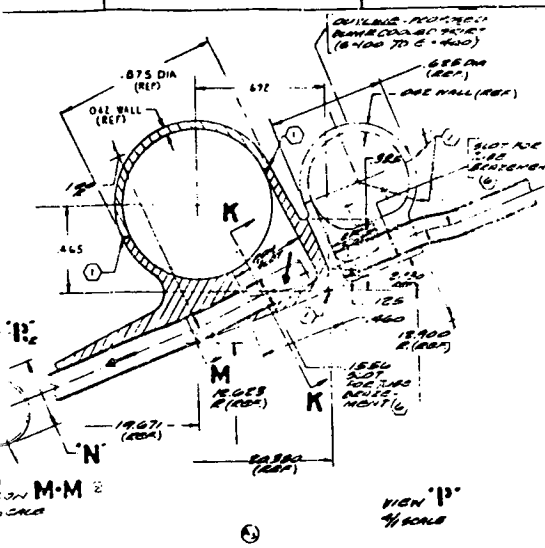


Figure 104. 700 Cycle Life Zr-Cu Combustor Wall Temperature Distribution
 ($P_c = 1900 \text{ psia}$ or $1.31 \times 10^7 \text{ N/m}^2$, $MR_{T/C} = 6.5$)



ISOMETRIC DRAWING



CHANNEL (NOT ON WALL COORDINATES - C.B. TO C-10)

SR	X	Y	N	H	T	L	INJ
20	10.000	2.483					
19	9.160	2.483	000	040	040		078
18	8.000	2.475					097
17	7.500	2.472					096
16	7.000	2.480					094
15	6.500	2.490					092
14	6.000	2.498					091
13	5.500	2.440					087
12	5.000	2.275					081
11	4.500	2.220					076
10	4.000	2.180					071
9	3.500	2.060					066
8	3.000	1.970					061
7	2.500	1.860	000	040	040		057
6	2.000	1.750					052
5	1.500	1.630					047
4	1.000	1.520					042
3	800			028			037
2	500	1.370		028			032
1	200			028			027
0	0	1.240					022
1	200	1.377					017
2	300						012
3	415	1.400					007
4	428	1.474					002
5	500						000
6	650	1.605	000	150	0		000
7	770	1.762					000
8	975	1.910					000
9	1000		000	150	0		000
10	1.119	2.028					000
11	1.278	2.148					000
12	1.441	2.274					000
13	1.500			180	040		000
14	1.628	2.413					000
15	1.823	2.500					000
16	2.084	2.785					000
17	2.509	2.920					000
18	2.601	3.187					000
19	2.984	3.276	000	180	040		172
20	3.325	3.000					000

(TOTAL NO OF CHANNELS = 100) (4)

1. REVISED CHANNEL HGT'S. IN TABLE AND HEAT UP STRUCTURE TO 032 IN.	2. REVISED INLET & OUTLET MANIFOLDS, ACC'D 1050
---	---

Figure 105. 700 Cycle Life Zr-Cu Channel Wall Combustor/A-286 Tubular Nozzle Configuration ($P_c = 1900 \text{ psia}$ or $1.31 \times 10^7 \text{ N/m}^2$, $MR_{T/C} = 6.5$)

CHANNEL (NOT ON WALL COORDINATES - C.B. TO C-100)

SR	X	Y	N	H	T	L	INJ
20	3.125	3.060	050	050	020		020
19	3.548	3.018	057	020	020		020
18	3.785	3.180	034	020	020		020
17	4.022	3.183	007	020	020		020
16	4.263		078	020	020		020
15	4.648	3.882	024	020	020		020
14	4.887		082	020	020		020
13	5.017		087	020	020		020
12	5.030		042	020	020		020
11	5.500	7.014	045	020	020		020
10	10.485	8.108	043	020	020		020
9	12.180	9.400	182	020	020		020
8	15.849	10.600	128	020	020		020
7	15.888	11.483	170	020	020		020
6	17.105	11.483	143	020	020		020
5	17.119	11.985	131	020	020		020
4	18.071	12.028	180	020	020		020
3	20.380	12.110	143	020	020		020

(TOTAL NO OF CHANNELS = 500) (2)

163

-050	INLET	020	020
-049	INLET	020	020
-047	INLET	020	020
-045	INLET	020	020
-043	INLET	020	020
-041	INLET	020	020
-039	INLET	020	020
-037	INLET	020	020
-035	INLET	020	020
-033	INLET	020	020
-031	INLET	020	020
-029	INLET	020	020
-027	INLET	020	020
-025	INLET	020	020
-023	INLET	020	020
-021	INLET	020	020
-019	INLET	020	020
-017	INLET	020	020
-015	INLET	020	020
-013	INLET	020	020
-011	INLET	020	020
-009	INLET	020	020
-007	INLET	020	020
-005	INLET	020	020
-003	INLET	020	020
-001	INLET	020	020

(1) CHANNELS NOT ON WALL COORDINATES - C.B. TO C-100
 (2) CHANNELS NOT ON WALL COORDINATES - C.B. TO C-100
 (3) CHANNELS NOT ON WALL COORDINATES - C.B. TO C-100
 (4) CHANNELS NOT ON WALL COORDINATES - C.B. TO C-100
 (5) CHANNELS NOT ON WALL COORDINATES - C.B. TO C-100
 (6) CHANNELS NOT ON WALL COORDINATES - C.B. TO C-100
 (7) CHANNELS NOT ON WALL COORDINATES - C.B. TO C-100
 (8) CHANNELS NOT ON WALL COORDINATES - C.B. TO C-100
 (9) CHANNELS NOT ON WALL COORDINATES - C.B. TO C-100
 (10) CHANNELS NOT ON WALL COORDINATES - C.B. TO C-100

FOLDOUT FRAME

TABLE XXII. CYCLE LIFE PERTURBATION SUMMARY

F: 20,000 Pounds (8.896×10^4 N)
 P_c: 1900 psia (1.31×10^7 N/m²), MR_{T/C}: 6.5 Cooling Circuit: Split-Flow (Regeneratively Cooled to $\epsilon = 100$)
 ϵ : 400-to-1

Component	Cycle Life	71 Cycle Life	300 Cycle Life	700 Cycle Life
<u>Nozzle</u>		525	525	525
Number of Tubes			0.05 (0.127 cm) 685 (636 K)	0.05 (0.127 cm) 685 (636 K)
Minimum Unformed Tube Outside Diameter, inch		0.05 (0.127 cm) 685 (636 K)		
Maximum Gas-Side Wall Temperature, F				
<u>Combustor</u>		100	100	100
Number of Channels				
Minimum Channel Dimensions:				
Width, inch		0.04 (0.1016 cm)	0.04 (0.1016 cm)	0.04 (0.1016 cm)
Height, inch		0.094 (0.239 cm)	0.045 (0.1143 cm)	0.028 (0.0712 cm)
Land, inch		0.0427 (0.1084 cm)	0.0427 (0.1084 cm)	0.0427 (0.1084 cm)
Combustor-Nozzle Joint Area Ratio		8	8	8
Minimum Hot-Gas Wall Thickness, inch		0.029 (0.0737 cm) 1271 (962 K)	0.027 (0.0686 cm) 900 (756 K)	0.027 (0.0686 cm) 698 (644 K)
Maximum Gas-Side Wall Temperature, F				
Critical Location Stress and Life Parameters:				
Yield Safety Factor		1.21	1.42	1.25
Ultimate Safety Factor		1.41	2.05	2.46
Damage Fraction: $(4(\theta_c + \theta_p))$		$4(0.04 + 0.065) = 0.421$ For N = 30 Cycles	$4(0.001 + 0.249) = 1.00$	$4(0.001 + 0.249) = 1.00$
<u>Chamber</u>				
Combustor Coolant Pressure Drop, psi		194 (1.339×10^6 N/m ²)	608 (4.9×10^6 N/m ²)	2230 (1.53×10^7 N/m ²)
Nozzle Coolant Pressure Drop, psi		36 (2.485×10^5 N/m ²)	36 (2.485×10^5 N/m ²)	36 (2.485×10^5 N/m ²)
Combustor Liner and Nozzle Tube Weight, lb		15.5 (7.03 kg)	14.0 (6.35 kg)	12.6 (5.72 kg)

$P_c = 1600 \text{ psia } (1.103 \times 10^7 \text{ N/m}^2)$
 $MR_{T/C} = 6.5$
 Tube Material: A-286
 Coolant Inlet: $\epsilon = 100$
 Combustor-Nozzle Joint: $\epsilon = 8$
 Tube Wall Thickness: 0.007-Inch (0.01778 CM)
 (Constant)

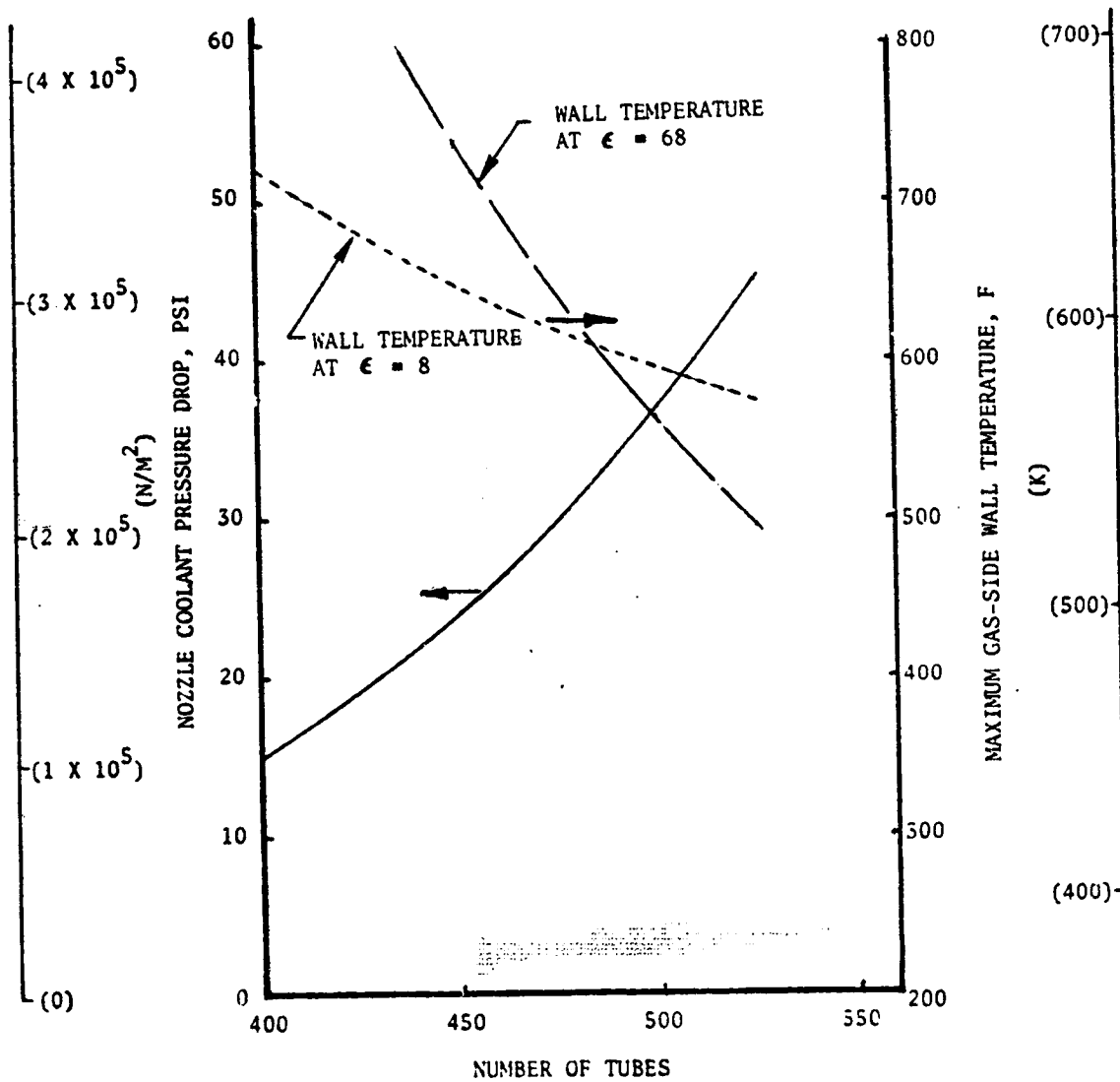


Figure 106. A-286 Nozzle Split-Flow Circuit (Round Tubes) Coolant Pressure Drop and Wall Temperature Variation With Number of Tubes ($P_c = 1600 \text{ psia or } 1.103 \times 10^7 \text{ N/m}^2$), $MR_{T/C} = 6.5$

$P_c = 1600 \text{ psia } (1.103 \times 10^7 \text{ N/M}^2)$
 $MR_{T/C} = 6.5$
 Tube Material: A-286
 Coolant Inlet: $\epsilon = 100$
 Combustor-Nozzle Joint: $\epsilon = 8$
 Tube Wall Thickness: 0.007-Inch (0.01778 CM)
 (Constant)

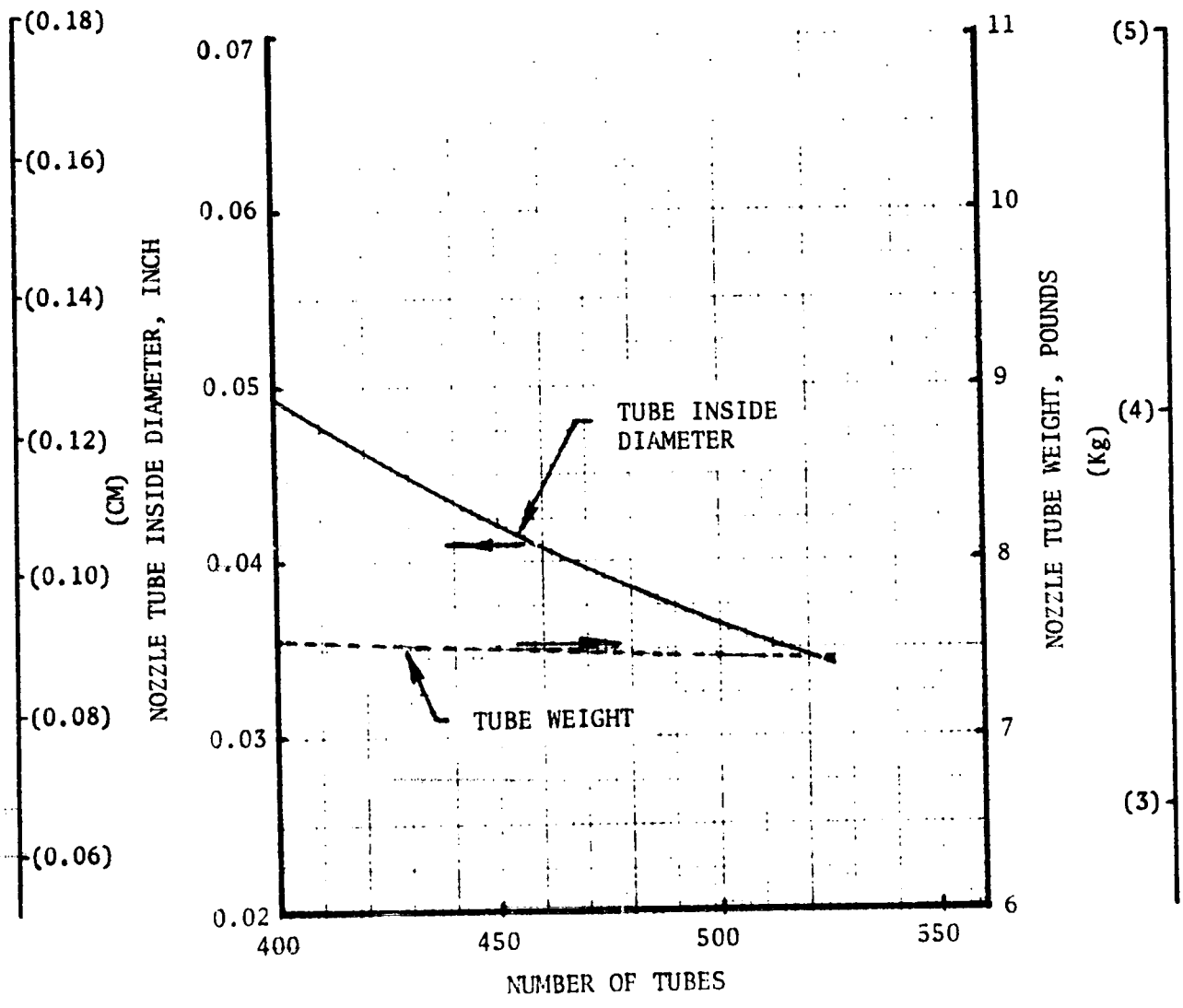


Figure 107. A-286 Nozzle Split-Flow Circuit (Round Tubes) Tube Diameter and Weight Variation With Number of Tubes ($P_c = 1600 \text{ psia}$ or $1.103 \times 10^7 \text{ N/m}^2$), $MR_{T/C} = 6.5$

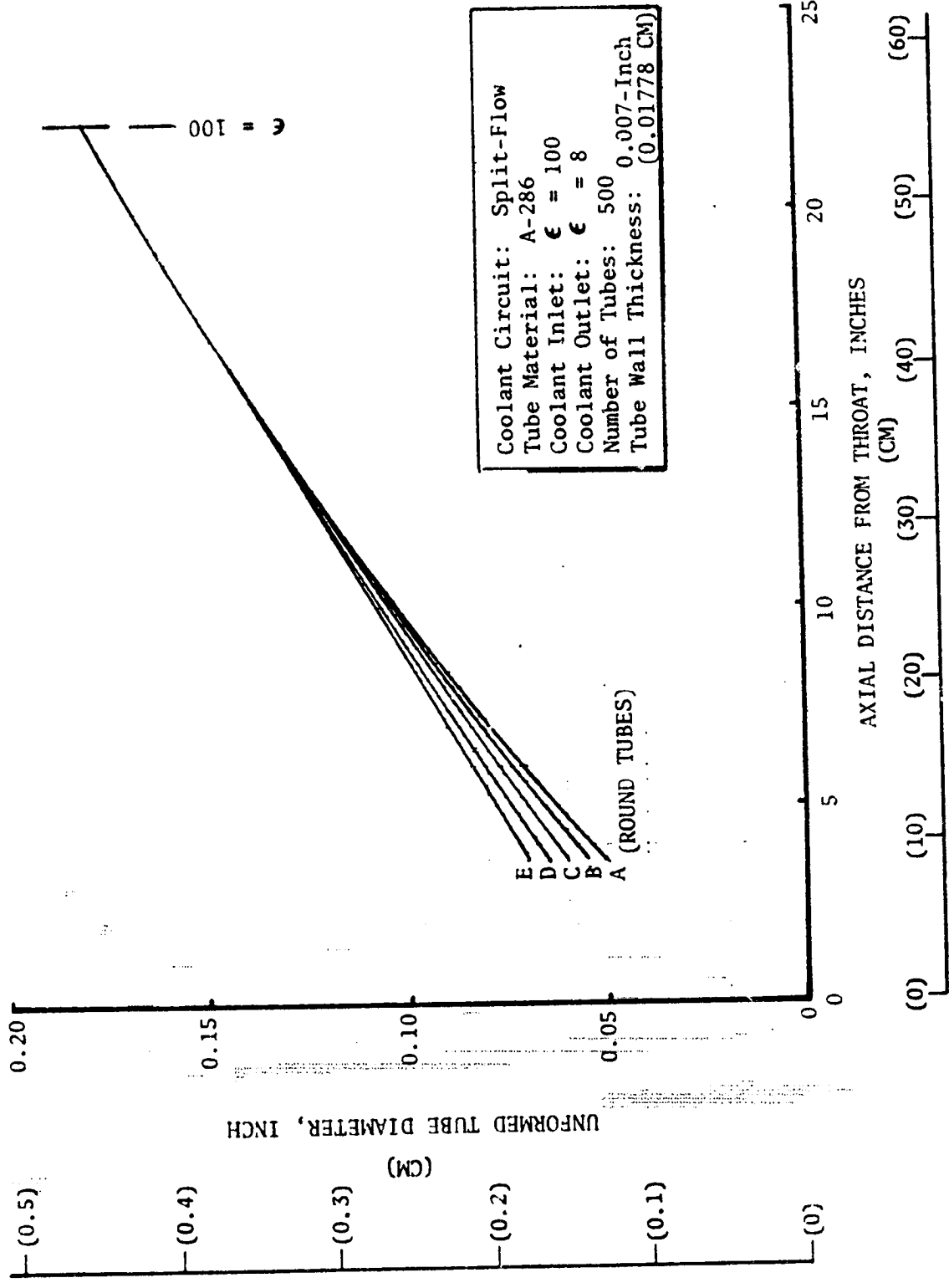


Figure 108. Booked A-286 Nozzle Configurations (Split-Flow Cooling Circuit) --
 $P_c = 1600$ psia (1.103×10^7 N/m²), $MR_{T/C} = 6.5$

$P_c = 1600 \text{ psia}$, $MR_{T/C} = 6.5$
 $(1.103 \times 10^7 \text{ N/m}^2)$
 Coolant Circuit: Split-Flow
 Tube Material: A-286
 Coolant Inlet: $\epsilon = 100$
 Coolant Outlet: $\epsilon = 8$
 Number of Tubes: 500
 Tube Wall Thickness: 0.007-Inch
 (0.01778 CM)

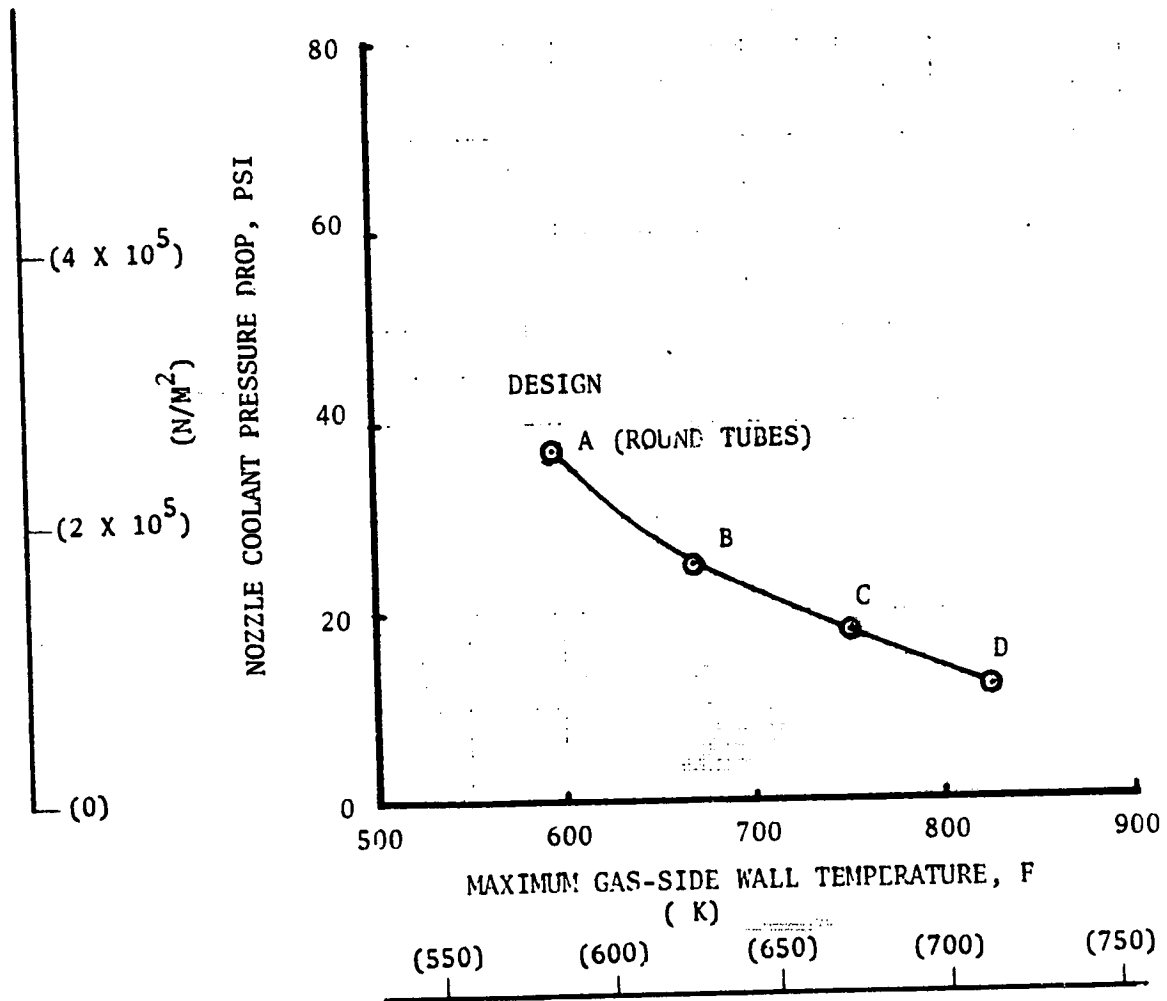


Figure 109. Nozzle Coolant Pressure Drop Influence on Maximum Wall Temperature ($P_c = 1600 \text{ psia}$ or $1.103 \times 10^7 \text{ N/m}^2$, $MR_{T/C} = 6.5$)

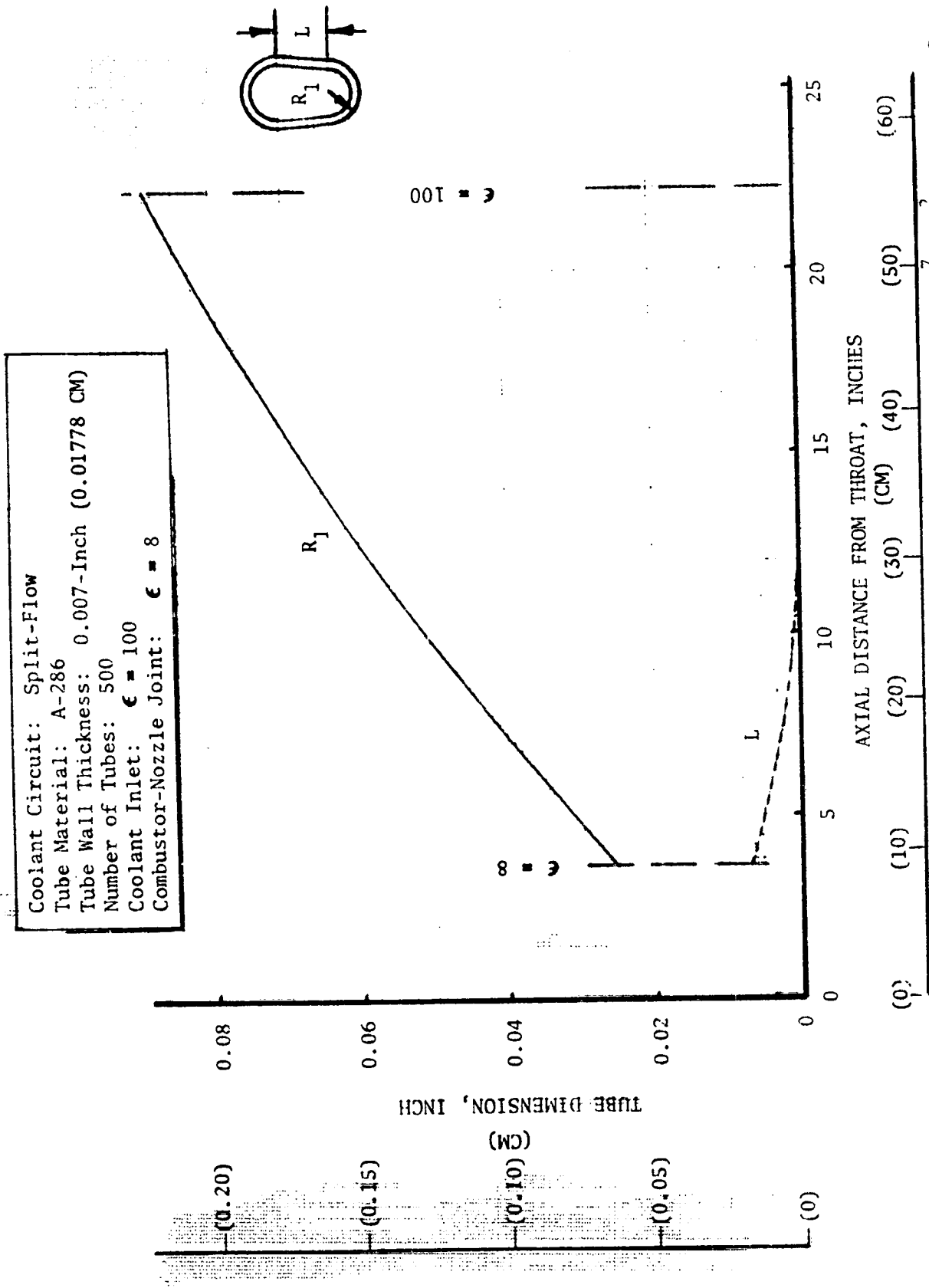


Figure 110. A-286 Tubular Nozzle Tube Dimensions ($P_c = 1600$ psia or 1.103×10^7 N/m², $MR_{T/C} = 6.5$)

Coolant Circuit: Split-Flow

Coolant Inlet: $\epsilon = 100$

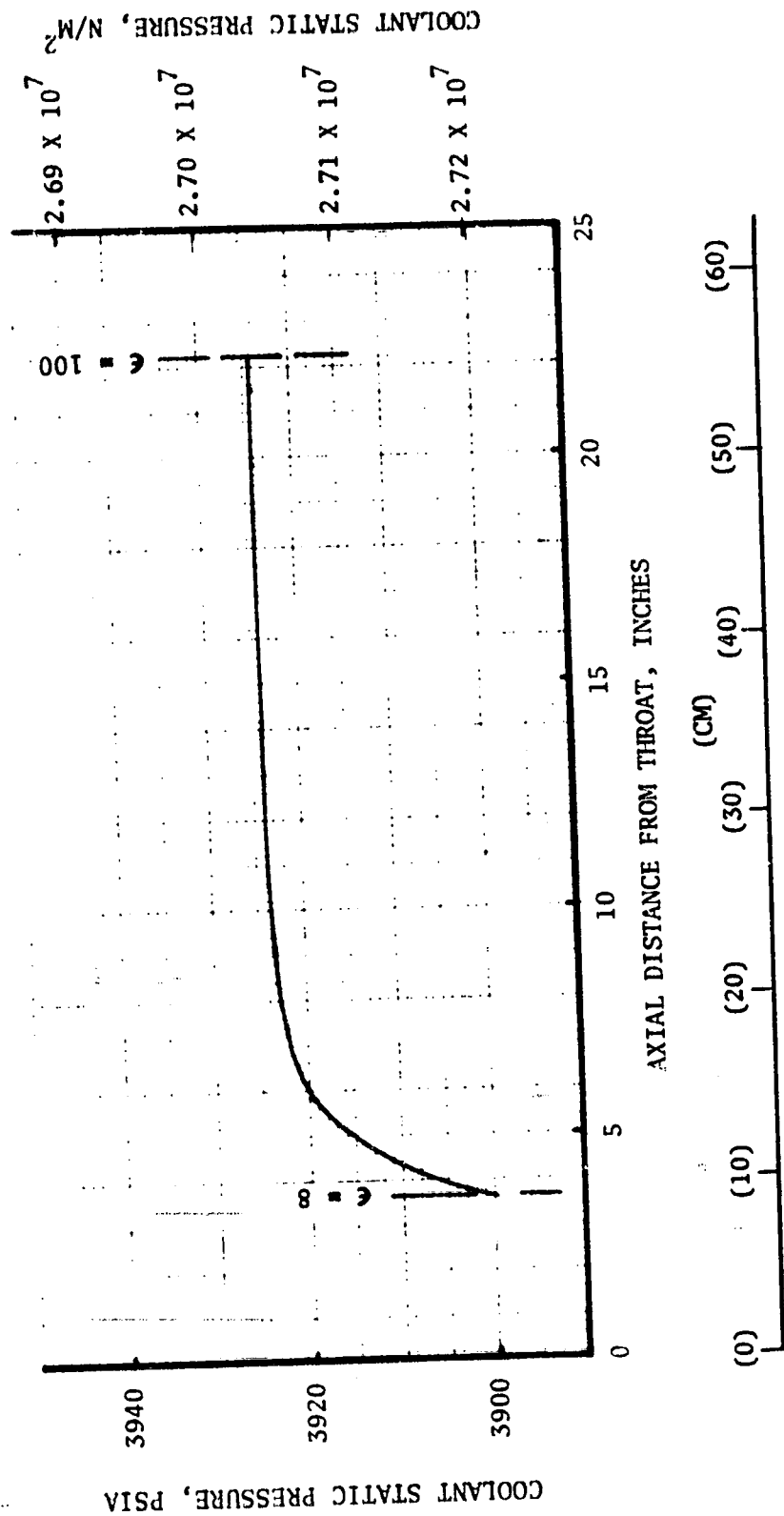


Figure 111. Nozzle Coolant Static Pressure Distribution ($P_c = 1600$ psia or

1.103×10^7 N/m², $MR_T/C = 6.5$)

Coolant Circuit: Split-Flow
 Tube Material: A-286
 Tube Wall Thickness: 0.007-Inch (0.01778 CM)
 Number of Tubes: 500
 Coolant Inlet: $\epsilon = 100$
 Combustor-Nozzle Joint: $\epsilon = 8$

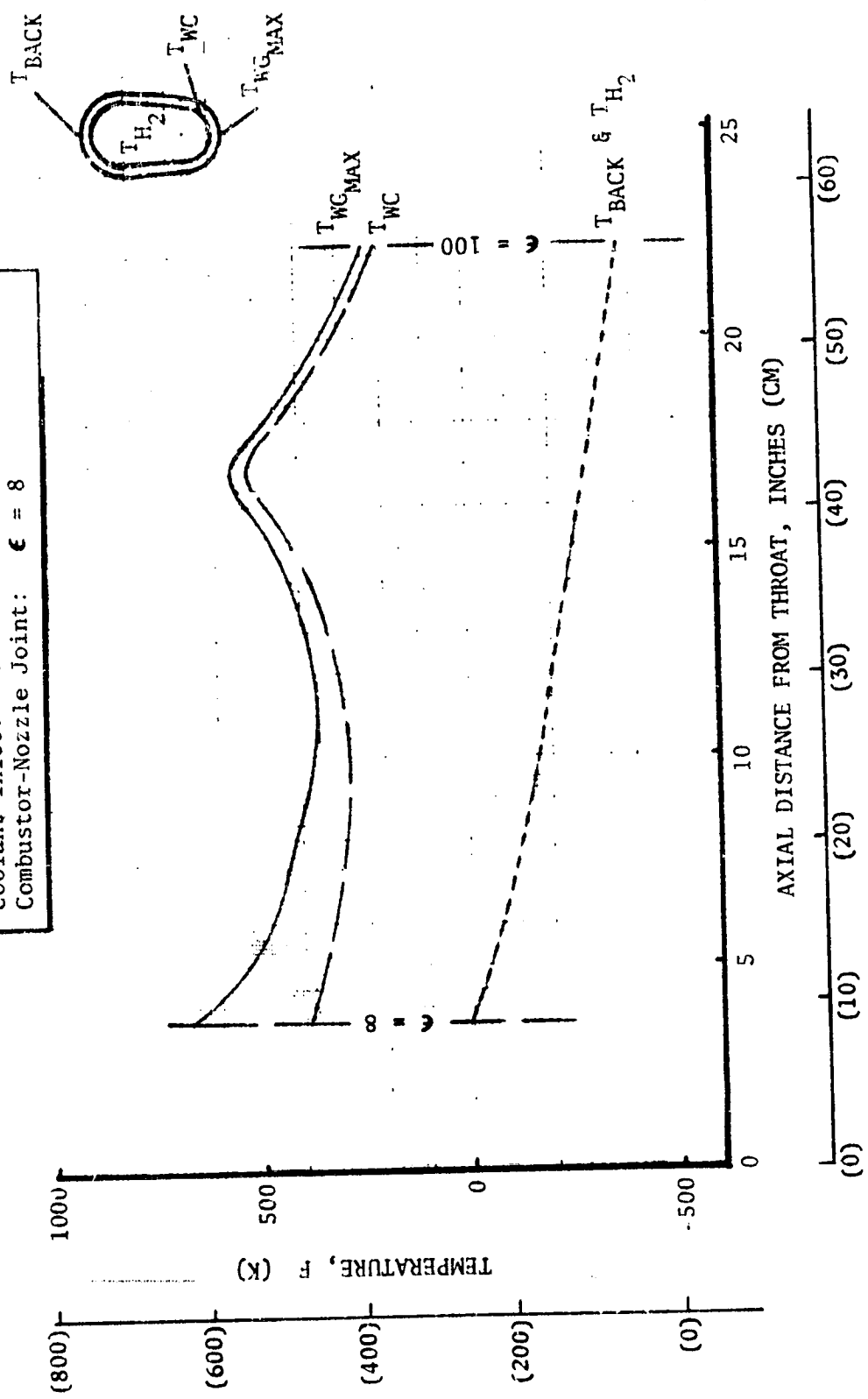


Figure 112. Nozzle Temperature Distributions ($P_c = 1600$ psia or 1.103×10^7 N/m², $MR_{T/C} = 6.5$)

combustor in the same manner as for the 1900-psia ($1.31 \times 10^7 \text{ N/m}^2$) thrust chamber designs performed in Task I. As shown in Fig. 113, a combustor-nozzle joint area ratio of 8-to-1 minimized the combustor coolant pressure drop for a maximum gas-side wall temperature of approximately 880 F (745 K) and 910 F (762 K). Using this selected joint area ratio, the influence of the number of channels was investigated for a 0.040-inch minimum channel width. As was discovered in Task I, the optimum land width appears to occur at values below the 0.040-inch (0.1016 cm) minimum value selected based on fabrication difficulty (Fig. 114). As shown in Table XXI, the wider minimum channel width of 0.045-inch (0.1143 cm) resulted in an acceptable design, but resulted in a higher coolant pressure drop than the 0.040-inch (0.1016 cm) minimum channel width. Therefore, the combustor design having a 0.040-inch (0.1016 cm) channel width and 0.042-inch (0.1068 cm) land width (110 channels) was selected. As shown in Table XXIII, finite element stress analysis indicated a maximum gas-side wall temperature of approximately 880 F (745 K) was required to satisfy the 300-cycle life requirement. Also, the 1.2 factor on the effective strain range, computed using the simplified method, resulted in an excellent correlation with the finite element analysis results.

The channel dimensions of the selected combustor design as shown in Fig. 115 resulted in a minimum channel size of 0.04-inch by 0.056-inch (0.1016 cm by 0.1422 cm) and a coolant pressure drop of 338 psi ($2.33 \times 10^6 \text{ N/m}^2$). The coolant static pressure and wall temperature distribution of the selected design are presented in Fig. 116 and 117. The design drawing of the 1600-psia ($1.103 \times 10^7 \text{ N/m}^2$) chamber pressure thrust chamber is shown in Fig. 118.

2100 psia ($1.448 \times 10^7 \text{ N/m}^2$) Chamber Pressure Thrust Chamber

The design of the A-286 tubular nozzle for 2100-psia ($1.448 \times 10^7 \text{ N/m}^2$) chamber pressure thrust chamber was performed in the same manner as for the other chamber pressure design. The final selected design, shown in Fig. 119, has 540 tubes with a constant 0.007-inch (0.01778 cm) wall thickness. The tube dimensions, coolant static pressure, and wall temperature distributions for the nozzle are presented in Fig. 119 through 121. This design resulted in a coolant pressure drop of 41 psia ($2.83 \times 10^5 \text{ N/m}^2$), a maximum gas-side wall temperature of 608 F (593 K), and a coolant tube weight of 5.6 pounds (2.54 kg).

As shown in Fig. 122, a combustor-nozzle joint area ratio of 9.5 minimized the combustor coolant pressure drop, and therefore, was selected as the joint area ratio. Also as shown in Table XXIV, a maximum gas-side wall temperature of 934 F (775 K) was allowed for the 300-cycle thrust chamber life for the 2100-psia ($1.448 \times 10^7 \text{ N/m}^2$) chamber pressure design. A factor of 1.0 on the simplified analysis effective strain range provided better correlation with the finite element analysis. The resultant Zr-Cu combustor characteristics are presented in Fig. 123 through 125. The selected design had minimum channel dimensions of 0.040-inch by 0.042-inch (0.1016 cm by 0.1068 cm), a combustor coolant pressure drop of 893 psi ($6.15 \times 10^6 \text{ N/m}^2$), and a liner weight of 7.4 pounds (3.36 kg). The design layout of this configuration is shown in Fig. 126. Because of the higher combustion gas pressure, the INCO 718 jacket thickness was increased to 0.035 inch (0.0889 cm).

$P_c = 1600 \text{ psia } (1.103 \times 10^7 \text{ N/M}^2)$
 $MR_{T/C} = 6.5$
 Cooling Circuit: Split-Flow (Regeneratively Cooled to $\epsilon = 100$)
 Combustor Liner Material: Zr-Cu
 Minimum Gas-Side Wall Thickness: 0.027-Inch (0.0686 CM)
 Minimum Channel Width: 0.040-Inch (0.1016 CM)
 Number of Channels: 110

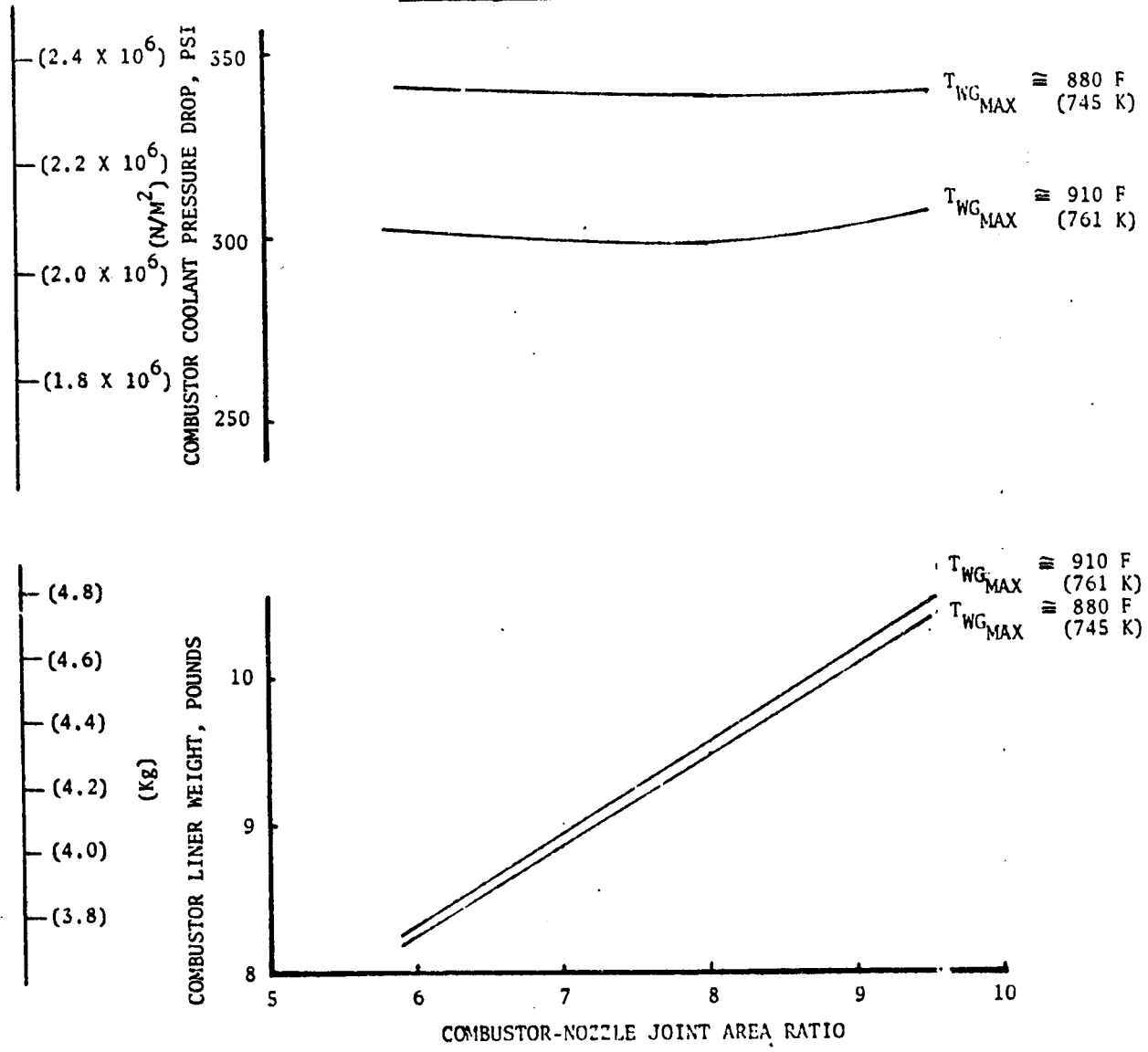


Figure 113. Combustor Coolant Pressure Drop and Liner Weight Variation With Combustor-Nozzle Joint Area Ratio ($P_c = 1600 \text{ psia}$ or $1.103 \times 10^7 \text{ N/m}^2$, $MR_{T/C} = 6.5$, 300 Cycle Life)

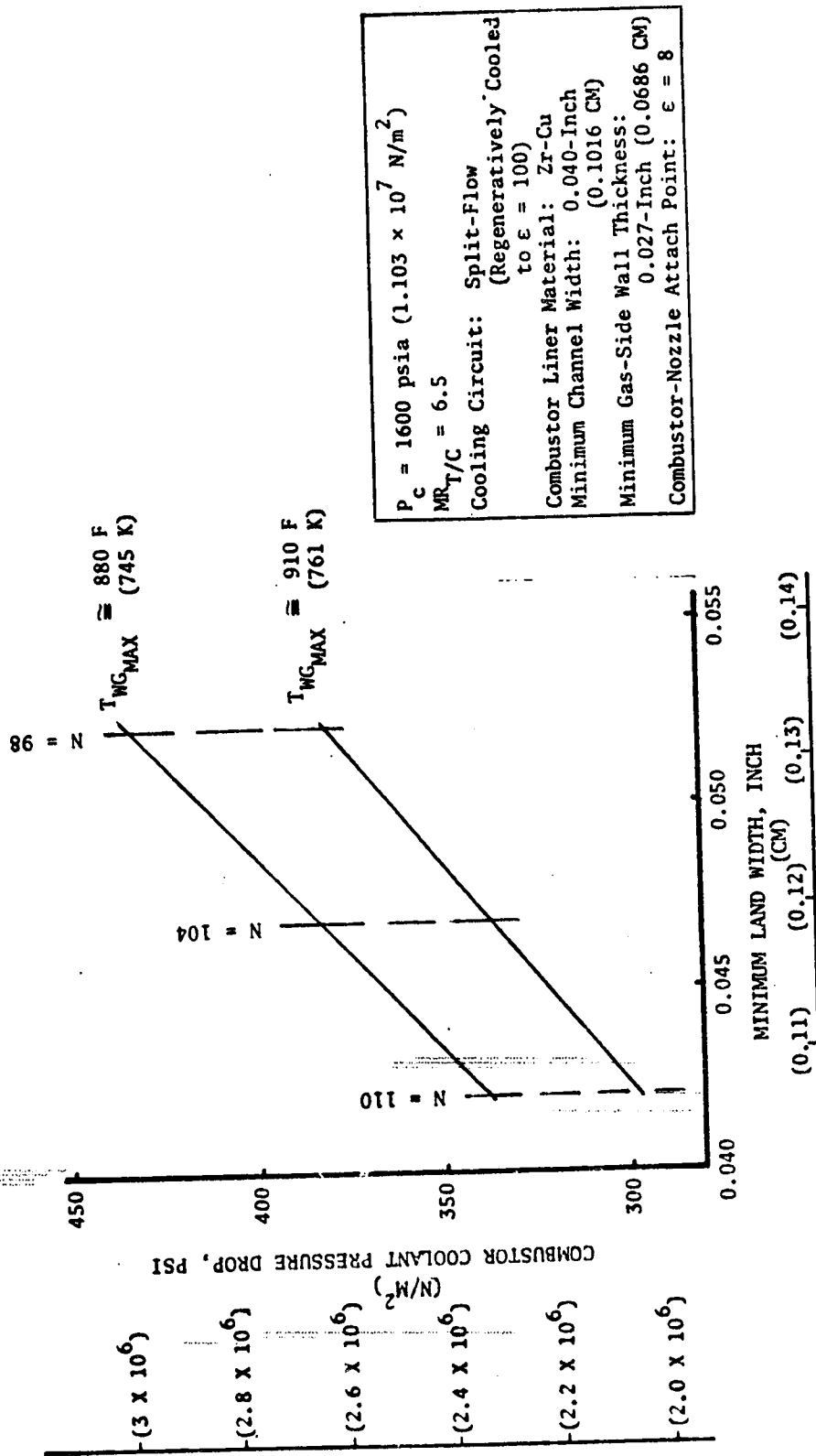


Figure 114. Minimum Land Width (Number of Channels) Influence on Combustor Coolant Pressure Drop ($P_c = 1600$ psia or 1.103×10^7 N/m², $MR_{T/C} = 6.5$, 300 Cycle Life)

TABLE XXIII. 1600 PSIA (1.103×10^7 N/m²) CHAMBER PRESSURE
THRUST CHAMBER STRESS/CYCLE LIFE RESULTS

Cycle Life: 300 Cycles

MPa/C: 6.5

Combustor Liner Material: Zr-Cu

Critical Location: X = -0.5-Inch (-1.27 cm)

Channel Width (inch)	Gas-Side Wall Thickness (inch)	Coolant Pressure (psia)	Max Gas-Side Wall Temp. (F)	1.2 ϵ_{eff} (in/in)	N_f	ϕ_f	ϕ_c	$4(\phi_f + \phi_c)$	Yield Safety Factor
0.040 (0.1016 cm)	0.027 (0.0686 cm)	3345×10^7 N/m ² (2.307 x 10 ⁷ N/m ²)	879 (744 K)	0.0216	1250	0.24	10^{-4}	0.96	1.57
0.045 (0.1143 cm)	0.027 (0.0686 cm)	3387×10^7 N/m ² (2.333 x 10 ⁷ N/m ²)	881 (745 K)	0.0216	1250	0.24	10^{-4}	0.96	1.38
0.040 (0.1016 cm)	0.027 (0.0686 cm)	3334×10^7 N/m ² (2.295 x 10 ⁷ N/m ²)	871 (740 K)	0.0214	1260	0.238	10^{-4}	-0.95	1.57
0.040 (0.1016 cm)	0.027 (0.0686 cm)	3340×10^7 N/m ² (2.3 x 10 ⁷ N/m ²)	909 (760 K)	0.0223	1160	0.259	10^{-4}	1.03	1.53
0.04 (0.1016 cm)	0.027 (0.0686 cm)	3345×10^7 N/m ² (2.307 x 10 ⁷ N/m ²)	879 (744 K)	0.022	1200	0.25	10^{-4}	1.00	1.57

Modified Simplified Stress/Cycle Life Analysis

Finite Element Stress Analysis

¹The 1.2 factor only applies to values computed using the modified simplified stress/cycle life analysis

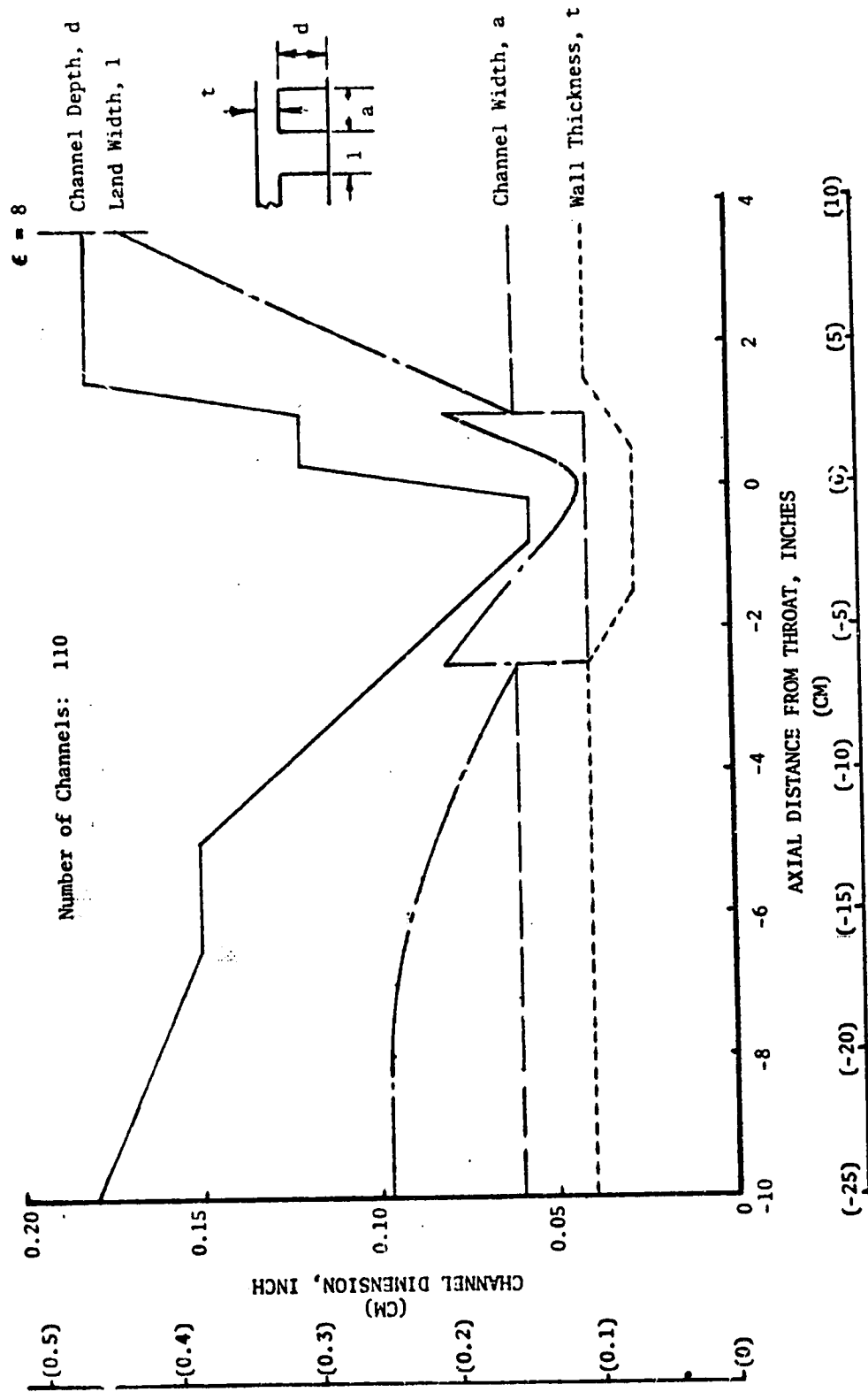


Figure 115. Zr-Cu Combustor Channel Dimensions ($P_c = 1600$ psia or 1.103×10^7 N/m², $MR_{T/C} = 6.5$, 300 Cycle Life)

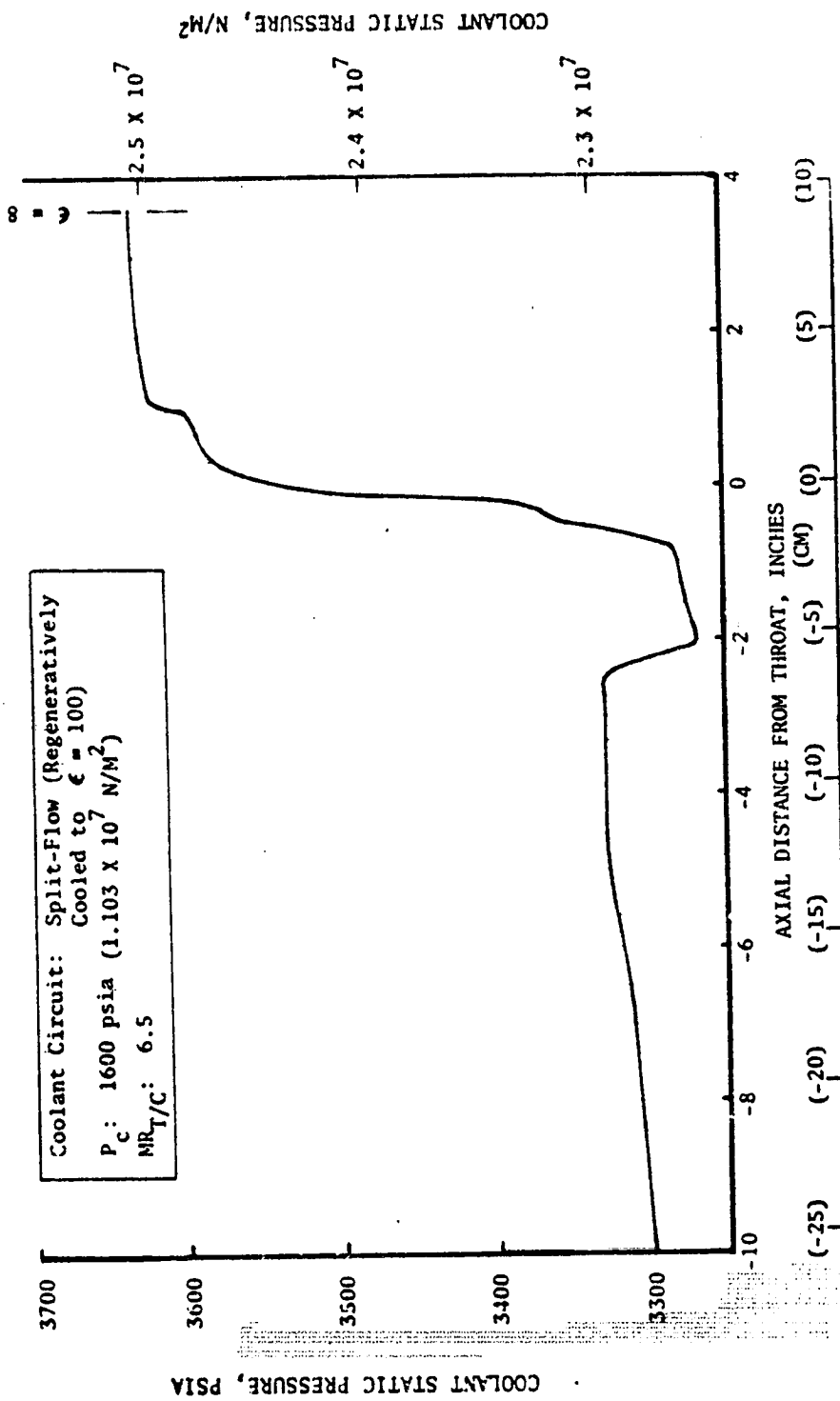


Figure 116. Zr-Cu Combustor Coolant Static Pressure Distribution ($P_c = 1600$ psia or 1.103×10^7 N/m², $MR_{T/C} = 6.5$, 300 Cycle Life)

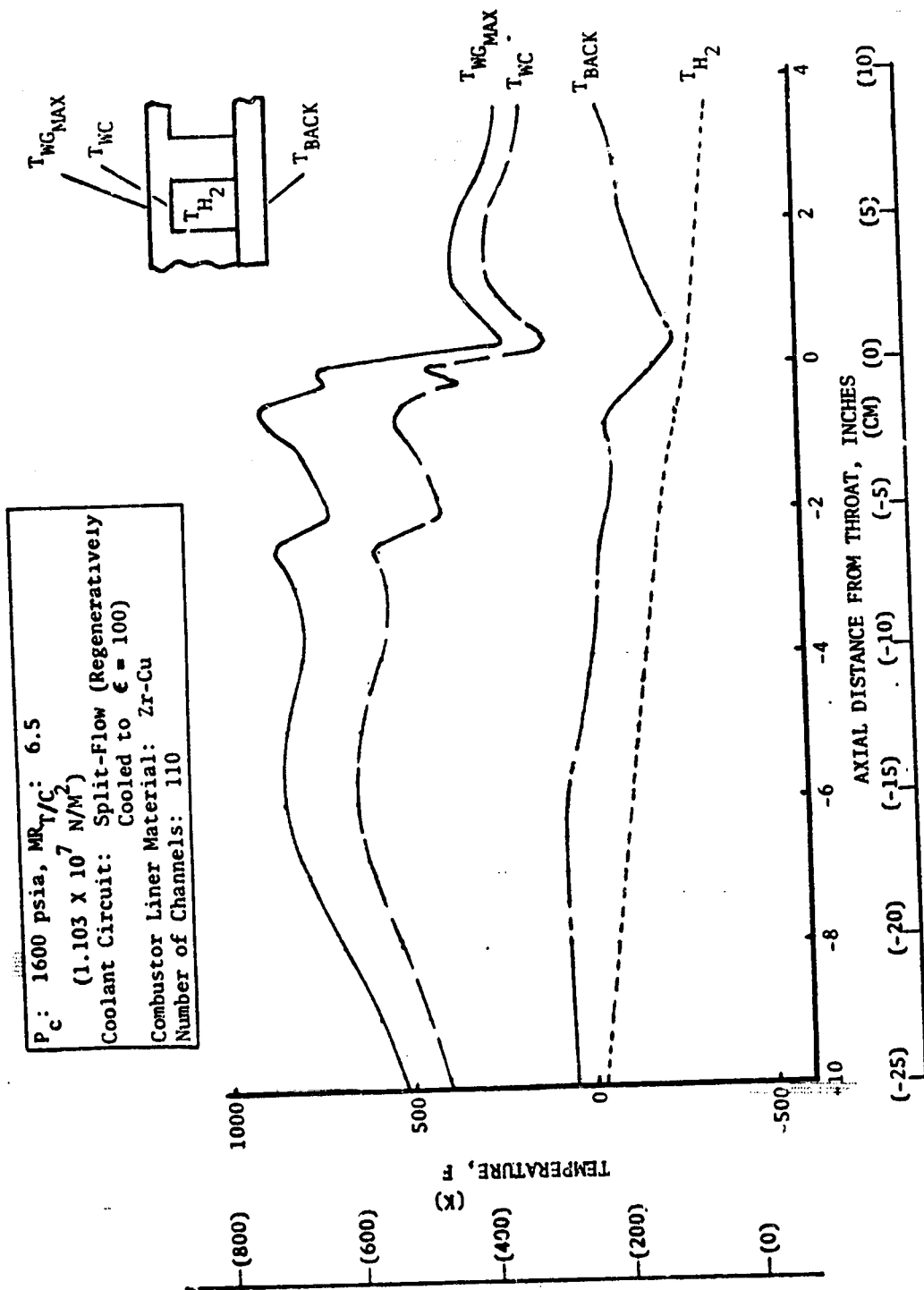
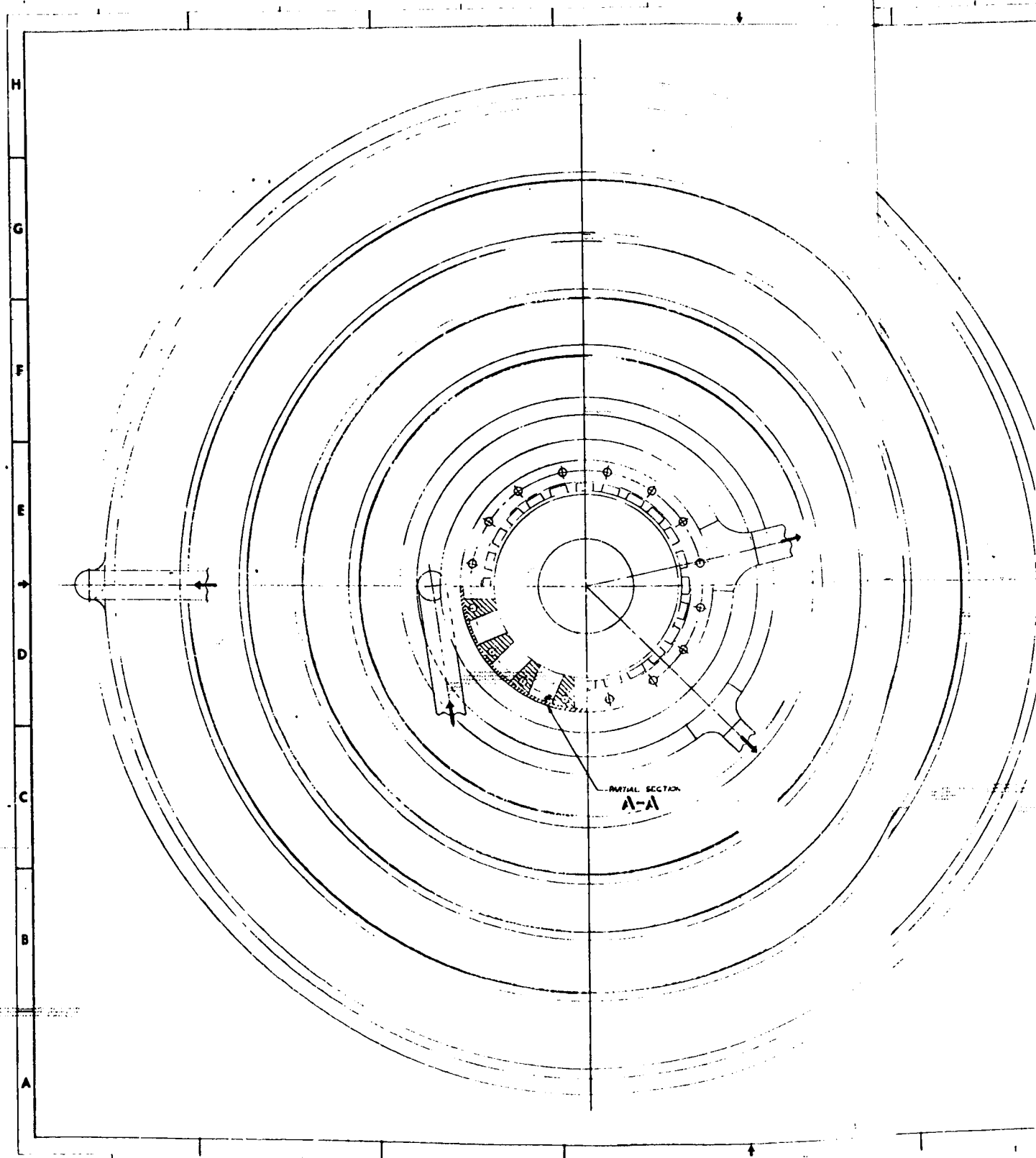


Figure 117. Zr-Cu Combustor Wall Temperature Distribution ($P_c = 1600$ psia or $1.103 \times 10^7 \text{ N/m}^2$, $MR_{T/C} = 6.5$, 300 Cycle Life)



FOLDOUT FRAME

027 MANIFOLD 1REQD
028 MANIFOLD 1REQD
029 MANIFOLD 1REQD

043 MANIFOLD 1REQD
010 MANIFOLD 1REQD

026 MANIFOLD 1REQD

17 28

15 78

16 78

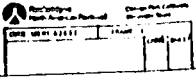
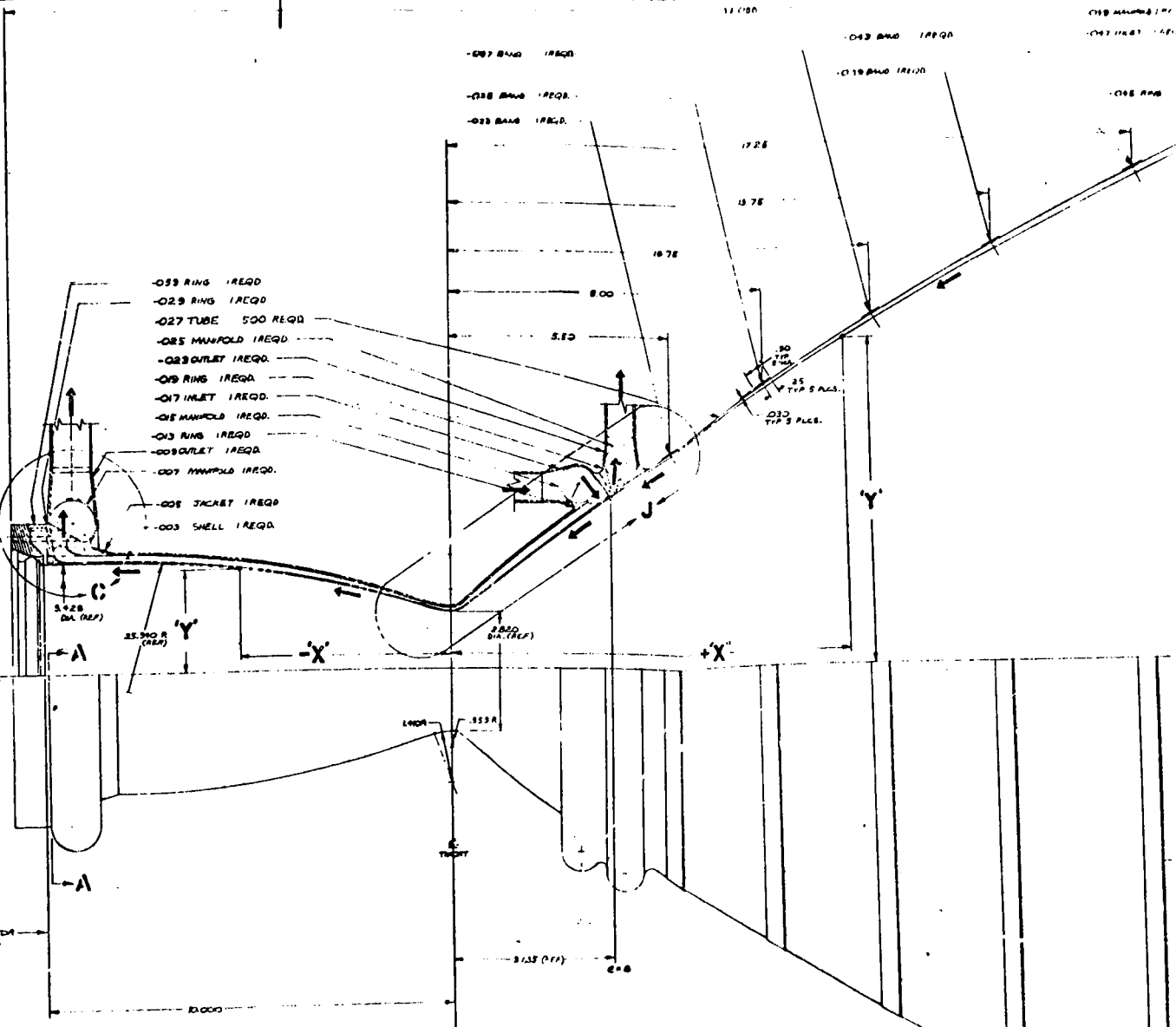
8 00

5 50

30
120
25
TYP 5 PLS.

033
TYP 3 PLS.

- 023 RING 1REQD
- 029 RING 1REQD
- 027 TUBE 500 REQD
- 025 MANIFOLD 1REQD
- 028 OUTLET 1REQD
- 018 RING 1REQD
- 017 INLET 1REQD
- 015 MANIFOLD 1REQD
- 013 RING 1REQD
- 008 OUTLET 1REQD
- 007 MANIFOLD 1REQD
- 006 TACKET 1REQD
- 003 SHELL 1REQD



FOLDOUT FRAME

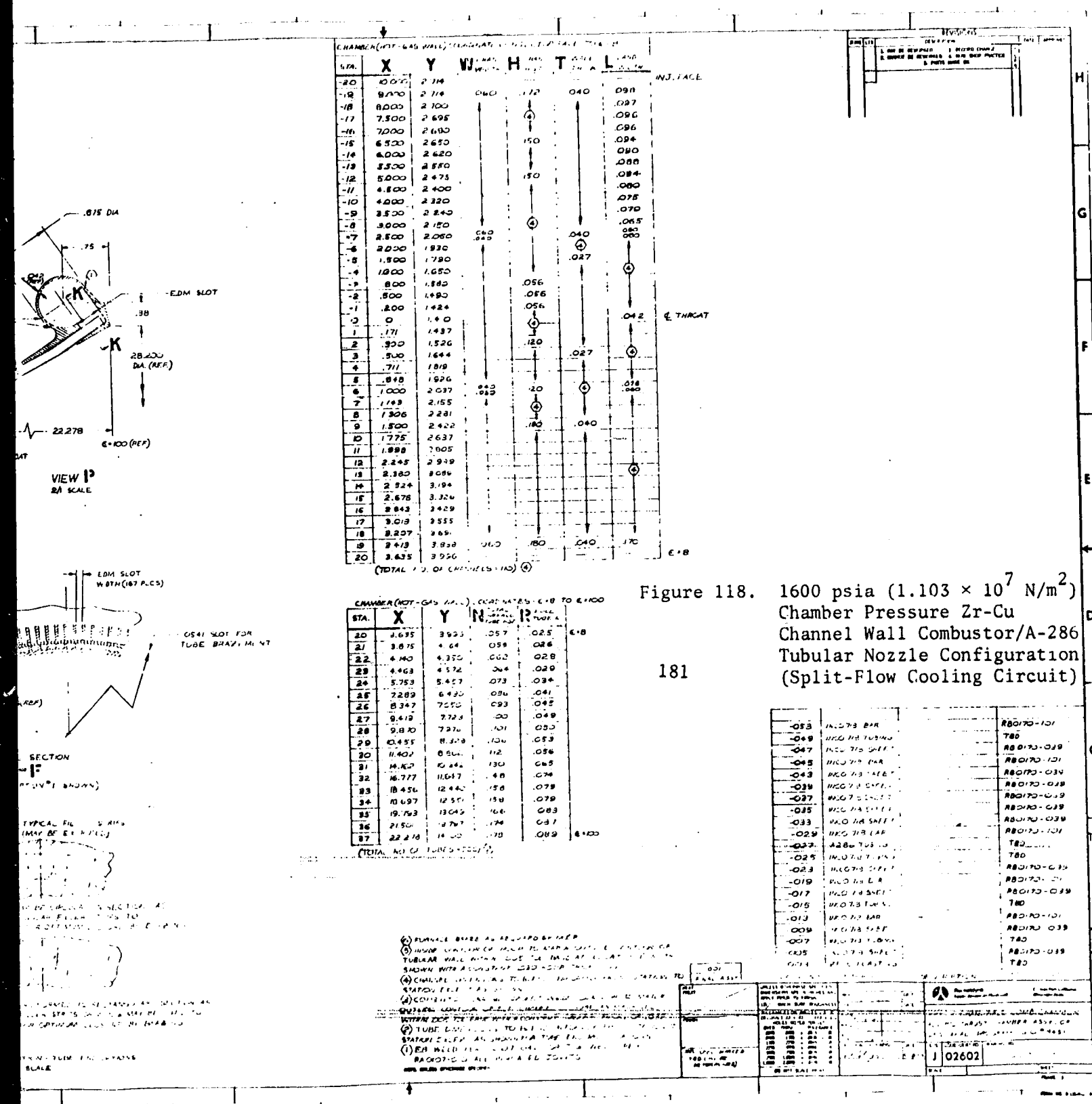
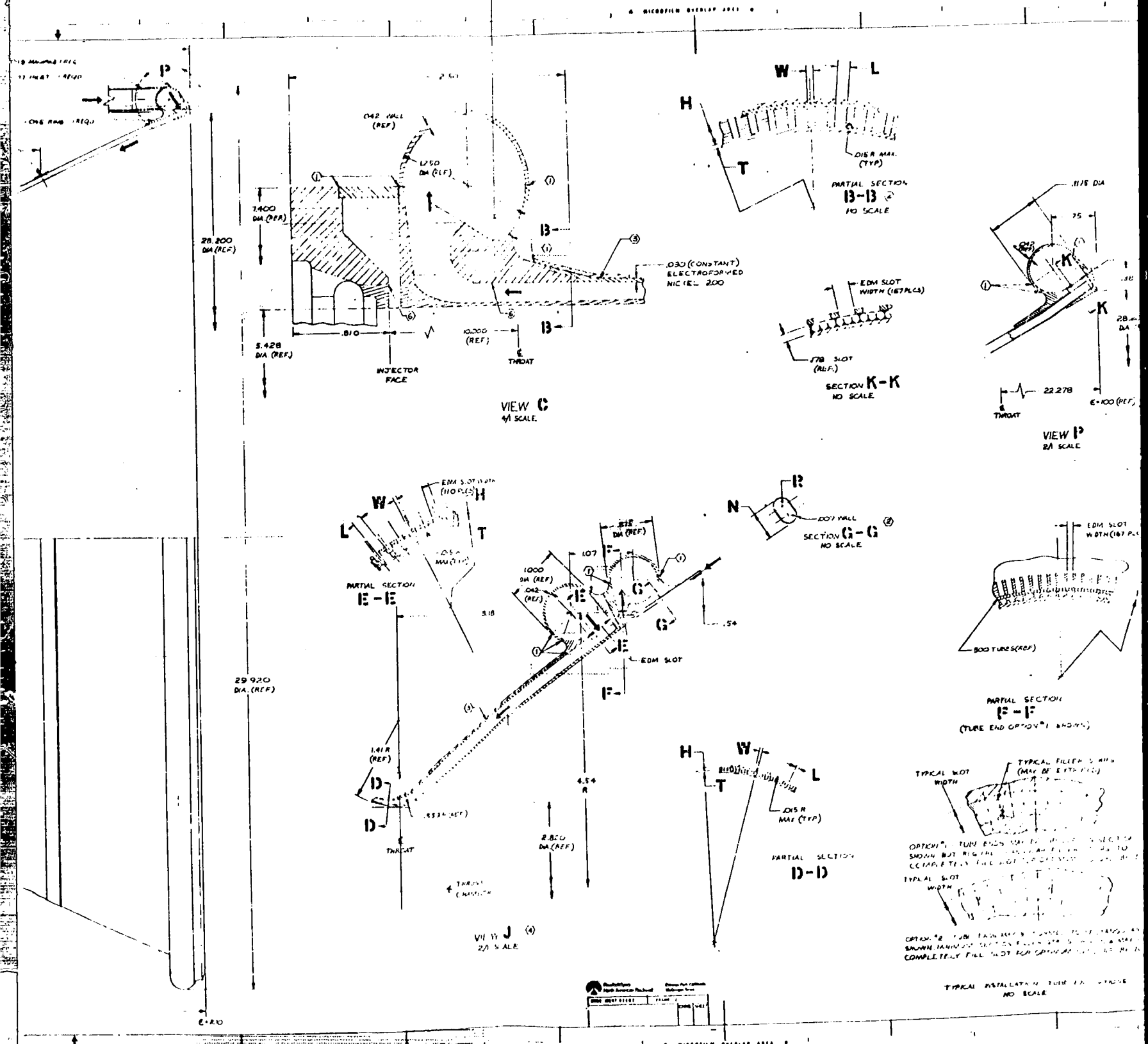


Figure 118. 1600 psia ($1.103 \times 10^7 \text{ N/m}^2$) Chamber Pressure Zr-Cu Channel Wall Combustor/A-286 Tubular Nozzle Configuration (Split-Flow Cooling Circuit)

WALLET BOARD

FOLDOUT FRAME

4/

Coolant Circuit: Split-Flow
 Tube Material: A-286
 Tube Wall Thickness: 0.007-Inch (0.01778 CM)
 Number of Tubes: 540
 Coolant Inlet: $\epsilon = 100$
 Combustor-Nozzle Joint: $\epsilon = 9.5$

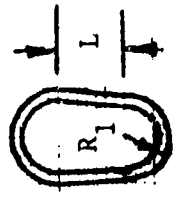
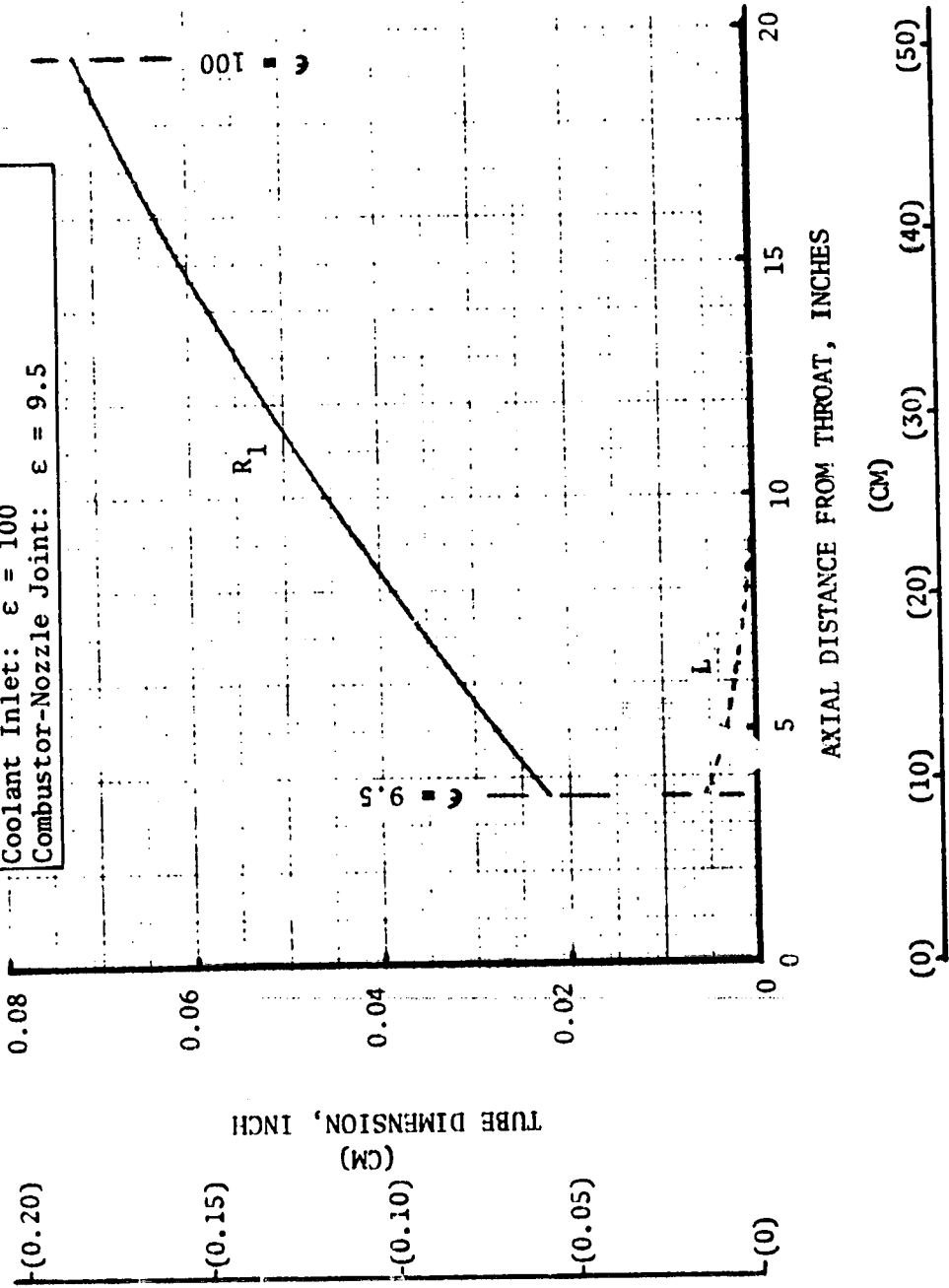


Figure 119. A-286 Nozzle Tube Dimensions ($P_c = 2100$ psia or 1.448×10^7 N/m², $MR_{T/C} = 6.5$)

Coolant Circuit: Split-Flow
 Coolant Inlet: $\epsilon = 100$

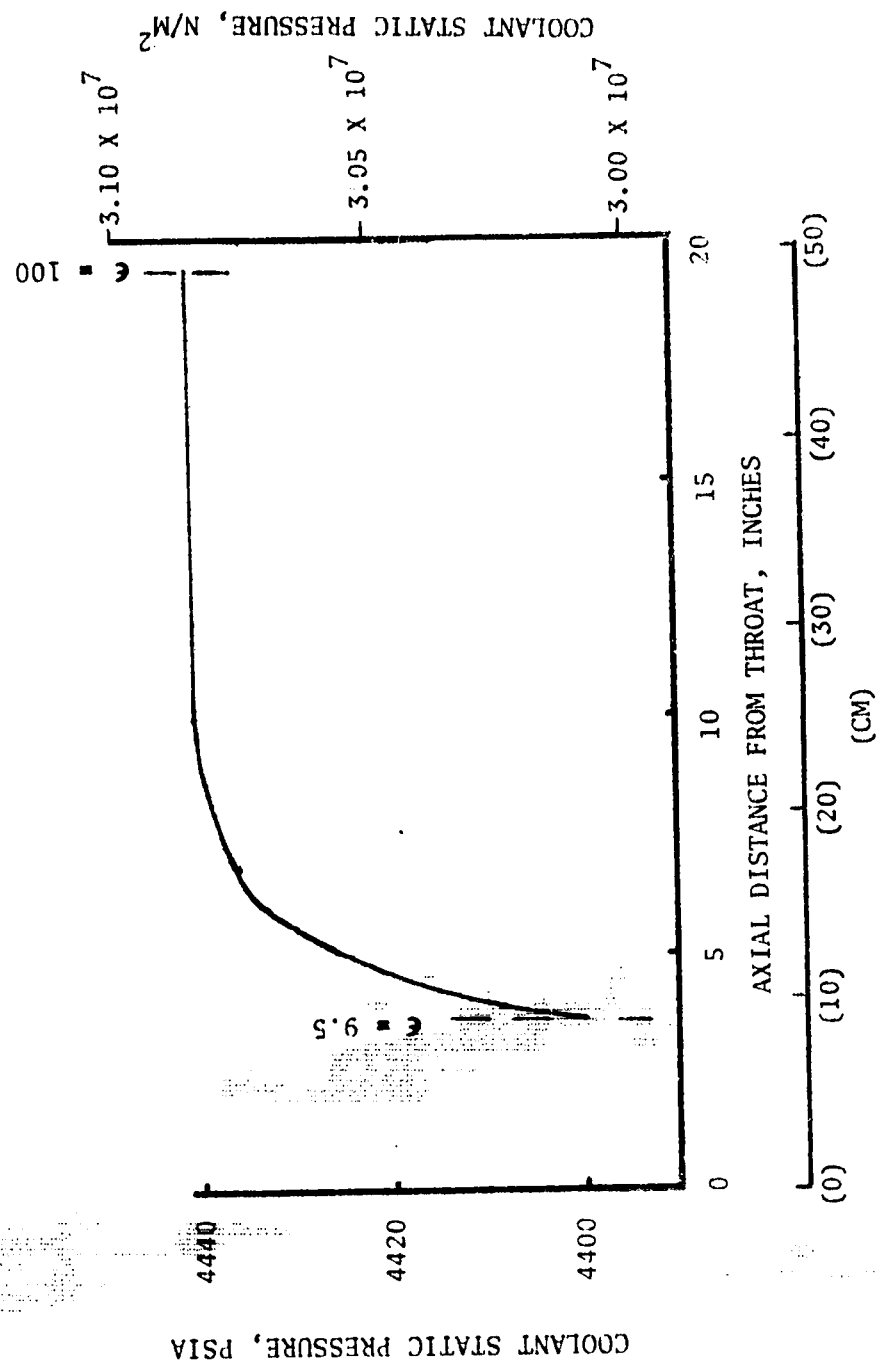


Figure 120. Nozzle Coolant Static Pressure Distribution ($P_c = 2100$ psia or 1.448×10^7 N/m², $MR_{T/C} = 6.5$)

Coolant Circuit: Split-Flow
 Tube Material: A-286
 Tube Wall Thickness: 0.007-Inch (0.01778-CM)
 Number of Tubes: 540
 Coolant Inlet: $\epsilon = 100$
 Combustor-Nozzle Joint: $\epsilon = 9.5$

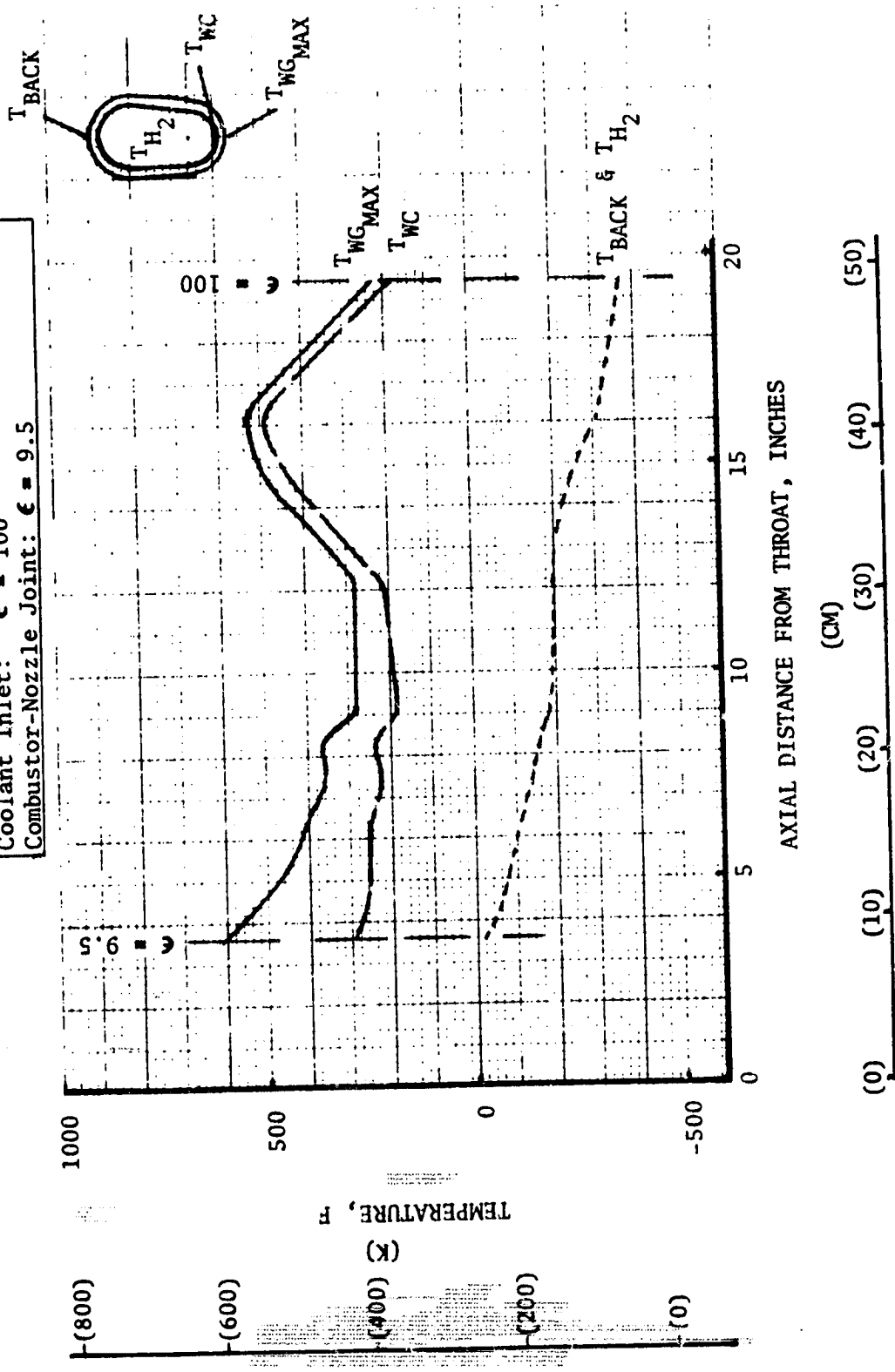


Figure 121. A-286 Nozzle Temperature Distributions ($P_c = 2100$ psia or 1.448×10^7 N/m², $MR_{T/C} = 6.5$)

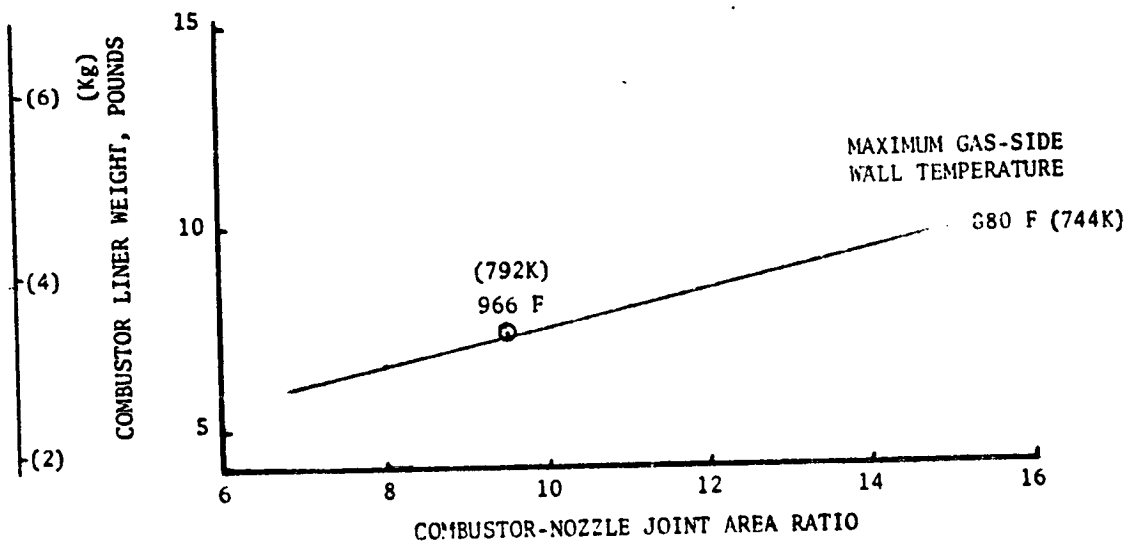
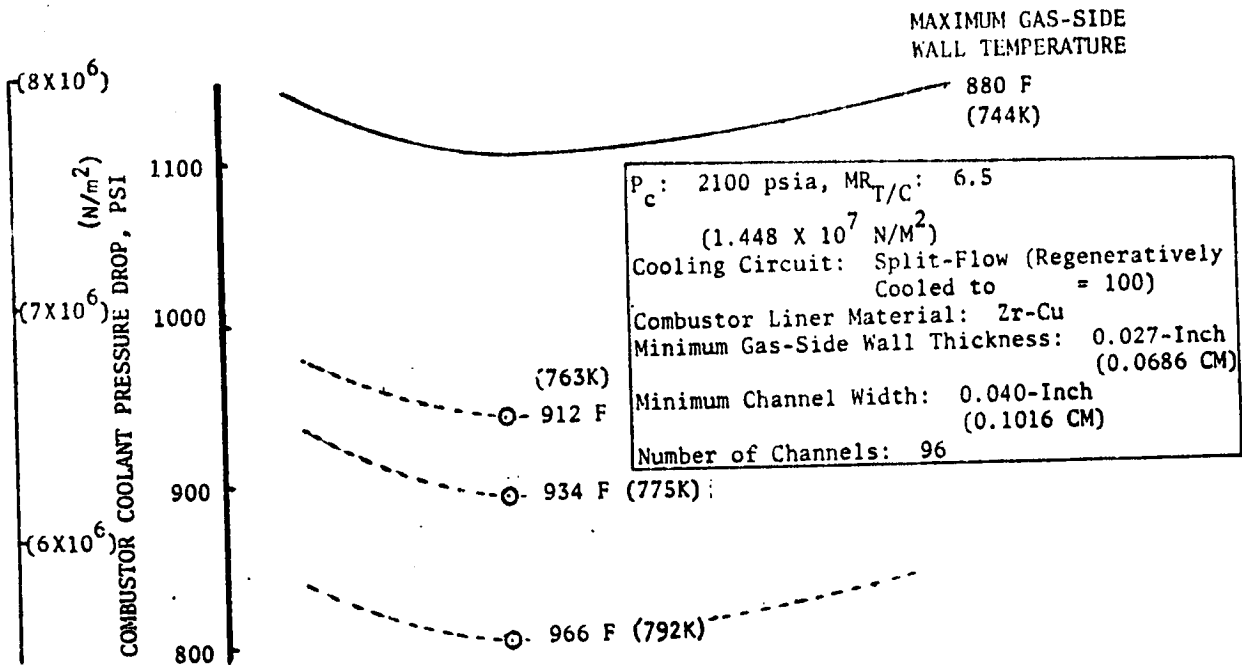


Figure 122. Combustor Coolant Pressure Drop and Liner Weight Variation With Combustor-Nozzle Joint Area Ratio ($p_c = 2100$ psia or $1.448 \times 10^7 \text{ N/m}^2$, $MR_{T/C} = 6.5$, 300 Cycle Life)

TABLE XXIV. 2100 PSIA ($1.448 \times 10^7 \text{ N/m}^2$) CHAMBER PRESSURE
THRUST CHAMBER STRESS/CYCLE LIFE RESULTS

Cycle Life: 300 Cycles

MR_{T/C}: 6.5

Combustor Liner Material: Zr-Cu

Critical Location: X = -0.5-Inch (-1.27 cm)

Channel Width, (inch)	Gas-Side Wall Thickness, (inch)	Coolant Pressure, (psia)	Max Gas-Side Wall Temp, (F)	$1.2 \epsilon_f^i$, (in/in)	N_f	θ_f	θ_c	$4 (\theta_f + \theta_c)$	Yield Safety Factor
0.04 (0.1016 cm)	0.027 (0.0686 cm)	4113 (2.835×10^7 N/m ²)	882 (746 K)	0.0216	1250	0.24	10^{-4}	0.96	1.29
		4090 (2.82×10^7 N/m ²)	882 (746 K)	0.0216	1250	0.24	10^{-4}	0.96	1.30
		4235 (2.92×10^7 N/m ²)	879 (744 K)	0.0214	1240	0.242	10^{-4}	0.968	1.25
0.04 (0.1016 cm)	0.027 (0.0686 cm)	4091 (2.82×10^7 N/m ²)	934 (770 K)	0.0226	1120	0.268	10^{-4}	1.072	1.24
0.04 (0.1016 cm)	0.027 (0.0686 cm)	4091 (2.82×10^7 N/m ²)	934 (770 K)	0.022	1200	0.25	10^{-4}	1.0	1.24

Modified Simplified Stress/Cycle Life Analysis

Finite Element Stress Analyses

The 1.2 factor only applies to values computed using the modified simplified stress/cycle life analysis

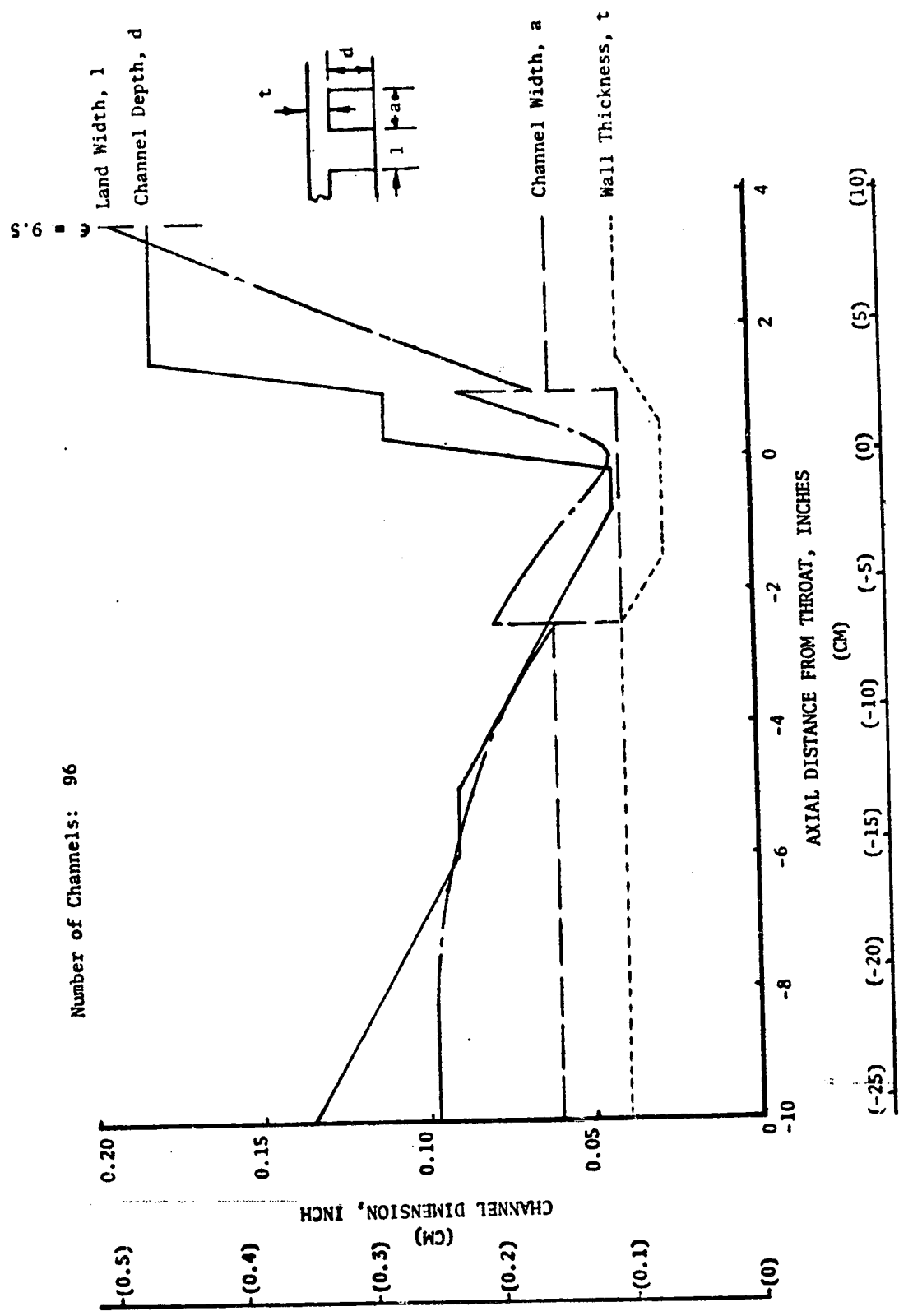


Figure 123. Zr-Cu Combustor Channel Dimensions ($P_c = 2100$ psia or 1.448×10^7 N/m², $MR_{T/C} = 6.5$, 300 Cycle Life)

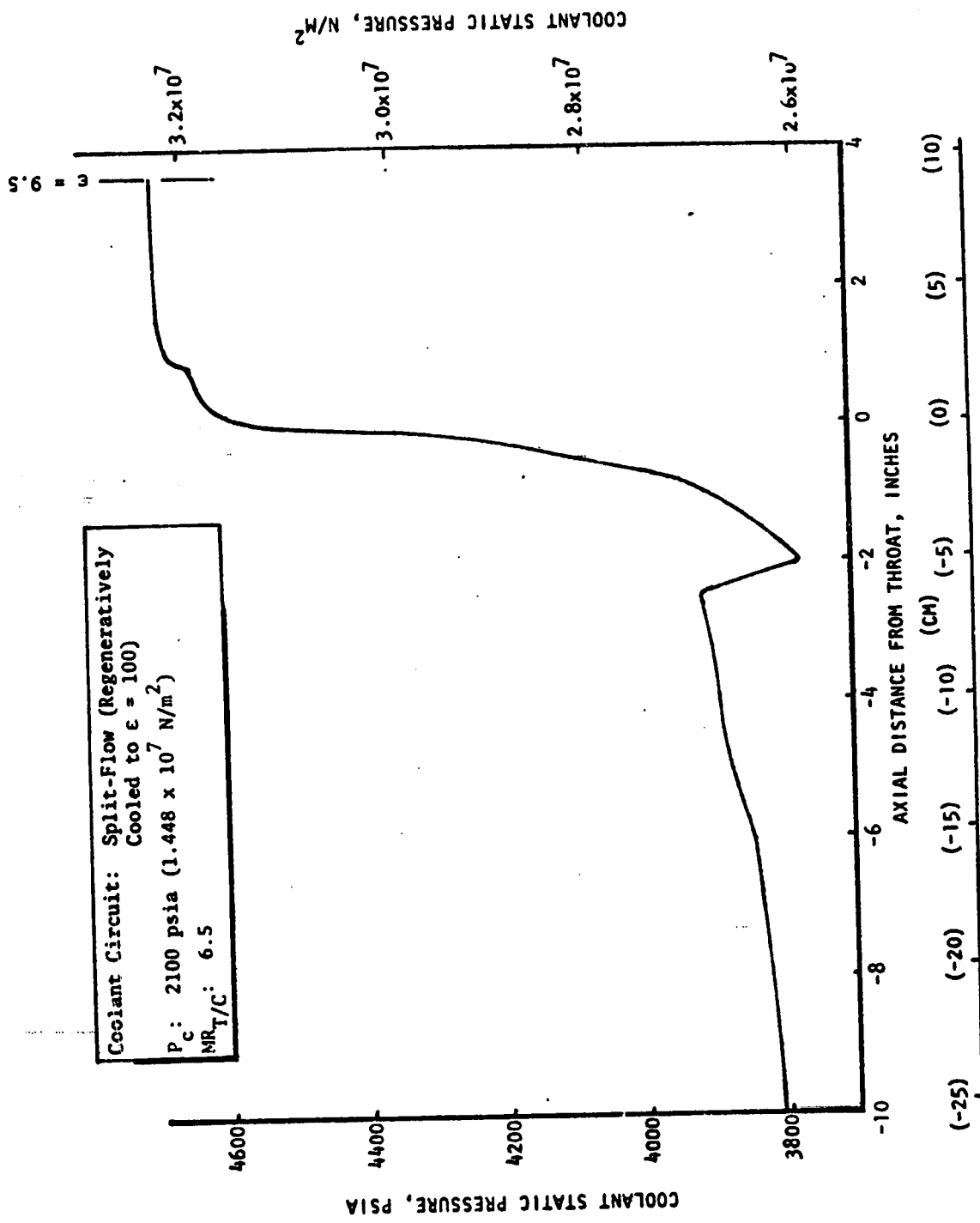


Figure 124. Zr-Cu Combustor Coolant Static Pressure Distribution ($P_c = 2100$ psia or 1.448×10^7 N/m², $MR_{T/C} = 6.5$, 300 Cycle Life)

P_c : 2100 psia, $MR_{T/C}$: 6.5
 $(1.448 \times 10^7 \text{ N/M}^2)$
 Coolant Circuit: Split-Flow (Regeneratively Cooled to ≈ 100)
 Combustor Liner Material: Zr-Cu
 Number of Channels: 96

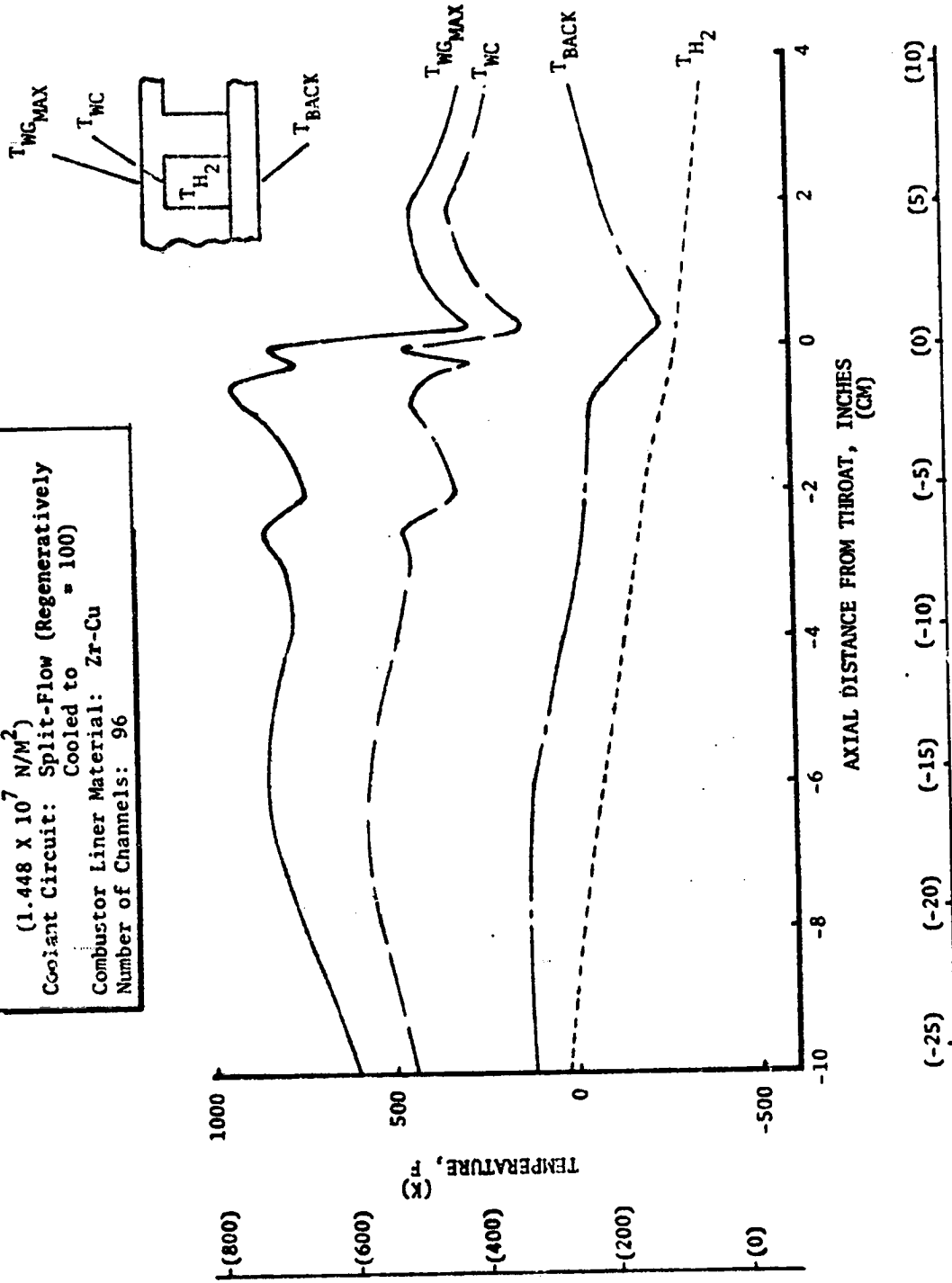
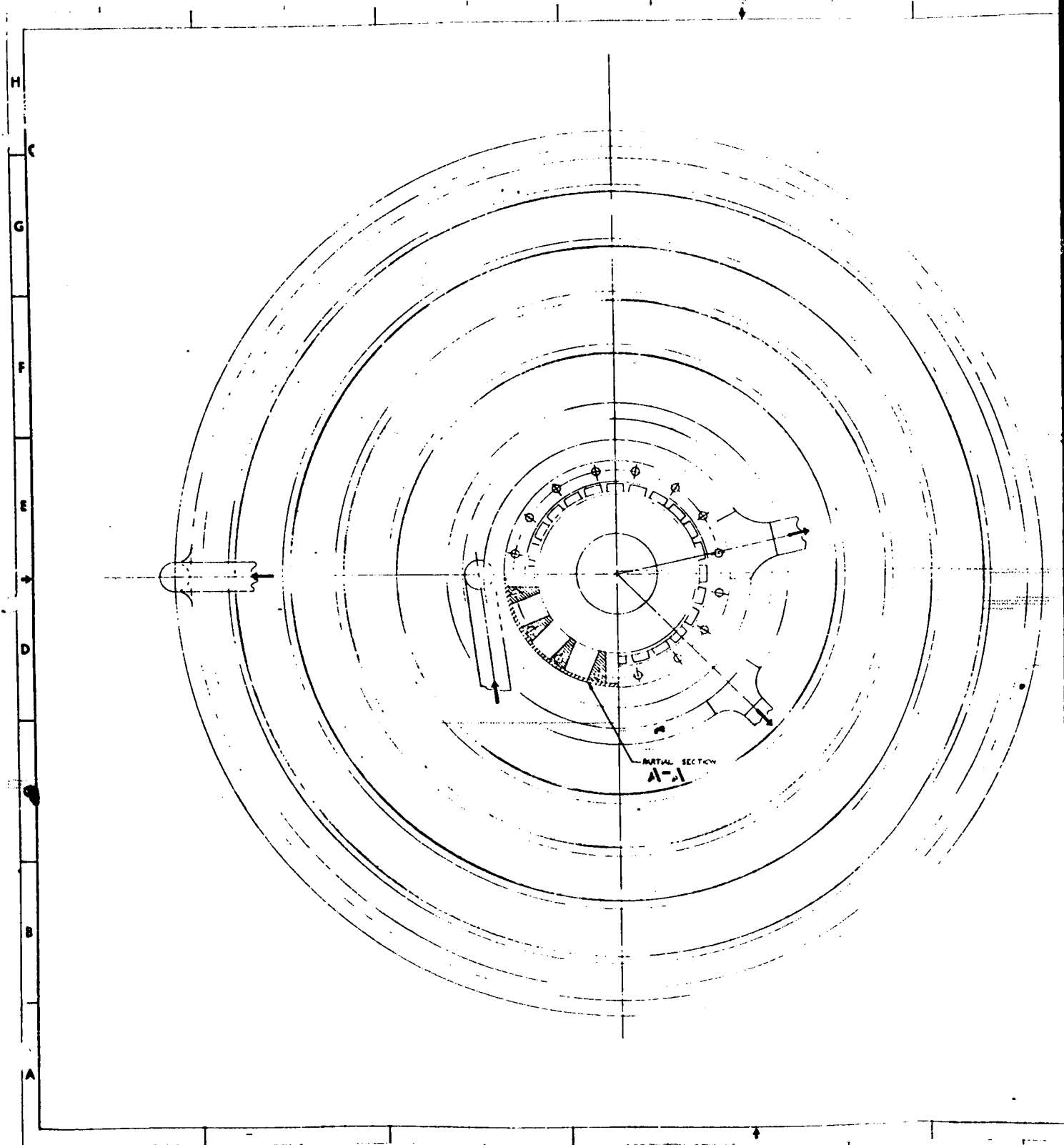
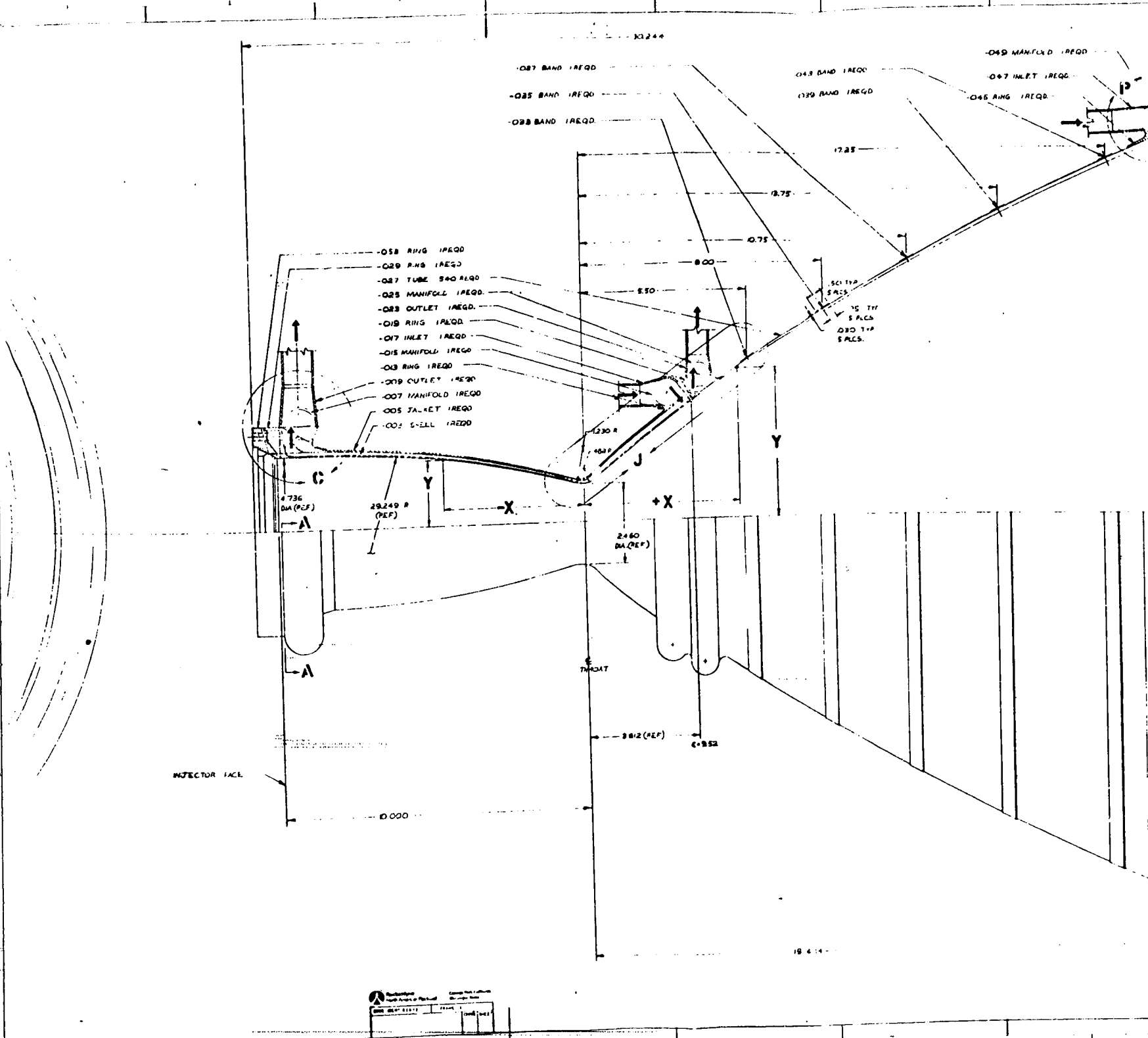


Figure 125. Zr-Cu Combustor Wall Temperature Distribution ($P_c = 2100$ psia or $1.448 \times 10^7 \text{ N/m}^2$, $MR_{T/C} = 6.5$, 300 Cycle Life).

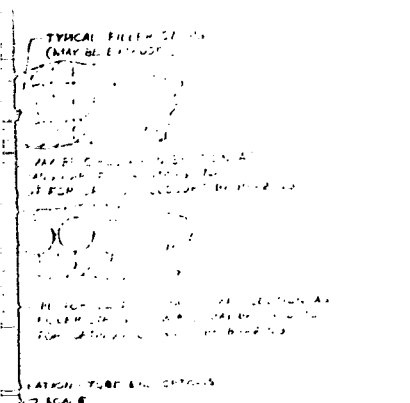
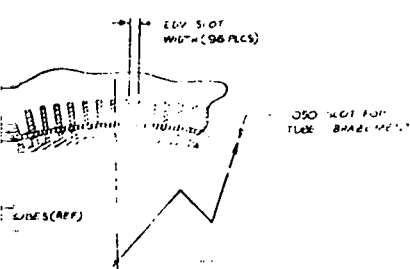
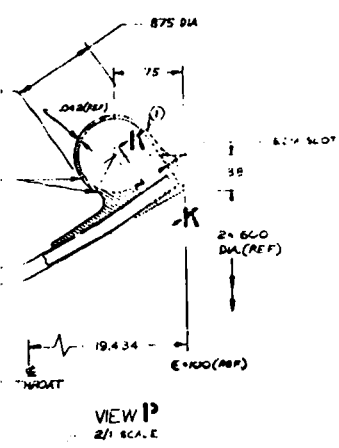


FOLDOUT FRAME



Part No.	REV	DATE	BY	CHKD
100-100000	1	10/1/50	J. H. B.	J. H. B.

FOLDOUT FRAME



CHAMBER (NOT-SAW WALL) COOLING SYSTEM

STA	X	Y	W	H	T	L	INT. FACE
20	0.000	2.261					09A
19	0.000	2.262					097
18	0.000	2.267					096
17	7.000	2.350					096
16	7.000	2.385					094
15	6.500	2.385					088
14	6.000	2.270			090		085
13	5.000	2.238			090		086
12	5.000	2.180			090		082
11	4.000	2.130					078
10	4.000	2.070					072
9	3.000	1.980					065
8	3.000	1.880					062
7	3.000	1.780			040	040	050
6	2.000	1.680			040	040	040
5	1.500	1.570			040	040	040
4	1.000	1.450			040	040	040
3	0.500	1.320			040	040	040
2	0.000	1.180			040	040	040
1	0.000	1.030			040	040	040
0	0.000	0.880			040	040	040
1	1.066	1.272					042
2	3.000	1.440			040	040	040
3	5.000	1.690			040	040	040
4	7.000	1.990			040	040	040
5	8.640	2.260			040	040	040
6	1.000	2.527			040	040	040
7	1.000	2.796			040	040	040
8	1.500	3.065			040	040	040
9	2.000	3.334			040	040	040
10	2.500	3.603			040	040	040
11	3.000	3.872			040	040	040
12	3.500	4.141			040	040	040
13	4.000	4.410			040	040	040
14	4.500	4.679			040	040	040
15	5.000	4.948			040	040	040
16	5.500	5.217			040	040	040
17	6.000	5.486			040	040	040
18	6.500	5.755			040	040	040
19	7.000	6.024			040	040	040
20	7.500	6.293			040	040	040

(TOTAL NO. OF CHANNELS = 96) (1)

Figure 126. 2100 psia (1.448×10^7 N/m²) Chamber Pressure Zr-Cu Channel Wall Combustor/A-286 Tubular Nozzle Configuration (Split-Flow Cooling Circuit)

CHAMBER (NOT-SAW WALL) COOLING SYSTEM

STA	X	Y	N	R	L	INT. FACE
20	0.000	2.795	040	040	040	040
21	3.893	2.890	040	040	040	040
22	5.000	4.740	050	050	050	050
23	6.358	5.600	060	060	060	060
24	7.282	6.450	070	070	070	070
25	8.206	6.797	070	070	070	070
26	8.600	6.950	080	080	080	080
27	9.121	7.265	080	080	080	080
28	9.547	7.731	080	080	080	080
29	10.358	8.020	090	090	090	090
30	11.635	8.460	090	090	090	090
31	12.500	8.740	100	100	100	100
32	13.500	9.040	100	100	100	100
33	14.266	9.330	110	110	110	110
34	15.716	9.710	110	110	110	110
35	16.400	10.000	120	120	120	120

(TOTAL NO. OF CHANNELS = 96) (2)

085	WCO 78 BAR	ABO70-101
086	WCO 78 BAR	ABO70-101
087	WCO 78 TUBING	T80
088	WCO 78 TUBING	ABO70-029
089	WCO 78 SHEET	ABO70-101
090	WCO 78 BAR	ABO70-029
091	WCO 78 SHEET	ABO70-029
092	WCO 78 SHEET	ABO70-029
093	WCO 78 SHEET	ABO70-029
094	WCO 78 SHEET	ABO70-029
095	WCO 78 SHEET	ABO70-029
096	WCO 78 SHEET	ABO70-029
097	WCO 78 SHEET	ABO70-029
098	WCO 78 SHEET	ABO70-029
099	WCO 78 SHEET	ABO70-029
100	WCO 78 SHEET	ABO70-029
101	WCO 78 SHEET	ABO70-029
102	WCO 78 SHEET	ABO70-029
103	WCO 78 SHEET	ABO70-029
104	WCO 78 SHEET	ABO70-029
105	WCO 78 SHEET	ABO70-029
106	WCO 78 SHEET	ABO70-029
107	WCO 78 SHEET	ABO70-029
108	WCO 78 SHEET	ABO70-029
109	WCO 78 SHEET	ABO70-029
110	WCO 78 SHEET	ABO70-029
111	WCO 78 SHEET	ABO70-029
112	WCO 78 SHEET	ABO70-029
113	WCO 78 SHEET	ABO70-029
114	WCO 78 SHEET	ABO70-029
115	WCO 78 SHEET	ABO70-029
116	WCO 78 SHEET	ABO70-029
117	WCO 78 SHEET	ABO70-029
118	WCO 78 SHEET	ABO70-029
119	WCO 78 SHEET	ABO70-029
120	WCO 78 SHEET	ABO70-029

- ① FINISH AS SHOWN BY SPEC.
- ② AS SHOWN BY SPEC. WITH TOLERANCES AS SHOWN BY SPEC.
- ③ TUBE VENTS AS SHOWN BY SPEC. WITH TOLERANCES AS SHOWN BY SPEC.
- ④ WELD AS SHOWN BY SPEC. WITH TOLERANCES AS SHOWN BY SPEC.
- ⑤ ADDITIONAL NOTES AS SHOWN BY SPEC.

02602

Chamber Pressure Perturbation Summary

As shown in Table XXV, the combustor coolant pressure drop is approximately proportional to the chamber pressure, and the combined liner and tube weight decreased with increase in chamber pressure. From a general thermal durability standpoint, the three chamber pressure designs are comparable with maximum wall temperatures ranging from 879 F (744 K) to 934 F (775 K) and also, from a fabrication standpoint, no significant difference resulted, since the number of nozzle tubes, number combustor channels, and the minimum channel size are approximately the same.

TABLE XXV. CHAMBER PRESSURE PERTURBATION SUMMARY

F: 20,000 Pounds (8.896×10^4 Newtons)
 Cycle Life: 300
 Cooling Circuit: Split-Flow (Regeneratively Cooled to $\epsilon = 100$)
 ϵ : 400-to-1, $MR_{T/C}$: 6.5

Component	Chamber Pressure, psia	$1600.7 \times 10^7 \text{ N/m}^2$ ($1.103 \times 10^7 \text{ N/m}^2$)	$1900.7 \times 10^7 \text{ N/m}^2$ ($1.31 \times 10^7 \text{ N/m}^2$)	$2100.7 \times 10^7 \text{ N/m}^2$ ($1.448 \times 10^7 \text{ N/m}^2$)
<u>Nozzle</u>				
Number of Tubes		500	525	540
Minimum Unformed Tube Outside Diameter, inch		0.055 (0.1397 cm)	0.05 (0.127 cm)	0.043 (0.122 cm)
Maximum Gas-Side Wall Temperature, F		668 (627 K)	685 (636 K)	608 (593 K)
<u>Combustor</u>				
Number of Channels		110	100	96
Minimum Channel Dimensions:				
Width, inch		0.04 (0.1016 cm)	0.04 (0.1016 cm)	0.04 (0.1016 cm)
Height, inch		0.056 (0.1423 cm)	0.045 (0.1143 cm)	0.042 (0.1068 cm)
Land, inch		0.0427 (0.1084 cm)	0.0427 (0.1084 cm)	0.0423 (0.1075 cm)
Combustor-Nozzle Joint Area Ratio		8	8	9.5
Minimum Hot-Gas Wall Thickness, inch		0.027 (0.0686 cm)	0.027 (0.0686 cm)	0.027 (0.0686 cm)
Maximum Gas-Side Wall Temperature, F		879 (744 K)	900 (756 K)	934 (775 K)
Critical Location Stress and Life Parameters:				
Yield Safety Factor		1.57	1.42	1.24
Ultimate Safety Factor		2.46	2.05	1.91
Damage Fraction ($4(\phi_c + \theta_c)$)		$4(1 \times 10^{-4} + 0.25) = 1.00$	$4(0.001 + 0.249) = 1.00$	$4(1 \times 10^{-4} + 0.25) = 1.00$
<u>Chamber</u>				
Combustor Coolant Pressure Drop, psi		338 ($2.33 \times 10^6 \text{ N/m}^2$)	608 ($4.19 \times 10^6 \text{ N/m}^2$)	895 ($6.15 \times 10^6 \text{ N/m}^2$)
Nozzle Coolant Pressure Drop, psi		25 ($1.724 \times 10^5 \text{ N/m}^2$)	36 ($2.485 \times 10^5 \text{ N/m}^2$)	41 ($2.85 \times 10^5 \text{ N/m}^2$)
Combustor Liner and Nozzle Tube Weight, lb		17.0 (7.72 kg)	14.0 (6.35 kg)	13.0 (5.9 kg)

TASK IV: COMPUTER PROGRAMMING

Computer program modifications and improvements (Task IV) made to the regenerative cooling design/analysis computer program were performed in parallel to the analysis tasks (Task I, II, and III). This was accomplished to ensure that normally encountered computer programming, checkout, sample test case, and operational case run phases would not interfere, but rather supplement the analysis effort. Modifications and improvements made to the program during this contract included:

1. An improved two-dimensional tube or channel thermal model.
2. Transient analysis capability using a quasi two-dimensional thermal solution.
3. Simplified stress and cycle life analysis method. This method is presented in Appendix A.
4. Capability of using two separate roughness values for heat transfer and pressure drop calculations.
5. Option to determine the influence of tube or channel tolerance.
6. Option for a perfect gas coolant requiring only the specific heat ratio, molecular weight, and viscosity.
7. Capability of reading in nozzle contour cards punched out by a design program.
8. Option for evaluating the coolant enhancement factor using an equation developed for hydrogen.

The modified regenerative cooling design/analysis computer program with operational manuals was submitted to NASA-LeRC separately. Also the Rocketdyne finite element computer program and three copies of the appropriate manual were submitted.

APPENDIX A

STRESS AND LIFE CYCLE EVALUATION

Life evaluation consists of assessing the accumulation of damage to material as cycles of operation occur. The length of time under load as well as repetitions of load are evaluated.

Cyclic influence is evaluated by using the materials fatigue properties. Length of time under load is evaluated by using the materials stress rupture properties. Damage to the material is expressed in terms of the fractional part of a materials capability that is used in order to satisfy the service requirements.

The formulation of a life equation is dependent on safety factor policy and failure definition. A safety factor of 4 and typical materials properties are used in the life equation and failure of the hot wall or thrust chamber liner is said to have occurred when a leaking crack appears. This definition of failure for the hot wall does not ordinarily result in failure of the thrust chamber, because it will usually continue to function normally for many cycles and extensive operating time after a leaking crack appears.

FATIGUE PROPERTIES

The property of concern is the materials thermal fatigue capability. This may be evaluated in various ways:

1. Universal Slopes Equation
2. Isothermal fatigue test data
3. Thermal fatigue test data
4. Hardware operating data

Isothermal fatigue tests have been conducted at Rocketdyne on NARloy-Z and zirconium copper. The test temperature range was from 70 to 1200 F.

Figure 127 and 128 are plots of the typical thermal fatigue capability of these materials in the range of temperatures from 70 to 1200 F.

The Universal Slopes Equation will be used to evaluate thermal fatigue properties of other materials in this program, if test data are not available.

STRESS RUPTURE PROPERTIES

Stress rupture testing has been conducted at Rocketdyne on NARloy-Z and zirconium copper. Both materials were in the condition of being heat treated and aged with no subsequent cold work. This is expected to be the condition of these materials when used as tubes or channels in a thrust chamber wall. The data are plotted in Fig. 129 and 130 and is considered as the typical stress rupture capability. The Larson Miller equation (Ref. 2) was used to extend the range of test data where required.

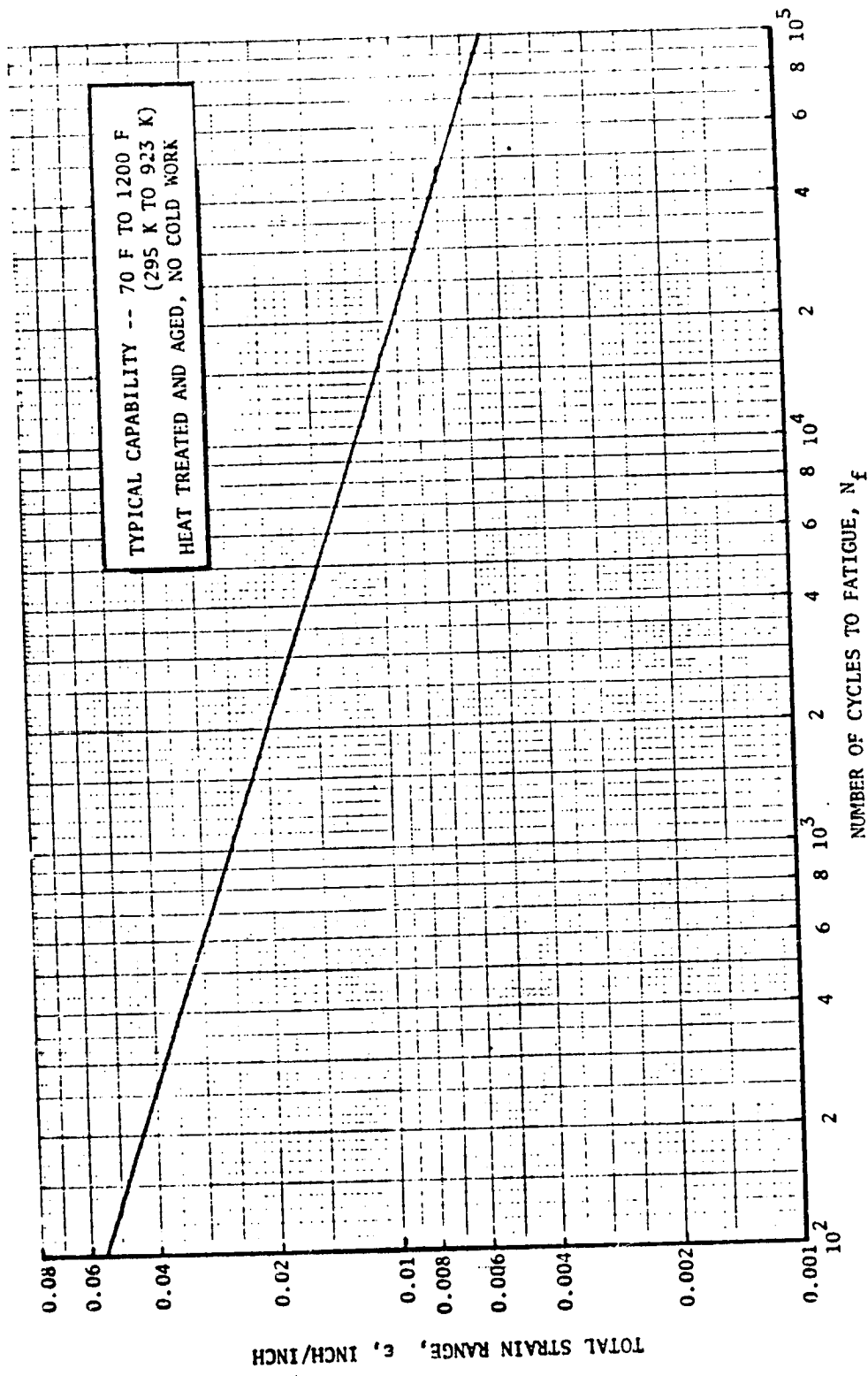


Figure 127. NARloy-Z Thermal Fatigue Life

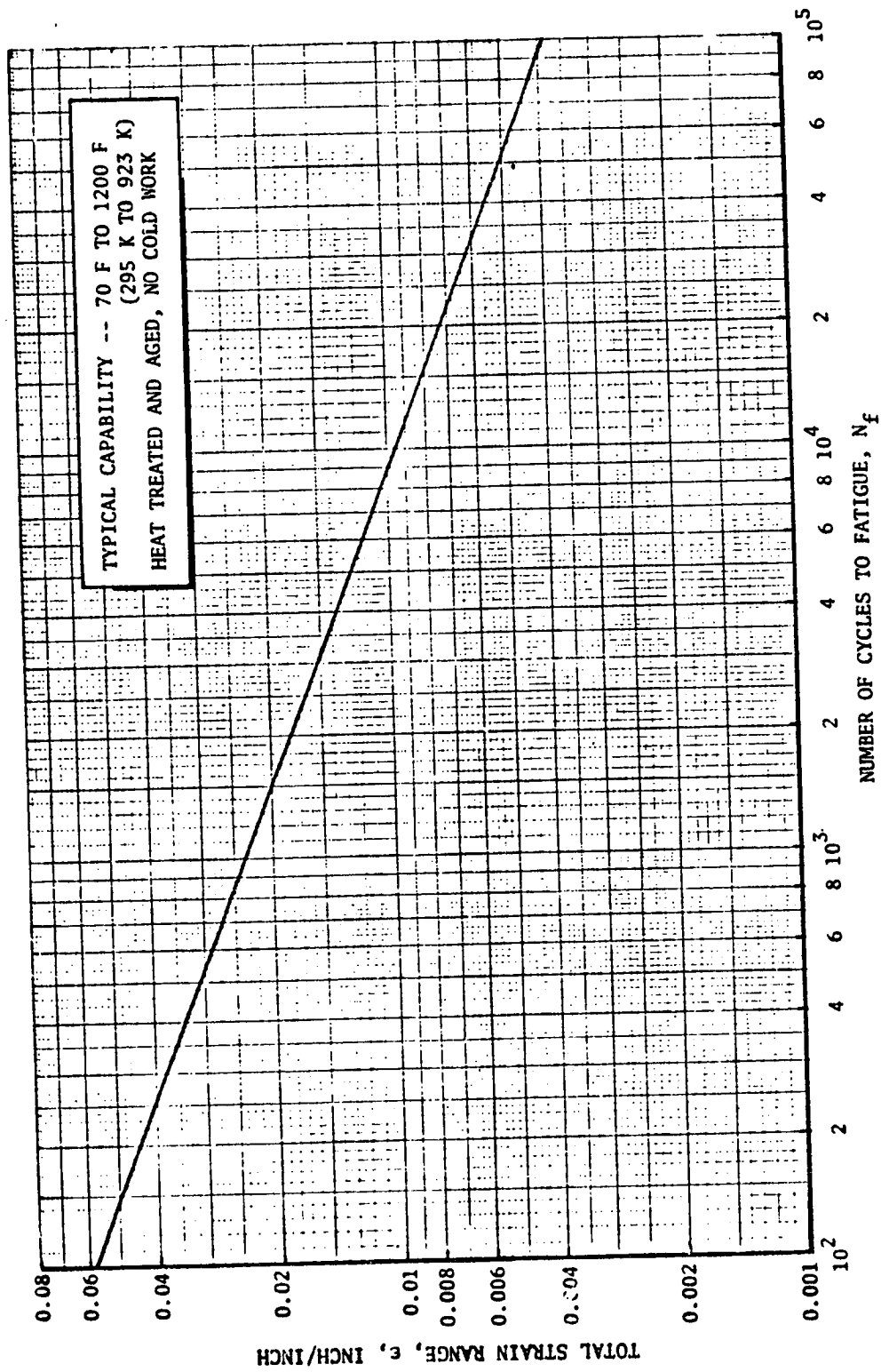


Figure 128. Zirconium-Copper Thermal Fatigue Life

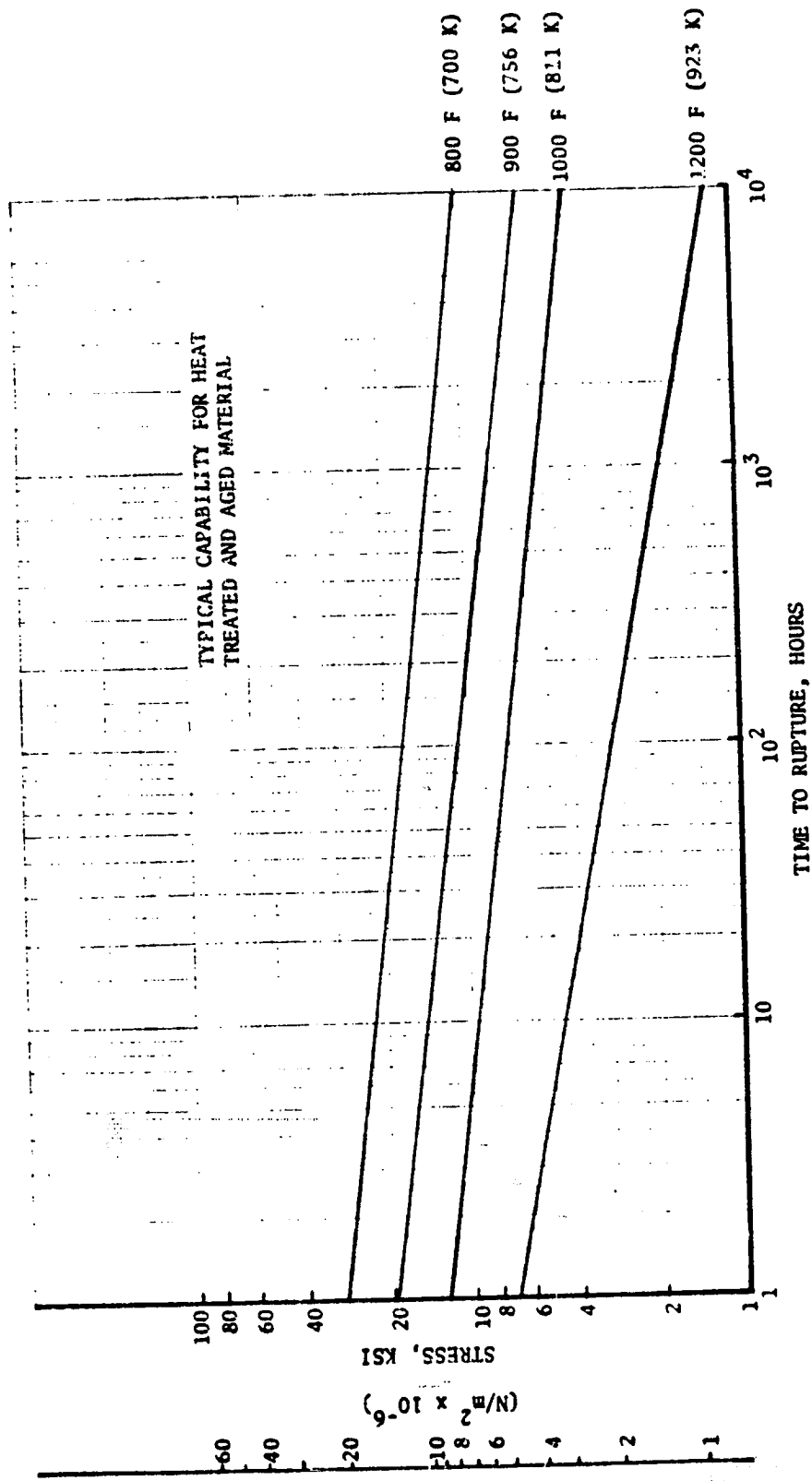


Figure 129. NARloy-Z Stress Rupture

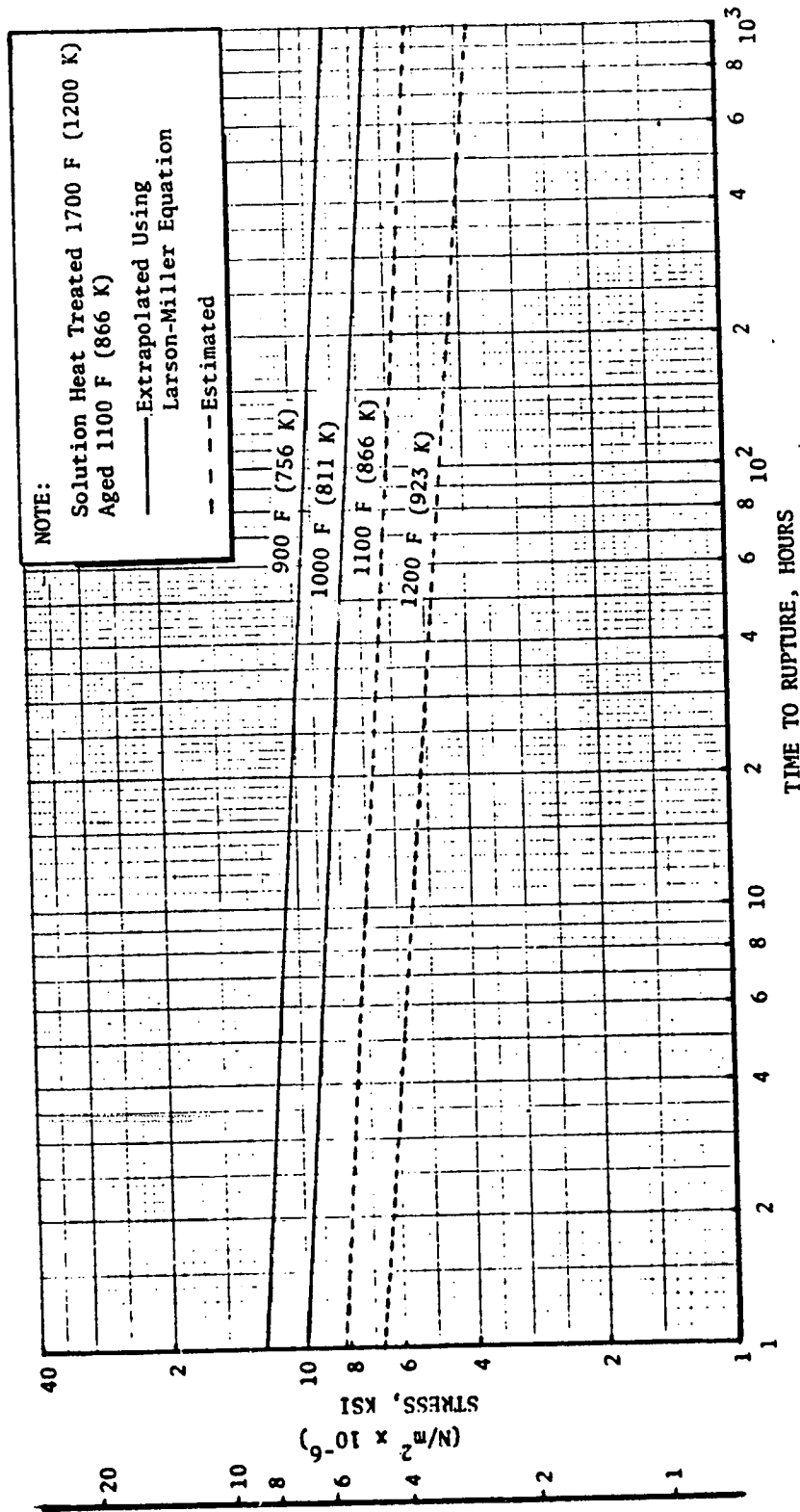


Figure 130. Zirconium-Copper Stress Rupture

Stress rupture data are available for many other materials that may be included in this program.

MATERIAL DAMAGE FRACTIONS

Material damage is expressed in terms of fractions that relate material capability to service requirements. Fatigue damage fraction is:

$$\phi_f = \frac{n}{N_f}$$

where

n = Number of cycles of loading applied

N_f = Number of cycles of loading to cause fatigue failure

Creep damage fraction is:

$$\phi_c = \frac{T}{T_r}$$

where

T = Number of hours load is applied

T_r = Number of hours to produce rupture under the applied load and temperature

LIFE EQUATION

The Life Equation is:

$$4 (\phi_f + \phi_c) \leq 1$$

This equation includes a safety factor of four. It is theorized that the total material damage is $(\phi_f + \phi_c)$. Therefore, when $(\phi_f + \phi_c) = 1$, failure would result.

The definition of failure concerns the condition of the thrust chamber hot wall. Failure of the hot wall is said to have occurred when a leaking crack appears. N_f and T_r are selected in accord with this definition of failure.

It should be noted that the above definition of failure of the hot wall does not in general constitute failure of the thrust chamber. Thrust chambers ordinarily will function satisfactorily for many cycles and a large accumulation of firing time after a leaking crack appears in the hot wall. Ordinarily, no degradation of performance can be detected with numerous leaking cracks.

The life equation described above will be used for all designs and materials in this program.

STRESS AND STRAIN ANALYSIS

Preliminary analysis methods suited to hand computation was used for a major portion of the design study. Finite element stress and strain analysis conducted by electronic digital computer was used for final detailed computations. Preliminary structural computations may be separated into three categories:

1. Stress calculation for basic structural criteria.
2. Stress calculation for determination of creep damage fraction, ϕ_c .
3. Cyclic strain range calculation for determination of fatigue damage fraction, ϕ_f .

Stress and strain analysis is the same for all materials, but differs between tube and channel designs.

Basic Structural Criteria

The following analysis is used for tubes:

$$\sigma = \frac{PR}{t}$$

$$\sigma = \leq \frac{F_{tu}}{1.5}$$

$$\sigma = \leq \frac{F_{ty}}{1.2}$$

where

- σ = Average hoop stress
- P = Coolant pressure
- R = Tube inside radius
- t = 90 percent of nominal tube wall thickness
- F_{tu} = Minimum guaranteed ultimate tensile strength of material at the average steady state operating temperature through the hot wall (Fig. 131 and 132 for Zr-Cu and NARloy-Z)
- F_{ty} = Minimum guaranteed yield tensile strength of material at the average steady state operating temperature through the hot wall (Fig. 131 and 132 for Zr-Cu and NARloy-Z)

The more critical stress, bending or shear, is used to define the structural requirements for channels.

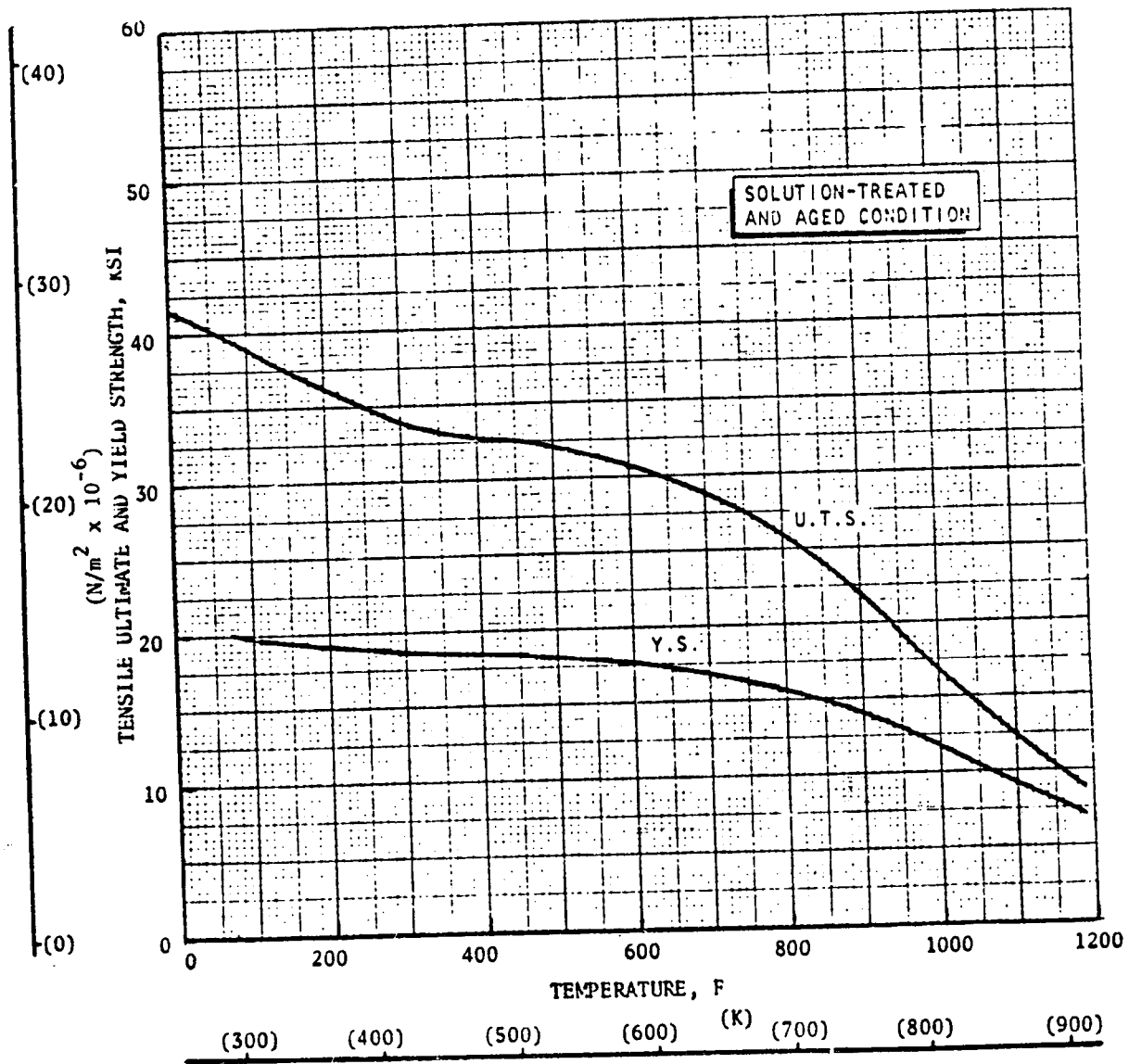


Figure 131. NARloy-Z Yield and Ultimate Strengths

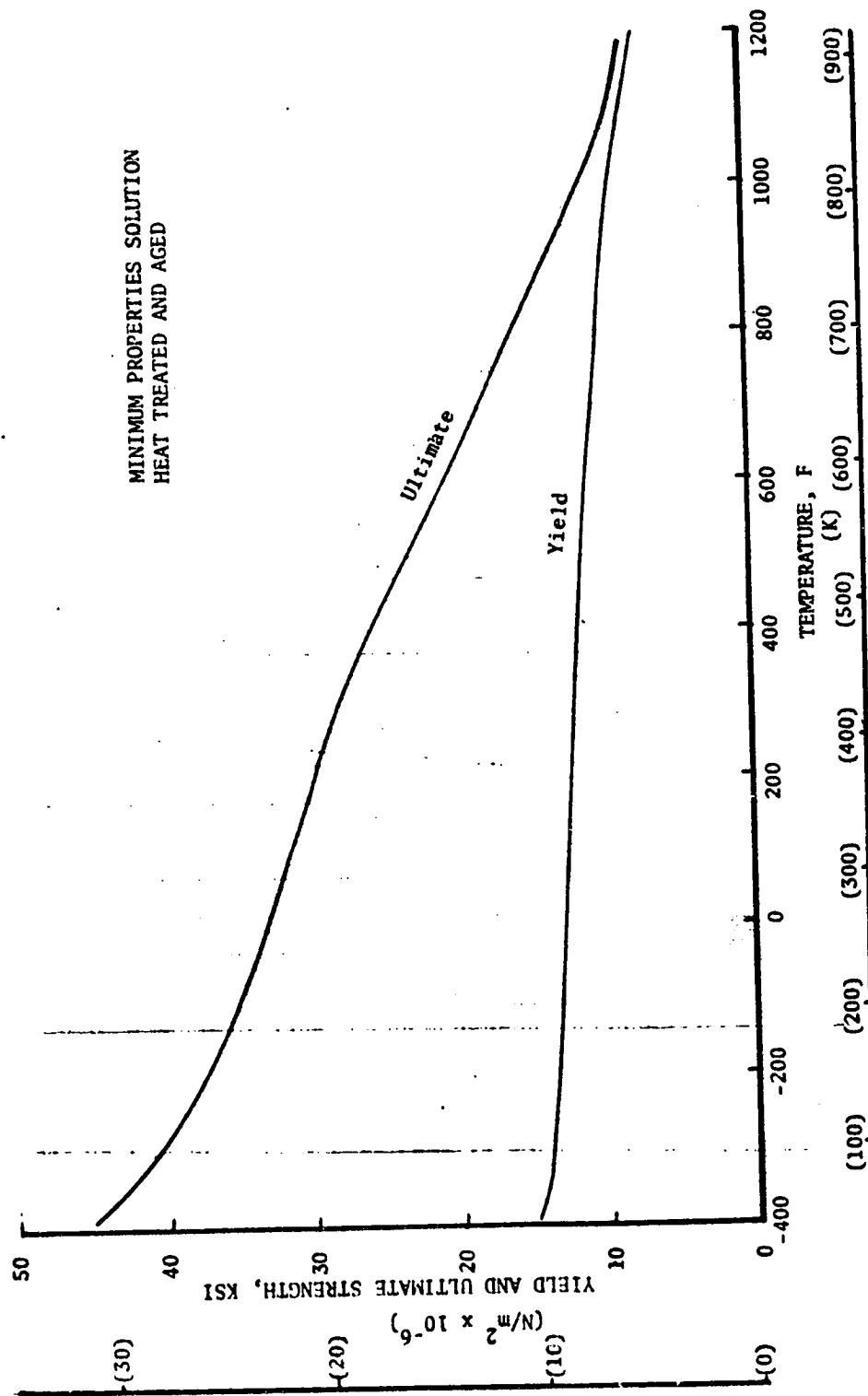


Figure 132. Zirconium-Copper Yield and Ultimate Strengths

Bending Stress

$$\sigma = \frac{Pa^2}{2t^2}$$

$$\sigma \leq \frac{F_{tu}}{1.5}$$

$$\sigma \leq \frac{F_{ty}}{1.2}$$

Shear Stress

$$\tau = \frac{3}{2} \frac{Pa}{2t}$$

$$\tau \leq \frac{0.6 * F_{ty}}{1.2}$$

$$\tau \leq \frac{0.55 * F_{tu}}{1.5}$$

where

σ = Maximum fixed end beam bending stress

τ = Maximum hot wall shear stress

P = Coolant pressure

a = Channel width

t = 90 percent of nominal hot wall thickness spanning the channel

F_{tu} = Same as for tubes

F_{ty} = Same as for tubes

Creep Damage Fraction

The following analysis is used for tubes:

$$\sigma = \frac{\Delta PRK}{t}$$

$$\phi_c = \frac{T}{T_r}$$

where

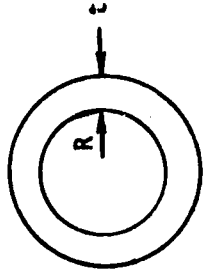
σ = Tube outer diameter hoop stress

P = Coolant pressure minus hot gas pressure

R = Tube inside radius

K = Thick wall tube factor for converting average hoop stress to outer surface stress (Fig. 133)

*In section 1.4.6.3, page 1-11, of MIL-HDBIC-5B, the ratio of the strength in shear to the strength in tension is given as 0.55 for proportional limit. From yield strength test data of common materials (MIL-HDBK-5B) this factor is found to be approximately 0.6. Since no reference was available for the ultimate strength, the 0.55 factor was used.



THICK WALL TUBE HOOP STRESS FACTORS

$$\sigma_{ID} = K_1 \frac{PR}{t} \quad (\text{HOOP STRESS AT INNER DIAMETER})$$

$$\sigma_{OD} = K_2 \frac{PR}{t} \quad (\text{HOOP STRESS AT OUTER DIAMETER})$$

P = INTERNAL PRESSURE

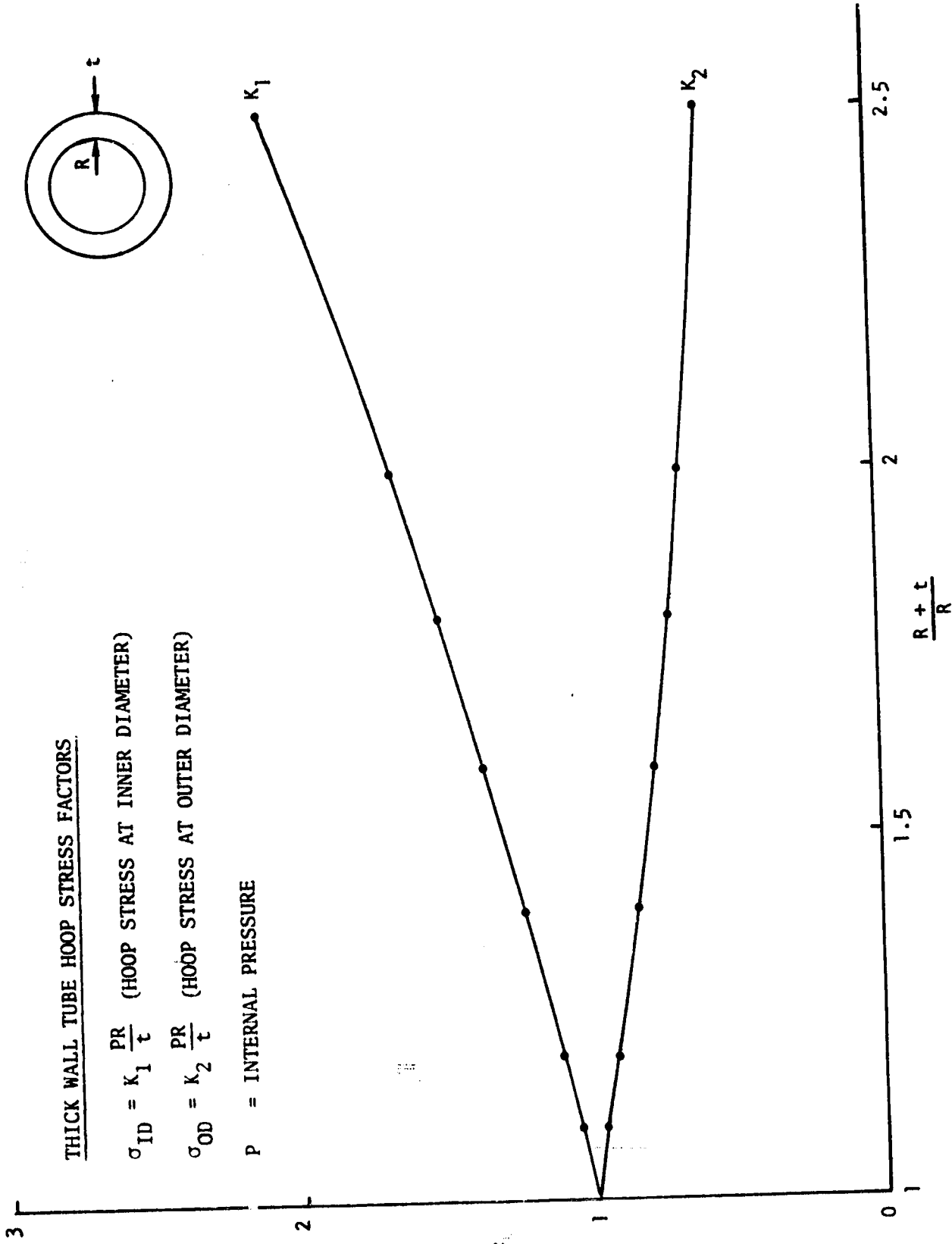


Figure 133. Thick Wall Tube Hoop Stress Factors

- t = 90 percent of nominal tube wall thickness
 T_r = hours to rupture at stress of σ and temperature equal the hot gas face temperature
 T = Hours of firing time

The following analysis is used for channels:

$$\sigma = \frac{\Delta P a^2}{2t^2}$$

$$\phi_c = \frac{T}{T_r}$$

where

- σ = Maximum fixed end beam bending stress
 ΔP = Coolant pressure minus hot gas pressure
 a = Channel width
 t = 90 percent of nominal hot wall thickness spanning the channel
 T and T_r are same as for tubes

Cyclic Strain Range Calculation

The following analysis is used for tubes:

$$\epsilon_{ai} = \alpha_j (T_{ji} - 70) - \alpha_w (T_{wi} - 70)$$

$$\epsilon_{as} = \alpha_j (T_{js} - 70) - \alpha_w (T_{ws} - 70)$$

$$\epsilon_{atot} = \epsilon_{as} - \epsilon_{ai}$$

$$\epsilon_c = \frac{\alpha_w (T_{wc} - T_{ws})}{2}$$

$$\epsilon_e = 1.155 \sqrt{\epsilon_{atot}^2 + \epsilon_{atot} \epsilon_c + \epsilon_c^2}$$

where

- ϵ_{ai} = Initial hot gas surface axial strain
 ϵ_{as} = Steady state operating hot gas surface axial strain

- ϵ_{atot} = Hot gas surface axial strain range
- ϵ_c = Hot gas surface circumferential strain range
- ϵ_e = Equivalent uniaxial strain range
- α_j = Jacket material coefficient of thermal expansion
- α_w = Tube material coefficient of thermal expansion
- T_{ji} = Initial temperature (F) of jacket
- T_{wi} = Initial temperature (F) of hot gas surface
- T_{js} = Steady state operating temperature (F) of jacket
- T_{ws} = Steady state operating temperature (F) of hot gas surface
- T_{wc} = Hot gas wall coolant side temperature (F)

The following analysis is used for channels:

$$\epsilon_I = \alpha_j (T_{ji} - 70) - \alpha_w (T_{wi} - 70)$$

$$\epsilon_s = \alpha_j (T_{js} - 70) - \alpha_w (T_{ws} - 70)$$

$$\epsilon_{tot} = \epsilon_s - \epsilon_I$$

$$\epsilon_e = 2 \epsilon_{tot} \beta$$

where

- ϵ_I = Initial hot gas surface axial or lateral strain
- ϵ_s = Steady state operating hot gas surface axial or lateral strain
- ϵ_{tot} = Hot gas surface axial or lateral strain range
- ϵ_e = Equivalent uniaxial strain range
- β = Correction factor to make the strain range agree with finite element analysis results

Fatigue Damage Fraction

The equivalent uniaxial cyclic strain range is used to enter the fatigue plot to find the number of cycles to cause fatigue failure, N_f . The fatigue damage fraction is then calculated as:

$$\phi_f = \frac{n}{N_f}$$

where n is the design requirement for number of cycles. In the event that cycles of a different type occur, each type of cycle is analyzed separately and a damage fraction calculated for each. The total fatigue damage, ϕ_f , is then:

$$\phi_f = \sum \frac{n_1}{N_{f2}} + \dots + \frac{N_n}{N_{fn}}$$

APPENDIX B

DUTY CYCLE LIFE EVALUATION METHOD

FATIGUE DAMAGE

To evaluate the fatigue damage for cycling loading, the accumulation of damage for each change in loading is calculated and summed. Each change in loading is treated as half cycle. The fatigue damage fraction for each change in loading is:

$$\phi_{fm} = \frac{N_{\text{design}}}{2 N_{fm}}$$

where ϕ_{fm} is the fatigue damage fraction for the m^{th} change in loading. From this, the total fatigue damage is:

$$\phi_f (\text{total}) = \sum_1^n \phi_{fm}$$

The predicted cycles to failure, N_{fm} , for each loading step are obtained from the zirconium-copper thermal fatigue life curve. The effective strain range for each step is the change in effective strain that occurs during a change in loading. The effective strain range is given as:

$$\Delta \epsilon_{\text{eff}} = 1.2 (\epsilon_{em} - \Delta \epsilon_{e(m-1)})$$

where ϵ_{em} is the effective strain after the m^{th} change in loading. The constant 1.2 was found to bring this type of simplified analysis into agreement with the computer finite element analysis for this particular thrust chamber design. Δ signifies the range of ϵ .

CREEP DAMAGE

The creep damage at each step is evaluated as outlined in Appendix A. The creep damage fraction for the n^{th} step is:

$$\phi_{cn} = \frac{t_n}{t_{rn}}$$

where t_n is the specified design time at the n^{th} step, and t_{rn} is the predicted time to rupture for the n^{th} step. The total creep damage fraction is:

$$\phi_c (\text{total}) = \sum_1^n \phi_{cn}$$

TOTAL DAMAGE

The total damage fraction is:

$$\emptyset (\text{total}) = \emptyset_f (\text{total}) + \emptyset_c (\text{total})$$

The design requires a factor of four which results in the following life equation:

$$4 \emptyset (\text{total}) \leq 1$$

Failure is defined as occurring when a leaking crack develops in the thrust chamber wall.

REFERENCES

1. Report No. AFRPL-TR-72-4, O_2/H_2 Advanced Maneuvering Propulsion Technology Program, Engine System Studies Final Report, Vol. II, December 1971.
2. Larson, F. R., and J. Miller; A Time-Temperature Relationship for Rupture and Creep Stresses, Transactions of the ASME, July 1952, pp. 765-775.